Mineralogy and Geochemistry of the Carbonaceous Mudstones, and Coal Petrogenesis of the Grootegeluk Formation in the Waterberg Coalfield, South Africa.

by

Kevin Faure

A thesis submitted in fulfilment of the requirements for the degree of Doctor of Philosophy

Department of Geological Sciences
University of Cape Town

September, 1993

CONTENTS

LIST of FIGURES

LIST of TABLES

ABSTRACT

The Grootegeluk Formation in the Waterberg Coalfield consists of coal and mudstone layers that were deposited during the Late Permian. In the south-central part of the Waterberg Basin rapid subsidence resulted in the formation of strata (~70 m thick) which consist of relatively thin coal beds interbedded with a multitude of mudstone and carbonaceous mudstone layers. Mudstones from the Grootegeluk Formation, the underlying upper Vryheid Formation and the base of the overlying Beaufort Group were obtained predominantly from borehole cores. The thesis integrates thin-section petrography, mineralogy, maceral composition, maximum vitrinite reflectivity and geochemical analyses to investigate: (1) the source of the sediments and the palaeo-environment of formation of the coal and mudstone layers; (2) the stratigraphical correlations of some South African coal formations and the formation of coal, on a continental scale, during the Late Permian and Triassic times; (3) the possibility of contamination to the environment by the waste products of coal-mining (carbonaceous mudstones) and coal-burning in a local power-station (fly ash and bottom ash).

The lower portion of the Grootegeluk Formation is dominated by kaolinite, quartz and minor amounts of anatase, and the upper parts of by quartz, kaolinite and minor amounts of montmorillonite-illite and microcline. These minerals are *predominantly* allogenic. Mineralogical evidence from the mudstones suggests that the base of the Grootegeluk Formation was relatively more distal and the upper portions more proximal to the source of the sediments. The maceral variation of the coal seams and the organic matter in the mudstones reveal that conditions for the preservation of organic matter were more suitable during the deposition of the sediments in the upper (vitrinite-rich) rather than the lower (inertinite-rich) Grootegeluk Formation.

At the base of the Grootegeluk Formation a 2 m thick carbo-tonstein occurs that is dominated by kaolinite, organic matter (~40 weight %), siderite, calcite and and minor proportions of apatite. The carbo-tonstein has mineralogical, maceral and chemical characteristics distinctive from the other mudstones.

Syn-depositional calcite lenses occur predominantly in the upper-half of the Grootegeluk Formation. Early diagenetic globular pyrite and spherulitic siderite occur in the coals and organic rich-mudstones of the Grootegeluk Formation. Globular pyrite and granular siderite are present predominantly in the organic-poor mudstones of the Grootegeluk Formation and Beaufort Group. Marcasite sometimes occurs along bedding planes and calcite is generally present as cleat-filling in the coal seams.

Based on their geochemistry, the Grootegeluk Formation and Beaufort Group mudstones have the same provenance, dominantly "granitic", possibly granodioritic in composition (Late Proterozoic Sm-Nd model ages). The provenance of the Vryheid Formation was relatively more mafic (Early Proterozoic Sm-Nd model ages). Smooth, systematic changes in the mineralogy and major element chemistry make major element whole-rock chemistry an ideal stratigraphic-indicator tool for the Grootegeluk Formation. The mudstones had very low concentrations of the alkali and alkaline-earth elements suggesting that the rocks had undergone very high degrees of chemical alteration. Trace elements in the carbonaceous mudstones are predominantly hosted in the mineral fraction. The carbo-tonstein had anomalously high concentrations of all the trace elements except S, Co, As and Zn, which, in addition to its mineralogical character, make the carbo-tonstein an important (chrono-) stratigraphic marker for local and intra-basinal correlation. Anomalous concentrations of the chalcophile elements in the mudstones from the overlying lower Beaufort Group mudstones are considered to have been concentrated as a result of diagenesis and(or) reduction-oxidation reactions.

The concentrations of trace elements and stable isotope data suggest that the sediments were deposited in fresh rather than in marine waters.

Evidence from organic ^{13}C analyses and palynological studies indicates that $\delta^{13}C$ values can be used in stratigraphical correlations and as palaeo-ecological indicators. The $\delta^{13}C$ values of the Permian and Triassic terrestrial organic matter suggest a change in the atmospheric $^{13}C/^{12}C$ ratio during this time.

Leachable concentrations of trace elements which may be toxic to plants, animals or humans are too low in coal mining discards to be of any concern. Mudstones that immediately overlie the Grootegeluk Formation coal-mudstones have leachable concentrations of elements that exceed the critical concentrations believed to be harmful to the environment. Experiments on fly ash and bottom ash samples from the Matimba power station revealed that the fly ash had unacceptably high concentrations of leachable elements, such as As, Cd and Mo. Leachates of bottom ash samples had very low concentrations of potentially harmful elements.

ACKNOWLEDGEMENTS

I would like to express my gratitude to my supervisor James Willis for proposing this project, for his guidance and support during the research and especially during the final preparation of the thesis. The project was funded by the Foundation for Research Development (FRD) and a generous studentship from James Willis.

The assistance of staff members and technicians in the Departments of Geological Earth Sciences and Archaeology is appreciated. I would like to thank John Lanham for the maintenance of the mass spectrometer and Julie Lee-Thorpe for assistance on the carbon stable isotope line in the Department of Archaeology. In the Department of Geological Sciences my thanks to: James Willis and Andy Duncan who were my mentors on XRF spectrometry; Chris Harris for maintenance of the stable isotope facility; Gavin Doyle for the maintenance of the XRD spectrometer; Ron Watkins for supervision on the Gradient Ion Chromatograph; Dick Rickard for help on the electron microprobe; Andy Duncan, Dave Hill and Gavin Doyle for their assistance with the departmental computer systems; Isobel Laithwaite and Nicky Wilson-Harris for helping with all sorts of administrative work; Bruce Cairns, "Chalky" Stout and Bernard Grove for maintenance of sample preparation equipment; Henry Hendricks, Robert Oliver and Dave Wilson for their helpful co-operation and expertise in making thin-sections; Dave Reid who always had an "open-door" for a chat and advice on anything under the sun and; the departmental assistants, Ivan Wilson, Neville Buchanan and Patrick Sieas for their work in the department and cheerful demeanour. I am grateful to Nick Steven and Chris Harris who had the arduous (odious!) task of reading the first draft of the thesis and deciphering my "boertjie" English. In particular I would like to thank Richard Armstrong for analysing several of my samples for their Sm/Nd ages, and also for his enthusiasm in getting involved in a project which had absolutely nothing to do with the upper mantle, MORB, Karoo lavas, etc. The cost of the Sm/Nd analyses was funded by Richard's FRD research grant. I acknowledge the collaboration of Hendrik Schloeman, a fellow student, in testing and deciding on a suitable leaching method, and translation of German papers.

The Geological Survey in Pretoria and the analysts, Dr. Deiter Bühmann, Mr. Trojak and Mr. Labuschagne, are thanked for providing cost-free XRD and Au analyses. Robbie Robért at MINTEK in Johannesburg provided advice and assistance with leaching experiments and analyses of leachates.

ISCOR are thanked for providing core samples and permission to present the data from this study. The geological staff at the Grootegeluk Coal Mine, in particular Claris Dreyer, Tom and Catherine Richards, and Leon Roux are thanked for their hospitality and sharing their in-depth knowledge of the area. I am also grateful to the geological staff of

ISCOR's Tshikondeni Coal Mine in the N.E. Transvaal, especially field-geologists John and Diedre Sullivan, and mine-geologist "PG" Lourens, for their "Low-veld" hospitality and visit to the coal-mine.

Several people, from many different disciplines, have provided thought-stimulating discussions that have succeeded in knocking the edges off a die-hard hardrock geologist and made me appreciative of the complexities and enormous potential of sedimentary geochemistry in S.A. In this regard I want to thank: my supervisor James Willis; Chris Hartnady and especially Maarten de Wit for discussions on Gondwana tectonics and comments on Chapter 8 (coal, and Permo-Triassic tectonics and mass extinctions); Colin MacRae from the Geological Survey in Pretoria for providing samples from the Vryheid and Pietermaritzburg Formations in the Waterberg Basin (for organic $\delta^{13}C$ analyses), and for discussions on palynology; Pedro Monteiro from Sea Fisheries in Sea Point, for discussions on organic carbon stable isotopes and Permo-Triassic mass extinctions and; Bruce Cairncross from the Department of Geology at RAU for his comments on Chapter 5 (coal petrogenesis).

Lastly, I would like to thank all those people who have offered their moral support, especially my parents, Sue and Bram. Thanks to Sophia for sharing her bedroom with my office and putting up with keyboard and paper noises through the night. Finally, a special thanks to my wife Brigette, who has been a constant source of strength and encouragement during the "lows and highs" of the thesis, and for all her hard work in supporting our family.

1. INTRODUCTION

1.1 GENERAL

The coal deposits of southern Africa form part of the Karoo Sequence which where deposited on the supercontinent of Gondwana during Lower Permian to Middle Triassic times. The Karoo Sequence is best preserved in the Main Karoo Basin (MKB) which covers more than half of South Africa (Fig. 1.1). Subsidiary Karoo basins to the north of the main basin include the southern terminus of the East African Rift system, represented by the north trending Lebombo and east trending Soutpansberg Basins in the northern Transvaal (Tankard et al., 1982). There are also the widespread, mainly thin Karoo deposits of the Kalahari Basin and Springbok Flats. The Waterberg Basin in the north-western Transvaal is considered to be an embayment of the much larger Kalahari Basin (Rust, 1975) which is separated from the MKB by the Cargonian palaeo-highlands (Visser, 1990; Fig. 1.1). A generalised stratigraphic column of the Karoo Sequence in the Waterberg Basin is presented in Figure 1.2.

The vast majority of coal beds in South Africa occur in the Ecca Group (lower and middle Permian) with most of the coal mining taking place in the north-west, north and north-eastern portions of the MKB (Fig. 1.1). Coal mining is assuming increasing significance in the subsidiary basins north of the main Karoo depository. Coal also occurs in the younger Molteno Formation (Lower to Middle Triassic) of the Beaufort Group which is confined to the central parts of the main basin (Fig. 1.1). These younger coals are of relatively lesser economic importance.

Coal was discovered in the north-western Transvaal in 1920 during a water-drilling project on the farm Grootegeluk (459 LQ), near the village of Ellisras (Alberts and Liebenberg, 1982). Exploration by the Geological Survey of S.A. in the 1940's established the extent of the coalfield, now called the Waterberg Coalfield. In the early 1970's the Iron and Steel Corporation (ISCOR) conducted intensive exploration and in 1980 established the Grootegeluk Coal Mine (GCM). The GCM opencast mine produces mainly power station coal which is supplied to the nearby dry-cooled Matimba Power Station. A significant but minor amount of blend coking-coal is also produced for the making of steel.

1.2 GEOMORPHOLOGY, CLIMATE AND VEGETATION

The landscape of the area is exceedingly flat and featureless. The drainage system is poorly developed and outcrop is sparse, as most of the surface is covered with sand and, locally, superficial calcretes and recent conglomerates and grits. This is in contrast to the mountains approximately 100 km to the south which consist of quartzites and conglomerates of the Early Proterozoic Waterberg Group (Fig. 2.1). The only obvious topographic feature

to the west of the Mogol river is a sandstone hill from the Beaufort Group, called Nelson's Kop on the farm Nelsonskop (484 LQ). East of the Mogol river a few low hills are underlain by mudstones of the lower portion of the Pietermaritzburg Formation (Lower Ecca Group) on the farm Grootfontein (501 LQ).

The vegetation consists mainly of dry woodland, thornbush and grassland. Rain falls in summer (~300 mm/yr) while the winters are dry (Fullard, 1967). Summer day-time temperatures are usually higher than 30°C and above 20°C in winter (Fullard, 1967). Water is very scarce and is obtained from boreholes and a nearby dam.

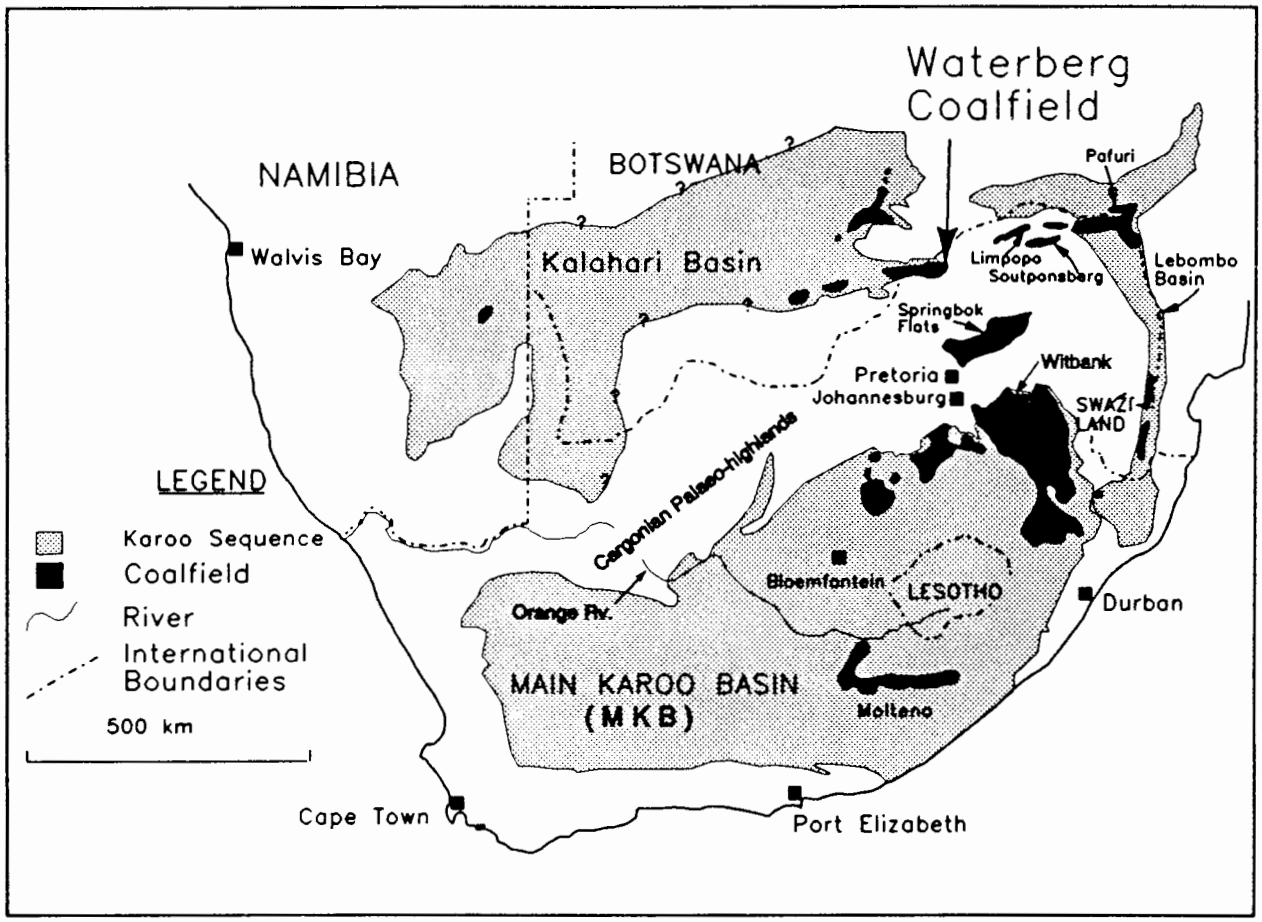

Figure 1.1 The distribution of the Karoo Sequence and the coalfields of southern Africa (modified after Tankard et al., 1982) and Visser (1990). The Waterberg Coalfield is considered to be an embayment of the Kalahari Basin rather than the Main Karoo Basin. Coal mining occurs mainly in the northern portion of the MKB, but is becoming increasingly important in the northern subsidiary Karoo basins.

1.3 COAL MINING IN THE WATERBERG COALFIELD

Although the Waterberg Coalfield covers a relatively small area in relation to the other coalfields in South Africa, it contains approximately 44% (de Jager, in Dreyer, 1991) of the South African *in situ* reserves of bituminous coal. Estimates indicate that 34 000 and 52 000 million tons (Mt) of the coal are mineable by opencast and underground methods respectively (Dreyer, 1991). The flat-lying coal seams are intercalated with carbonaceous mudstones which have thicknesses varying from millimetres to a few metres. The total

thickness of the Ecca coal and mudstone package is about 110 m in the Grootegeluk area. The run-of-mine (ROM) coal and carbonaceous mudstone is beneficiated at GCM to remove a substantial proportion of the inorganic fraction to obtain the required product. Thirty five percent of the ROM after beneficiation is a high ash coal (35-45% ash content) for Matimba Power Station and approximately 10% of the ROM is a low ash blend coking-coal (10% ash content) for the steel industry. The remaining 55% of the ROM is coal and carbonaceous mudstone with an ash content generally greater than 45% which is not utilised and is stored as discard dumps.

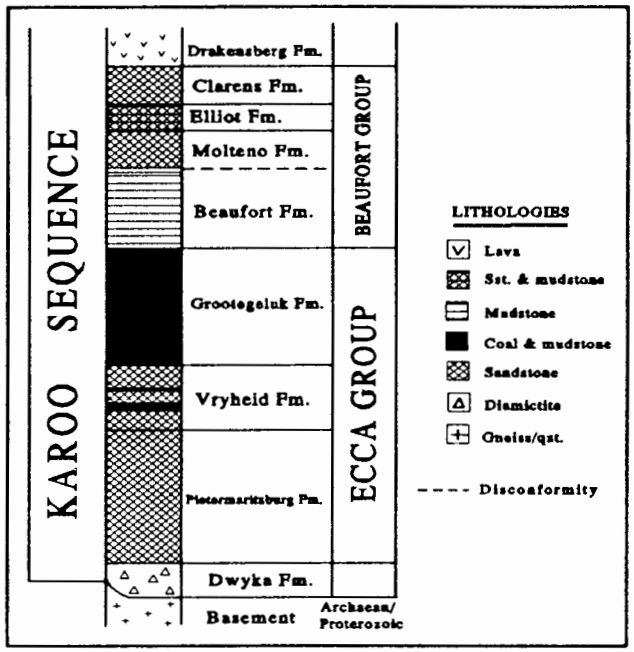

Figure 1.2 Stratigraphic column of the Karoo Sequence in the Waterberg Basin, not according to scale. Compiled from Beukes (1985), de Jager (1986) and Siepker (1986).

The only coal mine in the Waterberg Coalfield at present is the GCM opencast mine. The development of other mines in the area has been hampered mainly by the high ash content of the coal, long distances from market places and the shortage of water. The distance factor was eliminated when the Electricity Supply Commission (ESCOM) built the Matimba power station, especially designed for the high ash coal produced at GCM, about 5 km from the mine. GCM is able to supply Matimba with its full quota of coal. GCM has also partially overcome the need for large amounts of water by recovering water from slurries, and as a result is also recovering fine coal (Venter and van Loggerenberg, 1992).

1.3.1 COAL MINING DISCARDS

Although other sources of electricity, such as hydro-electricity, from countries north of South Africa may become available in the future, it is expected that the demand for power station coal in southern Africa will probably increase, because of the increasing demand for electricity by a growing population and a possible demand for electricity from neighbouring countries. The coal mines in the MKB have been in production for approximately 50 years and have a relatively short life span compared to the subsidiary Karoo Basins (Barker, 1986). If the shortage of water in the Waterberg Coalfield can be overcome, it can be regarded as the future coal-mining region of South Africa because of its enormous coal reserves. This view is supported by the fact that a variety of products can potentially be obtained from the Waterberg Coalfield, e.g., an activated carbon product for

the carbon-in-pulp (CIP) process, fuel for SASOL (oil from coal) and products from the petrochemical industry (Dreyer, 1991).

It has been estimated that a total of about 86 000 Mt ROM coal can potentially be mined from the Waterberg Coalfield (Dreyer, 1991). If this is the case then approximately 47 000 Mt discard material will be produced at current beneficiation rates of ROM. The coal-mining discard material (carbonaceous mudstones) is presently stockpiled, but after about 15 years will be back-filled into the mined-out pits (C.J. Dreyer, pers. comm., 1991). Even though the carbonaceous mudrocks will eventually be replaced into the pits, they have nevertheless been taken out of their natural environment and exposed to air, water and weathering. The constituents of the carbonaceous rocks can be released into the air from burning dumps or by leaching into groundwaters (Sciulli et al., 1986), especially in this area which has a highly seasonal rainfall. Carbonaceous rocks generally contain a broad array of trace elements, many of which are of considerable concern because of the low tolerances for them by plants, animals and humans (Torrey, 1978; Chadwick and Lindman, 1982; Valković, 1983; Thornton, 1983; Sciulli et al., 1986).

Establishing the mineralogy and chemistry of the geological strata that will be exposed and characterising the leachates from the discards in the Waterberg Coalfield is especially important because of the high proportion of discard material that will be generated over the many decades and the shortage of water in the area. In other coal mining countries, such as the U.S.A. and Australia, where mining and beneficiation results in discards, the coal-mining discards are leached to determine which elements may be released into the environment (Heaton et al., 1982; Bell et al., 1986; Clarke et al., 1990; Bell and Krol, 1990).

1.4 PREVIOUS WORK

Even though extensive exploration drilling has been done in the Waterberg Coalfield (Wyberg, 1928; Venter, 1944; Cillié and Visser, 1946; Cillié, 1951; Cillié, 1957), previous geological work was mainly restricted to stratigraphic correlation and the determination of the extent and quality of the coal horizons. Visser (1961) reviewed the general geology and Alberts and Liebenberg (1982) summarised the geology and mining potential of the Waterberg Coalfield. More recently Beukes (1985) and Siepker (1986) carried out sedimentological studies to identify the different facies in which the rocks of the Karoo Sequence in the Waterberg Basin where deposited. Anderson (1977) and MacRae (1988) undertook palynological studies on the Karoo Sequence of the Waterberg Basin and correlated the Sequence with other coal deposits. Siepker (1986) identified the microlithotypes present in the Grootegeluk Formation. In the Waterberg Coalfield only the *coal fractions* have been analyzed for their major, minor and trace element composition

(Botha, 1984). Spears et al. (1988) identified a tonstein at the base of the Grootegeluk Formation in the west Waterberg Coalfield area.

Botha (1984), Beukes (1985) and Siepker (1986) and mine geologists from the GCM have identified cycles and sub-cycles of coal and mudstone (hereafter referred simply to as coal-mudstone) variation. The cycles and sub-cycles are classified visually and by down-the-hole geophysical logging (Siepker, 1986; Dreyer and Roux, 1991). The base of a cycle has a high coal-to-mudstone ratio which decreases upward within each cycle. Sub-cycles of upward decreasing coal-to-mudstone ratio are also recognised. Most of the coal-mudstone layers are laterally persistent and so the cycles are also broadly preserved throughout the Waterberg Coalfield. However, the coal-to-mudstone ratios have not been formally quantified nor are there generally accepted boundaries where the cycles start and finish, nor any nomenclature scheme for the cycles and sub-cycles. To the untrained eye the coal beds in the Waterberg Coalfield are a confusing sequence of inter-bedded coals and grey-black mudstones (Fig. 2.3).

Most interpretations of the palaeo-environment of formation of the coal-mudstones have been based on sedimentological interpretation, maceral-microlithotype and fossil spore and pollen variation within the coal. The palaeo-environments that have been proposed for the formation of the Grootegeluk Formation are summarised in Table 1.1.

1.5 AIM OF STUDY

Relatively little is known about the geochemistry of South African coals *per se* and even less is known about the geochemistry and mineralogy of the host rocks of coal seams. This is also the case for the carbonaceous mudstones which interbed the coal seams of the Grootegeluk Formation. In this study emphasis is placed on the mudstones that were obtained from two boreholes which intersect the coal-mudstone sequence of the Grootegeluk Formation (approximately 70 m thick). The borehole cores, which were made available by ISCOR, were drilled close to the present opencast pit at the GCM and were spaced about 250 m apart (Fig. I.1). Spacings between samples from the cores were generally less than 0.6 m to ensure that small-scale chemical and mineralogical variations within and between cores could be observed. The sampling procedure is described in detail in Appendix I.

The aims of this project were broadly:

I To determine the palaeo-environment of formation of the Grootegeluk Formation coal-mudstones. The palaeo-environment reconstruction encompasses sediment provenances,

Table 1.1 Summary of palaeo-depositional environments proposed for the Grootegeluk Formation in previous studies.

Ryan (1966)	The sedimentary environment was distal in relation to the source area, with low topographic relief and with the fine-grained or argillaceous sediments reflecting periods of increased subsidence. These alternated with periods of slower movement during which thin coal seams formed.
Alberts and Liebenberg (1982)	The coal and coal-bearing strata were considered to have originated in a fluvial environment.
De Jager (1983)	Peat formation occurred at times of regional interruption in sedimentation.
Botha (1984)	The succession was deposited in a fluvial environment during rapidly changing climatic conditions and related pH-Eh fluctuations which led to the forming of the thin layered coal seams which differ in character.
Beukes (1985)	The succession formed on a poorly drained densely vegetated flood plain, the coals representing events of basinal subsidence when the flood plain was sufficiently "wet" to promote marsh formation and subsequent peat accumulation. The basin would then have been filled by prograding fine carbonaceous muds. The base of the formation was considered to have been deposited in a more proximal and the upper portion in more distal portion of the basin.
Siepker (1986)	Basin infilling caused poor drainage which led to the development of extensive poorly drained swamp environments within the flood-basin. The cycles within the succession are due to cyclic basin subsidence and(or) periodic mud input. The mud was introduced from a source external to the basin (melting glaciers to the north). The basal portion of the formation was more proximal to the source of the mudstones, and the upper portion was more distal, had deeper waters and was more stable (less subsidence).
MacRae (1988)	Palynological evidence suggests warmer, humid and generally milder climatic conditions in the lower half of the Grootegeluk Formation (Biozone D). Fossil pollen and spore data from the upper portion of the Grootegeluk Formation (Biozone E) suggest a possible drying up of the basin (silting up). The pollen and spore data also indicate a climatic change(?).

palaeo-climate, sediment and organic deposition, and diagenetic processes. Even though most of the samples studied are mudstones which usually have <50 weight % organic matter, it must not be forgotten that coal itself is also a sedimentary rock that was deposited as layers, buried and modified by diagenetic processes. So the conclusions derived for the mudstones are also pertinent to the formation and quality of the coal. The palaeo-environment reconstruction was based on data obtained from vitrinite reflectivity and maceral composition of the coal, whole-rock chemical compositions, mineralogy,

stable isotope compositions of the carbonates and organic fraction, and radiogenic isotope analyses of selected mudstones. The data from borehole core, that has been sampled in detail, will make it possible to establish the presence of strategic minerals/elements and evaluate the possibility of selective mining for these resources which are presently being discarded. The data also provide stratigraphic markers for local and regional correlation.

II To discuss the formation of coal in the Waterberg Coal Field with respect to the other coal fields in South Africa, the break in global coal formation at the end of the Permian Period, marine and freshwater mass extinctions during Permian-Triassic boundary times, and using the carbon stable isotope values of organic matter as a palaeo-ecological tool and for establishing the Permian-Triassic boundary in freshwater sediments.

III To investigate the present-day environmental consequences of producing and dumping vast amounts of coal-mining discards. Environmental impact studies consist of many aspects but the focus in this study will determine the concentrations of selected elements which may be naturally leached from the coal-mining discard dumps and Matimba power station ash. Utilising controlled leaching experiments it is possible to identify the elements which pose a threat to human, animal or plant life and also the magnitude of that threat. Mining in the Waterberg Coalfield is fortunately still in its infancy and so there still is an opportunity to anticipate and plan for possible disturbances to the environment as a result of mining.

2. GEOLOGY

2.1 INTRODUCTION

The Waterberg Basin in the north-western portion of South Africa consists of a sedimentary-volcanic succession that is fault-bounded in its northern and southern portions (Fig. 2.1). This study focuses primarily on the mudstones that occur in the coal-mudstone beds of the Grootegeluk Formation, specifically on the farm Grootegeluk in the south-central part of the basin (Fig. 2.1). The coal-mudstones are part of a continuous sedimentological sequence, the Ecca Group, that underlie the sediments of the Beaufort Group, and the volcanics of the Drakensberg Formation (Fig. 2.1). The general geology of the area will be discussed to place the Grootegeluk Formation into context with its host rocks, and a brief review of the coal formations in the Waterberg Basin. The terminology of clay-bearing rocks will be examined to clarify some of the terms that are used in this study.

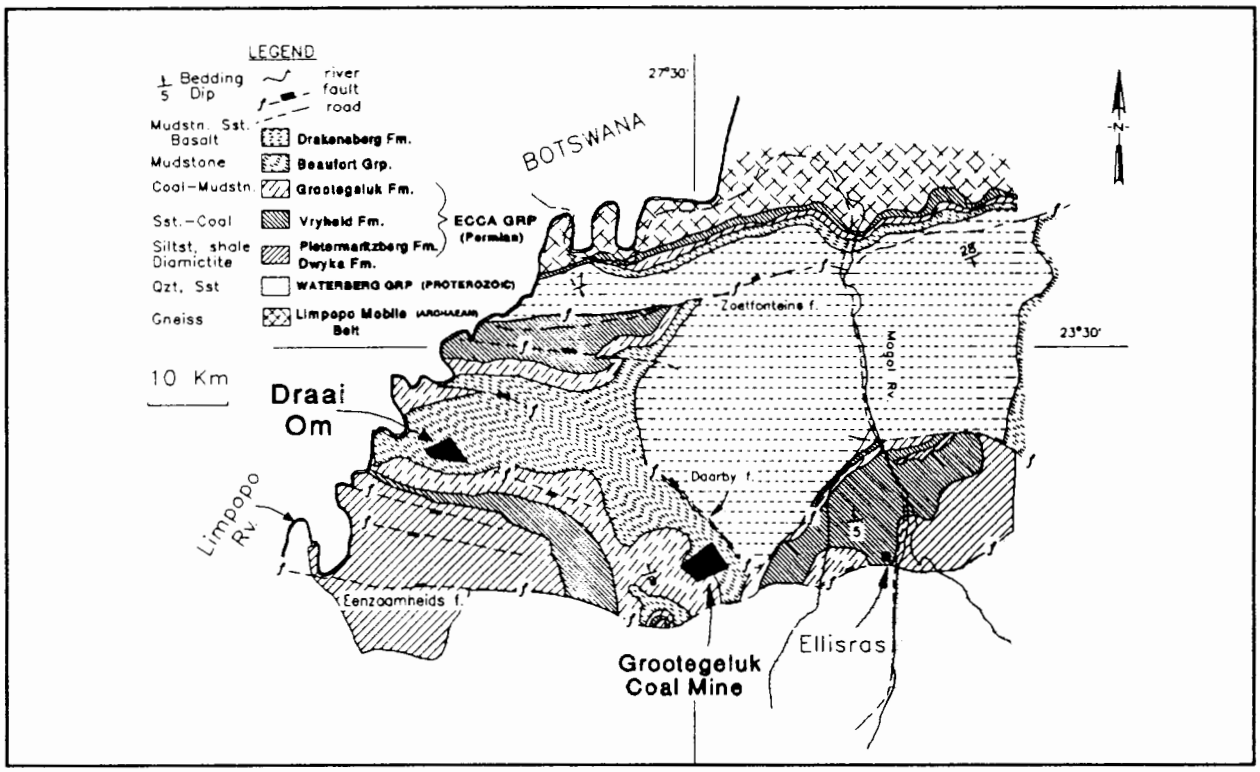

Figure 2.1 The general geology of the Waterberg Basin in the north-western Transvaal (modified after Cillié, 1951). Coal is open-cast mined on the farm Grootegeluk which is approximately 25 km west of Ellisras. Coal occurs within both the Vryheid and the Grootegeluk Formation in this portion of the Karoo Sequence but only the coal from the Grootegeluk Formation has up until now been economically recovered.

2.2 GENERAL GEOLOGY

2.2.1 LITHOSTRATIGRAPHY

The Waterberg Basin lies discordantly (Haughton, 1969) on the Archaean rocks of the Limpopo Mobile Belt and the Early Proterozoic Waterberg Group (Siepker 1986). To

the north of the Zoetfontein fault the basin is underlain by the gneissic rocks of the Limpopo Mobile Belt, to the east by the granites, gabbros and norites of the Bushveld Igneous Complex, and in the south by the quartzites and conglomerates of the Proterozoic Waterberg Group (Fig. 2.1). The Waterberg Basin is considered to be an embayment of the much larger Kalahari Basin in the north-western Transvaal (Rust, 1975; Fig. 1.1).

Cillié (1957) sub-divided the Karoo rocks of the Waterberg Basin utilizing information from 143 boreholes. He grouped the sediments into different lithologies based on the stratigraphy of the MKB. The South African Committee for Stratigraphy (S.A.C.S.; 1980) decided that there was not enough detailed information on the Karoo Sequence in this area to propose a lithostratigraphic nomenclature. Beukes (1985) re-evaluated the sediments and concluded that all the clastic lithostratigraphic units of the Karoo Sequence (S.A.C.S., 1980) are developed in the Waterberg Basin and that this justifies the use of the nomenclature as proposed for the MKB.

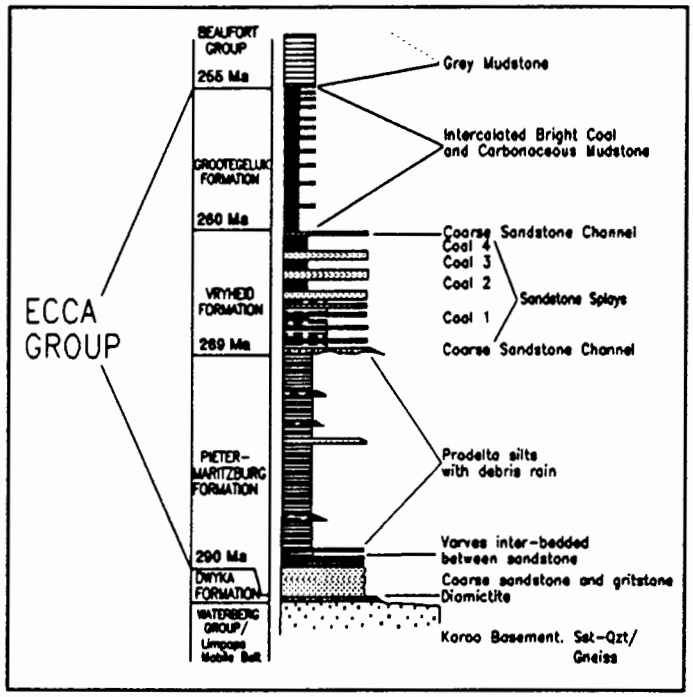

Figure 2.2. Generalised stratigraphy of the Waterberg Basin modified after Beukes (1985). Ages at formation boundaries are based on palynological data from MacRae (1988) and according to the time scale of Harland et al. (1990).

The interpretation of the Waterberg Karoo Sequence concluded from sedimentological information and facies analyses by Beukes (1985) and Beukes et al. (1991) was generally in good agreement with the interpretation of Siepker (1986). The stratigraphy proposed by these authors is briefly reviewed, and the subdivisions of the Lower Karoo Sequence in the Waterberg Basin are compared and correlated with the MKB (Figs. 2.2 and 2.4).

1. The first sediments encountered above the erosional surface of the basement are the diamictites of the **Dwyka Formation** (Fig. 2.2). Beukes (1985) recorded ground moraine tilloid, poorly sorted braided outwash conglomerate, grits and coarse sandstone, and lacustrine varves and turbidites.
2. The **Ecca Group** overlies these lithologies and is divided into the Pietermaritzburg, Vryheid and Grootegeluk Formations (Fig. 2.2).

2a) The **Pietermaritzburg Formation** consists of a coarsening-upward sequence of prodelta siltstones with inter-bedded glaciogenic debris flow and debris rain deposits that accumulated after a major transgression of the shoreline (Beukes, 1985).

2b) The **Vryheid Formation** is composed of delta front coarse sandstones, delta plain gritstone and(or) coarse sandstone channel deposits, and siltstone and(or) sandstone splay deposits capped by a thin dull coal (Coal 1; Fig. 2.2). This is overlain by east-west trending coarse gritty to sandy upward-fining fluvial channel deposits. The fluviatile conditions were interrupted and resulted in the accumulation of coal seams 2 and 3. The channel deposits are overlain by a complex unit of coal, mudstone, siltstone and sandstone that was interpreted to have resulted from intermittent periods of proximal flood-plain development with channels, splays and mudflows alternating with times of fine carbonaceous mud and peat formation (Coal 4; Beukes, 1985; Siepker, 1986). Siepker (1986) suggested that mudstone and sandstone mudflows, small channels, and crevasse splays, building tributary alluvial fans from the north, inter-fingered with fluvial and swamp deposits to the south, introducing mainly muds to these environments. The mudflows, which are developed predominantly in the northern portion of the basin, were considered to have been derived from glaciers retreating to the north. Siepker (1986) suggested that the mudflows should be differentiated and called the Goedgedachte Formation.

2c) Overlying the Vryheid Formation is a repetitious sequence of carbonaceous mudstones with interbedded bright coal seams. Beukes (1985) called this sequence the **Grootegeluk Formation** (Figs. 2.2 and 2.3). No alternating carbonaceous mudstone and coal seam sequence is present in the MKB. Stratigraphically Beukes (1985) correlated the formation with the Volksrust Formation in the MKB (Fig. 2.4) and suggested that the facies-association characteristics within this coal-mudstone unit justified the definition of the new Grootegeluk Formation. This nomenclature has, however, not yet been ratified by S.A.C.S. (1980). The Grootegeluk Formation is about 70 m thick in the south-central portion of the basin, and composed of stacked metre-thick sedimentary cycles of bright coal with mudstone partings grading upwards into mudstone with thinner coal partings (Fig. 2.3). Beukes (1985) interpreted these to have formed on a poorly drained, densely vegetated flood plain. In the western-most portion of the basin in South Africa, on the farm Draai Om (Fig. 2.1), Spears et al. (1988) proposed that a 2 cm mudstone layer was an acid air-fall tuff – termed a tonstein. The mudstone layer, which occurs 23 m below the top of coal-mudstone succession, was taken to represent the basal portion of the Grootegeluk Formation in the western Waterberg Coalfield. The tonstein, however, has not been identified elsewhere in the Waterberg Coalfield.

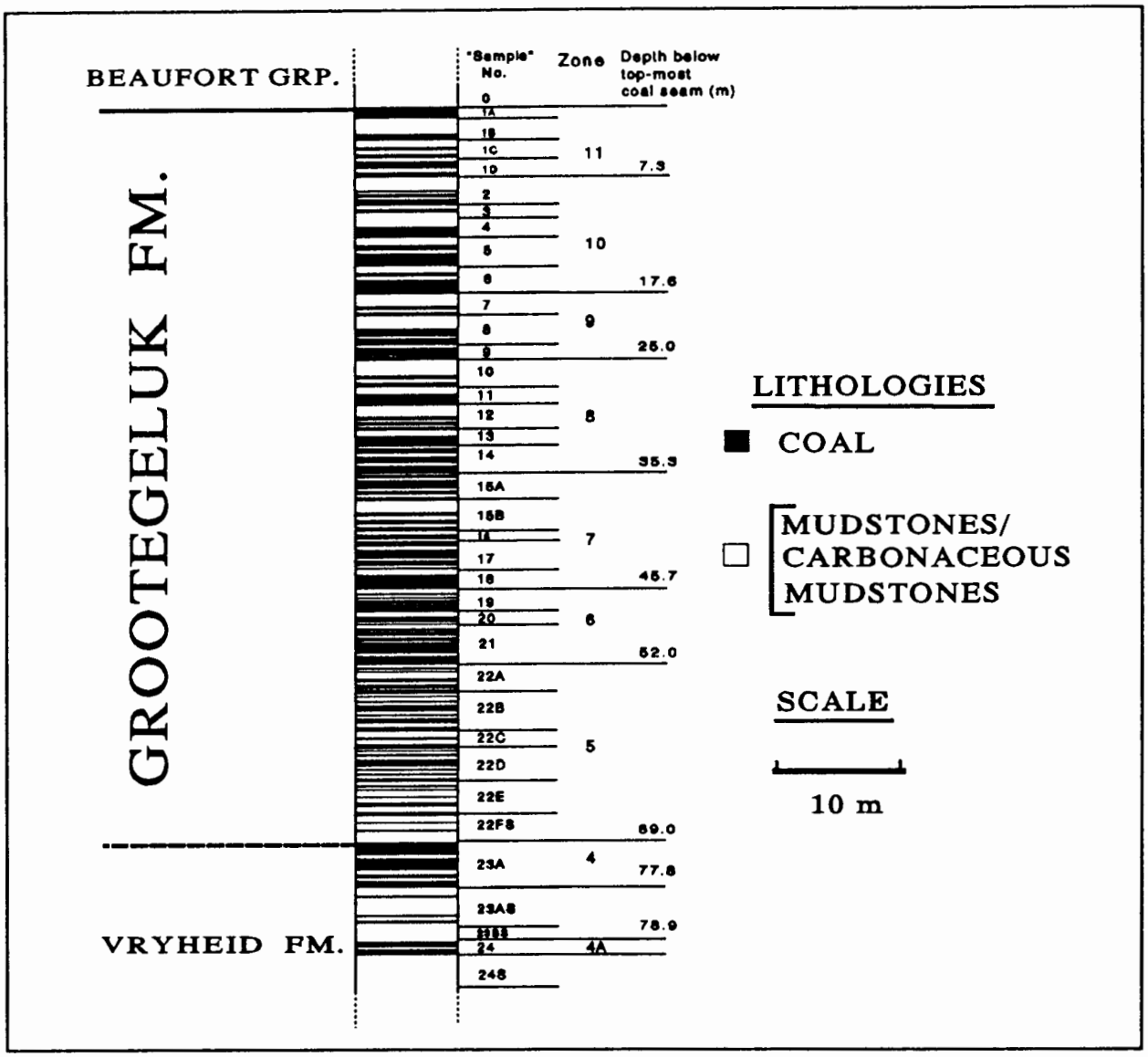

Figure 2.3 Stratigraphic column of the Grootegeluk Formation of the Waterberg Coalfield in the GCM area. The diagram displays the subdivisions used in this study, based mainly on the work of the geologists from the GCM. The sub-divisions of the zones and "sample numbers" are discussed in Section 2.3 and Appendix I. It is evident from the diagram that division and subdivision of the coal and mudstones is complicated by the multitude of layers. It is not possible to illustrate the intercalation of coal and mudstones which have thickness of centimetres and millimetres because of the scale of the diagram. Carbonaceous mudstones are defined as mudstones with more than 50 % organic matter.

3. The coal-mudstone cycles are overlain by medium to light grey massive mudstones of the **Beaufort Group**. These are considered to have originated in a well-drained, distal floodplain setting (Beukes, 1985). It is accepted by most authors (Haughton, 1969; Beukes, 1985; Siepker, 1986) that the Ecca-Beaufort Group contact is where the first sediments above the uppermost coal seams start. On the other hand, J.C. Dreyer (pers. comm., 1992) disagreed and suggested that the boundary is higher-up in the succession where the mudstones become the green-purple colour distinctive of the Beaufort Group mudstones in the MKB.

Due to the thinning of certain stratigraphic units towards the northern and north-eastern edges of the basin, the deterioration and(or) the disappearance of certain of the lower coal seams, and the presence of poorly sorted rock types in the north, it appears that the original edges of the basin towards the north and east could not have been very far away from the present ones (de Jager, 1976; Beukes, 1985; Siepker, 1986). To the south, however, the edge of the original basin may have been at a relatively greater distance (de Jager, 1976, Beukes, 1985, Siepker, 1986).

Only a few dolerite dykes are known on the surface in the Waterberg Coalfield and no sill has ever been encountered in any borehole (Alberts and Liebenberg, 1982). Dolerite dykes and sills, however, occur throughout the Soutpansberg Coalfields in the Limpopo Mobile Belt.

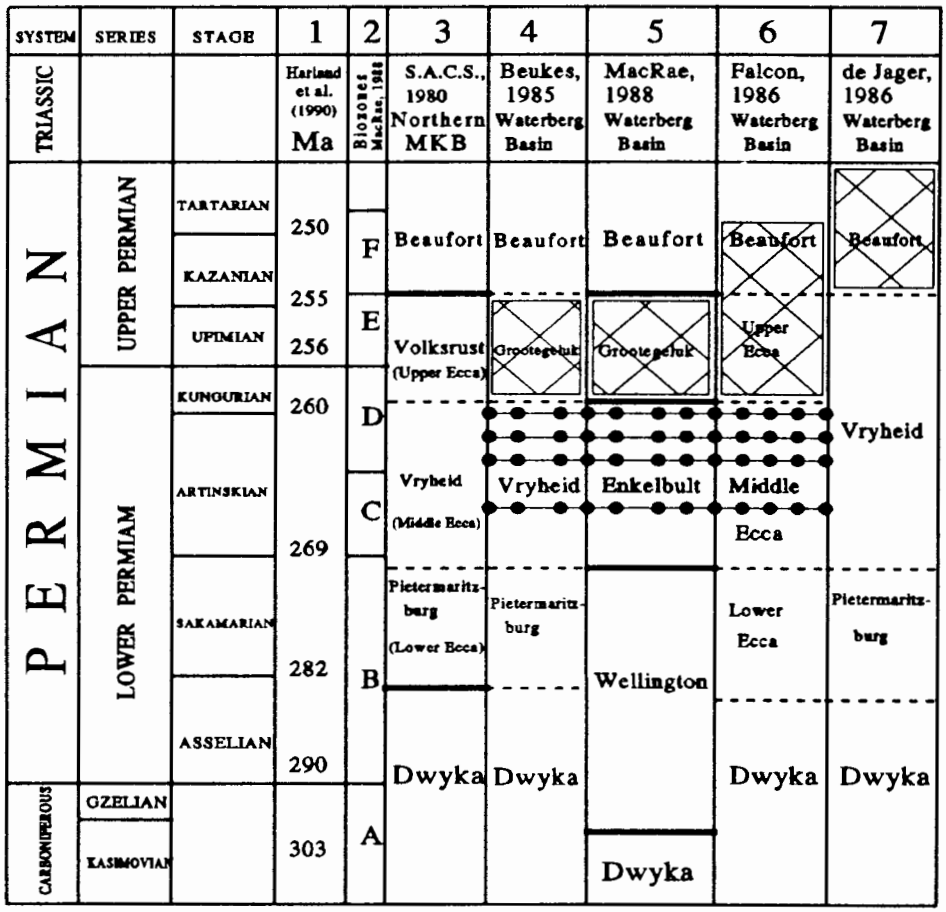

Figure 2.4. This figure schematically compares the stratigraphic interpretations of the Dwyka Formation, the Ecca and Beaufort Group of the Waterberg Basin (columns 4-7) and the northern MKB (column 3). Formation contacts with solid lines are ages (Harland et al., 1990) established from palynological data, and dotted contacts approximate ages. The 4 beaded lines symbolise the lower coal beds and the cross-hatched zones the position of the coal-mudstone succession as proposed by the different authors. S.A.C.S. (1980) accepted Upper Dwyka Formation and Ecca Group ages of Anderson (1977). Biozones of MacRae (1988) are based on data from palynological studies and are discussed further in Chapter 5.

2.2.2 TERMINOLOGY OF CLAY-BEARING ROCKS

There seems to be very little consensus on the classification of mudrock material. Several classifications exist, some are based on field observations, a number are based on laboratory experiments (Picard, 1971; Lewan, 1978), and most predate the development of modern analytical instrumentation. Because terms are not precisely defined several meanings are used for the same term leading to further confusion.

The main nomenclature problem is the dual meaning of the term clay, i.e., size and mineralogy. The term "clay mineral" has been used as a synonym for the term phyllosilicates but with the added connotation of fine grain size. Many sediments, however, contain phyllosilicates that are of silt size.

The term "mudrock" was proposed by Ingram (1953) and was defined as a rock that has more than 50% of its particles smaller than sand size (62μm-Wentworth scale). Mudstones are divided by Blatt et al. (1980) into siltstones, mudstones and claystones on the basis of the silt and clay size fraction, i.e. siltstones have ⅔ silt size fraction, mudstones have greater than a ⅓ and less than ⅔ clay size fraction and claystones have greater than ⅔ clay size fraction. This classification, however, is based only on grain size and mineralogy is not mentioned.

Clarke (1954) defined a shale as a detrital rock whose particles have a diameter of less than 62μm. Thus defined, the term is all-inclusive of silt and mudstones. Blatt et al. (1980) and Pettijohn (1975) suggest that the term shale should be used for a laminated (fissile) rock with a high proportion of clay material. As noted by Ingram (1953) fissility is a derived property and, in addition to being a function of particle orientation and bedding, is determined by weathering, temperature and water content. The fissility thus could be either primary (settling), secondary (compaction) or result from the fine interlaminations of organic material within mudstones. Therefore fissility should not be used in the classification of mudstones because the lithogenesis of laminated shales is doubtful.

Ideally a simple classification based on the percentage or dominant phyllosilicate and grain size is needed but has up now not been proposed. In this study the term mudstone or carbonaceous mudstone will be a sack-name used to describe a rock that;

a) has more than 50% inorganic material (black to grey in colour),

b) in which the inorganic fraction can be predominantly phyllosilicate or quartz, and

c) has a grain size less than sand-size (62μm).

A carbonaceous mudstone which has more than 50% organic material is considered to be coal.

2.2.3 STRUCTURE

The Waterberg Coalfield is structurally less complicated than the Soutpansberg Coalfield situated further eastward on the Limpopo Mobile Belt (Fig. 1.1). The Waterberg Coalfield lies in a basin between the Zoetfontein fault in the north and the Eenzaamheids fault in the south (Fig. 2.1). The Zoetfontein fault was the only fault active before deposition of the Karoo Sequence. It has been suggested that a Zoetfontein fault-scarp was present during the deposition of the Proterozoic Waterberg Group and that there was post-Waterberg Group, pre-Karoo movement along the Zoetfontein Fault (Crockett and Jones, 1975). It is also possible that the Zoetfontein fault could have been active during Karoo times (Beukes et al., 1991), producing fault-scarps that resulted in the deposition of poorly sorted sediments. The uplift was to the north of the Zoetfontein fault during pre- and syn-Karoo sedimentation whereas the post-Karoo faulting was downthrown to the north of the basin (Fig. 2.1; Green et al., 1980).

The sinuous-shaped Daarby fault (Fig. 2.1), with a vertical displacement of approximately 300 m divides the coalfield into a shallow western part, suitable for opencast mining, and a deep north-eastern part from where the coal can only be extracted by underground mining (Alberts and Liebenberg, 1982). Shallow-level coal seams are extracted at GCM on the western side of the Daarby fault.

2.3 COAL IN THE WATERBERG BASIN

Coal in the Waterberg Basin is generally present as 4 seams of dull coal in the sandy succession of the Vryheid Formation and as numerous seams of bright coal inter-layered with carbonaceous mudstone in the Grootegeluk Formation (Fig. 2.2). Coal seams in the Vryheid Formation vary between 1.5-8 m in thickness, those of the Grootegeluk Formation between millimetres and 2 metres. The Vryheid Formation coals are more enriched in the less reactive macerals but are suitable for steel making using new technology (Dreyer, 1991). The bright coal seams in the Grootegeluk Formation show a fine oscillation of quite clean vitrain with dull bands of clay-rich vitrain. The coal beneficiated from the Grootegeluk Formation is suitable mainly for power stations and as a blend coking-coal.

The Grootegeluk Formation coal-mudstone beds appear to be a chaotic sequence of inter-bedded coal-mudstone layers (Fig. 2.3). The coal-mudstone layers, however, do display some cyclic repetition based on the ratio of the thicknesses of coal to mudstone layers (Siepker, 1986; Botha, 1984). Generally the coal to mudstone ratio decreases upwards within certain zones. The top of each zone is considered to be a mudstone (with relatively little coal) that is overlain by a coal layer of the next zone. Sub-cycles have also been recognised within zones (Siepker, 1986; Botha, 1984). This coal-mudstone relationship has been used

by the GCM geologists who use natural gamma downhole logging for grade control and detailed logging of core for stratigraphic correlations (Dreyer and Roux, 1991).

The Ecca Group coals of the Waterberg Basin were originally divided into zones 1, 2, 3, 4A, 4, 5A, 5B, 5C, 6A, 6B, 6C and 7 numbered from the bottom up (de Jager, 1976). However, the geological staff at the GCM renamed the coal beds into twelve coal zones (Table 2.1). The predominantly dull coal seams 1, 2, 3, 4A and 4 of the Vryheid Formation retained their original numbering by de Jager (1976) as these seams correlate well from borehole to borehole. In the Grootegeluk Formation, with its multitude of intercalated bright coal and mud layers, the zones were numbered 5 to 11 (Table 2.1). For better stratigraphic and grade control the GCM geologists have further divided the zones into units called "samples" (Table 2.1; Fig. 2.3; Appendix I). The sub-divisions of the cycles and sub-cycles have not been formally defined and accepted by S.A.C.S. For convenience the nomenclature and subdivisions applied by the geologists at GCM will be adopted (Table 2.1; Fig. 2.3). It is generally accepted that the four lower coal seams of the Vryheid Formation in the Waterberg Coalfield (Fig. 2.2, Table 2.1) have similar lithological characteristics as the coal seams of the Vryheid Formation in the northern MKB (De Jager, 1976, 1983, 1986; Beukes, 1985, Falcon, 1986; MacRae, 1988; Fig. 2.4). The MKB represents a deltaic progradation into a more stable craton (Cairncross, 1989) and as a result the coal beds in the main basin, in contrast to the Waterberg Basin, are fewer in number but individually thicker and more aerially extensive.

Table 2.1. Divisions of the coal and mudstone layers of the Grootegeluk and Vryheid Formation as defined and used by the GCM (Botha, 1986). The Ecca Group coal and mudstones are broadly divided into "zones" (1-11) but these zones are further subdivided into units called "samples", mainly for stratigraphic correlation and grade control purposes.

STRATIGRAPHIC POSITION	COAL ZONE	GCM "SAMPLE"	PREDOMINANT COAL TYPE
Grootegeluk Formation (± 70 m thick)	11	1A-D	Vitrain (bright coal)
	10	2 to 6	
	9	7 to 9	
	8	10 to 14	
	7	15A to 18	
	6	19 to 21	
	5	22A-E	
Vryheid Formation (± 30 m thick)	4	23	Vitrain and Bituminous (dull coal)
	4A	24	
	3	25 to 29	
	2	30 and 31	
	1	32	

The upper coal seams of the Waterberg Coalfield are generally considered to be within the Upper Ecca Group (Visser, 1953; Haughton, 1969; Beukes, 1985; Siepker, 1986; MacRae, 1988). Falcon (1986), however, on the basis of petrological and palynological information correlates the upper portions of the Waterberg coal-mudstone seams with rocks of middle-Beaufort age in Zimbabwe (Fig. 2.4). Falcon (1986) suggested that coal forming sequences found in isolated inter-montane basins on and between cratons, such as the Waterberg Basin, are younger because sedimentation appears to have continued for a longer period of time than on the edges of the MKB. De Jager (1976, 1986) proposed that no stratigraphic equivalent of the Volksrust Formation in the MKB exists in the Waterberg Basin and therefore assigned the coal-mudstones to the Beaufort Group (Fig. 2.4, column 7). De Jager (1986) suggested that coal beds predominated at different stratigraphic levels in the MKB and the northern Karoo coalfields because very different climatic conditions prevailed during the periods of plant growth in the northern and southern regions of the coalfields of South Africa. In contrast MacRae (1988), on the basis of palynological evidence, tentatively assigns the upper coal zones (biozone E) of the Waterberg to the lowest part of the Kazanian Age, Upper Permian Series (Fig. 2.4). S.A.C.S. (1980) similarly accepts the age of the Upper Ecca to extend to the Kazanian Stages (Anderson, 1977).

2.4 DISCUSSION

It is not the aim of this study to examine the regional stratigraphy of the Waterberg Basin, although it is obvious from the synopsis of existing work that there are significant discrepancies. For example, the Dwyka Formation is considered to be of Carboniferous age by MacRae (1991), contrary to the S.A.C.S. (1980) accepted Asselian/Sakamarian age (Anderson, 1977; Fig. 2.4). The opinion of MacRae (1988) is also at odds with the view of Stapleton (1977) who, also on the basis of palynological evidence, believed that the Carboniferous System is not preserved in Southern Africa. More pertinent to this study are the differences of opinion on the age and(or) to which formation the upper coal-mudstone succession should be assigned (Fig. 2.4). The fact that the top of the Volksrust Formation in the MKB has been assigned to the same stage (Anderson, 1977) as the top of the Grootegeluk Formation (MacRae, 1988), both based on palynological data, would seem to support Beukes (1985) who stratigraphically correlated the Grootegeluk with the Volksrust Formation. De Jager (1973, 1986) and Falcon (1986) do not assign the formations to time stages, which makes chronostratigraphic comparisons difficult. De Jager (1973, 1986), in contrast to other interpretations, prefers to assign the whole coal-mudstone sequence to the Beaufort Formation, whereas Falcon (1986) visualises that the coal-mudstones start in the Upper Ecca (Grootegeluk Formation) and continue up to the lower half of the Beaufort Group. The top of the coal-mudstone sequence appears to be a convenient horizon for the

Ecca-Beaufort Group contact, but it has been suggested by Dreyer (pers. comm., 1992) that the contact may be higher-up in the grey mudstones overlying the coal-mudstone sequence.

It is evident that some work is still required to elucidate the chrono-stratigraphic status of the coal-mudstone sequence in the Waterberg Basin. Sedimentary rocks are commonly assigned to a geological age on the basis of their spore and pollen composition (palynology). However, the poor agreement between results (or conclusions) obtained from Karoo Sequence rocks does not inspire confidence in this technique.

If it is true that the tonstein at the base of the Grootegeluk Formation, described by Spears et al. (1988) in the western part of the basin, was an ash-fall tuff, then it holds very important possibilities for stratigraphic correlation across the basin and into the other coal basins, and also for determining the absolute age of the base of the Grootegeluk Formation from radiogenic isotope analyses.

3. ANALYTICAL CONDITIONS

3.1 X-RAY DIFFRACTION

3.1.1 INSTRUMENTAL CONDITIONS

Samples were prepared for qualitative powder X-ray diffraction (XRD) analysis by the grinding of samples to −300 mesh in a carbon steel mill and then drying overnight at 60°C. A small quantity of the powder was top loaded into an aluminium holder and scanned on a Phillips (PW1130/90) X-ray diffractometer, housed in the Department of Geological Sciences at the University of Cape Town (UCT). The diffractometer was operated at the following settings;

- Cu Kα radiation,
- 45 kV and 40 mA,
- NaI scintillation counter,
- step scan with counting time of 2 seconds and step size of 0.05°2θ,
- pre-slit (fixed) 2 mm,
- scans from 3–15°2θ were made using ½° divergent and receiving slits, then from 15–65°2θ with 1° divergent and receiving slits.

3.1.2 DATA COLLECTION AND MINERAL IDENTIFICATION

Intensity versus 2θ curves were plotted using an in-house program GSCAND, and GRAFIT® (Graphicus, Inc.) software. Minerals were identified from d-spacings and relative peak intensities using the JCPDS PDF-2 DATA BASE RETRIEVAL/DISPLAY SYSTEM (International Centre for Diffraction Data).

3.2 X-RAY FLUORESCENCE SPECTROMETRY

X-ray fluorescence (XRF) spectrometry was used to determine the whole-rock chemical composition of the carbonaceous mudstones. Analyses were determined with a Siemens SRS-303AS and a Phillips PW1400 XRF spectrometer. The operating conditions used were those adopted for routine analysis in the Department of Geological Sciences at UCT and described by Duncan et al. (1984). Intensity data were converted to concentrations with the aid of the Hewlett-Packard 9000 computer system and in-house data-processing programs.

3.2.1 SAMPLE PREPARATION

The samples were crushed and milled to -300 mesh (~50 μm) powders using an agate vessel and a Siebtechnik swingmill. The powders were used to make fusion discs and pressed powder briquettes. Discs were prepared using the Norrish and Hutton (1969) fusion method.

Ashed samples were mixed with lithium tetraborate flux with La as heavy absorber (Johnson Matthey Spectroflux 105) and $NaNO_3$ as oxidant. The flux and sample mixture were fused in 95%Pt-5%Au crucibles and cast into glass discs. Briquettes were made by pressing the powders into 30 mm diameter pellets at 10 tons psi.

3.2.2 H_2O^- AND LOSS ON IGNITION (LOI) DETERMINATION

The loss of adsorbed water (H_2O^-) in the carbonaceous shales was determined from the mass lost by heating the milled samples at 110°C for at least 12 hours. Subsequently, these powders were ashed with the temperature increased stepwise up to 850°C, the further loss in weight being attributed to the loss on ignition (LOI). Stepwise heating (Table 3.1) was applied to minimise the possibility of losing material from the carbonaceous mudstones through the production of smoke.

Table 3.1 Step-wise heating procedure to minimise the loss of material through the production of smoke.

Temperature (°C)	Time (hours)
350	2
400	2
450	2
500	1½
550	1
600	½
850	overnight

3.2.3 MAJOR AND MINOR ELEMENTS

Major and minor element concentrations (SiO_2, TiO_2, Al_2O_3, FeO, MgO, CaO, K_2O and P_2O_5) were determined using the fusion discs. Na_2O was determined separately on the powder briquettes. The intensity data were converted to concentrations using in-house programs NAVAL, SMSAM, MAJOR, and AVERG.

3.2.4 TRACE ELEMENTS

The concentrations of 29 trace elements (S, Sc, V, Cr, Mn, Co, Ni, Cu, Zn, Ge, As, Se, Br, Rb, Sr, Y, Zr, Nb, Mo, Ag, Cs, Ba, La, Ce, Nd, Pb, Bi, Th and U) were determined on pressed powder briquettes. Trace element intensities were corrected for absorption effects, elemental and tube spectral interferences, and background. Enhancement interactions for trace elements in most geological materials are not considered to be significant (Willis, 1989). The physical matrix effects were minimised by grinding the samples as fine as practically possible. The mass absorption coefficients (MACs) for the determination of S, Co, Mn, Cr, V, Ba, Sc and REE (La, Ce, Nd) were calculated from the major element concentrations, using the in-house program HIMAC (MAC tables from Heinrich, 1986). The analyte lines of the remaining trace elements are on the high energy,

short wavelength side of the shortest wavelength major element absorption edge (Fe Kabs). The MACs (calculated at the Mo Kα wavelength) for these trace elements were determined from Rh Kα Compton peak intensities. A single determination of MAC at the Mo Kα wavelength could be used for all the elements whose wavelengths were shorter than the Fe Kabs edge, because there were no major or minor element absorption edges between the RhKαC and Fe Kabs wavelengths. Concentrations were calculated using the in-house program TRACE.

Selected samples were analysed for their Au concentrations by atomic absorption at the Geological Survey of South Africa. Reported lower limits of detection were ~5 ppb Au.

3.2.5 INFINITE THICKNESS

The infinite thickness requirements for the carbonaceous shales were determined by preparing briquettes of different thickness, using a sample with the lowest ash content (40 weight %). A metallic disc containing a high concentration of Sn was placed in turn on top of briquettes containing 6, 8, 10 and 12 g of sample. The samples were scanned over the Sn Kα peak to determine whether they were infinitely thick for that wavelength. It was found that only the disc with 12 g of sample was infinitely thick at the Sn Kα wavelength. On the basis of this experiment all briquettes were therefore made using at least 12 g of sample.

3.2.6 COUNTING ERRORS AND DETECTION LIMITS

As counting errors and the detection limits vary with sample composition, the values for the errors and detection limits should be quoted for each sample. Because only one type of rock (mudstone) was analysed, it suffices to quote in ppm the average counting errors (S_d) and lower limits of detection (LLD; Table 3.2). Presuming that other errors such as sample and equipment errors are insignificant there is a 99% chance that the calculated concentration is within $\pm 3S_d$ of the real concentration of the sample. The equations for the calculations of the LLD and the S_d are given below:

$$LLD = \frac{6}{(cps/ppm)} \times \sqrt{\frac{R_b}{T}} \qquad S_d = \frac{100\sqrt{2}}{\sqrt{T}} \times \sqrt{R_p + R_b}$$

where LLD = lower limit of detection (99 % confidence limit)

S_d = standard deviation of net peak intensity

R_p = gross peak count rate in cps

R_b = total background count rate (background and spectral overlap) in cps

cps = net peak intensity in counts per second (R_p - R_b)

ppm = concentration in parts per million (in % for major elements)

T = total counting time (peak and background)

For major elements the counting error is only a minor portion of the total error. So for the major elements the absolute average difference (AAD), i.e. the mean difference between the accepted standard concentrations and measured standard concentrations, is reported. The results of the LLD, S_d and AAD calculations are given in Table 3.2.

Table 3.2. X-ray fluorescence average absolute differences (AAD) for major elements (%) and average counting errors (S_d) for trace elements (ppm). The lower limits of detection (LLD) for major elements (%) and trace elements (ppm) are quoted at the 99% confidence limits.

Element/ oxide	AAD/S_d	LLD	Element/ oxide	AAD/S_d	LLD	Element/ oxide	AAD/S_d	LLD
SiO_2	0.13	0.03	FeO	0.12	0.015	Na_2O	0.10	0.08
TiO_2	0.02	0.004	MgO	0.15	0.04	K_2O	0.03	0.003
Al_2O_3	0.10	0.017	CaO	0.06	0.008	P_2O_5	0.01	0.011
Mn	0.7	1.8	Co	1.6	2.8	Pb	2.9	4.2
S	6.1	7	Cr	1.2	2.3	As	0.3	0.9
Ba	2.7	5.5	V	2.4	4.3	Se	0.4	0.8
Sc	0.5	1.0	Zn	0.5	1.4	Bi	1.0	3.2
Rb	0.3	1.2	Cu	1.1	1.9	Br	0.3	0.9
Sr	0.2	1.1	Ni	0.8	1.1	La	2.2	3.3
Y	0.3	1.8	Ge	0.5	1.1	Ce	3.3	5.8
Zr	0.9	1.2	W	1.1	2.8	Nd	2.2	3.4
Nb	1.0	1.5	U	2.1	3.4			
Mo	0.2	0.5	Th	2.5	3.9			

3.3 RARE-EARTH ELEMENT ANALYSIS

Twelve of the rare-earth elements (REE) were determined by gradient ion chromatography (Dionex® *4000* i instrument), in the Department of Geological Sciences at UCT. Analyses were done on volatile-free samples, ashed in a furnace according to the procedure described in Table 3.1. Concentrations were not obtained for Ho, due to interference by Y, or for Lu which was not sufficiently well resolved from Yb. The detection limits of REE by gradient ion chromatograph were at the part per billion level, which was well below the expected values of the samples in this study. The analytical conditions routinely used, precision and accuracy are described by le Roex and Watkins (1990).

3.4 STABLE ISOTOPE ANALYSIS

Carbon and oxygen stable isotope values of carbonate minerals were determined in the Department of Geological Sciences, and organic carbon stable isotope values were

determined in the Department of Archaeology, at UCT. Data are reported in the δ notation where:

$$\delta_x = \frac{(R_x - R_{std})}{R_{std}} \times 10^3 \quad ‰$$

R_x = $^{18}O/^{16}O$, $^{13}C/^{12}C$ and R_{std} = corresponding ratio in standard e.g. V-SMOW

3.4.1 C and O STABLE ISOTOPE ANALYSES of CARBONATE MINERALS

The carbonate minerals calcite, ankerite and siderite were analysed for their carbon and oxygen stable isotope values. Whole-rock samples were milled to −300 mesh. Individual minerals which were hand-picked from partially crushed samples while viewed under a binocular microscope, were crushed using an automatic agate mortar and pestle for 1½ hours. Powders were dried at 50°C for at least 48 hours before analysis. Carbon dioxide was extracted at a temperature of 25.2°C from calcite following the method of McCrea (1950). The powdered samples were loaded into glass reaction vessels and 5 ml of 100 % H_3PO_4 were loaded into a separate arm of the reaction vessel. The samples and acid in the reaction vessels were degassed on a vacuum line, then placed in a water bath to equilibrate the sample and acid to the required reaction temperature. The acid was poured onto the sample after equilibration and the vessel left in the bath until the reaction reached completion. The following reaction:

$$3\ CaCO_3 + 2\ H_3(PO_4) \rightarrow 3\ CO_2 + 3\ H_2O + Ca_3(PO_4)_2$$

shows that both water and carbon dioxide are liberated from the carbonate. CO_2 and H_2O will fractionate oxygen isotopes. The H_2O-CO_2 isotope fractionation has been experimentally determined at 25.2°C by McCrea (1950) and it was important to make sure that the reaction did take place at that temperature.

Reaction rates for dolomite and siderite at 25°C are impractically slow. For example, at 25°C only ~30% of dolomite will have reacted with phosphoric acid after 24 hours, and siderite requires about 14 days for complete reaction at 50°C! The other problem that frequently occurs is that all three carbonates coexist in the same sample and cannot be physically separated.

Rosenbaum and Sheppard (1986) reacted carbonates with phosphoric acid at elevated temperatures and empirically determined fractionation equations for siderite, dolomite and ankerite. Al-Aasm et al. (1990) used mixtures of pure carbonates and differential reaction rates of carbonates with phosphoric acid, under variable reaction temperatures (20° to 50°C), to determine the minimum requirements to attain the true $\delta^{18}O$ values for the different carbonate minerals. Based on the results of these two studies, calcite was reacted at 25.2°C,

ankerite at 50°C and siderite at approximately 100°C. For samples that contained more than one carbonate mineral that could not be separated a sequential procedure was followed:

1. Sample and acid were degassed on a vacuum line, and thermally equilibrated in water-bath at 25.2°C.
2. After thermal equilibration the acid was poured onto the sample, allowed to react for 2 hours, and CO_2 captured in a glass tube.
3. The reaction vessel was placed back into the 25°C bath for 24 hours and the resultant gas pumped away under vacuum. The residual calcite-acid reaction would have reached completion.
4. The reaction vessel was placed into a 50°C bath for 4 hours and the CO_2 from the ankerite was captured.
5. The reaction vessel was placed into a liquid paraffin bath at a stable temperature of approximately 90°C for ½ hour and the resultant gas removed under vacuum. The residual dolomite(ankerite)-acid reaction would have reached completion.
6. The reaction vessel was placed back into the bath until the siderite-acid reaction was complete, within about 3-4 hours. The reaction temperature was noted and used in the fractionation equation to calculate the fractionation factor between CO_2 produced and the mineral appropriate to the reaction.

For each CO_2 sample, the reaction vessel was opened and liberated gases frozen in a liquid nitrogen trap and the incondensable gases pumped away. The condensable gases were transferred to a pressure gauge through a liquid nitrogen cooled propanol trap (~ -40°C) to separate and remove the CO_2 from any water or acid contaminants present.

Carbon dioxide samples were analysed on a VG Micromass 602E mass spectrometer and $\delta^{18}O$ and $\delta^{13}C$ were calculated from the mass spectrometer measurements using the relevant $\alpha_{CO2\text{-}mineral}$ factor. The Rosenbaum and Sheppard (1986) oxygen fractionation factor equations for α, between the $\delta^{18}O$ value of the carbonate and that of the acid-extracted CO_2, used in this study are:

$$\textit{Ankerite} : \quad 10^3 \ln\alpha = 6.68 \times 10^5 (1/T^2) + 4.15$$

$$\textit{Siderite} : \quad 10^3 \ln\alpha = 6.84 \times 10^5 (1/T^2) + 3.85$$

T = temperature in Kelvin

Selected samples were done in duplicate and isotope data are reported in the usual δ notation with $\delta^{18}O$-values reported relative to the V-SMOW standard and the $\delta^{13}C$ values reported relative to the Peedee Belemnite (PDB) standard. The differences between duplicate samples were all better than 0.15 ‰. Seven analyses of an in-house standard

(Namaqualand marble) gave an average $\delta^{18}O$ of + 25.37 ± 0.12‰ and $\delta^{13}C$ of + 2.84 ± 0.10‰ (1 standard deviation).

A possible problem of reacting whole-rock carbonaceous mudstones with a 100% H_3PO_4 at elevated temperatures of 90°C, is that some of the organic matter may react and contribute to the carbonate $\delta^{13}C$ value. To test this possibility a sample of pure siderite was selected as an internal standard. The siderite was analysed 5 times and had a mean $\delta^{13}C$ value of −8.26 ± 0.09 (1 std. dev.). Three mixtures of the internal standard siderite and decarbonated coal with siderite:coal proportions of 1:10, 1:30 and 1:50 were analysed for their $\delta^{13}C$ values at a temperature of 110°C. The $\delta^{13}C$ values of the three mixtures were −8.50, −8.36 and −8.40 ‰ respectively, within 3 standard deviations of the mean $\delta^{13}C$ value of the pure siderite. It would therefore appear that carbon from coal does not significantly contaminate the CO_2 produced from the carbonate.

The mineral-H_2O fraction equations that have been used in this study are:

Calcite; $10^3 \ln\alpha = 2.78 (10^6 T^{-2}) - 2.89$ (O'Neil et al., 1969)
Dolomite; $10^3 \ln\alpha = 3.20 (10^6 T^{-2}) - 1.50$ (Northrop and Clayton, 1966)
Siderite; $10^3 \ln\alpha = 3.18 (10^6 T^{-2}) - 5.86$ (Golyshev et al., 1981)

3.4.2 ORGANIC CARBON STABLE ISOTOPE ANALYSES

The $\delta^{13}C$ values of organic material in the carbonaceous mudstones were determined at the Archaeology Department of UCT. The −300 mesh powder samples were digested with excess weak HCl for 48 hours at 50°C to remove carbonate minerals. Thereafter the samples were washed with deionized water, centrifuged, the liquid portion decanted, and the samples freeze-dried for at least 24 hours before analysis. The quantity of sample analysed (10-120 mg) depended on the amount of organic matter in a sample.

The samples, with about 2 g of CuO, were loaded into a quartz tube and evacuated to about 10^{-3} mbars, sealed, and combusted in a furnace at 850°C for twelve hours. Carbon dioxide was extracted on a vacuum-line, incondensable gases pumped away, and H_2O removed by liquid nitrogen-cooled ethanol (about −100°C). The CO_2 was analysed for both $\delta 45$ and $\delta 46$ on the VG Micromass 602E mass spectrometer in the Department of Archaeology and the $\delta^{13}C$ values were calculated from $\delta 45$ values corrected for ^{17}O interference. Selected samples were run in duplicate and gave $\delta^{13}C$ values with absolute differences of less than 0.1‰. The international graphite standard NBS 21 was analysed twice and gave $\delta^{13}C$ values of −28.14 and −28.16‰ versus the recommended value of −28.13‰.

3.5 ORGANIC PETROGRAPHY

The petrographic analyses (maceral and reflectivity) of the coal and carbonaceous mudstone were carried out by ISCOR's Department of Material Research in Pretoria. Samples were set in epoxy resin blocks and polished.

3.5.1 MACERAL ANALYSIS

The polished blocks were analysed at an enlargement of 320X under oil immersion with an optical microscope equipped with a point-counter. The macerals identified were vitrinite, liptinite (sometimes called exinite), reactive semifusinite (RSF) and inertinite.

3.5.2 REFLECTIVITY

The average maximum reflectivity ($\bar{R}_o max$) of vitrinite immersed in oil was obtained by an automated photometric-reflectance microscope at a 500X magnification. The reflectivity measurements were done according to the International Standards Organisation (I.S.O.) specifications.

3.6 EXPERIMENTAL LEACHING OF COAL MINING DISCARD MATERIAL

3.6.1 INTRODUCTION

No national or international controlled leaching method exists to simulate, in the laboratory, the weathering that occurs in a typical exposed coal discard (waste) pile. Leaching tests, however, are commonly used, and even compulsory by law, to predict the environmental effects of disposed waste materials. For example, the currently mandated leaching test in the U.S.A. is the EPA Toxicity leaching procedure (EPA, 1990). Unfortunately this leaching test is unsuitable when applied to coal mining, or coal conversion solid wastes (fly ash and gasification ash) because the procedure was designed for the determination of leaching phenomena in municipal landfills.

Probably the most comprehensive study on coal discards was done in the U.S.A, by the Los Alamos National Laboratory in New Mexico. Over a period of 8 years (1975-1983; Heaton and Wagner, 1983 - final program report) it assessed the nature of, and amounts of trace elements in, drainage from coals and coal preparation wastes. In 1980 there were about 5000 active and abandoned coal refuse dumps in the U.S.A., and about half of these posed some type of health, environmental or safety problem. Much of the research on coal-mine drainage chemistry was conducted a decade ago, but an increased environmental awareness has brought about a renewed interest.

3.6.2 EVALUATION of DIFFERENT ANALYTICAL PROCEDURES

Several leaching methods, including methods used in other disciplines such as agriculture, were considered for this study. Some of the methods were tested in trial experiments on the carbonaceous mudstones to asses their suitability. A brief description and discussion of the methods tested is given below.

1. Toxicity Characteristic Leaching Procedure (TCLP; EPA, 1990). This test is designed to provide information relevant to leaching in a municipal landfill. This test will soon become the official EPA regulatory leaching test, replacing the present EPA toxicity extraction procedure (EPA, 1980). The test uses dilute acetic acid as the leaching solution. A sample to extractant ratio of 20:1 is used with 18 hours of end-over-end agitation. The test calls for the periodic addition of acetic acid to maintain a pH of 5.0.

2. The University of North Dakota Synthetic Groundwater Leaching procedure (SGLP) for coal conversion products (Hassett, 1987). The SGLP method differs from the TCLP (EPA, 1990) mainly in that the leaching solutions are defined as whatever is appropriate to simulate the conditions the waste material is likely to encounter under natural conditions, e.g. a sodium sulphate bicarbonate-buffered solution with the following composition (in mg/l): 436 Na; 388 SO_4; 726 HCO_3; pH=8.3-8.7.

3. Los Alamos National Laboratory Shaker Leaching Procedure for coal refuse material (Heaton et al., 1981). Samples leached were not greater than 9 mm in particle size. De-ionized water was used as an extractant with a sample-to-liquid ratio of 1:5. The flasks were fitted with glass chimneys to allow air access while preventing liquid from splashing out during agitation. The refuse-water mixtures were placed on a platform shaker and agitated for a duration of 1 to 5 days. After leaching samples were removed from the shaker and filtered by vacuum filtration. The Los Alamos Laboratory also used a more cumbersome method called the Column Leaching Procedure (Heaton et al., 1981). This method involved the packing of solid sample into a column and passing deionized water through the sample at a constant rate or irregular rates (simulating different climates) by means of a peristaltic pump. Measurements of leachate flow and pH were made at the column outlet. Samples of leachate were collected periodically for analysis of total dissolved solids and trace element composition.

4. HNO_3 leaching test (proposed and tested in this study). The extractant, HNO_3 (pH=4), was mixed with 1 part sample to 10 parts extractant, agitated for 4 hours and the mixture filtered.

5. Citric acid leaching test for agricultural purposes (Mr G.R. Thompson, Department of Agriculture and Water Supply, Elsenburg; pers. comm.). The extractant, citric acid (pH=2.7), was mixed with 1 part sample to 10 parts extractant, agitated for 4 hours and the mixture filtered.

6. Extraction of heavy metals from soils to establish their availability to plants and the risk of ground water pollution, described by von Prüeß et al. (1991). The extractant is NH_4NO_3 (pH=4.7), 4 parts sample to 10 parts liquid (1:2.5), agitated for 2 hours and leachate filtered.

During the course of evaluating the different leaching methods, it became clear to the author why there is no internationally (or nationally) accepted leaching procedure to establish whether coal discard products pose a threat to the environment. There are a multitude of variables that have to be considered to achieve realistic and meaningful results. Elemental concentrations obtained from different leaching methods may bear little resemblance to naturally occurring leachate concentrations. Some of the variables that have to be taken into consideration when deciding on a suitable leaching method are:

1. Sample particle size;
2. Type of leaching solution and concentration, and whether the pH of the extractant must be monitored and(or) kept constant;
3. The sample-to-liquid ratio or if leaching should be "dynamic" (one pass through sample);
4. Temperature of leaching solution;
5. The type (if any) of agitation (orbital, end-over-end, horizontal);
6. The duration of the extraction procedure, e.g. using water (difficult to reproduce natural conditions and time-scales) and;
7. Whether the sample should be open to air during to extraction.

Before most of these variables can be decided on it is necessary to know which elements will be analysed, the lower limit of detections required and if the analytical facilities are available to meet these requirements.

One of the biggest handicaps of these type of leaching experiments is the significance of the results obtained. Different extractants will result in different concentrations in the leachate and some leaching solutions will be so weak that nearly all trace elements will be

below detection limits for the analytical technique to be used. The concentration of the trace elements in the leachates of the different methods examined are dependent partly on the pH of the leaching solution. The concentrations of elements found in leachates in this study were in the following order: citric acid (method 5) > ammonium nitrate (method 6) > nitric acid (method 5) > sodium sulphate (method 2) ≈ water (methods 1 & 3). The concentrations of elements in the sodium sulphate and water leaching methods were higher for higher sample-to-liquid ratios and increased time.

If the Cd concentration, for example, in the leachate of method X is 100 ppm what exactly does this value mean? How accurately do the tests simulate conditions that will occur in a real waste pile? How hazardous is this sample if rain-water filters through an exposed coal waste dump and into the groundwater? Also different trace elements have different toxicity levels in humans, animals and plants, so concentrations that may be toxic for one may be essential for another.

For the following reasons it was decided that the leaching method of von Prüeß et al. (1991), method 6, was the *most* suitable to predict experimentally the elements that were likely to go into solution during weathering of the mudstones:

1. The method is an established one, has been proposed as a legislatory leaching method in Germany and as an internationally recognised leaching method (von Prüeß, pers. comm., 1993).
2. Concentrations of most elements analysed in the leachates were generally higher than the lower limits of detection for the analytical techniques used in this study.
3. Most other leaching techniques were devised primarily for municipal land-fill wastes, combustion residues or specifically for agricultural purposes.
4. During agitation the pH of the leachate usually stabilizes within the acid range.
5. The procedure is simple and rapid.
6. Von Prüeß et al. (1991) established the highest acceptable elemental concentrations in the NH_4NO_3 leachates that were acceptable for the health of humans, animals, plants and soil organisms. The results of their study therefore makes it possible to quantify the contamination potential of the samples under investigation in this study. The highest acceptable elemental concentrations were based on correlations of elemental concentrations found in the NH_4NO_3 soil-leachates with elemental concentrations found in plants that were grown on the analysed soils. Von Prüeß et al. (1991) also suggested actions to be taken if the concentrations exceed recommended values. The recommendations were made on the basis of different soil usage:
   a) Soils used for the growth of plants used in human consumption.
   b) Soils used for the growth of plants used in animal consumption.
   c) Soils used to grow plants not to be used for consumption.

d) If the risk for the soil-fauna has to be evaluated.

e) If the risk for the ground water has to be evaluated.

Von Prüeß (1992) demonstrated why a molarity of 1M (NH_4NO_3), a leaching solution to solid ratio of 2.5, and an extraction time of 2h is most favourable for the extraction of mobile trace elements. The positive effect of the pH buffer capacity of NH_4NO_3 leaching solution on the mobility of the elements under investigation is discussed in the same publication. The reproducibility of data from 10 different laboratories analysing three soil samples was shown to be acceptable for most elements.

Extraction and analyses of leachable elements from carbonaceous mudstones were carried out at the Analytical Division of MINTEK, in Johannesburg. The leachates were analysed using inductively coupled plasma - optical emission spectrometry (ICP-OES) and ICP - mass spectrometry (ICP-MS).

3.6.3 LEACHING PROCEDURE

Fifty millilitres of 1M NH_4NO_3 (No. 1188, Merck) was added to 20 g of pulverized sample (~ −300 mesh) in 120 ml polyethylene containers. It was decided to use −300 mesh sample because there is no representative sample size on the discard dumps and the grain size of mudstones from the Grootegeluk Formation are less than silt-size. The results from the leachates therefore can be compared to one another and would give maximum leachable concentrations. The mixture was thoroughly agitated on a horizontal moving shaker-table for 2 hours at approximately 20°C. The mixture was then centrifuged (2000 rpm) for 15 minutes and the supernatant filtered (Whatman No.1 qualitative paper). The clear leachate was stabilized by adding 1 ml concentrated HNO_3 (65%) p.a. and stored in 120 ml polyethylene bottles. Five blank samples were also prepared and analysed as samples. The blanks contained the same amount of acid, agitated and filtered in the prescribed way, but without sample added. One blank was analysed approximately every 10 analyses.

The clear leachate from sample 137_0c (done in triplicate) turned yellow and a small amount of black precipitate formed, when the HNO_3 was added. One drop of H_2O_2 was added that cleared the leachate and re-dissolved the precipitate. All the samples were analysed within 7 days after extraction.

3.6.4 ICP-MS INSTRUMENTAL CONDITIONS

The ICP-MS instrument used at MINTEK is a VG-II$^+$ Plasmaquad instrument. A polypropylene V-groove de Galan type nebuliser, manufactured at Mintek, was used together with a Gilson Miniplus 3 peristaltic pump. For quantitative analyses data were acquired in the pulse counting mode, either by scanning or peak jump acquisition. The instrumental parameters are listed in Table 3.3.

Because the ICP-MS at MINTEK is used to analyse a large number of samples and variety of materials, the instrument was specially stripped and thoroughly cleaned before analysis of the samples and blanks in this study, to improve the detection limits and minimise the chances of contamination.

3.6.4.1 Spectral Interference

There are several possible sources of spectral interference e.g. isobaric overlap, high concentrations of oxides and hydroxides, combination ions (e.g. combination of matrix element with argon or nitrogen that are present in the plasma), background interference (ions associated with plasma gas, water and hydrogen - only important for elements up to mass 80) and matrix interference. Matrix interference becomes more severe the heavier the matrix element and the lighter the analyte element. The matrix interference can be compensated for by using the ratio of the element responses to the responses obtained for 3 elements (Sc, In and Re) added as internal standards. The interface cones and ICP torch injection tube all have small orifices through which the ions and sample solution respectively must pass. These orifices become easily blocked and because the ICP-MS is an extremely sensitive technique, the total dissolved solids in sample solutions must be kept below 0.2%. This meant therefore that the leachates had to be diluted 50 times with concentrated HNO_3 (analytically pure), mainly due to the presence of the 1M NH_4NO_3 in the leachate.

Table 3.3 ICP-MS operating conditions.

ICP PLASMA	Argon
FORWARD POWER	1.35 kW
REFLECTED POWER	<10 W
COOLANT GAS FLOW	16 ℓ/min.
AUXILIARY GAS FLOW	0.30 ℓ/min.
CARRIER GAS FLOW	0.80 ℓ/min.
NEBULISER PRESSURE	2 bar
SOLUTION UPTAKE RATE	0.8 mℓ/min.
SAMPLER CONE APERTURE	1 mm
SKIMMER CONE APERTURE	0.7 mm

3.6.4.2 Precision

Precision was checked on a weekly basis and the ICP-MS calibrated on a daily basis. The precision was reported by the chief analyst (Mr. R.V.D. Robért) to be < 2% relative over 10 measurements.

3.6.4.3 Limits of Determination

Limits of determination are greatly influenced by the background signal. The background signals from the leaching agent NH_4NO_3 used in these experiments were relatively high and negatively affected the limits of determination of the various elements. The lower limit of determination (lld; not LLD - lower limit of detection) for elements analysed by ICP-MS were considered to approximate 2 times the sample standard deviation in five blank samples. The lld for the ICP-MS are tabulated below (Table 3.4 and 3.5). In Table 3.5 the recommended maximum llds (DIN V 19730) are compared to the llds achieved in this study. The purpose of the recommended maximum llds is to ensure that elemental concentrations, usually encountered in leachates from uncontaminated soil samples, can be determined with confidence. For most of the elements reported in the DIN V 19730 the llds are lower and therefore acceptable (Table 3.5). The llds of Be and Cd, however, are too high.

3.6.5 ICP-OES INSTRUMENTAL CONDITIONS

The ICP-OES used at the MINTEK is a Spectroflame ICP system. Routine operating conditions are listed in Table 3.6. No interference corrections are required for elements measured at the ppm level. It is considered by the analyst (Mrs G. Russell) that meaningful, reproducible data can only be obtained at approximately ten times the detection limit. The value of ten times the detection limit is referred to as the lower limit of determination (lld). The low end of the calibration range is therefore determined by the lld. The calibration ranges of the elements analysed by ICP-OES are tabulated below (Table 3.4 and 3.7). Sc was used as an internal standard element and is added in equal amounts to all samples. All elemental intensities were ratioed to that of Sc and then the concentrations calculated. Matrix interferences are overcome by running matrix matched standards. All the spectral lines used were free of any significant spectral overlap.

Table 3.4 Table comparing the results of elements in samples that were leached and analysed in duplicate by both ICP-OES and ICP-MS; the lower limit of determination (lld) of elements analysed by ICP-OES and ICP-MS; correlation of values obtained for elements that were analysed by both instruments in the replicate samples and; the analytical results that were considered to be the most reliable and were used in this study.

ELEMENT	ICP-OES Duplication	ICP-OES Calibration Range (lld) (ppm)	ICP-MS Duplication	ICP-MS lld (ppb)	ICP-MS vs. ICP-OES	COMMENT	DATA USED
Al	Good	0.2-50	Poor	39	Poor	-	ICP-OES
Co	Good	0.05-5	Good	6	Fair	ICP-MS more sensitive	ICP-MS
Ni	Good	0.1-5	Poor	20	Poor	Most ICP-MS and -OES values < lld	ICP-OES
Cr	Good	0.02-5	(Poor-Fair)	8	Poor	Most ICP-MS and -OES values < lld	ICP-OES
Cu	Good	0.02-5	Good-Fair	43	Good-Fair	ICP-MS more sensitive	ICP-MS
Zn	Good	0.05-5	Poor	1139	Poor-Fair	-	ICP-OES
V	Good	0.01-5	Good (but spurious high values)	8	Fair	ICP-OES slightly more reliable	ICP-OES

Table 3.5 Comparison of duplicate sample analyses and the lower limit of determination (lld) for elements analysed **only** by ICP-MS.

Element	Duplication	Comments	Lower Limit of Determination (ppb)	Recommended maximum lld (ppb) (DIN V 19730)
As	Good	-	21	50
B	Good	-	111	-
Ba	Good	-	31	-
Be	Fair-Good	-	14	2.5
Bi	?	Most samples < lld	1.5	-
Cd	Fair	-	13	5
Mo	Poor-Fair	-	20	25
Pb	Good	-	18	50
Sb	(Good?)	Most samples < lld but two high values good	3.5	25
Se	Poor	Data unacceptable	115	-
Tl	Fair	-	1.2	12.5
U	Fair-Good	-	1.1	2.5

Table 3.6 ICP-OES operating conditions.

TORCH POWER SETTING	1.2 kW
Ar COOLANT	14 ℓ/min
AUXILIARY GAS	1 ℓ/min
CARRIER GAS FLOW	1 ℓ/min
OBSERVATION HEIGHT	10 mm above the coil

Table 3.7 The quality of data of duplicate analyses and the calibration ranges for elements analysed **only** by ICP-OES. The lowest value of the calibration range is also the lower limit of determination by ICP-OES

ELEMENT	DUPLICATION	CALIBRATION RANGE (ppm)
Ca	Good	0.02-50
Fe	Good to fair	0.02-5
K	Good	0.5-20
Mg	Good	0.01-20
Na	Good	0.5-50
P	Good	0.2-20
S	Good	0.2-25

3.6.6 LEACHATE ANALYSES

The elements *Al, Co, Ni, Cr, Cu, Zn, V,* Na, Mg, P, S, K, Ca, and Fe were analysed by ICP-OES and *Al, Co, Ni, Cr, Cu, Zn, V,* As, Se, Mo, Cd, Sb, Ba, Tl, Pb, Bi, Be, B, and U were analysed by ICP-MS. ICP-MS routinely analyses the above elements at the ppb level, whereas ICP-OES data are usually analysed at the ppm level. The two instruments are capable of analysing some elements better than others because of interference problems, so the elements that were analysed by both instruments (in italics above) were compared to decide which data were more acceptable.

Eight samples were analysed in duplicate, one in triplicate, and the results of the replicate analyses compared to determine the reliability of the data. Samples were given arbitrary numbers so analysts had no prior knowledge of which samples were replicates. Qualitative comparisons of all replicate analyses by both instruments were done by means of X-Y plots, and the findings are reported in Table 3.4. For Ni, Cr and V where most of the values were below or very close to the lld, the ICP-OES data was preferred because values above the lld were reproduced better than the ICP-MS data. The Al data from the replicate

samples analysed by ICP-MS was unacceptable, whereas the ICP-OES data was good and therefore used in this study.

The analyses of replicate samples tests not only the performance of the analytical technique but also examines the reproducibility of the leaching method. Figures 3.1A demonstrates that the reproducibility of the von Prüeß et al. (1991) leaching method is good. A comparison of the absolute values of elements analysed by both instruments, on replicate samples, revealed that the correlation was generally poor to fair. Cu was the only element that had a good to fair correlation of absolute concentration in samples analysed by both instruments (Fig. 3.1B). The results of the replicate analyses are reported in Appendix II (Table II.4).

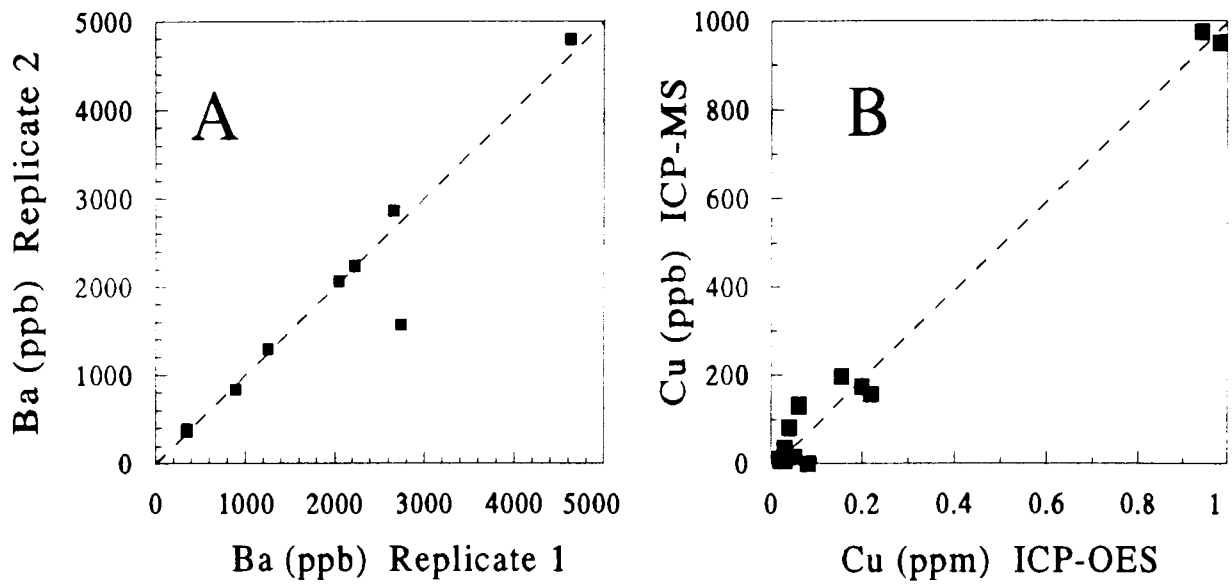

Figure 3.1. **A.** Plot of Ba versus Ba concentrations of replicate leachates using the method of von Prüeß et al. (1991) and analysed by ICP-MS. The results demonstrate that the method can provide reproducible results. **B.** Plot of Cu (ppb) versus Cu (ppm) concentrations of replicate leachates that were analysed by ICP-MS and ICP-OES respectively. The plot confirms that the leaching method does produce reproducible data, provided the analyses are reliable.

3.7 Sm-Nd RADIOGENIC ISOTOPE ANALYSES

Selected mudstone samples were analysed for their Sm-Nd isotopic ratios and concentrations in the FRD/UCT Radiogenic Isotope Facility, Department of Geological Sciences at the University of Cape Town. The sample preparation and analyses were performed by Dr. R.A. Armstrong.

The carbonaceous mudstones were ashed up to 850°C, according to the procedure described in Table 3.1. The ashed samples were dissolved in teflon beakers with double distilled hydrofluoric acid and nitric acid and finally perchloric acid. The solutions were spiked with a mixed Sm-Nd tracer and concentrations determined by isotope dilution. The

REE were separated in bulk using standard cation procedures. Sm and Nd separations were then done on a separate column using HDEHP-coated [Bis (2-ethylhexyl) hydrogen phosphate] teflon powder. The average Nd and Sm blanks were 60 pg and 30 pg respectively.

Isotopic analyses were done on a VG Sector Multicollector Thermal Ionization Mass Spectrometer. Average $^{143}Nd/^{144}Nd$ value for the La Jolla Nd isotope standard (n = 3) was 0.51182 ±1 (1σ). Nd isotope ratios were corrected for fractionation using the constant $^{146}Nd/^{144}Nd$ = 0.7219. Within-run values are quoted at 2 standard errors of the mean $^{143}Nd/^{144}Nd$. Errors of the Sm/Nd concentrations are estimated to be about 1%.

Model Nd_{CHUR} ages were calculated relative to a depleted mantle ($t_{Nd\text{-}DM}$). The $t_{Nd\text{-}DM}$ values were calculated from a 2nd order curve:

$$t_{DM} = AT^2 + BT + C$$

where $A = 1.53077 \times 10^{-23}$, $B = -1.44357 \times 10^{-12}$, $C = 0.513078$

The ^{147}Sm-^{143}Nd decay constant used in the calculations was 6.54×10^{-12}. All isotopic calculations have been performed using the GEODATE package of Eglington and Harmer (1991).

4. MINERALOGY and MINERAL CHEMISTRY

4.1 INTRODUCTION

A substantial portion of the Grootegeluk Formation consists of mudstones which have an organic fraction of less than 50% (Fig. 2.3). The mineral matter that is present in the carbonaceous mudstones of the formation is more than likely also present in the coal portions, except in much smaller concentrations than in the mudstones. Even though the organic portion is the most important part of coal, it is the abundance and composition of the inorganic material that often dictates the specific use of coal. Most uses of coal have specific limits as to the amount and(or) composition of the inorganic component in order for the coal either to be acceptable for the process or to optimize the use of the coal. Detrital minerals in coals, however, are difficult to study because only a very small portion of coal consists of inorganic matter. In the mudstone layers adjacent to coal seams, however, the minerals are more concentrated and are much easier to examine than the dispersed minerals in coal.

Mineral matter within coal is also of petrogenetic importance. The abundance and composition of the early diagenetic mineral components reflect the sedimentological and geochemical history of the early peat- and coal-forming environment. Information on the composition of the detrital minerals concentrated in the mudstones adjacent to coal seams is of great value in understanding the formation and quality of the coal. Increasing concern over the fate of trace elements during mining, processing, conversion and waste disposal has also resulted in greater interest in the types and modes of occurrence of trace minerals within coal and coal-mining waste products.

Three main mineral types have been identified in coal-bearing rocks: detrital, plant derived and authigenic minerals (Renton, 1982; Spears, 1987). It is possible that clay minerals in some coal-bearing rocks can be of vegetal-chemical origin, forming from aluminosilicate materials originally contained within swamp plants (Renton, 1982). Petrographic studies by Finkelman (1981), however, suggest that in coals with ash contents over 5 weight % most of the syngenetic minerals are detrital. The Grootegeluk carbonaceous mudstones considered here generally have an inorganic component in excess of 60% and therefore most of the minerals are considered to have a detrital origin. Although this study focuses mainly on the carbonaceous mudstones there are minerals, such as siderite, that occur more commonly and in major concentrations in the coal seams. Such minerals will also be examined.

The mineral components of the mudstones were identified by X-ray powder diffraction (XRD), and the chemical composition of selected minerals was determined by electron microprobe analysis. Even though argillaceous sedimentary rocks are usually too

fine-grained to resolve all the mineral constituents under an optical microscope, thin-sections of the mudstones were routinely made to obtain additional petrogenetic information.

It is virtually impossible to obtain meaningful information about the size of the minerals in a mudstone at the time of deposition because the minerals may have undergone diagenetic changes, and phyllosilicates, for example, could be deposited as either isolated flakes, books, floccules or rock fragments. Therefore no precise mineral-size analyses of the sediments were attempted.

4.2 RESULTS

XRD patterns of 12 selected mudstones, ordered according to depth in the Grootegeluk Formation, are presented in Figure 4.1. Qualitative results of the XRD analyses are as follows;

1. Kaolinite and quartz are the main mineral constituents in all the mudrocks.
2. Kaolinite crystallinity increases with increasing depth in the formation as manifested by the increased resolution of the 020, $1\bar{1}0$, $11\bar{1}$, $02\bar{1}$ and 021 kaolinite peaks.
3. Siderite is present in almost all samples in major (>1%) to minor (<1%) proportions.
4. Montmorillonite-illite and microcline are present in minor to trace proportions in samples from the upper portions of the Grootegeluk Formation.
5. Pyrite, calcite, ankerite and anatase are present intermittently in minor to trace proportions in the mudstones.

Mineral concentrations have not been obtained from XRD analysis because the mudstones have variable amounts of organic matter that prevent the accurate determination of the mineral concentrations. The organic matter causes a broadening of peaks and an increase in background intensities. A low temperature ashing technique to remove the organic portion of carbon-bearing rocks, with minimal thermal effect upon the inorganic minerals, was not available for this study. Although in this chapter mineral proportions of samples were approximated from thin-section studies, normative mineral proportions were calculated from whole-rock chemical compositions and will be discussed later in Chapter 6.

4.2.1 CLAY MINERALS

4.2.1.1 Kaolinite

XRD diffractograms demonstrated that the principal clay mineral present was kaolinite, and that the crystallinity of the kaolinite increased towards the base of the Grootegeluk Formation (Fig. 4.1). Optical microscope investigations of the carbonaceous mudstones established that the clay minerals are predominantly micro-crystalline kaolinite. However, ~64 m below the topmost coal seam, relatively large kaolinite grains of up to 2 mm in size occur in a 2 m thick zone (Fig. 4.2). The 2 m thick zone starts at "sample"

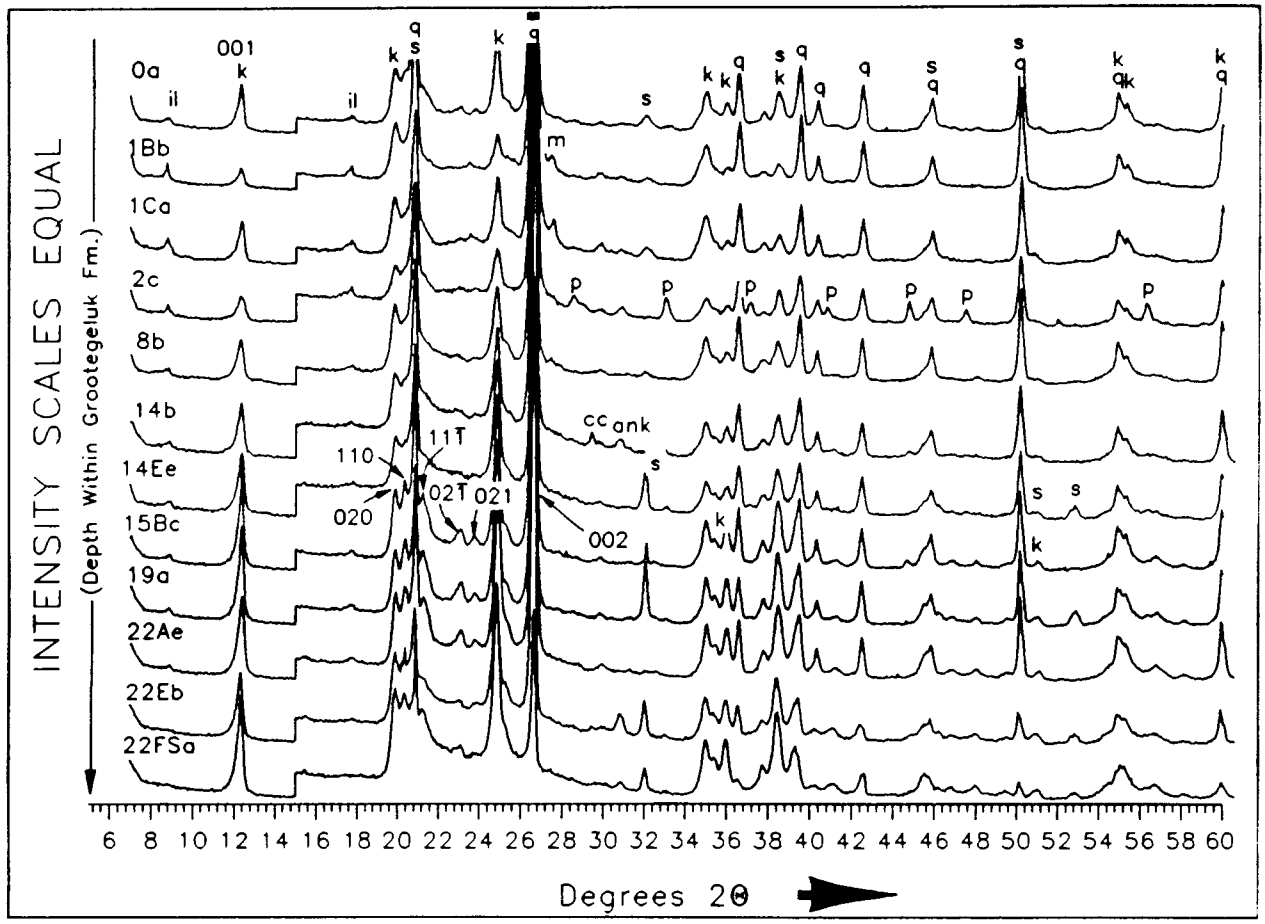

Figure 4.1 Stacked XRD patterns of selected Grootegeluk Formation mudstones representing the whole stratigraphic section. The intensity scale of each sample is the same and samples are ordered according to depth in the formation. Symbol classification: k = kaolinite, q = quartz, il = montmorillonite-illite, s = siderite, cc = calcite, ank = ankerite, p = pyrite and m = microcline. Some of the kaolinite peaks are labelled. Note the change of intensity at 15° 2θ because the secondary slits were changed from ½° to 1°. Samples irradiated with Cu Kα radiation.

22Eb and extends down to "sample" 22FSa in both the boreholes investigated in this study. The kaolinite crystals, which usually show strain, frequently have inclusions of apatite and calcite (Fig 4.3, 4.4). Calcite and apatite were positively identified by electron microprobe analysis. In plane polarized light the kaolinite crystals are colourless, yellowish or brownish due to staining by humic material. The kaolinite grains commonly possess a perfect basal cleavage (001) and are mantled by siderite, calcite, and carbonaceous material (Figs. 4.2, 4.3, 4.4). Simple kaolinite crystals (subhedral to anhedral) predominate but vermicular crystals are also developed (Fig. 4.2). Occasional subhedral prismatic kaolinite crystals exhibit simple twinning.

Macroscopically, the carbonaceous mudstone zone containing the kaolinite grains is not a discrete, well- defined layer. In hand-specimen the carbonaceous mudstones in this zone have conchoidal fractures, high organic contents (average LOI of 42.5 weight % for 12 samples), and grey-to-black sand-sized kaolinite grains. The kaolinite grains are not evenly dispersed within this zone but tend to occur in pockets or clusters of grains within

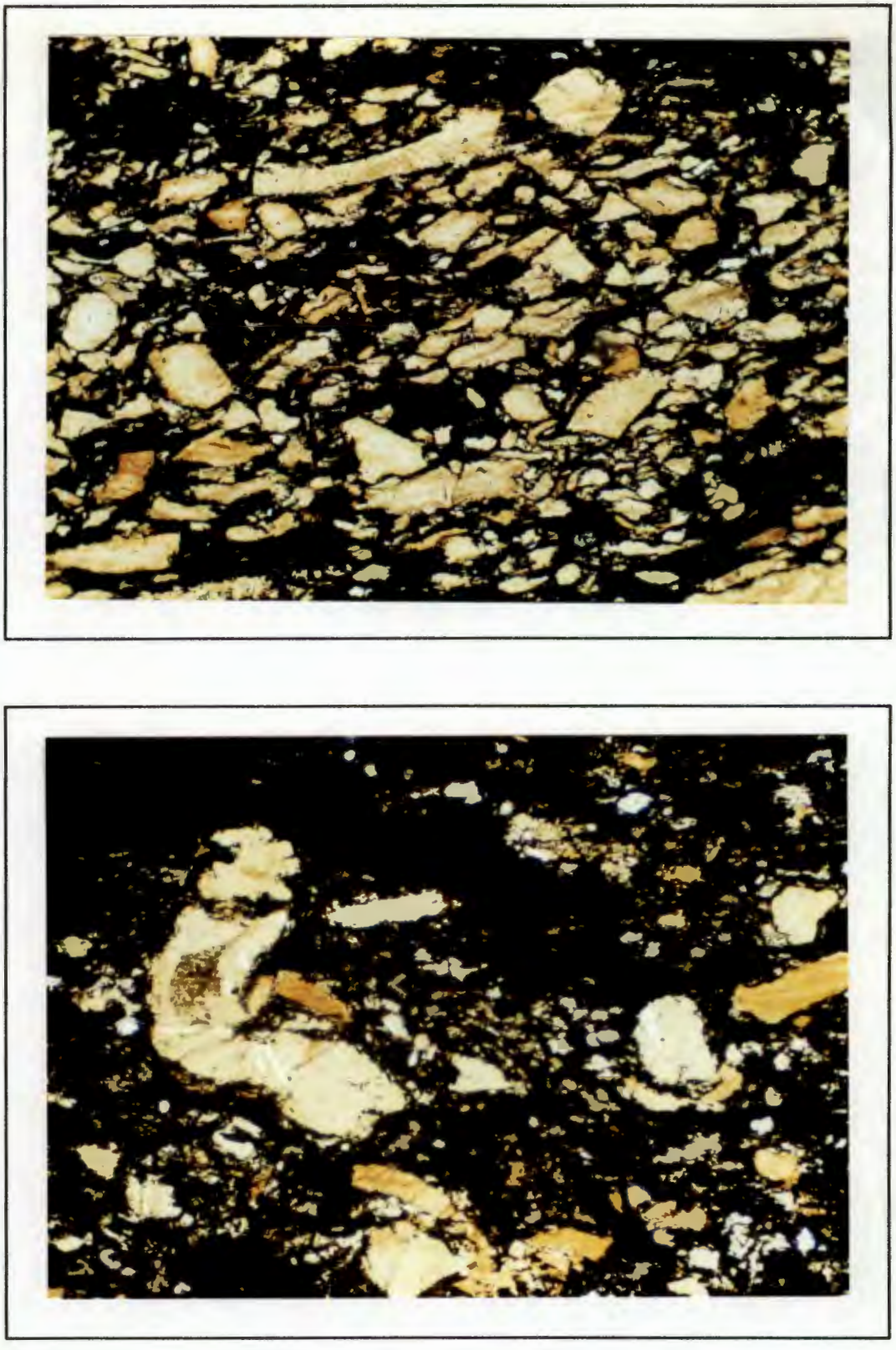

Figure 4.2 Photomicrographs of kaolinite grains which occur in a 2 m thick zone approximately 64 m below the topmost coal seam in the Grootegeluk Formation (sample 136_22Eb). Both photographs have a horizontal field of view of 2.5 mm and nicols parallel. The kaolinite grains can be up to 2 mm in length, commonly exhibit perfect basal cleavage and have a yellow to brown colour due to staining from the abundant organic material (black material in-between the kaolinite grains). The kaolinite crystals are usually subhedral to anhedral but prismatic and vermicular ("worm-like"; bottom photograph) do also occur. Kaolinite is present in the rest of the Grootegeluk Formation but have much smaller grain sizes, usually micro-crystalline. Quartz is a common mineral in the mudstones above the 2 m zone containing the kaolinite crystals, but is not observed in thin-sections of samples from the 2 m thick zone.

Figure 4.3 Photomicrographs of kaolinite grains (A) in sample 136_22Eb. Top photograph - horizontal field of view is 1.5 mm and nicols parallel. Bottom photograph - the horizontal field of view is 1.5 mm and nicols crossed. Kaolinite grains that are present in the 2 m thick zone at the base of the Grootegeluk Formation sometimes have inclusions of calcite (B: high interference colours) and apatite (not shown in photographs) that usually lie parallel to the kaolinite cleavage (see diagram in Fig. 4.4). Fine-grained calcite (high birefringence) is also disseminated in the organic and kaolinite matrix of samples from the base of the Grootegeluk Formation (bottom photograph).

the organic mudstones. This zone is difficult to identify in hand-specimen, and thin-sections of samples are required for positive identification. The best macroscopic characteristic of this zone probably is the conchoidal fracturing of the samples.

Approximate kaolinite modal mineral proportions for the lower and upper parts of the formation are 60-70% and 25-35% respectively.

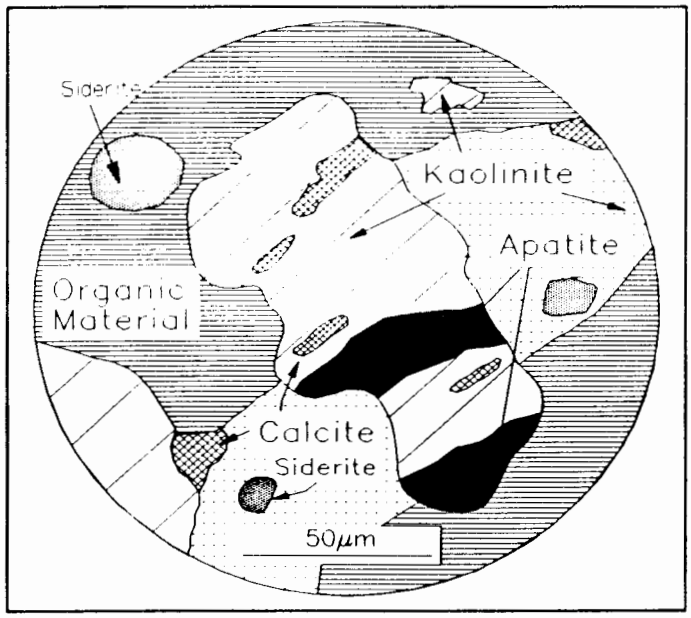

Figure 4.4 A schematic diagram of a kaolinite crystal that contains apatite and calcite inclusions. The calcite and apatite, where present, commonly lie along the kaolinite cleavage. The kaolinite grains occur in an organic and micro-crystalline kaolinite matrix (dotted shading). Other minerals present in the matrix are siderite, fine-grained calcite, and apatite. Spherulitic siderite generally occurs with the organic portion of the carbonaceous mudstones. The kaolinite grains occur in a 2 m thick coal-mudstone zone, ±64 m below the top most coal seam of the Grootegeluk Formation.

4.2.1.2 Montmorillonite-Illite

XRD analyses revealed that montmorillonite-illite is predominantly present in the upper portions of the Grootegeluk Formation (Fig. 4.1; top 10 m). It was not established whether predominantly mixed-layer clays were present or whether mixtures of discrete montmorillonite and illite were present. Thin-section studies confirmed that small flakes (<0.5 mm) of illite, highly birefringent in cross-polarised light, were present in the upper part of the formation. The flakes generally had a preferred orientation parallel to bedding.

Approximate montmorillonite-illite mineral proportions for the upper parts of the formation are 5-10%.

4.2.2 QUARTZ

X-ray diffraction results show that quartz is ubiquitous in the Grootegeluk Formation, but that intensities of quartz peaks, e.g. between 42° and 43° 2θ, for samples 22Eb and 22FSa near the base of the formation are substantially lower than in samples higher up in the formation (Fig. 4.1). No quartz was observed in optical examinations of samples near the base of the Grootegeluk Formation, but in the middle and upper parts of the formation quartz was easily recognisable and very common. The average grain size of quartz increases toward the top of the formation where the grains are on average silt-size. Modal estimates of the quartz in upper parts of the formation are 55-65%.

No samples in this study of the Grootegeluk Formation were seen to consist only of quartz, nor have sandstone units (defined by grain-size or composition), indicative of

channelling associated with overbank deposits, been observed in this formation or anywhere in the Waterberg Basin (de Jager, 1986).

4.2.3 IRON CARBONATES AND IRON SULPHIDES

The main iron-bearing mineral in the Grootegeluk Formation is siderite. Siderite occurs predominantly in the lower-to-middle carbonaceous mudstones of the formation (0-20% modal), but is also present in minor amounts in the upper portions. Two forms of siderite have been identified, spherulitic and granular siderite. Spherulitic siderite appears as roughly spherical nodules (1-5 mm in diameter) made up of acicular, radiating and sometimes concentrically zoned crystals (Fig. 4.5). The spherulitic siderites occur mainly within the coal seams, and to a lesser extent within the carbonaceous mudstone layers. Organic material is usually draped around the siderite spheres (Fig. 4.5). Siderite is also present, although less conspicuous than spherulitic siderite, as finer-grained granular aggregates (<0.5 mm), commonly dispersed within the clay matrix of the less carbonaceous mudstones in the upper Grootegeluk Formation (Fig. 4.6). The chemical composition of siderite, obtained by electron microprobe analysis, was fairly uniform for both spherulitic and granular siderite. The average chemical formula calculated from analyses of 18 siderites is $(Ca_{0.23}\ Mg_{0.10}\ Mn_{0.02}\ Fe_{1.66})\ CO_3$. The optical zonation of the spherulitic siderite was not related to any significant chemical zonation. Pyrite has been observed to mantle siderite in the Grootegeluk Formation (Siepker, 1986; J.C. Dreyer, pers. comm., 1991) but was not seen in any of the samples in this study.

Granular siderite is also present in the massive grey mudstones of the Beaufort Formation that occur above the Grootegeluk Formation.

In the samples analysed by XRD, pyrite is the dominant sulphide mineral. Marcasite (orthorhombic FeS_2) was observed in a few hand-specimen samples as radiating fibrous masses lying along bedding planes. Thin-section and hand-specimen observations established that pyrite occurs mainly as globular aggregates, but also as isolated euhedral crystals dispersed in the coal, as fossil leaf pseudomorphs along bedding planes, and less commonly as fillings in late fractures. The globular pyrite varies in size but can be up to about 10 cm in diameter. Although the globular pyrite is mainly developed in the organic-rich coal seams of the Grootegeluk Formation, high concentrations of pyrite have been observed, both in borehole core and the pit at the GCM, in the grey mudstones of the Beaufort Group just above the topmost coal seam. Thin mudstones and(or) coal layers were seen to pinch-out against or be cross-cut by the globular type of pyrite in the Grootegeluk Formation.

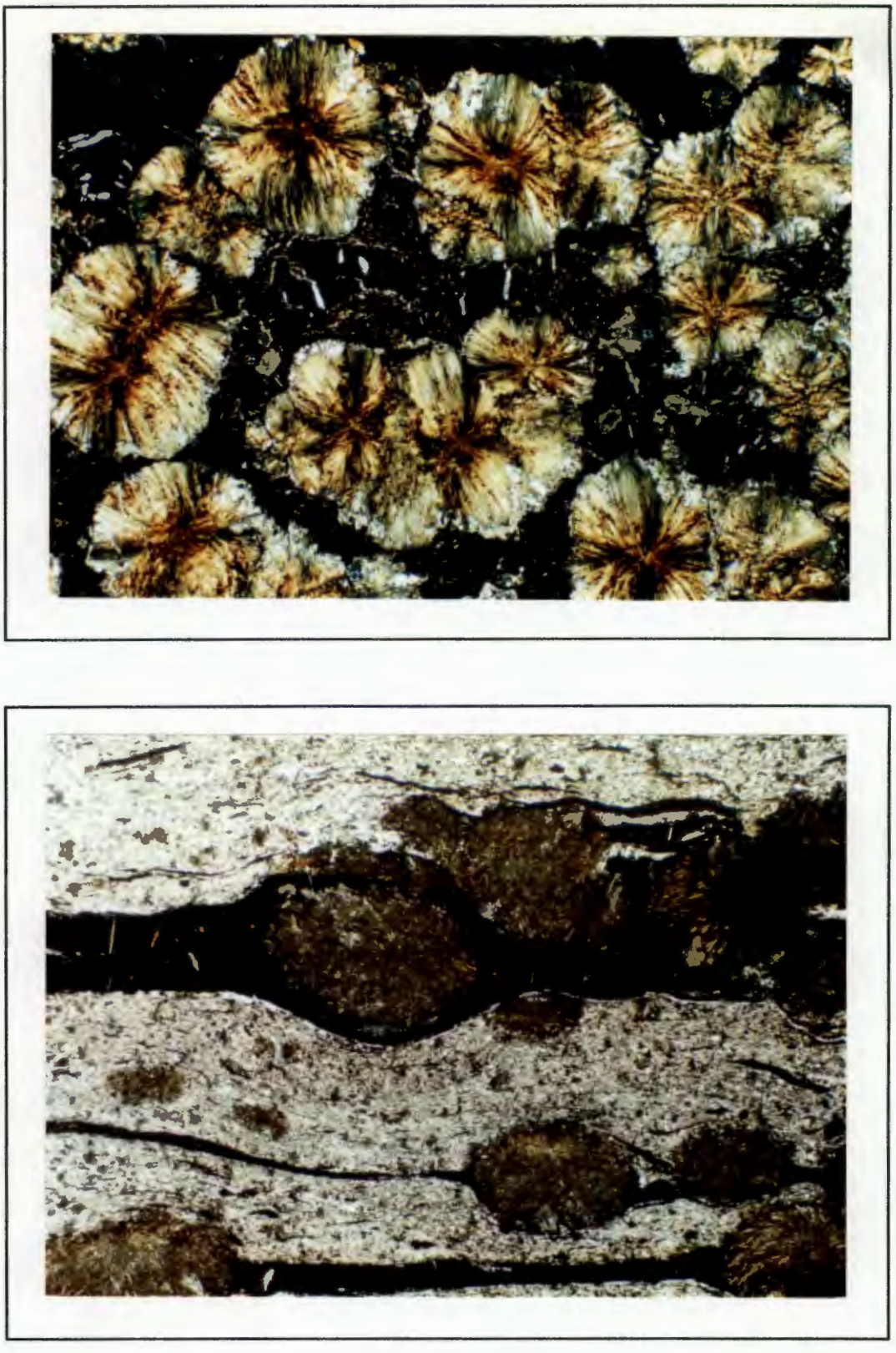

Figure 4.5 Photomicrographs of spherulitic siderite. Top photograph (136_19a) - the horizontal field of view is 6.5 mm and nicols parallel. Bottom photograph (136_14Ee) - the horizontal field of view is 3 mm and the nicols parallel. The spherulitic siderites are spherical to round in shape, sometimes concentrically zoned (optically) and tend to occur within coal seams and organic-rich portions of mudstones. Organic matter usually drapes around the spherulitic siderite.

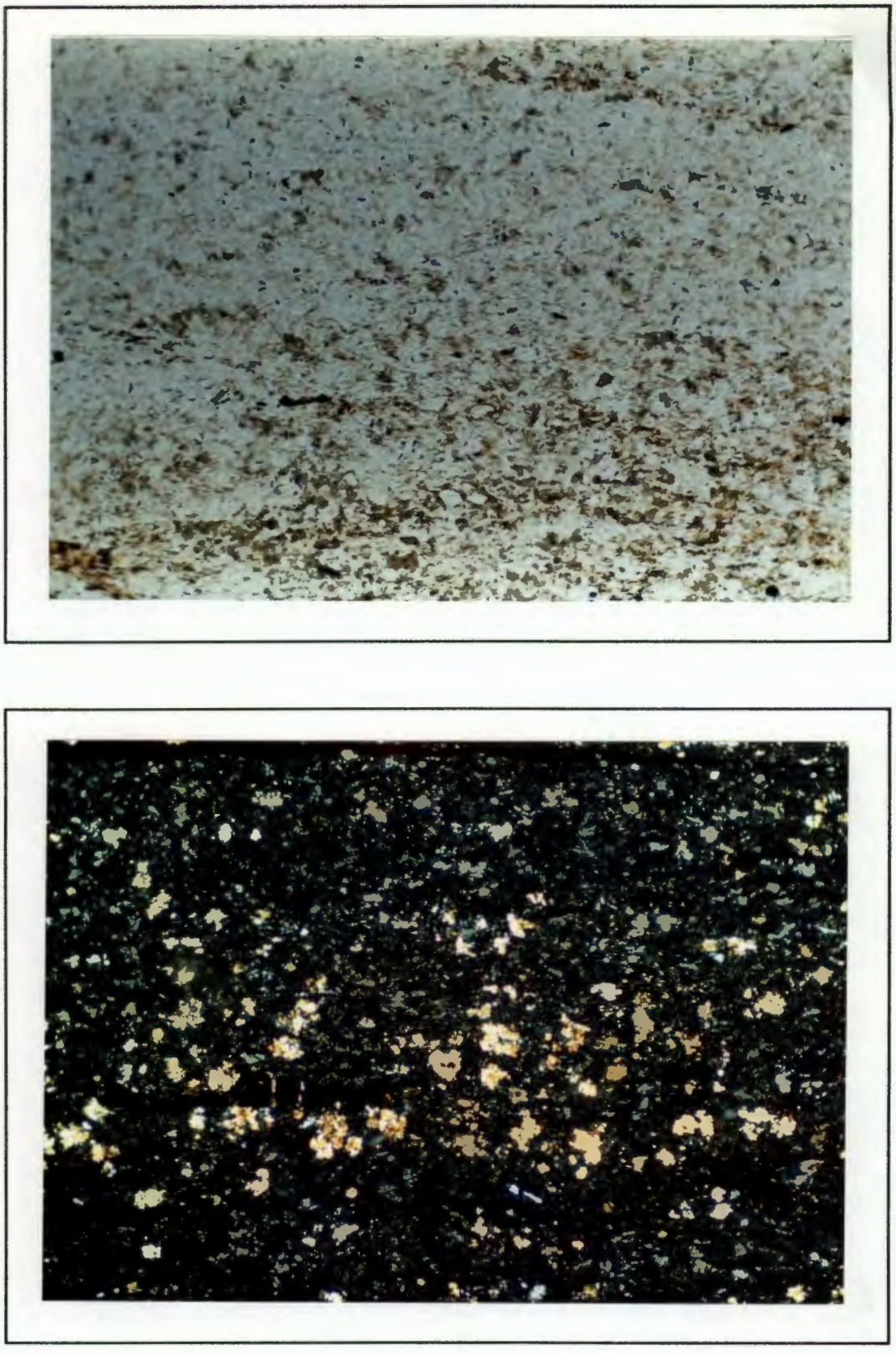

Figure 4.6 Photomicrographs of granulitic siderite (136_1Cc). Top photograph - the horizontal field of view is 3 mm and the nicols parallel. Bottom photograph - the horizontal field of view is 3 mm and the nicols crossed. The granulitic siderites have much smaller grain sizes (<0.5 mm) than the spherulitic siderites. The granulitic siderite occur preferentially within the organic-poor mudstones of the Grootegeluk Formation and the overlying Beaufort Group mudstones. Granulitic siderite is not easily identified in thin-section if nicols are parallel (top photograph) but can easily be distinguished by their high interference colours when the nicols are crossed (bottom photograph).

4.2.4 CALCITE

Four different forms of calcite have been identified in the Grootegeluk Formation:

(1) As lenses of pure calcite, 10-20 cm thick, present in the upper-half of the Grootegeluk Formation. The lenses have variable lateral dimensions but can be up to 50 m in length. Borehole information reveals that the calcite lenses do not occur in any specific horizon nor do they have any systematic distribution, except that they occur in the top half of the formation (Richards T., pers. comm., 1992; Fig. 4.9). In the opencast pit at GCM, the calcite lenses pinch out laterally, and appear to be syn-sedimentary (Fig. 4.7). Thin-section studies of the calcite lenses reveal that they have small-scale horizontal laminations (thin organic matter layers inter-bedded in the calcite), cross-cutting calcite-filled rootlet-like burrows (< 1 mm wide), and cracks filled-in by calcite that cross-cut the primary layering of the calcite lenses (Fig. 4.8).

(2) Calcite is present as inclusions in some of the relatively large kaolinite crystals described above (section 4.2.1.1; Fig. 4.3). The calcite inclusions commonly parallel the cleavage partings of the host.

(3) As a fine-grained mineral, dispersed predominantly in the mudstones at the base of the Grootegeluk Formation zone (Figs. 4.3 and 4.4; section 4.2.1.1). The concentration of the fine-grained calcite in this zone is 1-5 volume % of the mudstones.

(4) As cleat-filling within brittle vitrinitic coal seams. The cleat (joints in coals) surfaces are usually perpendicular to bedding and do not strike in any preferred direction.

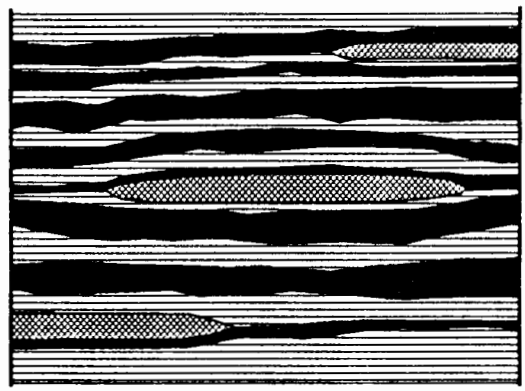

Figure 4.7 The diagram schematically illustrates the calcite lenses that occur sporadically, usually in the upper half of the Grootegeluk Formation. The calcite lenses are represented by cross-hatching, mudstone layers by horizontal lines and coal seams by solid areas. The lenses typically have a lateral extent of 50 m and thicknesses between 10 and 20 cm. Field relationships suggest that the calcite lenses are syn-sedimentary.

4.2.5 TRACE MINERALS

Apatite was not detected by XRD analysis but was observed in thin-section in samples that contained the kaolinite crystals in the zone near the base of the Grootegeluk Formation. Apatite occurs as high relief inclusions within the kaolinite crystals (Fig. 4.4) and was also detected by electron microprobe scanning as very small (~30 μm) anhedral grains within the organic and inorganic matrix of the carbonaceous mudstones. Electron microprobe analyses

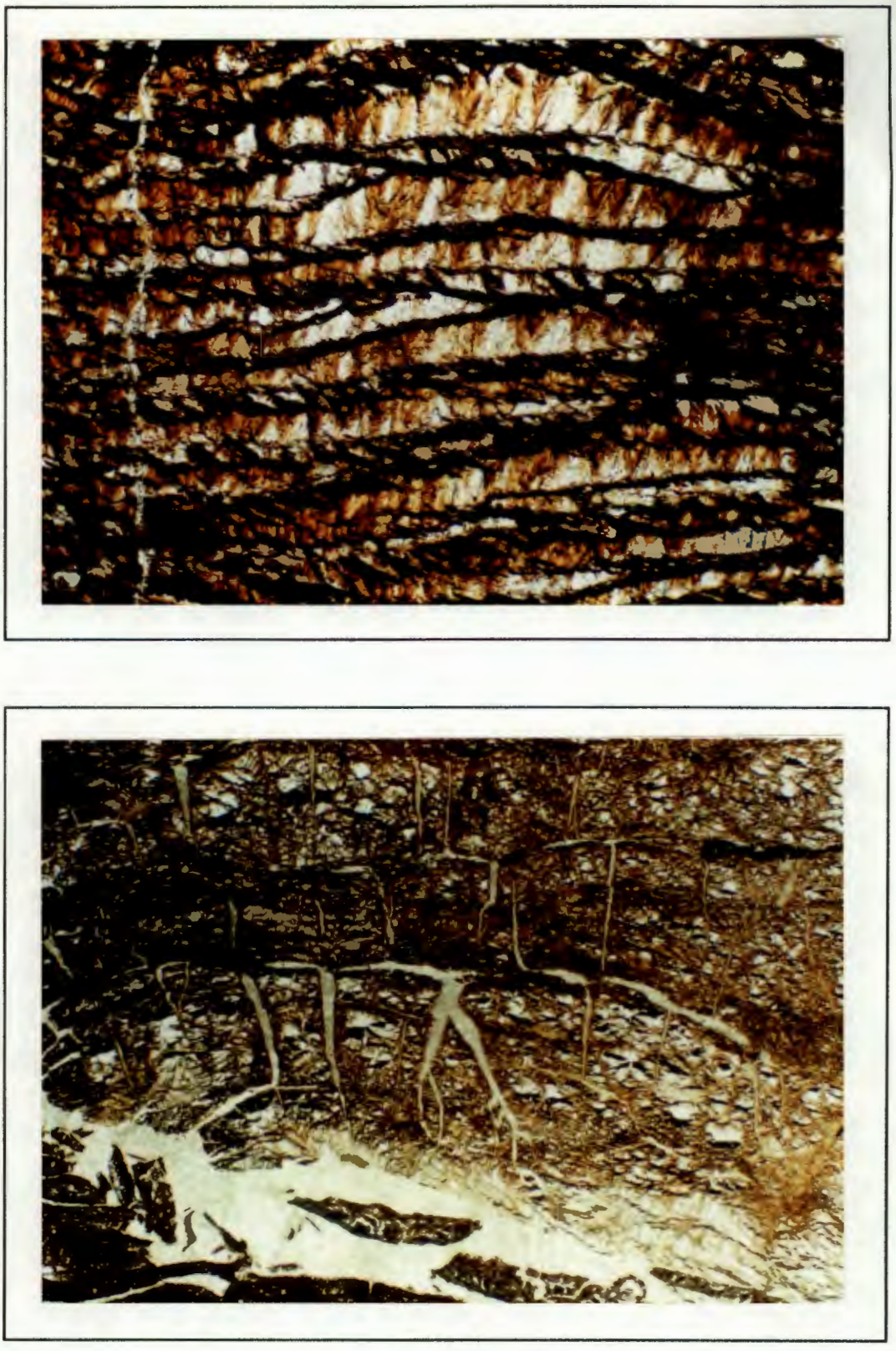

Figure 4.8 Photomicrographs of parts of two syn-sedimentary calcite lenses. Top photograph (hand-specimen from GCM pit, about 10 m below top most coal seam): horizontal field of view 3 mm; nicols parallel. Bottom photograph (137_6b): horizontal field of view 6.5 mm; nicols parallel. The lenses occur randomly in the top half of the Grootegeluk Formation. The lenses consist predominantly of calcite and thin horizontal layers of organic matter (top photograph). Thin (< 1 mm wide) cross-cutting rootlet-like burrows are common (top photograph). Cross-cutting secondary calcite that fill in vertical cracks may be desiccation cracks. Calcite-filled fractures that cross-cut all the different "types" of calcite formed very late, possibly during up-lift (base of bottom photograph).

of the apatites within the kaolinite and those dispersed in the mudstone matrix revealed that they are fluor-apatites (up to 4 % fluorine) and generally have very uniform compositions. The apatites were also analysed for Fe, Mg, Mn, La, Ce, Sr, and Ba but none of these elements were detected. Oxide totals of apatite frequently were about 2% short of a 100% and it is suspected that some OH may be present.

Ankerite, microcline and anatase were only identified by XRD analysis and it was not possible to determine their petrographic relationships. Microcline was only detected in samples from the topmost part of the formation and anatase in samples from the base of the formation (Fig. 4.1).

4.3 DISCUSSION

Figure 4.9 schematically summarises the relative variations of the minerals. A detailed analysis of the normative mineral variations in the mudstones will be performed in Chapter 6, and therefore observed variations in the mineral concentrations will only be discussed here in general terms.

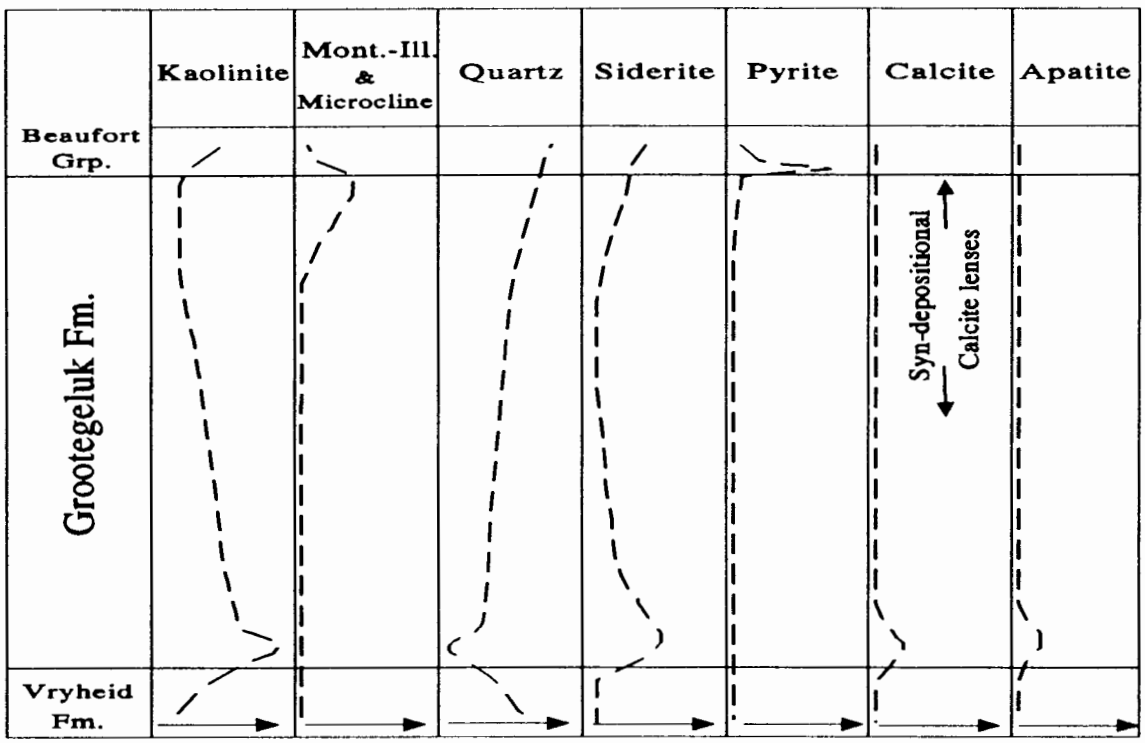

Figure 4.9 Schematic variation of the minerals with respect to depth in the stratigraphy. The plots illustrate the *general* concentration variations (not isolated occurrences) of the minerals in the mudstones based on XRD analyses and petrographic studies. The arrows at the bottom of the plots indicate increasing concentration.

4.3.1 MINERALOGY

4.3.1.1 Clay Minerals

4.3.1.1.1 Clay Mineral Structure and Nomenclature

Clay minerals are hydrous aluminosilicates with a sheet or layered structure and belong to two main groups (Deer et al., 1966; Tucker, 1981).

1) The *kandite group* (general formula $Al_4[Si_4O_{10}](OH)_8$), of which kaolinite is the most important, has a two-layered structure consisting of a silica tetrahedral sheet linked to an aluminium octahedral (gibbsite) sheet by common O(OH) ions. The lattice does not expand with varying water contents and no replacements by iron or magnesium in the gibbsite layer occurs.

2) The *smectite group* (general formula $(0.5Ca,Na)_{0.7}(Al,Mg,Fe)_4[(Si,Al)_8O_{20}](OH)_4.nH_2O$) has a three-layered structure in which an alumina octahedral layer is sandwiched between two layers of silica tetrahedra. Smectites have the ability to absorb water molecules which changes the basal spacing. Hence smectites are often called "expandable clays". Substitution of the Al^{3+} by Fe^{2+}, Mg^{2+} and Zn^{2+} can take place in montmorillonites. A net negative charge resulting from such substitutions is balanced by other cations such as Ca^{2+} and Na^{+}, that are contained in inter-layer positions. Montmorillonite is a common clay in the smectite group.

Illite (general formula $K_{1-1.5}Al_4[Si_{7-6.5}Al_{1-1.5}O_{20}](OH)_4$; only slightly expandable) has a crystal structure very similar to the mica, muscovite. It has a three-layered structure, like the smectites, but Al^{3+} substitution for Si^{4+} in the tetrahedral layers results in a deficit of charge that is balanced by K^{+} ions in inter-layer positions. Some OH^{-}, Fe^{2+} and Mg^{2+} ions also occur in illite. Bailey (1966), in summarizing the nature of illite, said, "sedimentary illite is....a heterogenous mixture of detrital $2M_1$ muscovite, detrital mixed layer micaceous weathering products, detrital weathering products partly reconstituted by K-adsorption or by diagenetic growth of chloritic inter-layers, plus true authigenic 1Md and 1M micas - some having mixed layering also". Illite therefore has a variable and heterogenous nature. Views from different disciplines and the different stages of alteration of illite probably are reasons for a lack of consensus about its nature.

Mixed-layer clays are also common. The structure of this group is the result of ordered or random stacking of basic clay mineral units one upon the other in the c-direction, in particular illite, montmorillonite and chlorite.

Because of their crystal structure, fine crystal size and presence of unsatisfied bonds, clay minerals are important in the process of ion exchange. Ions in aqueous solutions can be adsorbed onto and desorbed from clays, with the water chemistry controlling the exchange process. In general, montmorillonite shows a large ion exchange capacity, kaolinite very slight and illite intermediate capacity.

4.3.1.1.2 Clay Minerals as an Indication of Palaeo-environment

In coals carbonaceous clay bands, which are usually detrital in origin, generally originate from sudden influxes of sediment-laden water into the swamp. Such influxes usually are related to the formation of crevasse splays in a fluviatile environment or widespread flooding (Spears, 1987). The predominance of kaolinite in the clay bands is favoured by acid conditions and low cation activities (Na^+, K^+, Ca^{2+}, Mg^{2+}) and associated with good drainage (Garrels and Christ, 1965; Pettijohn, 1975; Curtis, 1983). Sedimentary environments with higher pH values and total dissolved solids favour the formation of illite (Renton, 1982; Deer at al., 1966). The transition from kaolinite to illitic mudrocks has been well documented and has often been attributed to differential flocculation with increasing salinity (Edzwald and O'Melia, 1975). Coals that have formed in freshwater depositional environments are characteristically kaolinite-rich while illite formation in coals is favoured by alkaline conditions, possibly but not necessarily marine conditions (Renton, 1982).

There is, however, no unanimous agreement that clay minerals are universal palaeo-environmental indicators that permit reconstruction of the environment where they were formed or ultimately deposited. Krauskopf (1967) regarded observational evidence to be ambiguous. He suggested that clay minerals preserve a record of the environment from where they came rather than of the environment in which they were finally deposited. Weaver (1960) considered clay minerals to be inert and to behave as any other detrital mineral, i.e. clay minerals do not correlate with fresh, a brackish, or marine water deposition. A major difficulty, therefore, is that the clay minerals in a sediment may have been inherited from the weathering of a parent rock and transported to the depositional site. Alternatively, the clay minerals may have been formed in place by diagenesis or metamorphism.

Kaolinite-rich clays that sometimes occur immediately below coal seams are called underclays (Pettijohn, 1975). Underclays are considered to be the soil upon which vegetation grew and formed the coal (Pettijohn, 1975). The clay-rich mineralogy of the underclays represent substantial alteration of detrital material by vegetation (Wnuk and Pfefferkorn, 1987).

Kaolinite-rich mudrocks have been noted in coal seams and in the adjacent sediments in many coal deposits around the world (Burger, 1985). Some of these kaolinitic mudrocks which usually have sharp contacts, and a lateral continuity possibly greater than that of the associated sedimentary facies, have been termed tonsteins (Williamson, 1970 for review). It is now generally agreed that many, if not all, tonsteins represent altered volcanic ashes (Triplehorn, 1990). Tonstein is a non-genetic term and the volcanic origin of the kaolinite beds cannot be solely based upon its kaolinite percentage. Tonsteins will be discussed further in Section 4.4 below.

A tentative interpretation of the palaeo-environment of formation of the Grootegeluk Formation mudstones, based on the clay proportions (Fig. 4.9) is that: (1) most of the lower to middle part of the formation, which is dominated by kaolinite, was formed in an acidic environment, and pore-waters had relatively low ionic activity because the basin was relatively well-drained or had high water-to-rock ratios during diagenesis, and (2) in the upper part of the formation, where the proportion of the clay mineral montmorillonite-illite increases, conditions became more alkaline, and pore-water ionic activities were higher because the swamp was poorly drained or water-to-rock ratios were low during diagenesis. The presence of the feldspar, microcline, exclusively within the upper sediments is a manifestation of the less acidic depositional environment proposed for the upper sediments or more rapid (proximal) deposition and therefore less weathered.

4.3.1.1.3 Clay Minerals and Diagenesis

Changes in clay mineralogy with diagenesis of sediments are well documented (Hower, 1981). The changes in clay mineralogy during diagenesis take place principally as a result of the rise in temperature that accompanies burial. Due to the systematic variation in clay mineral composition with depth (i.e. temperature), hydrous layer silicates have been used as palaeo-temperature indicators between 80° and 300°C (McDowell and Elders, 1980). Therefore, studies of clay mineralogy, combined with measurements of the rank of associated coal can give an indication of the temperatures to which the sequence as whole has been subjected.

Kaolinite is generally abundant in the early and middle stages of diagenesis, while usually absent in the last stages (Hower, 1981). However, the stability of kaolinite is dependent on prevailing chemical conditions. For example, it has been demonstrated experimentally that kaolinite in a solution which has a $[K^+]/[H^+]$ ratio equal to 10^6 is transformed to illite at 100°C, whereas at a ratio equal 10^3 a temperature of 200°C is required to achieve the same transformation (Hemely, 1959). If potassium and aluminium are present in interstitial pore water and the temperature is between 90° and 100°C, smectite is converted to illite (Powell et al., 1978). Smectite and mixed-layer clays generally do not survive temperatures in excess of 100°C; illite on the other hand is stable from 25°C to lower greenschist conditions (Powell et al., 1978). The crystallinity of illite has been used by Weaver (1960) as a diagenetic indicator but it is valid only at the late stages of diagenesis or in the early stages of metamorphism.

The ratio of illite to kaolinite in a mudstone would therefore be expected to increase with depth of burial (temperature), assuming no introduction of heat from other sources such as dykes, sills etc. In the Grootegeluk Formation, however, the illite to kaolinite ratio decreases with depth (Fig. 4.9). Because no dykes or sills have been identified in the

Waterberg Basin, the change in clay mineral ratio is considered to have occurred as a result of changing chemical environments, during either erosion of the source rocks or deposition and diagenesis of the sediments, rather than in response to a rise in temperature with increased burial. The presence of the smectite montmorillonite indicates that the Grootegeluk Formation was not subjected to temperatures much greater than 100°C. Palaeo-temperatures of formation can also be obtained from organic matter and mineral stable isotope data, and will be discussed further in subsequent chapters.

4.3.1.2 Quartz

Pettijohn (1975) estimated that the average shale is composed of two parts silt and one part clay. He proposed that the clays were end-products of weathering and the silt (quartz and feldspar), products of abrasion. The composition and proportion of silt is therefore dependent on the relief and climate, and also the mineralogy of the source area. Sediments that have very low quartz contents would represent very low energy depositional conditions and(or) strong chemical weathering of the source area. An increase in quartz implies higher depositional energies and(or) an increase in mechanical weathering in the source area. Detrital quartz is considered to be introduced into peat swamps as overbank deposits of streams, and from wind (Renton, 1982).

In the Grootegeluk Formation the upward increase in the proportion and grain-size, up to silt-size, of quartz implies that the mudstones that are intercalated with the coal were deposited in a higher energy depositional environment than the mudstones lower in the formation (Fig. 4.9). The increase in the quartz size and proportion, and the concomitant presence of microcline in the upper mudstones, indicates possibly that abrasion of rocks and minerals became more important than chemical weathering in the source area, and that *in-situ* alteration of minerals during deposition and diagenesis was less important than in the lower portion of the formation. Changes in the sedimentological and chemical environment should be reflected in the quality of the coal. This idea will be explored further in the next chapter.

No sandstone layers or channels have been observed within the 70 m thick coal-mudstone sequence anywhere in the Waterberg Basin (de Jager, 1986), suggesting an overall very low energy environment for the Grootegeluk Formation. Any sedimentological model for this formation must account for the complete absence of channels and also the remarkable inter-layering of the coal-mudstones formation, in a basin that was originally much bigger than the present fault-bounded basin (Beukes, 1985; Siepker, 1986).

4.3.1.3 Siderite and Pyrite

The stability fields of iron-bearing minerals are very important in establishing chemical conditions during the deposition and burial of sediments. Some of these minerals could form

during early diagenesis and be important palaeo-chemical indicators. The chemical environment of the sediments will change with burial and up-lift, so petrographic evidence is important in establishing the relative timing of formation of the minerals.

The conditions under which siderite is thermodynamically stable are severely restricted and may be summarized according to Berner (1971), Curtis and Spears (1971), and Stumm and Morgan (1981):

(1) a reducing environment is essential both for thermodynamic stability of siderite and for mobilization of sufficient amounts of Fe^{2+} (Eh < 0.0 V at pH 7 Figure 4.10);

(2) low sulphide concentration; at a concentration exceeding 10^{-7} molℓ^{-1} HS^-, any Fe is precipitated as sulphide;

(3) pCO_2 of > 10^{-6} atm.; in natural aquatic environments CO_2 is mostly supplied from distinct sources, e.g. microbial organic matter degradation (Hangari et al., 1980), sulphate and iron reduction (Pye et al., 1990), and volcanic gas (Bahrig, 1988).

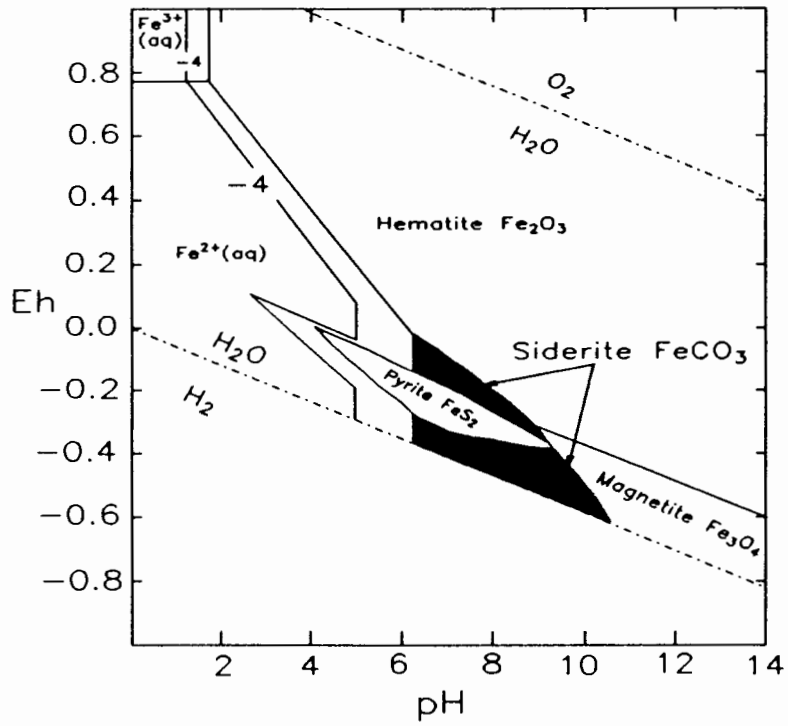

Figure 4.10. Stability relations of Fe-oxides, sulphides and carbonate in water at 25°C and 1 atmosphere pressure. Total dissolved sulphur = 10^{-6} molality (m). Total dissolved carbonate = 10^0 m. After Garrels and Christ (1965).

The restricted physical and chemical conditions for the formation of siderite have been used as an indicator of an anoxic environment lacking substantial sulphate reduction and are not typical for marine sediments (Berner, 1971). In marine settings, the onset of siderite precipitation only occurs once sulphates in the pore water have been reduced, and also wherever the rate of iron reduction exceeds the rate of sulphate reduction, such that insufficient dissolved sulphide is available to precipitate all the available dissolved ferrous iron (Pye et al., 1990).

By comparison, siderite is a relatively common constituent of ancient non-marine sediments where it is normally found in association with coal beds and fresh-water clays (Matsumoto and Iijma, 1981; Curtis and Coleman, 1986). This association is a predictable result of thermodynamic stability (Berner, 1971). Iron is made available by the reduction of ferric iron oxides and hydroxides from clay-bearing soils, while (early) fermentation and (later) thermal decarboxylation of organic matter provided the bicarbonate. Fresh waters are usually low in dissolved sulphate so that the anaerobic bacterial decay of organic matter may enable the attainment of a low Eh and high pCO_2 without the formation of appreciable H_2S. In mixed waters (fresh-brackish-marine), the principal control on the precipitation of siderite and pyrite appears to be sulphate concentrations in the pore water (Curtis and Coleman, 1986). Where the interstitial solutions contain significant concentrations of the sulphate ion, pyrite (and marcasite) form.

The diagenetic iron minerals (and organic matter) record the predominant environments that left their mark on the sediments. This mark of the predominant environment, however, can often erase the record of earlier environments (Berner, 1971). For instance many sediments are deposited in oxic waters but soon become anoxic during burial due to rapid consumption of oxygen in the interstitial waters. Detrital ferric oxides pass rapidly through the post-oxic stage and then undergo reaction with H_2S (formed via bacterial sulphate reduction) to form pyrite, or react with HCO_3^- or CH_4 to form siderite (activity of reduced sulphur low). Therefore the early diagenetic minerals do not necessarily indicate that oxic conditions did not exist in the overlying water during early diagenetic stages (Curtis and Coleman, 1986).

In the Grootegeluk Formation the globular pyrite which is generally restricted to the organic-rich coal seams, was seen to cross-cut thin mudstones and(or) coal seams. This field-relationship indicates that the globular pyrite grew at or near the sediment-water interface. The precipitation of pyrite in the anoxic environment would only have been possible when enough reduced sulphate, from organic matter, was available. Marcasite, which usually forms at low temperatures in sedimentary rocks and was observed only along bedding-planes, could have formed during early diagenesis or up-lift of the sediments where the concentration of dissolved sulphate was high enough to precipitate the iron sulphide. It has been reported that pyrite sometimes mantles siderite in the Grootegeluk Formation (Siepker, 1986; J.C. Dreyer, pers. comm., 1992). This would be as a result of the localized changing chemistry and(or) source of the pore waters during diagenesis. The formation of pyrite and siderite is highly dependent on the rate of supply of a suitable source of sulphur, iron and carbon, as discussed above. The only stratigraphic level where a substantial amount of pyrite is present in the mudstones is at the base of the Beaufort Group just above (about 0.5 m) the topmost coal seam of the Grootegeluk Formation. Although the Beaufort Group mudstones have not been

examined in detail in this study, field evidence from the pit at Grootegeluk suggests that globular pyrite is well developed at this stratigraphic level. In light of the absence of evidence for deposition in a marine environment, it is most likely that the presence of pyrite in these mudstones, now barren of coal, acquired sulphur from the degradation of organic material.

When and(or) where the conditions changed sufficiently, siderite became the stable iron-bearing mineral. The near spherical shapes of the spherulitic siderite imply that the siderite probably grew under little pressure from overburden. Zonation and the sphericity also imply that the spherulitic siderite's chemical constituents were supplied equally to all areas of the minerals. The above features of the siderite, and the fact that organic material is usually draped around the spheres, indicate an early diagenetic growth for the siderite, and a higher compaction of the organic host material (Fig. 4.5). It is envisaged that the spherulitic siderite also formed during very early diagenesis, probably not at the water-sediment interface but at least before advanced compaction. Because of the predominance of early formed siderite and the uniform composition of the siderite, it is proposed that the Grootegeluk Formation sediments were deposited in fresh waters. The amount of siderite precipitated was probably governed by the pCO_2 rather than a supply of reduced iron, because even the organic poor sediments have small amounts of inconspicuous "granular" siderite.

4.3.1.4 Calcite

Calcite is a common mineral in many depositional environments, but those environments interpreted to be marine generally have higher calcite concentrations (Renton, 1982). In the Grootegeluk Formation the calcite occurs predominantly as cleat in-filling in the coal seams. Early ideas on the formation of cleats in coal, and joints in other sedimentary rocks, are reviewed by Price (1966). The explanation advanced by Price (1966) is that with uplift there is a decrease in the lateral stresses at a different rate to the reduced gravitational loading and hence lateral extension fractures form. In addition to the tectonic control, Ting (1977) showed that cleat frequency is not only related to coal type but also rank, reaching a maximum at the low-volatile bituminous stage in studies from peat through to high rank coal. Cleat studies from other coalfields reveal that several mineral phases are present in cleats (sulphides, silicates, and carbonates in that order) and that the depositional sequence forms in response to pore-fluid evolution and movement during burial diagenesis (Spears and Caswell, 1986). Cleat-filling in the Grootegeluk Formation is essentially mono-mineralic. This suggests that cleat formation probably occurred during later stages of the coal formation, most probably during up-lift. The coal beds in the Grootegeluk Formation are not homogenous due to the presence of many mudstone layers in-between the coal seams. This inhomogeneity would probably result in a non-uniform response to the stress field during up-lift, or

subsidence, and therefore result in cleats that have no preferred strike, as is the case in the Grootegeluk Formation.

The syn-sedimentary calcite lenses with calcified root-hair trace-fossils suggest that shallow water-levels occurred sporadically during the deposition of the upper Grootegeluk Formation mudstones. If the vertical cracks, filled-in by secondary calcite, are desiccation cracks, then it suggests that relatively dry periods occurred during the deposition of the upper half of the formation (Fig. 4.8).

The calcite (and apatite) within kaolinite crystals near the base of the Grootegeluk Formation, is quantitatively very small but important in understanding the genesis of the kaolinite crystals. The grain-sizes and shapes of the kaolinite and presence of the minerals within the kaolinite, hampers the interpretation that kaolinite is authigenic and formed from percolating pore-waters during diagenesis (Figs. 4.2 and 4.3). It is more probable that the kaolinite crystals formed from alteration of pre-existing minerals and that the calcite and apatite are alteration remnants, probably of feldspar.

In the mudstones which contain the kaolinite crystals, fine-grained calcite is dispersed within the matrix (Fig. 4.3, 4.4) unlike the mudstones from the rest of the formation. This calcite must have formed much earlier than the cleat-calcite, probably during burial and diagenesis of the sediments.

4.3.1.5 Trace Minerals

Finkelman (1981) demonstrated that, in many cases, the trace-element content of coal can be directly attributed to the occurrence of specific trace minerals, rather than to the incorporation of trace elements within the major and minor components. It is therefore important to account for as many of the trace minerals as possible to facilitate the interpretation of whole-rock chemical compositions.

Apatite is only observed in samples from a 2m thick zone at the base of the Grootegeluk Formation. Apatite is most apparent within the sand-sized kaolinite crystals but was also detected by electron microprobe scanning as very small (~30 μm) anhedral grains within the organic and inorganic matrix of the mudstones. One possible source of phosphorous for the apatite is from the break down of organic material. However, an additional source of P_2O_5 must be evoked because no apatite is associated with any of the other organic-bearing mudstones in the Grootegeluk Formation, and it is also highly unlikely that the phosphorous, from the break-down of organic material, would have crystallised (with Ca) as apatite in the kaolinite crystal structure. It is therefore suggested that the apatite, like calcite, in the kaolinite is an alteration product resulting from the break-down of previous minerals.

4.3.2 TONSTEINS

4.3.2.1 Introduction

Tonsteins are compact argillaceous rocks with sharp contacts, usually thin (1-3 cm), containing the clay mineral kaolinite in a variety of forms, often with considerable lateral extent (hundreds of kilometres), and commonly occurring in coal seams (Williamson, 1970). Coal-bearing sequences that contain tonsteins are of varying ages and geographic location (Burger, 1985; Burger et al., 1990). In spite of the clay content they are characteristically hard and show a conchoidal fracture due to their kaolinitic nature (Spears, 1987).

In the past the occurrence of thin kaolinite-rich beds ("tonsteins") in coal-bearing sequences has led to conflicting views of their origin, but there is now general agreement that most, if not all, tonsteins formed from the alteration of volcanic ash (Price and Duff, 1969; Spears and Duff, 1984; Hill, 1988). Volcanic ashes that were deposited into peat swamps, mostly as distal air-falls from violent eruptions of siliceous material, may serve as useful chronostratigraphic markers on an intercontinental or even global scale (Burger, 1985; Triplehorn 1990). Recent technological improvements in radiometric dating provide great opportunities in using tonsteins as absolute time horizons.

4.3.2.2 The Waterberg Basin Tonstein

Spears et al. (1988) were the first authors to identify a tonstein in a South African coalfield. The tonstein was recorded in borehole-core on the farm Draai Om approximately 35 km west of the farm Grootegeluk in the western part of the Waterberg coalfield (Fig. 2.1). The tonstein is 2 cm thick and occurs 23 m from the top of a coal-mudstone sequence, taken to be the bottom of the Volksrust Shale Formation (Grootegeluk Formation equivalent). The tonstein was interpreted by Spears et al. (1988) to be of volcanic origin based upon XRD analysis, thin-section and geochemical evidence. One of the interesting findings of Spears et al. (1988) was the presence of small amounts of goyazite and gorceixite (Sr and Ba aluminum phosphates) in the tonstein at Draai Om. Aluminum phosphate minerals of the crandallite group ($(Ca,Sr,Ba)Al_3(PO_4)_2(OH)_5H_2O$) are becoming more frequently recognised in tonsteins of volcanic origin (Price and Duff, 1969; Triplehorn and Bohor, 1983; Hill, 1988; Triplehorn, 1990).

If the 2 cm thick tonstein described by Spears et al. (1988) is an altered volcanic tuff, then it probably extends 35 km east to the farm Grootegeluk. To date no similar mudstone at the base of the Grootegeluk Formation has been identified elsewhere in the Waterberg Basin. It is evident that the thickness of the Grootegeluk Formation changes laterally. The base of the formation is ~70 m below the topmost coal seam at the GCM whereas it is 23 m below at Draai Om. The substantial change in thickness of the formation from the western part of the basin to Grootegeluk suggests that conditions of basin formation such as: (1)

basinal subsidence and (2) the rate of organic accumulation, which is a balance between the rate of organic production and destruction (Clymo, 1987), differed considerably in the two regions. These may in part be the reasons why the tonstein is difficult to recognise and has not been recorded elsewhere in the basin. Nevertheless there are some similarities which suggest that the tonstein at Draai Om described by Spears et al. (1988) is related to the 2 m thick organic-rich mudstone at the base of the Grootegeluk Formation in this study.

There are two main reasons why these sediments are stratigraphic equivalents and may have a similar origin. The first point is that the Spears et al. (1988) tonstein and the 2 m zone in this study both occur at the base of the Grootegeluk Formation. The second point is that some of the mineralogical evidence from the sediments in the 2 m zone cannot be reconciled with a normal detrital origin, and a volcanic origin is far more likely source for some of the inorganic material.

If the original sediments at the base of the Grootegeluk Formation were volcanic ashes, deposited and possibly reworked in a rapidly subsiding acidic peat swamp, the minerals and textures of the high temperature volcanic material would not have been preserved after diagenesis in this corrosive chemical environment. The only primary minerals that would have survived the acidic environment within the peat swamp would have been zircon. Volcanic material would be unstable under these conditions and would rapidly alter resulting in the formation of minerals such as kaolinite. The increase in ionic activity in pore-fluids and a change in chemical conditions (Eh, pH) could result in the precipitation of authigenic minerals such as siderite, calcite and apatite.

If the kaolinite grains at the base of the Grootegeluk Formation had an authigenic origin then the kaolinite would be micro-crystalline, filling open spaces such plant-cells, not be vermicular and not occur as sand-sized grains with calcite and apatite in its structure. If the calcite and apatite inclusions in the kaolinite grains were enclosed by authigenic kaolinite, then one would expect that detrital and other early diagenetic minerals, e.g. kaolinite, quartz and siderite, and organic matter would also have been enclosed. However, no other inclusions in the kaolinite grains were observed.

The fact that quartz was identified only by XRD, in significantly reduced proportions compared to the other samples, and was not observed in thin-sections of samples from this zone, suggests an authigenic, not detrital, source for the quartz. The silica may have been derived from the break-down of the unstable high temperature volcanic silicate minerals, e.g. tridymite, and glass. Spears et al. (1988) reported the presence of some of the crandallite group minerals in the tonstein at Draai Om: none of these minerals were identified in thin-section, XRD or electron microprobe scanning in the Grootegeluk mudstones. However, the reason for the presence of the crandallite group of minerals in some tonsteins is still not

understood (Triplehorn, 1990), so it may be that chemical and(or) thermodynamic conditions were not suitable for their formation in the carbonaceous mudstones at Grootegeluk.

The major difference between the Draai Om tonstein and the sediments in question at Grootegeluk, is that the latter has about 40% (by weight) more organic matter and is much thicker than the 2 cm thick tonstein at Draai Om (Fig. 4.11). Although high organic production and low degradation rates at Grootegeluk would account for a major portion of the difference in thicknesses at the two localities, an additional 40 wt.% organic matter to a 2 cm tonstein, which has no organic matter, does not result in a 2 m thick tonstein. Tonstein that have formed from volcanic ash are usually thin, having formed over a relatively short time-span. It may be that volcanic ash, possibly in addition to detrital kaolinite that was being deposited in a low energy environment, was washed into the Grootegeluk part of the basin over a period of time. In addition the volcanic material may have been reworked after deposition in the swamp because it is plausible that organic material may be transported some distance, with only a negligible introduction of inorganic material, to form allochtonous peats (McCabe, 1991).

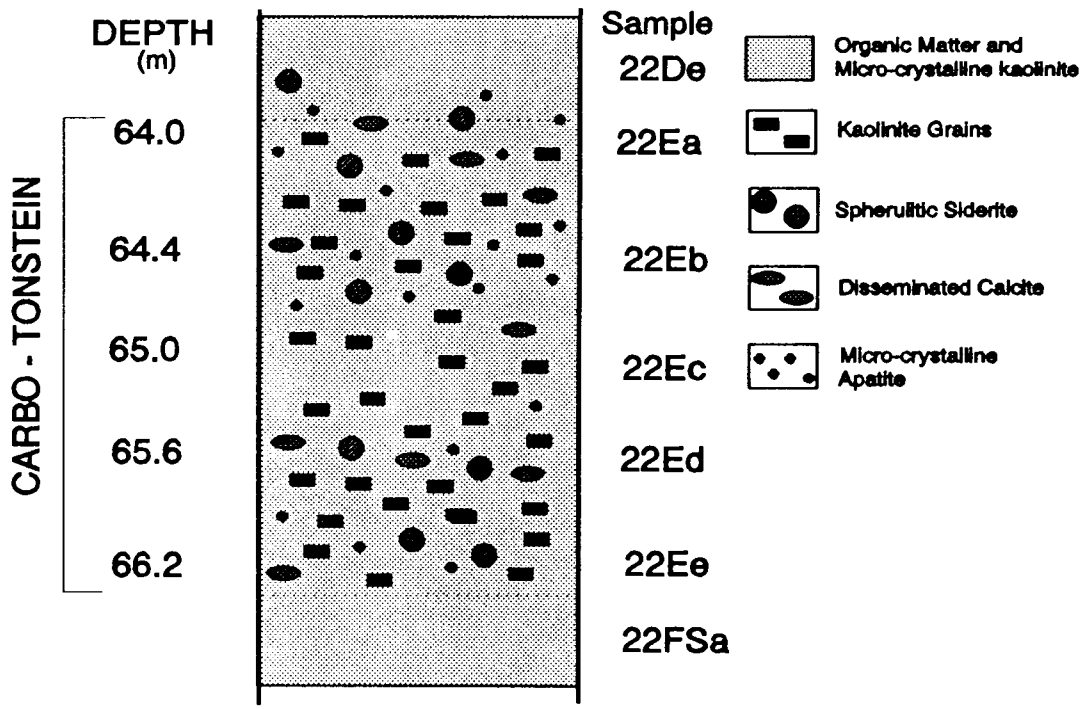

Figure 4.11. A schematic diagram of the mineralogical features of the carbo-tonstein zone (see Figs. 4.2, 4.3 and 4.4). The upper and lower contacts of the carbo-tonstein are not well defined mainly because of the high organic content and the small grain-sizes of the minerals. However, the distinct mineralogical features of the zone are clearly apparent in thin-sections of the carbo-tonstein samples. Kaolinite can have grain-sizes up to 2 mm, shapes that are subhedral to anhedral, sometimes vermicular (worm-like), and have inclusions of apatite and calcite. The kaolinite grains are set in a matrix of organic matter (~40 weight %), micro-crystalline kaolinite (can not see individual crystals in thin-section), siderite and, disseminated calcite and minor apatite. Quartz was not observed in thin-section but minor amounts were identified by XRD.

It is therefore proposed that the 2 m thick zone of carbonaceous mudstone, approximately 64 m below the topmost coal seam, is the lateral extension of the tonstein described by Spears et al. (1988) on the farm Draai Om, and that most of the minerals in the 2 m thick zone at Grootegeluk originated from volcanic derived material. The upper and lower contacts of the tonstein zone are not macroscopically well defined, but thin-section studies reveal the distinctive nature of the mudstones (Fig. 4.11). According to the Williamson (1970) descriptive classification of tonstein types, the tonstein at Grootegeluk is referred to as a carbo-tonstein. It is suggested that the (carbo-)tonstein at the base of the Grootegeluk Formation be called the Grootegeluk Tonstein.

4.3.3 MINERAL MATTER and COAL UTILISATION

Studies of the minerals that occur in coals are not only of geological interest but are also of economic and environmental importance. If the mode of occurrence and proportion of major and trace elements is known, steps may be taken during mining, coal beneficiation, and waste disposal to remove the minerals that are undesirable or considered harmful, or to concentrate those minerals that are beneficial.

4.3.3.1 Metallurgical

Coals suitable for coking have very low ash contents (< 6 wt.%), low total S (< 1 wt.%), low Cl (causes deterioration of coke-oven walls) and low P (has detrimental effect within the blast furnace). Most phosphate in coal is concentrated in the mineral matter as apatite or a member of the crandallite group (Al-phosphate with variable Ca, Ba and Sr). Particular attention is also now being paid to the content of the alkali metals in the coal. The relative abundance of the clay minerals is an important criteria to consider because minerals such as illite are a major source of potassium.

4.3.3.2 Combustion

The problems encountered in combustion are either technical or environmental. Environmental problems mainly concern the emission of sulphur dioxide. One of the foremost tests of coals to be used for steam-raising is the determining of the calorific value of the coal. Other tests of significance include the investigation of the properties of the coal's ash (mineral matter) at high temperatures. The elements responsible for most combustion problems are the alkali elements, sodium and potassium, and the alkali earths, Ca and Mg, along with Si, Al, Fe, S, Cl and Ti. The ash-fusion temperature of coal ash is most affected by Si, S, Fe and Ca contents of the ash. Increased Si tends to increase ash-fusion temperature and increases in Fe, S and Ca tend to decrease ash-fusion temperature. Ferrous iron oxide depresses ash-fusion temperature more then ferric iron (Renton, 1982). Once fused, the Si and Fe oxide

contents of ash also affect the viscosity of slag (Sage and McIllroy, 1959 in Renton, 1982). In general, as the concentration of silica decreases relative to the iron and the alkaline-earth oxides, and as the ratio of ferric oxide to ferrous oxide in the ash decreases, the viscosity of the slag decreases, i.e. as the (Fe+alkali+alkali-earth oxides/Si+Al+Ti oxides) ratio increases, the viscosity decreases. During the combustion process, the products of the alkali metals (especially Na), iron and sulphur stick to boiler surfaces, and when heated to the molten state, the deposits react with and consume the metal surface (Cain and Nelson, 1961 in Renton, 1982).

Most modern coal-burning equipment requires the coal to be ground to a fine powder (pulverized) before it is fed into the combustion chamber. Coarse particles of hard mineral matter, such as quartz, can cause significant abrasion of grinding surfaces in the pulverising equipment.

4.3.3.3 Storage and Handling

One of the most important problems in handling large quantities of coal is the generation of acid conditions by pyrite oxidation in the mine or washery waters. This leads to corrosion of mining and preparation equipment as well as to pollution control problems when waters are discharged to the environment. Acid run-off may also be developed from exposed stockpiles of coal, or from refuse and overburden materials, which are often more enriched in pyrite than the coal itself.

The clay mineral species can also cause problems. If the coal and the carbonaceous material is rich in "expandable" clays, such as smectites, coal stockpiles and waste dumps are subject to swelling and shrinkage with changes in humidity. The coals with expandable clays crack and disintegrate forming an undesirable excess of fine particles and allowing access of air and water to promote oxidation of pyrite. The swelling clays can also make stockpiles and waste piles subject to slope instability (Taylor and Smith, 1986).

4.3.3.4 Discussion

As has been mentioned, the amount, type, and mode of occurrence of mineral matter in coal seams will determine the beneficiation process required, the ultimate use of the product, and the safe disposal of the waste-product. The mineralogical character of the mudstones is especially important for mining in the Waterberg Coalfield because of the intercalated nature of the coal and mudstone layers. Even though it is not the aim of this study to suggest ways of optimizing mining, beneficiation, and utilization of coal, a brief discussion follows to emphasize the importance of a mineralogical study in coal utilization. The environmental impact of waste products from coal-mining and beneficiation in the Waterberg Basin will be investigated in detail (Chapter 8).

Mineralogical analyses established that apatite is present in the 2 m carbo-tonstein zone at the base of the formation. Because of the presence of the coal seams and the highly carbonaceous mudstones, this part of the formation is a target for mining. It has been mentioned that P has a detrimental effect on furnaces, so the ROM would first have to be beneficiated to obtain a desirable product. If the apatite was solely an alteration mineral within the kaolinite, the beneficiation process would be fairly simple because the kaolinite is relatively coarse and can easily be separated from the lighter organic fraction. But electron microprobe scanning revealed that very small (~30 μm) apatite grains were also distributed within the organic matter. This means that the ROM will have to be ground extremely fine which makes beneficiation of these coal-mudstones a lot more difficult, time consuming and expensive. An alternative use for the carbo-tonstein zone may be more cost effective. For example the high organic and kaolinite content makes the mudstones a very suitable raw material for the production of building bricks, tiles etc.

With regard to grinding and use of coal in the Matimba power station it would be possible to maximise the life of grinding machines and also to deliver a more constant product to the power station if coal from the upper and lower parts of the formation were blended before pulverisation. The upper part of the formation has a high proportion of silt-size quartz and minor montmorillonite-illite, whereas the lower part of the formation is dominated by kaolinite and an increased proportion of spherulitic siderite nodules.

4.4 SUMMARY

The proposed relative timing and sequence of mineral formation is schematically summarised in Figure 4.12.

The predominant minerals in the ~70 m thick Grootegeluk Formation mudstones are kaolinite and quartz. Kaolinite is the dominant mineral from the base to the middle portions of the formation, and quartz dominates in the upper portions. Thin-section studies reveal that approximately 64 m below the topmost coal seam a 2 m thick carbonaceous mudstone zone contains kaolinite grains which can be up to 2 mm in length. This zone is dominated by kaolinite, organic matter (40 wt.%), siderite, disseminated calcite and minor apatite, and although quartz was detected by XRD analysis, no quartz was observed in thin-sections of samples from this zone. The dominance of kaolinite in the middle and lower portions of the formation suggests a very low energy depositional environment, that chemical conditions were predominantly acidic, and that pore-water ionic activities were low as a result of good drainage of the basin or high water-to-rock ratios prevailed during diagenesis. The quartz concentration and grain-size increase upward in the formation indicating a change in the energy of the sedimentary depositional environment, and(or) that physical weathering (abrasion) became more important than chemical weathering in the source area. The clay

mineral montmorillonite-illite is present only in the upper part of the formation suggesting that the depositional environment became more alkaline, pore-water had higher ionic activities because the swamp was less well drained or low water-to-rock conditions prevailed during diagenesis. The exclusive presence of microcline in the upper part of the formation indicates that chemical weathering in the source area and acidic alteration became less important during the deposition of the upper parts of the Grootegeluk Formation. The absence of microcline and montmorillonite-illite in the middle and base of the Grootegeluk Formation, and in the Vryheid Formation and Beaufort Group mudstones, does not exclude the possibility that the detrital material originally deposited in these zones did not contain the K-bearing minerals which were later altered *in situ* to kaolinite, as a result of the acidic conditions.

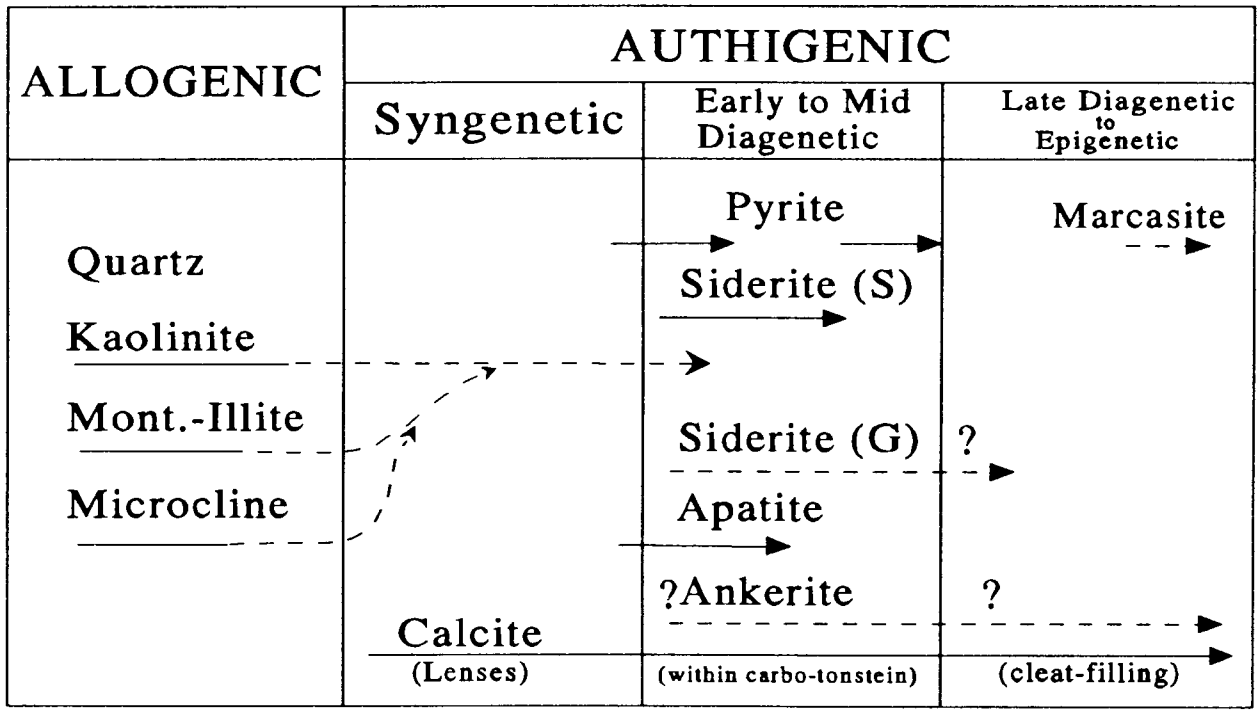

Figure 4.12 The proposed relative timing of mineral formation in the coal and mudstones of the Grootegeluk Formation. Siderite (S) = spherulitic siderite and siderite (G) = granular siderite. The terms used in this table are defined as follows: allogenic minerals - those minerals that have been derived from pre-existing rocks and transported into the basin, i.e. detrital; authigenic minerals - those formed in the rock of which they are a part, during deposition (syngenetic - before burial), and epigenetic minerals - those formed after maximum burial. The dashed arrows indicate that some of the kaolinite may be authigenic as a result of montmorillonite-illite and microcline alteration in acidic conditions.

Iron sulphide occurs predominantly as globular pyrite mainly in the organic-rich coal seams of the Grootegeluk Formation. The field relationship between the globular pyrite, and thin coal and mudstone layers suggest that the pyrite was formed at or near the sediment-water interface and(or) during the early stages of diagenesis. Pyrite that sometimes mantles siderite is considered to have formed much later during diagenesis. Major proportions of

pyrite was observed in the grey massive mudstones of the Beaufort Group, just above the topmost coal seam of the Grootegeluk Formation. The source of reduced sulphur for this pyrite may have been from the degradation of organic matter. The rapid decrease of montmorillonite-illite (and microcline), which is commonly associated with marine sediments, in the Beaufort Group mudstones indicates that the source of the sulphur was not marine. Sedimentological studies of the Beaufort Group mudstones also indicate freshwater deposition for the Beaufort Group mudstones (Beukes, 1985; Siepker, 1986). Marcasite which is a low temperature iron sulphide sometimes occurs along bedding planes and probably formed during uplift.

Siderite occurs as spherulitic siderite predominantly in coal seams, but is also present in the carbonaceous mudstones in the lower to middle parts of the formation. Microscopic granular siderite has been observed in organic-poor mudstones in the middle to upper parts of the formation and also in the overlying grey massive mudstones of the Beaufort Formation. The relative timing of the two types of siderite is difficult to establish because they tend to occur in different parts of the formation and the granular siderite has a very small grain-size. It is proposed that the spherulitic siderite which occurs predominantly in coal seams and organic-rich mudstones most probably formed during the early stages of diagenesis, at least before advanced compaction. Granular siderite occurs preferentially in the organic-poor mudstones could have formed at any stage of diagenesis.

Calcite is present throughout the formation and four types have been identified: (1) syn-sedimentary lenses that occur sporadically in the upper half of the formation, (2) inclusions within sand-sized kaolinite grains in a 2 m thick zone that occurs near the base of the formation, (3) disseminated, fine-grained matrix mineral only in the mudstones of the kaolinite zone at the base of the Grootegeluk Formation, and (4) filling in cleat structures that most probably formed during uplift and erosion of the units overlying the coal-mudstones. Ankerite was detected in a few samples by XRD analysis but was not seen in petrographic studies. It is assumed that the ankerite is authigenic and could have formed at anytime during burial or uplift of the sediments.

Apatite occurs as an inclusion mineral within the kaolinite grains and as small (~30 μm) disseminated grains in the organic and inorganic matrix of the zone containing the kaolinite crystals and calcite in the matrix of the mudstones. It is proposed that apatite formed during early diagenesis from the products of alteration of minerals that were deposited in the basin.

Evidence from minerals that formed during early diagenesis of the mudstones indicate that sedimentation occurred in fresh-water. The absence of sandstone layers or channels in the approximately 70 m thick coal-mudstone sequence in the Waterberg Basin, suggests an overall very low energy environment for the generation of the Grootegeluk Formation. It is

debatable whether the (carbonaceous) mudstones that intercalate the coal seams resulted from sudden influxes of sediment-laden water into a swamp as crevasse splays, in a fluviatile environment. It is proposed that the changes in the organic-inorganic proportions in the mudstones were due to basinal subsidence and, the rate of organic accumulation, which is a balance between the rate of organic production and destruction. The Grootegeluk Formation as a whole is three times thicker at Grootegeluk than at Draai Om, 35 km to the west, indicating that organic production predominated over organic degradation in the south central part of the Waterberg Basin, and that sedimentary conditions differed in the two localities.

The 2 m thick zone that occurs approximately 64 m below the topmost coal seam in the Grootegeluk Formation is interpreted to be a tonstein and is classified as a carbo-tonstein. The tonstein at Grootegeluk is regarded to be the lateral extension of the 2 cm thick tonstein described by Spears et al. (1988) on the farm Draai Om also at the base of the Grootegeluk Formation. The tonstein, however, differs in thickness, appearance and mineralogy at the two locations. At Grootegeluk, in the south-central Waterberg Basin, the tonstein is much thicker and does not have sharp contacts (Fig. 4.11) and, the crandallite group minerals that were identified at Draai Om were not observed at Grootegeluk. These differences in the tonstein can essentially be ascribed to the much higher proportion of organic matter that accumulated in the Grootegeluk tonstein area. It is also possible that volcanic ash material, in addition to detrital kaolinite, may have been washed in and(or) reworked in the (deeper?) Grootegeluk part of the basin over a period of time. It is proposed that the (carbo-)tonstein at the base of the Grootegeluk Formation be called the Grootegeluk Tonstein.

The palaeo-environment of formation of the Grootegeluk Formation will be discussed further in later chapters based on evidence from the organic fraction, whole-rock chemical composition of the mudstones, normative mineral variation, and stable isotope values of carbonate minerals and organic matter.

5. COAL PETROGRAPHY and PETROGENESIS

5.1 INTRODUCTION

Most of the world's coal was formed during three periods: (1) the Carboniferous period primarily in Europe, Russia and America, (2) the Permian period mostly in southern Africa, China, India and Australia and, (3) during the Cretaceous period chiefly in America and Europe. Unlike the hot, humid Carboniferous coal-forming swamps of the northern hemisphere (Laurasia) that developed along extensive lowlands, marginal to actively subsiding large geosynclines, the Permian swamps in the southern hemisphere (Gondwana) existed under cold to cool temperate conditions associated with the waning of an ice age (Falcon, 1986). During coal-forming times Gondwana migrated so that the South Pole shifted from central to southern Africa and then eastward to Antarctica, which at that time lay adjacent to the present east coast of southern Africa (Smith et al., 1981; Anderson and Anderson, 1985). With this eastward movement of the pole, the ice sheet began to melt, so that the ice caps and their surrounding glaciers reduced in size and swamps began to form in and around glacial lakes, in valleys, along riverbanks, on deltas, and in coastal back-swamps. Therefore relatively cold conditions prevailed initially and coals are considered to have originated in mossy tundra-type bog (Plumstead, 1969). The cold-climate floras were replaced in the early Permian by swamp-dwelling gymnosperms, with the subsequent Glossopteris deciduous forests dominating Gondwana through most of the Permian (Hobday, 1987). Several authors are in favour of a predominantly autocthonous (*in situ*) origin for Gondwana coal (Plumstead, 1969; Snyman, 1976; Falcon, 1977), including the Grootegeluk Formation coal (Siepker, 1986).

In contrast to the northern hemisphere coals and the coals from the MKB which occur as relatively thick and discrete seams, coal in the Grootegeluk Formation consists of innumerable coal seams with thicknesses varying from millimetres to meters. The coal seams are intercalated with mudstones that have variable organic contents (Fig. 2.3 and 5.1). The grey-to-black mudstones in the lower portion of the formation are usually more carbonaceous than the grey-to-white mudstones in the upper portions. The coal-mudstone contacts are also sharper in the upper parts of the formation and as a result units are generally more distinct. The coal-mudstone succession has been divided into several cycles based on the coal to mudstone ratio (see Chapter 2). Where the cycles are developed, the base of a cycle has a relatively high coal-seam to mudstone-layer ratio that decreases progressively upwards in the cycle. Within the cycles smaller sub-cycles on all scales have been reported (Beukes, 1985; Siepker, 1986). The divisions of the cycles are, however, subjective which makes correlation of sub-cycles and cycles difficult when comparing bore-hole logs from different sources, e.g. Beukes (1985) has 11 zones, Siepker (1986) has 38 zones, and ISCOR has 8 zones sub-divided into 28 "samples" (sub-zones). Nevertheless, it

is possible to correlate macro-cycles over most of the coalfield (Siepker, 1986; Beukes et al., 1991).

Beukes (1985) proposed that the coal-mudstones of the Grootegeluk Formation were deposited in an overbank swamp environment. He considered that the base of the formation was deposited in the more proximal, highly oxidising, part of the overbank deposit, and that the upper part of the formation was more distal and poorly drained. Siepker (1986) suggested that the basal portion of the Grootegeluk Formation was more proximal to the source of the mudstones, and that the upper portion was more distal, had deeper waters and that conditions were more stable (less subsidence?). Siepker (1986) also suggested that the source of the clastic material in the Grootegeluk Formation could have been sediment-laden glacial waters from retreating glaciers to the north of the Waterberg Basin.

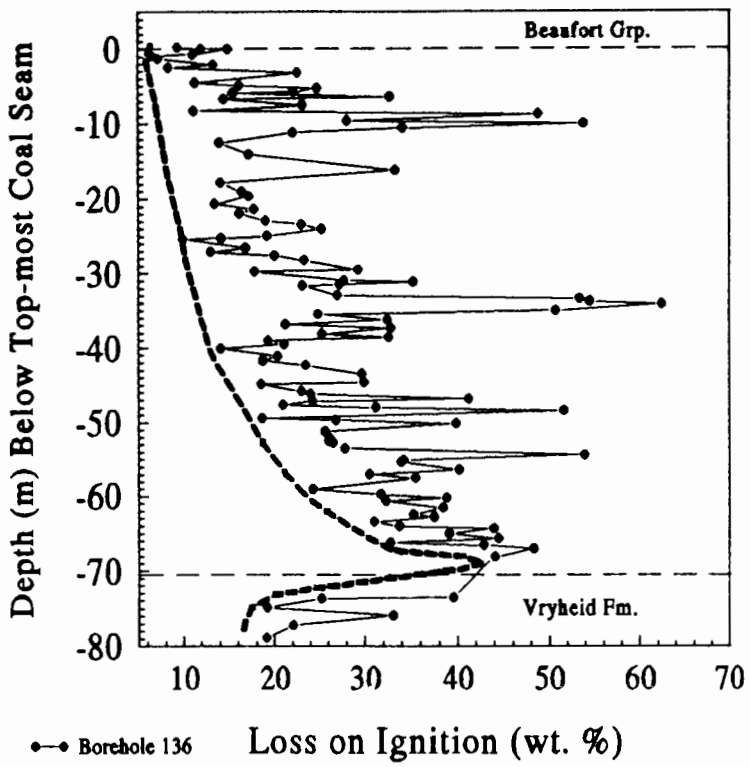

Figure 5.1 This graph demonstrates the variation of mudstone LOI values *vs.* depth in the Grootegeluk Formation. The LOI of the mudstones is a good approximation of the organic content. Although the organic fraction of the mudstones is highly variable, the thick dashed line which envelopes the minimum LOI values, indicates that the amount of organic matter in the lower mudstones of the formation generally is higher than in the upper mudstones. Observation of the Grootegeluk Formation in the pit at the GCM also shows that the coal and mudstone layers are better defined at the top of the formation.

Even though the organic and inorganic material in the Grootegeluk Formation have vastly different origins they were nevertheless deposited in the same physical and chemical environment, and buried to the same depths and temperatures. In many cases, studies of the organic material can be far more informative about the chemical conditions during deposition and later diagenesis. This is mainly as a result of the sensitivity of organic materials to Eh and pH and to changes throughout the entire range of diagenesis up to lower greenschist metamorphic facies (Bustin et al., 1990).

A brief review of coal petrography and coal formation is presented before the data from the organic matter in coal and carbonaceous mudstones of the Grootegeluk Formation are discussed. Evidence from the organic fraction of the coal and the carbonaceous mudstones, and the mineralogy of the inorganic fraction (Chapter 4) are used to interpret

the palaeo-environment of formation and the diagenetic history of the coal and mudstone layers.

5.2 BACKGROUND INFORMATION

5.2.1 COAL PETROGRAPHY

Microscopically coal is composed of a number of discrete organic constituents termed macerals and microlithotypes. Macerals in coals are analogous to minerals in rocks, and range in size from 1 to 50 μm (Falcon and Snyman, 1986). Associations of macerals are called microlithotypes (50 μm - 100 μm across) or lithotypes (at least several millimetres across; Falcon and Snyman, 1986). Microlithotypes may be considered as equivalents to discrete beds or laminae, made up of different mineral combinations, in clastic and non-clastic rocks. Macerals are grouped together into group macerals termed vitrinite, liptinite, and inertinite. Each group includes a series of macerals that can be regarded as belonging together, either because of similar origin (e.g. liptinite - spores, algae; vitrinite and inertinite - woody trunks, leaves, branches etc.) or because of the mode of degradation and preservation (Falcon and Snyman, 1986). A coal's maceral composition is important in determining its utilization. Chemical differences between macerals are important in determining such properties as the calorific value and the coking and liquefaction potential of coals. The physical properties of macerals may also be important in determining such factors as grindability and coking potential.

The changes in carbon and volatile matter content with rank are directly related to the amount of light reflecting from the surface of vitrinite (Hoffman and Jenker, 1932). The higher the carbon content the higher the reflectance and the higher the rank of the coal. For geological studies vitrinite reflectance is normally used as the rank parameter (Teichmüller and Teichmüller, 1975), and conventionally reported as the mean maximum vitrinite reflectivity or $\bar{R}_o$max. In contrast to chemical parameters (e.g. C/H ratio), reflectivity has the advantage that it can be measured not only on coal layers but also on clastic rocks that contain finely dispersed vitrinite. Vitrinite reflectance is a broadly accepted and standardized procedure, is sensitive to minor changes in the level of diagenesis and is applicable throughout the entire range of diagenesis from recent sediments to metamorphic rocks of the lower greenschist facies (Bustin et al., 1990). The $\bar{R}_o$max is influenced only by temperature and time and, therefore, is a better indicator of temperature than are silicate minerals, which are also affected by rock and fluid composition (Pevear et al., 1980). The time factor, however, can be particularly troublesome, because the same $\bar{R}_o$max could be produced by long heating at low temperatures or by short heating at higher temperatures. Castano and Sparks (1974) and Bostick (1979) also provided charts that relate $\bar{R}_o$max to palaeo-temperature. These charts are based on $\bar{R}_o$max and temperature values obtained

from drill-holes where the present temperature was thought to be close to the maximum palaeo-temperature. Pevear et al. (1980) have pointed out that temperatures obtained from these data, however, are minimum palaeo-temperatures.

With increasing levels of organic diagenesis the colour of kerogen observed in transmitted white light changes progressively. Such studies originated with palynologists in the oil industry, who observed changes in the colour of pollen and spores from translucent to greenish yellow, yellow, amber, brown and finally to black and opaque with increasing diagenetic level (Staplin, 1969). Even though the colour changes have been standardised by the use of reference materials, the determinations are subjective. One widely adopted scale based on changes in kerogen colour is the spore colouration index or the thermal alteration index (TAI; Staplin, 1969).

5.2.2 PALAEO-ENVIRONMENT OF PEAT ACCUMULATION AND PRESERVATION

The amount of peat that would ultimately accumulate and be subsequently transformed into coal depends upon the volume of plant debris accumulated and the rate of plant-debris degradation. The degradation of plant debris in peat-forming swamps is largely as a result of oxidation (accumulation temperatures > 25°C, too slow or to fast subsidence, low groundwater table) and bacterial activity. Bacterial activity is controlled by water pH as is the case for sulphate-reducing bacteria. Below pH 4.5 the activity is severely restricted but increases with increasing pH, peaking at pH 7 (Barnes et al., 1990). Conditions most favourable for the preservation of plant material therefore exist below pH 4.5, whereas at elevated pH conditions become increasingly less favourable, i.e. the organic material is dissolved and removed in solution (Renton, 1982; Barnes et al., 1990).

A thin layer of peat could therefore represent a small volume of plant debris accumulation under low pH and Eh conditions, or it could represent a larger volume of plant debris accumulation under neutral to alkaline pH and slightly positive Eh conditions. The former situation results in low-ash coal, whereas the latter results in high-ash coal formation. Acid conditions that favour the preservation of peat would also favour the formation of kaolinite (not carbonates). The presence of a higher ash coal could reflect the development of deep-water conditions (Ward, 1984), a high degree of bacterial degradation due to a pH above 4.5, or sub-aerial ablation or oxygenated waters. In conditions of low ground-water level or elevated topography, high aerobic oxidation of plant matter occurs, resulting in a high degree of fusinitisation and carbon enrichment, and the production of volatile-poor inertinite organic components. Shallow, open-water distal environments, lagoons, ponds, and distal deltaic settings typically accumulate very fine wind- and water-borne organic and inorganic matter, particularly algae, spores, and pollens (liptinite; Teichmüller, 1975).

It is apparent that peat will be preserved only under very specific conditions. The interplay of the different variables, however, hamper straight forward deductions of palaeo-environmental conditions.

5.2.3 PEAT DIAGENESIS

Coal is an organo-clastic sedimentary rock, composed essentially of the fossilised remains of plant debris that have undergone progressive physical and chemical alteration through geological time. Diagenesis of organic matter begins early and proceeds rapidly under surface conditions, compared to clastic material. Some changes take place during sedimentation and are thus pre-diagenetic e.g. oxidation. Diagenesis of organic matter is considered in terms of different stages (*review* Durand, 1980). In this study three stages of organic diagenesis will be considered: eogenesis, catagenesis and metagenesis summarized from Durand (1980), Tissot and Welde (1984), Barnes et al. (1990) unless otherwise referenced (Fig. 5.2). The eogenetic zone of diagenesis represents mainly biochemical reactions, whereas catagenetic and metagenetic reactions are chemical, in response to the temperature change with burial. Boundaries between the different stages are gradational.

5.2.3.1 Eogenesis

Eogenesis refers to those biological, physical, and chemical changes in organic matter that occur at temperatures less than those required for significant cracking (the breaking of C-C bonds) of hydrocarbons. Important processes that take place at this stage are chemical oxidation, aerobic and anaerobic microbial decomposition, bacterial sulphate reduction, reduction of ferric iron, and the production of CO_2 (aerobic processes), and CH_4 and NH_3 (anaerobic processes; Oremland and Kvenvolden, 1981).

The formation of the macerals during the early stages of peat accumulation is dependent on a number of factors including type of plant community, climatic controls, ecological conditions, the acidity (pH) and the redox or Eh value (Falcon and Snyman, 1986). In general, the parent substances and the initial decomposition soon after deposition will determine whether coal or petroleum forms (Teichmüller and Teichmüller, 1975). The precursor of coals are primarily lignin and cellulose from higher order plants, which experience a predominantly biochemical "humification" with restricted oxygen supply during peat formation.

5.2.3.2 Catagenesis

Temperature is the dominant factor controlling coalification reactions. Normally temperature is dependent on the depth of subsidence, the geothermal gradient and the heat conductivity of underlying and accompanying rocks (Teichmüller, 1987). It is now widely

recognised that both temperature and time must be considered in reconstructing the thermal history of strata (Lopatin, 1971 in Bustin et al., 1990). Lopatin (1971 in Bustin et al., 1990) proposed that the level of diagenesis increased exponentially with temperature and linearly with time. Increased pressure has little diagenetic effect on organic matter, other than compaction, and in fact may retard diagenesis (Teichmüller, 1987; Bustin et al., 1990).

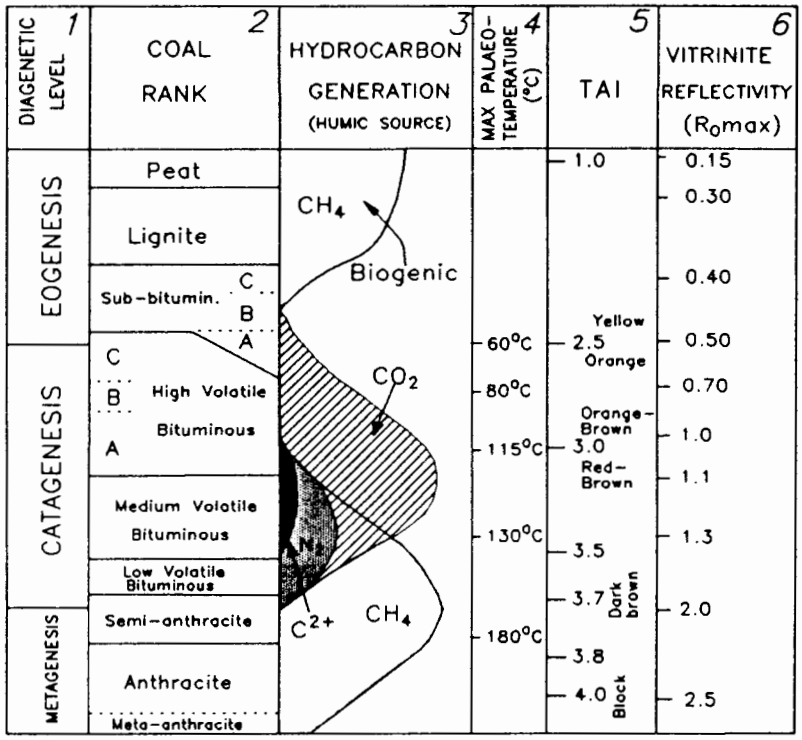

Figure 5.2 Correlation of major organic maturation indices and hydro-carbon generation from a dominantly humic, organic source. References used in columns 1 to 6 are: [1] Tissot and Welde, 1984; [2, 6] Teichmüller and Teichmüller, 1975; [3] Hunt, 1979; [4] Murchinson, 1987; [5] Bustin et al., 1990.)

Kerogen makes up the great bulk of organic matter present at the catagenic stage. Kerogens are commonly characterised by the use of bulk parameters, such as the H/C and O/C atomic ratios, obtained from elemental analyses and expressed as a "van Krevelen plot" (Fig. 5.3). Type 1 kerogens which are typically found in oil shales, have high initial H/C and low O/C ratios and source materials are mainly algae and(or) waxes from higher plants. Type 2 kerogen has intermediate ratios and both algal and higher plant sources appear to contribute to these kerogens (typically marine and lacustrine source organic matter). Type 3 kerogen has an initial low H/C and increased O/C ratios, and is derived dominantly from freshwater plants (predominantly vitrinite macerals). Vitrinite-rich kerogens are mainly gas sources (Powell and Snowdon, 1983). With increased maturation all the kerogen types become more carbon-rich.

Catagenesis takes place at moderate temperatures (60°-150°C) and pressures, corresponding to the zone of bituminous and semi-anthracite coal, oil, wet gas (liquid hydrocarbons) and gas generation, depending generally on the predominant precursor

material (Fig. 5.2). Kerogen from freshwater plant debris (type III) has commonly been considered to be a good source for hydrocarbon gas, compared with types I and II kerogen from marine and lacustrine sediments (Tissot and Welte, 1984). This, however, is not always the case because the Gippsland Basin in Australia contains giant oil fields produced from organic matter (liptinite) of freshwater plant origin (Smyth and Mastalerz, 1991).

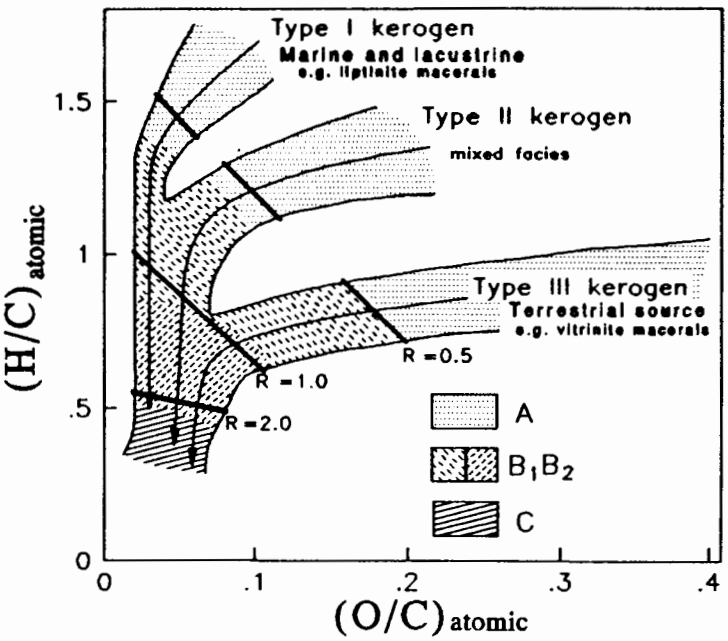

Figure 5.3. A "van Krevelen plot" demonstrating the chemical changes during the diagenetic stages of kerogen types and coal macerals: **A**, immature -- the field of humic acids overlap the region of immature Types I and II kerogen; **B**, mature -- the region between B_1 and B_2 is the region of maximum oil generation; **C**, over-mature; **R** -- iso-evolution as measured by vitrinite reflectance. Adapted from van Krevelen, 1961 and Durand, 1980.

5.2.3.3 Metagenesis

Metagenesis refers to the stage of diagenesis at which crystalline ordering of the organic matter begins (anthracite rank coal; Fig. 5.2). Aromatic nuclei increase in size and result in a cracking of hydrocarbons, generating methane.

5.3 COAL PETROGRAPHY OF THE GROOTEGELUK FORMATION

The maceral composition (normalised to 100%), mineral proportion (volume % of the sample) and mean maximum vitrinite reflectivity ($\bar{R}_o$max) of coal and carbonaceous mudstone samples were determined from borehole core samples of the Grootegeluk Formation by ISCOR (not the same samples as in this study; Chapter 3). The samples were divided into two groups because of the intercalated nature of the sediments. The one group of samples was composed predominantly of coal (Fig. 5.4 A) and the other group of samples consisted mostly of mudstone (Fig. 5.4 B). Both groups were separated into different relative density (RD) fractions and analysed for their maceral and mineral concentrations, and $\bar{R}_o$max. Group macerals, i.e. vitrinite, liptinite (sometimes called exinite), inertinite, and reactive semi-fusinite (RSF) were identified. Reactive semi-fusinite is a term used in the coal industry for macerals in the inertinite group that are partially degraded vitrinite (C.J. Dreyer, pers. comm. 1992). Coal separated at RD 1.40 (low ash) is used as a blend-coking coal and coal separated at RD 1.80 (middlings) is suitable for generation of electricity.

5.3.1 RESULTS

Vitrinite is the dominant maceral group in the Grootegeluk Formation coals and mudstones (Fig. 5.4 A,B; Table 5.1; and Appendix II Table II.1). The vitrinite content in coal and mudstone decreases with depth in the formation, whereas the concentrations of the other macerals, except liptinite, generally increase with depth (Fig. 5.4 A,B). The RSF content in the coal samples and the inertinite content in the mudstone samples increase rapidly in the carbo-tonstein zone at the base of the formation (Fig. 5.4 A,B). Generally the greater the mineral content (higher RD) of the coal and mudstone samples, the lower the vitrinite content and the higher the RSF and inertinite content (Fig. 5.4 A,B). Overall the mean maceral compositions of the two groups, for similar RD's, do not vary much (Fig. 5.4 A,B and Table 5.1).

The $\bar{R}_o$max of samples is generally uniform but values tend to increase progressively to higher $\bar{R}_o$max values at the base of the formation within the carbo-tonstein zone. The Grootegeluk Formation samples have $\bar{R}_o$max values between 0.52 and 1.06 (mean value of 0.72).

Table 5.1 The mean maceral compositions (%) of the samples separated at different relative densities (RD) from Group A and B (see Fig. 5.2). The maceral composition the two groups, for similar RD's, do not vary much but the differences in the means are significant between different RD's within each group.

GROUP A - samples predominantly coal					**GROUP B** - samples predominantly mudstone				
RD	Vitrinite	Liptinite	RSF	Inertinite	RD	Vitrinite	Liptinite	RSF	Inertinite
1.35	90	1.7	2.3	5	1.50	86	1.1	4	8
1.80	56	2.3	18	23	1.80	53	1.8	19	25
2.00	57	2.4	15	25	1.90	42	2.7	23	31
Avg	68	2.1	12	18	Avg	60	1.9	15	21

5.4 DISCUSSION

Petrographic studies have established that the predominant maceral group in the upper portion of the Grootegeluk Formation is vitrinite, in both coal and carbonaceous mudstone samples. The vitrinite content decreases, and the inertinite and RSF increases progressively with depth and increased RD, especially in the carbo-tonstein zone at the base of the formation. The liptinite proportion is variable and occurs only as a minor maceral group in the formation.

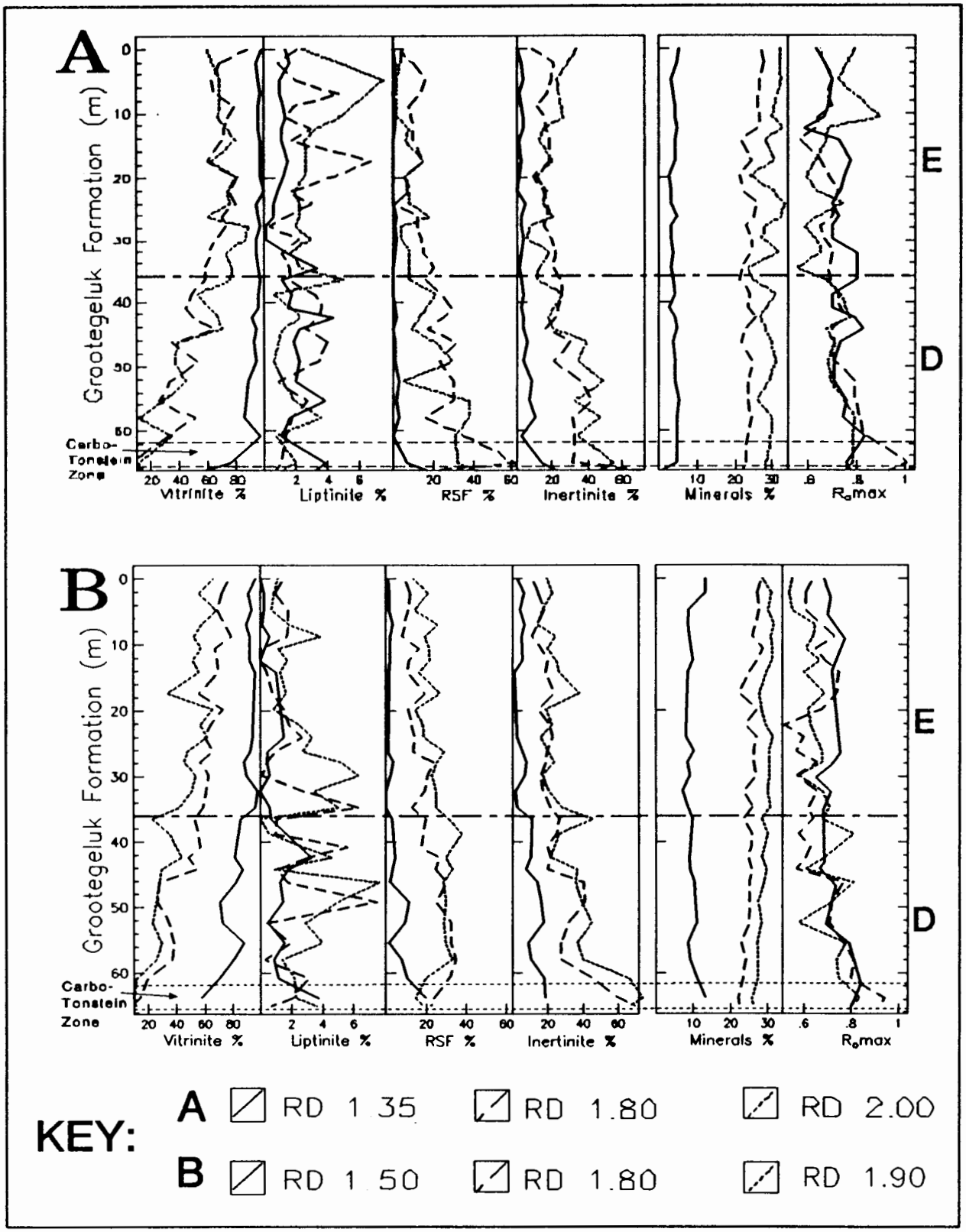

Figure 5.4. Maceral concentrations (normalised to 100%), mineral matter (volume % of sample) and mean maximum reflectivity ($\bar{R}_r max$) of samples separated at different relative densities (RD). **A** = samples predominantly coal and **B** = samples predominantly mudstone. The Grootegeluk Formation has been divided on the basis of palynological data into two biozones E and D (MacRae, 1988). The depth at which the carbo-tonstein zone occurs (at the base of the Grootegeluk Formation) is also illustrated on the graphs. The maceral, liptinite, is also referred to as exinite (Teichmüller, 1975).

5.4.1 PRECURSOR VEGETATION and MACERAL VARIATION

5.4.1.1 Vitrinite, Reactive Semi-fusinite and Inertinite

According to the van Krevelen (1961) classification (Fig. 5.3) the coals are Type 3 kerogen because they are composed essentially of vitrinite, indicating that the coals had a humic (continental) vegetation source. The original parent material of the inertinite group macerals were most probably similar to that of the vitrinite maceral group, except that for inertinite the plant material had been strongly altered and degraded in oxidising and(or) alkaline conditions in the peat stage of coal formation (termed fusinitisation; Teichmüller and Teichmüller, 1975). Reactive semi-fusinite is classified as part of the inertinite group, but it is not as degraded as semi-fusinite (C.J. Dreyer, pers. comm. 1992).

The overall increase in inertinite and RSF in the coals and mudstones in the lower portions of the Grootegeluk Formation (Fig. 5.4 A,B) suggest that these coals were subjected to higher degradation than the organic material in the upper parts of the formation. The RSF content in the coal group (Fig 5.4 A) and the inertinite content in the mudstone group (Fig. 5.4 B) increase abruptly in the carbo-tonstein zone, indicating that degradation of vitrinite was more intense in this part of the formation. In the mudstone group samples the RSF decreases in the carbo-tonstein zone (Fig. 5.4 B), in contrast to the coal samples (Fig. 5.4 A). The mudstone group, however, has a significantly greater proportion of inertinite in the carbo-tonstein zone indicating that the organic material had been more degraded in the mudstone than in the coal group samples.

The major maceral variation in the Grootegeluk Formation therefore is between the vitrinite and inertinite (and RSF) maceral group. The variation appears to be a manifestation of different degrees of maceral degradation rather than a *major* change in organic source.

5.4.1.2 Liptinite

Figure 5.4 A,B and Table 5.1 show that the liptinite maceral group (typically spores, pollen, algae, wax coatings of leaves, etc.) occurs only in very minor proportions, is highly variable and has different trends in the coal and mudstone groups (Fig. 5.4 A,B). The differences in the trends are interpreted to indicate that liptinite in the mudstone group was enriched mostly by degradation, and that an increase in liptinite in the coal-rich fractions indicates a primary enrichment (albeit small). The increase in the liptinite proportion in the upper part of the formation in the predominantly coal samples, corresponds approximately to the MacRae (1988) biozone E which is discussed below (Fig. 5.4 A).

5.4.2 SEDIMENT and PEAT DEPOSITION

5.4.2.1 Previous Work

5.4.2.1.1 Evidence from Sedimentology

Based essentially on sedimentological studies, Beukes (1985), Siepker (1986) and, Beukes et al. (1991) considered that the coal-mudstones in the lower portions of the formation which have higher proportions of inertinite and RSF, were formed in a poorly-drained proximal floodplain setting, whereas the vitrinite-rich upper parts formed in the well-drained distal floodplain facies of this formation. Beukes et al. (1991) suggested that this indicated that vitrinite had a very high post-depositional preservation potential, under conditions when most other macerals are not preserved, and may not necessarily reflect low Eh-pH conditions in the original depository. This proposal, however, is in complete contrast to the general consensus that the preservation of vitrinite is very sensitive to pH and especially Eh conditions of deposition (Teichmüller, 1975; Falcon and Snyman, 1986).

5.4.2.1.2 Evidence from Palynology

MacRae (1988) divided the Ecca Group rocks in the Waterberg Basin into five biozones, A to E from the bottom up, based on palynological data (Fig. 2.4). The lower portion of the Grootegeluk Formation was assigned to the top half of the biozone D and the upper portion to the E zone (Fig. 5.4 A,B). Spores and pollens occurred in equal proportions in biozone D but in biozone E the cryptogam spores (e.g. mosses, ferns, algae, fungi) dominated the higher order pollen producing organisms (MacRae, 1988).

Based on the quantitative characteristics and re-appearance of many species in biozone D (lower Grootegeluk Formation), MacRae (1988) suggested that climatic conditions were relatively warm, humid and generally milder than in the previous biozone C (lower Vryheid Formation, Fig. 2.4). In biozone E (upper half of the Grootegeluk Formation) the spores dominate over the pollen but the lack of knowledge of pollen and spore dispersal abilities did not permit MacRae (1988) to estimate the proportion of different parent plants. So the significance of the increased spore to pollen ratio in Biozone E is ambiguous (MacRae, 1988). It could on the one hand indicate wetter, swampier conditions as proposed by Beukes (1985) or it could indicate an environment closer to shore where the input from lower-order plants would have exceeded that of the higher order, predominantly wind-dispersed pollen producers some distance from the shore (MacRae, 1988). This would typically occur during silting-up of a depository and the reduction in the size of the water body (MacRae, 1988). MacRae (1988) also proposed that the palynological evidence "suggested some climatic change" from biozone D to E times.

5.4.2.2 Evidence from Mineralogy in this Study

MacRae (1988) did not observe any lithological changes that correlated with the Biozone D and E contact. However, evidence from the mineralogy of the Grootegeluk Formation mudstones that are inter-bedded between the coal seams (Chapter 4), and evidence from the normative variation of the major minerals to be discussed later, establishes that lithological changes do occur within the mudstones. The data show that the lower portions of the formation are dominated by kaolinite (~70%), and the upper portion of the formation is dominated by quartz (~60%; see Fig. 5.5 for qualitative variation). The grain-size of quartz also increases towards the top of the formation. The upper portion of the formation has about 25% kaolinite and minor proportions (~5%) of montmorillonite-illite and microcline. Microcline and montmorillonite-illite are not present in the lower part of the formation.

Evidence from the mineralogy was interpreted in Chapter 4 to indicate that the palaeo-environment of the carbonaceous mudstones from the lower Grootegeluk Formation was dominated by acidic and low energy depositional (therefore distal) environments. The mudstones in the upper portions were considered to have been deposited in a relatively higher energy (therefore more proximal) environment. The upper mudstones were buried with lesser amounts of organic matter and therefore postdepositional chemical alteration of the mudstones was less important than during deposition of the mudstones at the base of the Grootegeluk Formation.

5.4.3 PROPOSED DEPOSITIONAL ENVIRONMENT

The conclusions proposed in this study from the mineralogy and the organic fraction are consistent with the lower portion of the Grootegeluk Formation forming in a more distal setting and that the upper portion was more proximal to the source of the sediments. This is in contrast to the Beukes (1985), Siepker (1986), and Beukes et al. (1991) models which propose that the base of the formation was proximal and the upper parts distal.

The dominance of vitrinite in coal *and mudstone* samples in the upper part of the Grootegeluk Formation appears to be controlled by the sedimentological conditions that prevailed during deposition at this time. Although the mineralogy of the *mudstones* in the upper parts of the formation indicate relatively high pH conditions, which are not considered to be suitable for the preservation of vitrinite (Falcon and Snyman, 1986), the mineralogical data also indicate that the relatively unaltered mudstones at the top of the formation were deposited in a higher energy depositional environment (more proximal) than the mudstones in the lower part. The evidence that the proportion of organic matter in the mudstones generally decreases towards the top of the formation (Fig. 5.1) is consistent with an increased "rate" of sedimentation. The increased "rate" of sedimentation buried peat,

which accumulated during favourable periods in the upper parts of the formation, rapidly enough to prevent biochemical alteration by oxidation and preserving it as vitrinite. An increase in the energy of the depositional environment also decreased the accumulation of organic material in the sediments, and as a result less acids that could cause mineral alteration were formed during diagenesis, thus preserving minerals such as microcline (Fig. 5.5).

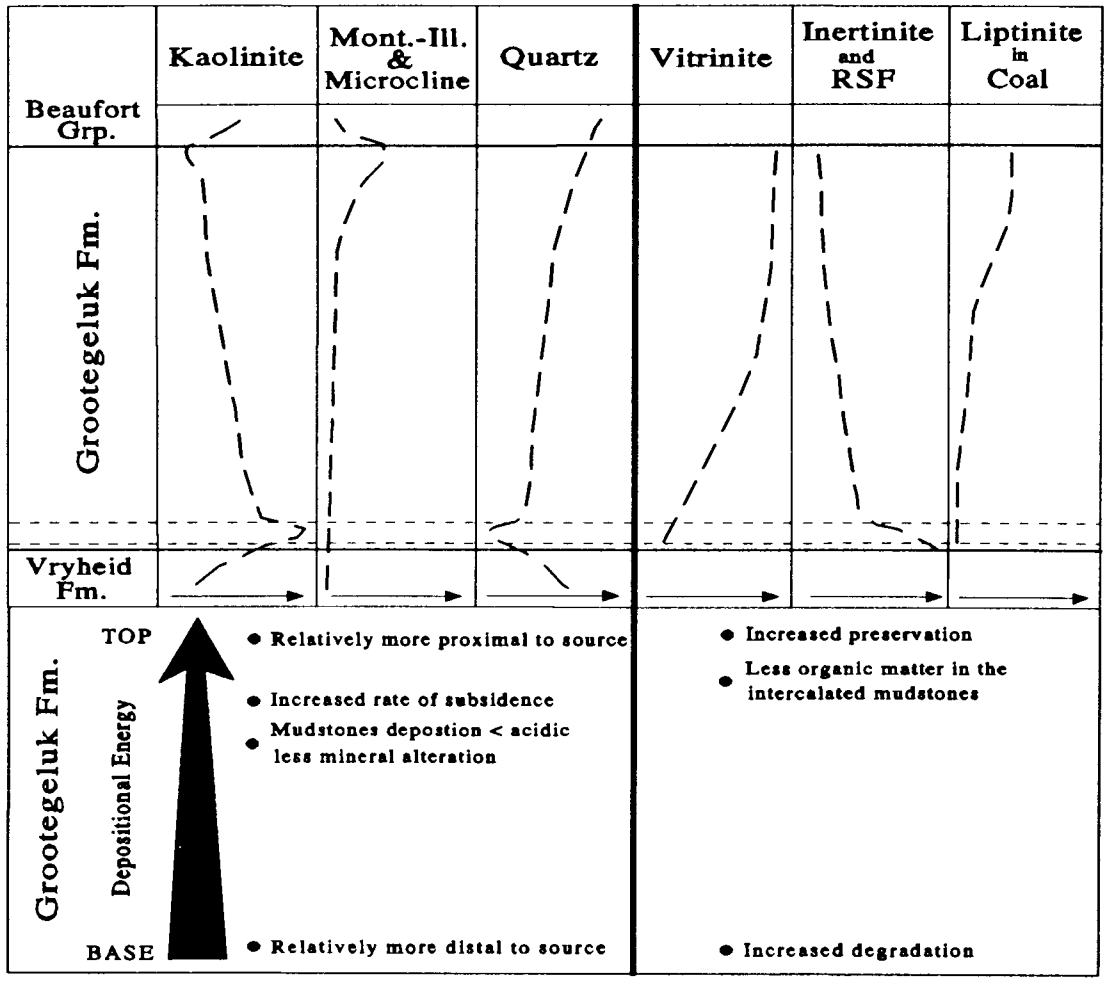

Figure 5.5. Schematic comparison of the detrital mineral and the maceral distributions of the Grootegeluk Formation. The maceral variation of the organic matter is considered to a manifestation of the changing sedimentological conditions during the deposition of the Grootegeluk Formation mudstones. The two dashed horizontal lines indicate the approximate borders of the carbo-tonstein zone at the base of the Grootegeluk Formation. Thin arrows at the base of the mineral and maceral plots indicate increasing concentrations.

An examination of clastic depositional environments and maceral contents of Triassic coals in Australia suggests that in passing from highly energetic fluvio-deltaic conditions towards a low-energy lacustrine regime, the proportion of inertinite increases at the expense of vitrinite and also, to some extent, liptinite. Inertinite, because of its already oxidised and fragmentary nature, can be transported further without alteration than other macerals and can remain in suspension in deeper, less turbulent environments (Smyth and Mastalerz, 1991). This is consistent with the interpretation of the Grootegeluk Formation that the organic material that was deposited with the argillaceous detrital matter in the lower parts

of the formation was deposited in more distal, possibly deeper waters, and was far more degraded.

MacRae (1988) proposed that palynological evidence from the upper Grootegeluk Formation (Biozone E) indicated a "shrinking basin", "silting-up of a depository" and "the reduction in the size of the water body". The evidence from this study does show that sedimentological conditions changed progressively upwards in the formation, however, the upward increase and high concentrations of vitrinite in the coal and mudstones from the top of the formation, suggest that conditions were still poorly drained preventing alteration by oxidation.

Assuming that the inorganic fraction of the carbo-tonstein zone did have a volcanogenic origin, the break-down of relatively fresh unstable high temperature minerals would result in a change of the ambient chemical conditions. Although the alteration of minerals in the carbo-tonstein zone would have involved "oxygen consuming" reactions, the pH of the sediments must have been sufficiently alkaline to precipitate the calcite dispersed in the mudstones during early diagenesis (Chapter 4), and therefore increase organic degradation.

The intercalated nature of the Grootegeluk Formation coal-mudstone sequences suggests that the basin was subsiding as it filled. The thicker coal seams indicate periods of equilibrium between subsidence and deposition. The repetitive nature of the coal-mudstone succession (Fig. 2.3), the lateral persistence of cycles, and the maceral and ash content of the coal-mudstone sequence indicate that the formation may have resulted from a combination of allogenic controls (tectonism and climate) and authigenic controls (environments of deposition).

5.4.4 THE ECCA FORMATION and BEAUFORT GROUP BOUNDARY

The contact between the uppermost coal seam and the overlying massive grey mudstones is conveniently regarded as the contact between the Grootegeluk Formation of the Ecca Group and the Beaufort Group in the Waterberg Basin (Fig. 1.2; Beukes, 1985; Siepker, 1986). Although these two lithostratigraphic units differ mainly in that the Beaufort Group mudstones contain no coal, there is no sedimentological break between the two lithostratigraphic units. As mentioned above, the vitrinite content, in all the RD fractions, increases continuously upwards in the Grootegeluk Formation (Figs. 5.4 A and B). In the Soutpansberg Coalfield (Fig. 1.1) to the east of the Waterberg Coalfield, a similar upward increase of vitrinite in coal occurs (John Sullivan pers. comm., 1992; Tshikondeni Coal Mine). In the Waterberg Coalfield the coal seams stop abruptly with no ostensible change in the maceral composition. This can be as a result of either of two possibilities: (1) that conditions suitable for producing and preserving peat deteriorated very abruptly, or (2) that

accumulation of peat continued as in the rest of the Grootegeluk Formation but was not preserved in the overlying grey mudstones now assigned to the Beaufort Group. There is no evidence to substantiate the former possibility. The latter may have occurred as a result of uplift after the peat had been buried to shallow depths, causing complete degradation of the peat before re-burial. Study of the Beaufort Group mudstones is outside the scope of this project but a few samples of the overlying massive mudstones have been sampled and analyzed and some ideas on their conditions of formation will be presented in later chapters.

5.4.5 ORGANIC PALAEO-THERMOMETRY

Palynological material from the Grootegeluk Formation generally have a dark orange colour (C.S. MacRae, pers. comm. 1992) and have been assigned a thermal alteration index (TAI) value of 3.0. The Grootegeluk Formation $\bar{R}_o$max varies between 0.52 and 1.06, with a mean value of 0.72 that corresponds to a coal rank of high volatile bituminous B in the catagenic zone (Fig. 5.2). Both the optical properties of vitrinite ($\bar{R}_o$max) and palynological data indicate that the maximum palaeo-temperature to which the Grootegeluk Formation organic material could have been subjected was about 100°C (minimum about 70°C; Fig. 5.2). This temperature is in close agreement with the temperature estimated from the curves of Bustin et al. (1990), that take both temperature and time into account, that was necessary to produce the $\bar{R}_o$max observed in the Grootegeluk Formation. Diagenesis of organic matter is progressive and irreversible, and therefore $\bar{R}_o$max and TAI reflect the maximum temperatures to which the organic materials were subjected.

5.5 SUMMARY

Evidence from the maceral concentrations of the Grootegeluk Formation establishes that the precursor material of the coal was humic (continental). Although the types of macerals vary in concentration through the formation, the predominant plant source material is considered not to have varied significantly.

The variation of the maceral concentrations is consistent with the evidence from the mineralogy of the mudstones that the base of the formation was deposited in the distal part of the basin and the upper the parts were deposited in a relatively more proximal setting (Fig. 5.5). The encroachment of the source area of the sediments is accompanied by the increase in vitrinite concentration in both coal and carbonaceous mudstones. The increase in vitrinite is in part accounted for by a relative increase in the depositional energy and an increased "rate" of deposition of the sediments (or basinal subsidence) that covered the organic matter and prevented organic degradation. The high vitrinite concentrations in the upper parts of the formation also indicate that conditions must have been poorly drained to prevent biochemical alteration by oxidation. The change in depositional energy is overall,

however, very small because no sediments coarser than siltstone-size are observed anywhere in the Grootegeluk Formation throughout the Waterberg Coalfield (Chapter 4). The more inertinite- and argillaceous-rich coal and, carbonaceous mudstones in the lower parts of the formation had been transported further than the upper parts of the formation. This study concurs with the recent findings of Smyth and Mastalerz (1991) that the water energy conditions can be an important factor controlling the composition of the organic matter in sediments.

The abrupt increase in the more degraded organic material in the carbo-tonstein zone is consistent with the deposition of relatively fresh unstable high-temperature volcanic material. The alteration of the minerals caused an increase in the pH of the organic-rich sediments resulting in a degradation of organic matter and an increase of inertinite and RSF. The increase in pH also provided suitable conditions for the precipitation of calcite in the matrix of these sediments which is not observed elsewhere in the formation.

The $\bar{R}_o max$ of vitrinite and palynological data indicate that the maximum palaeo-temperature that the Grootegeluk Formation organic material could have been subjected to was about 100°C.

6. WHOLE-ROCK CHEMISTRY

6.1 INTRODUCTION

The major and trace element composition of the carbonaceous mudstones that interbed the coal seams in the Grootegeluk Formation are presented and discussed in this chapter. Apart from establishing the chemical composition of the mudstones, the principal aim of the discussion is to assess the palaeo-environment of formation of the mudstones in conjunction with evidence already obtained from the mineralogy and organic matter. The whole-rock composition will also be important in assessing whether environmental contamination may occur as a result of the disposal of coal-mining waste material, but this possibility will be examined separately (Chapter 9).

6.1.1 PREVIOUS GEOCHEMICAL STUDIES

Few geochemical studies have been published for southern African Archaean (McLennan et al., 1983a; Wronkiewicz and Condie, 1987), Proterozoic (Schreiber et al., 1992), and Phanerozoic fine-grained sediments (Zawada, 1988). Hofmeyr (1971) conducted an extensive geochemical study of argillaceous rocks in southern Africa. He analysed samples (using XRF and emission spectrograph techniques) from sediments that range in age from the early Precambrian Fig Tree Group through to the Triassic Beaufort Group of the Karoo Sequence. However, the aim of Hofmeyr's (1971) work was only to establish the trace element composition of as many mudstone components of the southern African stratigraphic column as possible, and as a result the sampling distribution was rather random and scant. Dia et al. (1990) determined the Nd isotopic compositions and the $^{147}Sm/^{144}Nd$ ratios of 58 South African mudstones, with depositional ages ranging from 3.3 Ga to 200 Ma, to elucidate the development of continental crust through geological time in South Africa. Zawada (1988) published the only geochemical study of South African Phanerozoic argillaceous rocks used to solve a specific problem. He used selected trace elements of samples from the Ecca and Beaufort Group mudrocks in the Main Karoo Basin as palaeo-salinity indicators.

6.1.2 PRESENT STUDY

In this chapter the variation, association and concentration of elements will be evaluated to assess mainly palaeo-environmental processes. The major and trace element distributions in sedimentary rocks are controlled by several factors such as: source rock compositions (provenance); intensity of the weathering process, mainly related to tectonics and climate; sedimentation rates and depositional environments; and post-depositional changes (Taylor and McLennan, 1985). The composition of the Grootegeluk Formation

mudstones, and the sediments which immediately over- and underlie the Grootegeluk Formation, will be discussed with respect to these controlling parameters.

The chemical composition of the mudstones, however, also can be important in stratigraphic characterisation. For example, stratigraphic correlation of sediments which do not form a continuous horizon, due to erosion or in areas with poor exposure, can be identified and discriminated on the basis of their chemical compositions. In the case of the Grootegeluk Formation, where there is no distinctive rock unit-layer in the ~75 m thick coal-mudstone sequence, geochemical stratigraphic properties may be important.

The major and trace element compositions of 229 samples from two GCM borehole cores (prefixes 136 and 137) were determined in this study (see Appendix I for sampling procedure). Seventeen selected samples from the cores were also analysed for their rare earth element (REE) compositions because of the suitability of REE in provenance studies of argillaceous rocks (Taylor and McLennan, 1985).

The samples obtained from the cores were predominantly grey-black massive mudstones with organic matter proportions up to 62 weight %, but typically about 30 weight %. Three Beaufort Group samples per borehole, up to 0.5 m above the topmost coal seam, and several Vryheid Formation samples from approximately 70 m below the topmost coal seam were also analysed. Microscopic studies showed that the mudstones from the Beaufort Group and the Grootegeluk Formation are usually massive, whereas some of the Vryheid Formation mudstones have fine planar and cross-laminated bedding planes. Because of the profusion of mudstone partings and the cyclic variation of the coal-mudstone sequences, sampling widths (approximately 1 sample every 60 cm) were kept as small as practically possible to establish the presence of any geochemical trends or anomalies.

6.2 WHOLE-ROCK CHEMISTRY: XRF SPECTROMETRY RESULTS

The means and ranges of the major and trace element values are presented in Table 6.1 and all the whole-rock data are presented in Appendix II (Table II.2). In calculating the mean trace element values in Table 6.1, It was decided to include values that were below detection limits, so that means were not biased toward higher values. An arbitrary value of half the LLD for an element in a sample (not the average LLD) was included in the mean calculation reported in Table 6.1.

Several studies on coal, which usually have < 15 weight % mineral matter, have tried to ascertain whether trace elements occur predominantly in the organic fraction (either bonded, adsorbed or merely associated) or in the mineral fraction (for a useful review see Swaine, 1990). The majority of elements in coal tend to be associated with the mineral fraction but there are coals in which certain elements do have a predominantly organic association, for example Mo, S, Cu, Cr, V, etc. (Swaine, 1990). For some elements there is

no universal predominantly organic or inorganic association in carbonaceous sediments. In the case of the Grootegeluk Formation mudstones, which typically have mineral proportions of about 70 weight %, it was assumed that the major proportion of all the elements that were determined (C, H, and N were not determined) were associated with the mineral fraction, i.e. the organic matter is a diluent. Based on this assumption the whole-rock data, given in Table II.2, were recalculated on a volatile-free basis and used in all variation diagrams and compositional comparisons. The recalculation was done by normalising each analysis (major and trace) to a 100% volatile-free major element composition. The whole-rock data, recalculated volatile-free, are presented in Table II.3 (Appendix II). The variations of the elements (volatile-free) in the two boreholes are displayed in Figure 6.1.

6.2.1 GEOCHEMICAL VARIATION and ELEMENT ASSOCIATION

The concentrations of thirty eight elements in 229 mudstone samples were determined in this study. The presentation of results and discussion of this sizeable data base has been facilitated by means of a factor analysis (FA) that groups related variables (oxides and elements) into a smaller number of parameters called "Factors" (Table 6.2). The variables, which may have positive or negative loadings, that are loaded together in each Factor are often related by some (geo)chemical association. The depth of a sample below the topmost coal seam, and the LOI of each sample were also included as variables. Elements that were not included in the FA were: (1) Ge, Se, Br, Bi, Au, Cs, and Na because most of the concentrations were below detection limit for these elements or had very low concentrations and little variability (Au and Cs were analysed in samples from one borehole only); (2) U which was very weakly loaded on two Factors (1 and 3); and (3) Pb which was assigned alone to a Factor with the lowest variance in the FA. Sample 6b, a calcite lens, from borehole 137 was not included in the data set because it consisted almost entirely of calcite and a small proportion of organic matter. A SAS® program called FACTOR using the *prin* and *varimax rotation* options, was performed on the data base to obtain the Factor loadings on the variables (Table 6.2). Only variables with loadings ≥ 0.3 are listed in Table 6.2. It is appreciated that statistical techniques cannot replace direct scientific measurement and observation, but they are useful for "suggesting" geological association and co-variation for a large data base with many variables.

Oxides and element concentrations in the whole-rocks will be discussed together in their groupings as determined by the FA (Table 6.2) and with respect to their variation with depth in the formation (Fig. 6.1). The FA reduced the data for 31 variables (29 oxides and elements, LOI and depth in the formation) to 8 Factors that accounted for 90% of the variability (variance) in the data set (Table 6.2). Oxides and elements listed below in Factor

headings that have strong (≥ 0.5) positive or negative loadings are typed in bold, the rest are weaker (>0.3<0.5) loadings, with minus signs indicating a negative loading.

Table 6.1 The range, mean concentrations (n=228), 1 standard deviation and lower limit of detection of oxides and LOI's in weight %, and trace elements in ppm. Values that were lower than the detection limit were also included in the calculation of mean values, so that the mean values were not biased toward higher values. A half the LLD value was included in the calculation. In the case of elements which are generally below the LLD, such as Bi, the mean value for the formation is lower than the LLD.

wt. %	Minimum	Maximum	Mean	1 S. D.	LLD
SiO_2 %	53.99	77.44	68.79	4.92	0.03
TiO_2 %	0.52	2.25	1.07	0.29	0.004
Al_2O_3 %	11.09	40.76	26.31	4.73	0.017
FeO %	0.37	25.22	1.50	2.07	0.015
MgO %	0.16	1.91	0.39	0.22	0.04
CaO %	0.11	5.61	0.39	0.64	0.008
Na_2O %	0.03	0.21	0.12	0.03	0.08
K_2O %	0.37	3.10	1.30	0.68	0.003
P_2O_5 %	0.03	1.30	0.14	0.18	0.011
LOI %	6.47	62.43	26.74	11.66	-
S	450	121070	5720	9298	7.0
Sc	6.9	58	18.3	7.1	1.0
V	39	256	89	34	4.3
Cr	37	297	69	32	2.3
Mn	0.3	660	88	99	1.8
Co	1.0	109	7.1	8.4	2.8
Ni	0.7	161	13.8	14.6	1.1
Cu	6.2	76	27	9.5	1.9
Zn	12.2	108	42	19.9	1.4
Ge	0.4	60	1.0	4.0	1.1
As	0.5	245	7.9	17.9	0.9
Se	0.5	17	1.8	2.1	0.8
Br	1.5	8.5	2.4	1.3	0.9
Rb	29	212	109	39	1.2
Sr	51	944	227	170	1.1
Y	35	134	61	16	1.8
Zr	222	875	349	104	1.2
Nb	12.7	93	35	11.3	1.5
Mo	0.3	18.2	2.2	2.0	0.5
Cs	3.5	23	11.1	3.2	6.9
Ba	212	2435	593	409	5.5
La	28	132	67	16.2	3.3
Ce	64	294	142	34	5.8
Nd	26	125	63	14.8	3.4
W	1.7	24	9.2	3.0	2.8
Pb	0.3	1099	91	123	4.2
Bi	0.6	2.2	0.7	0.1	3.2
Th	20	86	38	10.0	3.9
U	4.3	52	9.0	4.1	3.4

Table 6.2 Results of the factor analysis (FA) on all the mudstones. The data used in this analysis were the whole-rock data re-calculated to a 100% major element volatile-free (Appendix II, Table II.3). Strong positive or negative loadings are ≥ 0.5 and weaker loadings > 0.3 < 0.5. The oxides and elements are ordered according to their factor loadings, with the highest factor loading in the top left and the lowest in the bottom right of each cell in the Table. The minerals and(or) rocks at the bottom of each factor column are the suggested minerals and rocks associated with the element(oxide) factor loadings. The data for the "variable" depth (in meters) in the FA, were positive values.

Factor	1	2	3	4	5	6	7	8
Cumulative Variance%	27	46	62	71	79	85	87	90
Strong Positive Loading	Zr, Nb, Sc, TiO_2, Al_2O_3, Th, Y, V, Cr, Cu, W	K_2O, Rb, SiO_2, Zn, MgO	Co, As, S, FeO, Ni	La, Ce, Nd,	Sr, Ba	CaO, Mn, P_2O_5	Al_2O_3, Th, Nb, SiO_2	P_2O_5, CaO
Weaker Positive Loading	Depth, Ni		Mo	Y, Cu	P_2O_5	FeO, MgO	TiO_2	MgO
Weaker Negative Loading	-LOI, -S	$-P_2O_5$	-Zn				-LOI	-V, -Cr
Strong Negative Loading		-LOI -Depth						
	Carbo-tonstein Factor. Kaolinite, zircon, anatase	Montmorillonite-illite Microcline Quartz	Pyrite	REE & Y	Sr- and Ba-bearing phosphate (?)	Carbonates and apatite.	Kaolinite	Apatite and calcite

6.2.1.1 Factor 1 **Zr, Nb, Sc, TiO_2, Al_2O_3, Th, Y, V, Cr, Cu, W**, Depth, Ni, -LOI, and -S.
Factor 7 **Al_2O_3, Th, Nb, SiO_2,** TiO_2, and -LOI

The Grootegeluk Formation mudstones consist predominantly of the two oxides Al_2O_3 and SiO_2. However, the oxides have opposite variations in the distribution of concentrations with depth in the formation (Table 6.2; Fig. 6.1). Al_2O_3 is positively loaded onto Factors 1 and 7 (Table 6.2). The reason for this can be seen in the Al_2O_3 variation diagram (Fig. 6.1) which shows that: (1) Al_2O_3 generally increases steadily with depth in the Grootegeluk Formation and then decreases in concentration in the Vryheid Formation; and (2) the Al_2O_3 (also kaolinite) increases abruptly to anomalously high concentrations at depths of about 64 m below the topmost coal seam. Figure 6.1 also demonstrates that the concentration of the other major oxide, TiO_2, and the trace elements which are positively loaded with Al_2O_3 onto Factor 1, also abruptly increase at a depth of 64 m. The variables positively loaded onto Factor 1 therefore appear to be those that have anomalous high concentrations at the base of the Grootegeluk Formation, hence the positive loading of

Figure 6.1 Variations of major and trace element compositions with depth below the topmost coal seam. Concentrations of major elements have been plotted for boreholes 136 (solid line) and 137 (dotted line). For the trace elements only concentrations from borehole 136 have been plotted, except where values differ significantly between the two boreholes and both are plotted. Although the major and trace element data have been normalised to a 100% major element volatile-free basis, the LOI values of the samples are also plotted. The LOI of the samples are not equal to their organic matter content but is a good approximation of the relative variation of organic matter within the formation. Bismuth has been analyzed but all of the values were below the detection limit for XRF spectrometry and have not been plotted in this figure. Three samples, in both boreholes, up to 0.5 m above the topmost coal seam that is traditionally considered to be within the Beaufort Group, have been analyzed and are included in the plots. The boundary between the underlying Vryheid formation occurs at about 70 m from the topmost coal seam (dash-dot line). The boundaries of the carbo-tonstein, established from mineralogy and mineralogical characteristics (Chapter 4), are displayed by two dashed lines at the base of the Grootegeluk Formation (64 and 66 m). All concentration values are in ppm except when indicated as "%".

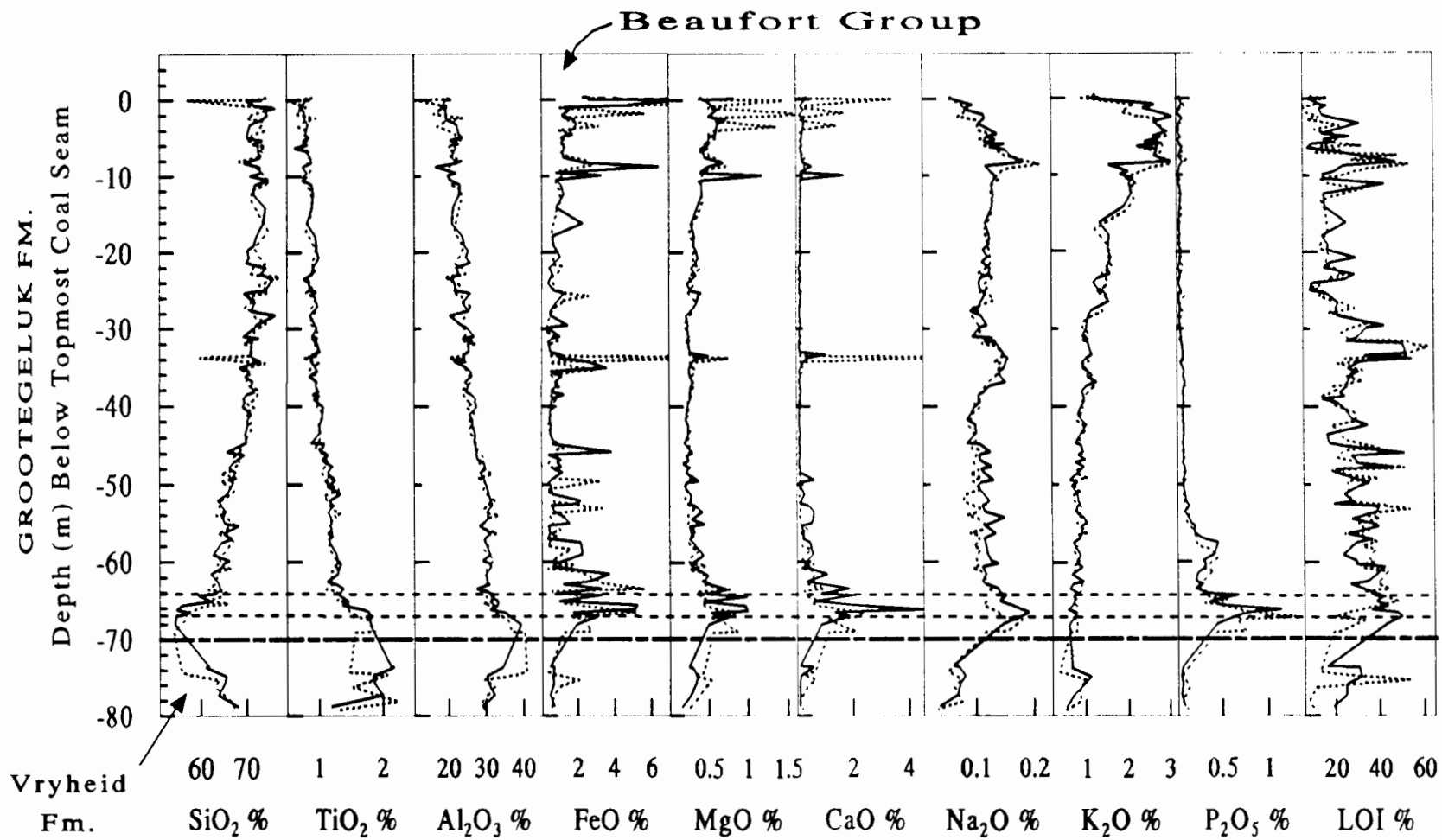

Figure 6.1 Continued.....

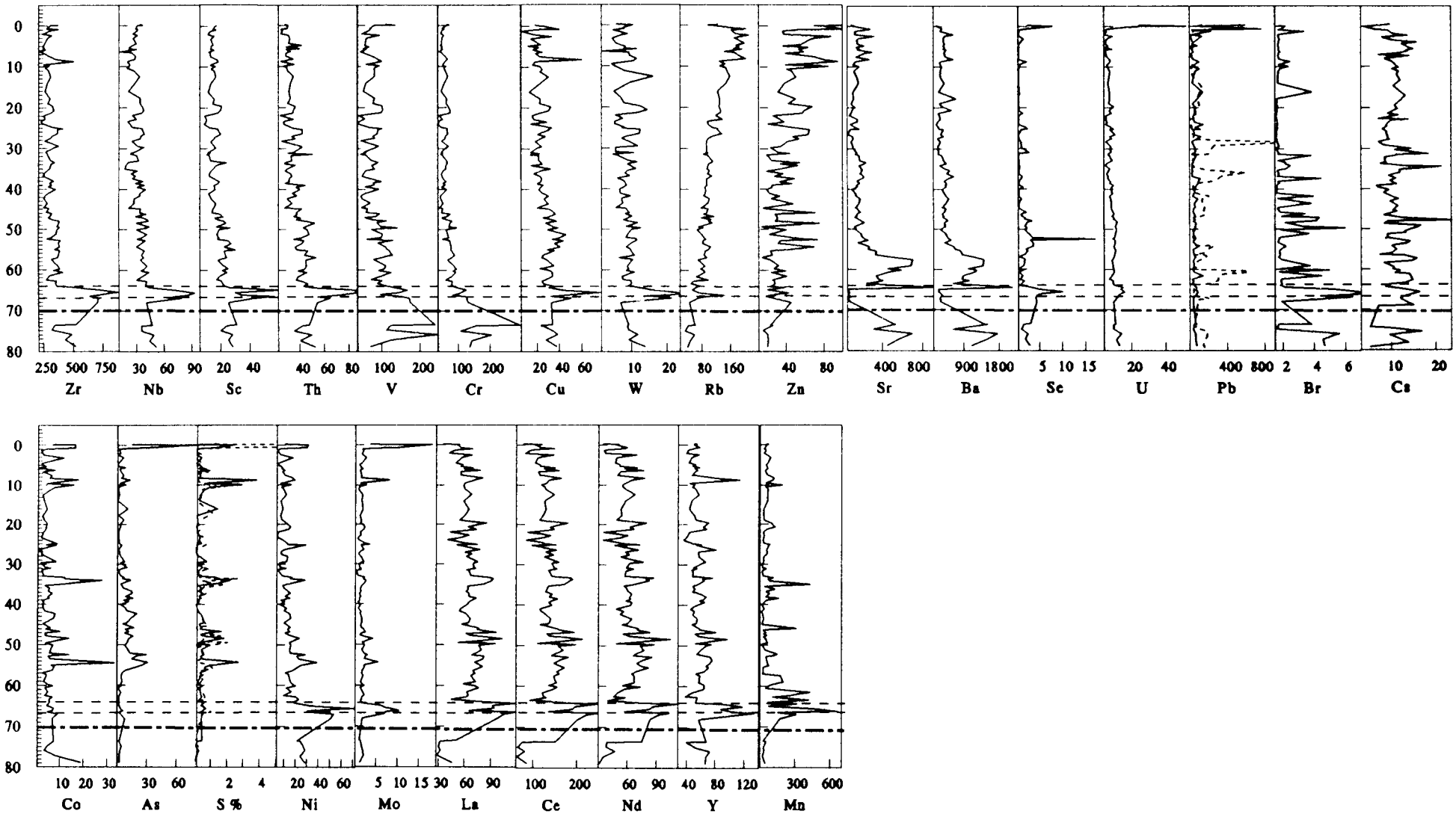

depth in the formation, for example TiO_2, Th, and Nb, whereas the other trace elements in Factor 1 do not necessarily co-vary with Al_2O_3 outside of the carbo-tonstein zone. It is not clear why the FA has assigned the "kaolinite" variables to another factor (Factor 7), but the variables are probably associated with samples from the entire borehole that have higher proportions of detrital matter (kaolinite and/or quartz) as indicated by a positive Al_2O_3 and SiO_2 loading and a negative LOI loading.

The negative loading of LOI on both Factors 1 and 7 signify that with higher proportions of organic matter the oxides and trace elements associated with the factors decrease in concentration. Also no oxides or elements, except S (presumably an organic association), in this study are positively correlated with LOI which would support the assumption made earlier that the elements are predominantly associated with mineral matter in the carbonaceous mudstones.

The almost identical distribution of TiO_2 and Al_2O_3 (Fig. 6.1), and the positive loading on Factor 7 of both these oxides indicates that Ti is closely associated with the clay fraction. Titanium is present probably in anatase (a low temperature polymorph of TiO_2) which was identified by XRD in samples from the carbo-tonstein zone at the base of the Grootegeluk Formation (Chapter 4).

The Zr concentration in the Grootegeluk Formation generally does not vary much except for the abrupt and anomalous increase in the carbo-tonstein zone (65.02 m - sample 136_22Ec) and the sharp but smaller increase toward the top of the formation (8.74 m - sample 136_2c). The concentrations of Zr are also slightly higher in some of the samples from the underlying Vryheid Formation (below depth 70 m; Fig. 6.1).

The variations of Nb and Th follow those of Zr in Figure 6.1. Although high concentrations of elements such as Nb, Sn, Ta, etc. are sometimes reported in rocks containing zircons, Deer et al. (1966) considers that these elements are probably present in inclusions of other minerals that often occur within zircon. Thorium and Nb are positively loaded onto Factor 1 and 7 with Al_2O_3 and may be an indication of a strong association (adsorption?) with kaolinite in the samples.

The variation of the yttrium concentration in the Grootegeluk Formation is highly erratic (Fig. 6.1). The Y variation is very similar to the REE, La, Ce, and Nd, but Y has additional peaks at 8.74 m (sample 136_2c) and in samples above the coal seams (sample 137_0c; not plotted see Table II.3 in Appendix II) that correlate with FeO, S, Zr, Co, Mo, (Ge, Se, and Br - excluded from FA) peaks.

Cu and Ni occur in most coals in sulphides and(or) associated with organic matter (Swaine, 1990). The FA of the mudstones indicates that neither Cu or Ni are strongly correlated with the S or the organic matter. In fact the S content of those samples in the carbo-tonstein zone which do have anomalous Cu and Ni concentrations are relatively low compared

to the rest of the samples. Anomalous Cu concentrations of samples in the upper portions of the Grootegeluk Formation (8.24 m - sample 136_2b) correlate with increased concentrations of oxides and elements such as Na_2O, K_2O, and Rb, rather than with samples that have high S and Fe concentrations which occur in sample 136_2c (8.74 m) immediately below sample 136_2b (Fig. 6.1). High Ni concentrations also occur in the samples just above the topmost coal seam (sample 137_0c) which are associated with high concentrations of mainly chalcophile oxides and elements, for example FeO, S, Zn, Co, As, Pb, U and Mo (Fig. 6.1, Table II.3). Although Cu and Ni are loaded onto Factor 1, their distribution in the sedimentary environment is complicated and dependent on several geological factors.

The Sc concentration increases overall by approximately a factor of 2 with depth and like the other variables from Factor 1 its concentrations abruptly increase to anomalously high values at 65.02 m (sample 136_22Ec), in the carbo-tonstein zone.

Chromium and V have positive loadings on Factor 1 even though these elements do not abruptly increase to anomalous concentrations in the carbo-tonstein zone, as do the other elements and oxides in this Factor. Figure 6.1. shows that the concentrations of V and Cr increase steadily with depth in the borehole, but increase rapidly in the samples of the Vryheid Formation. These two elements are included in Factor 1 because they have higher concentrations deeper in the borehole ("Depth"). The Cr and V anomalies in the Vryheid Formation are not correlated with any other elements except TiO_2. The distribution of Cr and V is most probably controlled by provenance compositions and adsorption onto the clay minerals. V concentrations which are much more variable than Cr may have an organic association (Swaine, 1990).

6.2.1.2 FACTOR 2 K_2O, Rb, SiO_2, Zn, MgO, $-P_2O_5$, -LOI and -Depth.

It is apparent from the variation diagrams (Fig. 6.1), and from the study of the mineralogy of the Grootegeluk Formation mudstones (Chapter 4), that the elements positively loaded on Factor 2 are indicative of the increased proportions of quartz, the clay mineral montmorillonite-illite, and also microcline, towards the top of the Grootegeluk Formation. Hence the strong negative loading of "Depth" (Table 6.2). The spike in the Na_2O plot coincides with K_2O and MgO peak in the same sample 136_2b (8.24 m). Based on typical compositions of microcline and montmorillonite-illite (Deer et al., 1966), the rapid decrease upward in the concentration of Na_2O above sample 2b (8.24 m) suggests a decrease in the microcline proportion towards the top of the formation whereas the K_2O concentration is sustained due to an increased contribution of K from illite. The K_2O concentration, however, decreases abruptly in the Beaufort Group mudstones that immediately overlie the topmost coal seam.

The strong co-variance of Rb with K_2O indicates that Rb is incorporated in K-bearing minerals such as illite and microcline. Rubidium and potassium have similar ionic radii and

charge (+1), and the co-variation of these elements supports their coherent geochemical behaviour (Fig. 6.1). Although the Zn concentration is generally highly variable there is a good correlation with the montmorillonite-illite and microcline components. This correlation is to be expected because Zn can easily substitute for Al in the smectite lattice (section 4.3.1.1.1). Heinrichs et al. (1980) reported that Zn is preferably concentrated in chlorite but that it is also strongly associated with illite.

The MgO concentrations which are generally very low, are positively loaded on the "montmorillonite-illite-microcline Factor" because of Mg in the montmorillonite structure (Deer et al, 1966). Other samples with anomalous MgO are associated with mineral phases such as carbonates (see Factor 6 below; Fig. 6.1).

The strong negative loadings of LOI and "Depth" is a manifestation of the general decrease in LOI (≈organic matter) upwards in the formation, as noted in the mineralogical study of the samples (Chapter 4). The weak negative loading of P_2O_5 on Factor 2 is probably due to the P_2O_5 peaks at 58 m and 64 to 70 m.

6.2.1.3 FACTOR 3 Co, As, S, FeO, Ni, Mo and -Zn.

The chalcophile elements, present predominantly as pyrite (Chapter 4), are strongly loaded on Factor 3. Cobalt, As and Ni are present in only very small amounts and are known to be present as impurities in pyrite (Deer et al., 1966).

Zinc, which is also a chalcophile element, however, is weakly negatively loaded on the "chalcophile Factor". The Zn concentration is highly variable and a sulphide (or organic) association may be statistically masked by the overall upward increase in the Zn concentration associated with increasing montmorillonite-illite. Inspection of the variation diagrams in Figure 6.1 suggest that indeed this

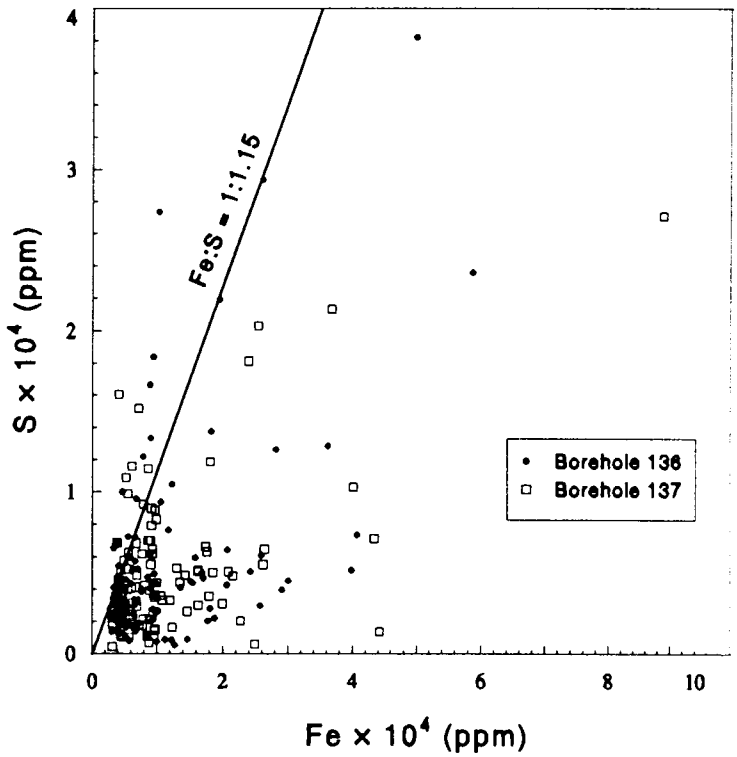

Figure 6.2. In the Fe (FeO recalculated as Fe) *vs.* S diagram for the mudstones, the Fe:S line displays where whole-rock Fe and S values would plot if Fe and S were present only in pyrite (FeS_2). Most of the values plot to the right of the Fe:S line supporting mineralogical evidence that Fe is predominantly present as siderite and to a lesser extent ankerite.

may be the case because Zn peaks do occur at the same depths as Fe and S peaks, for example, immediately above the topmost coal seam (sample 136_0c).

The Mo concentrations in the Grootegeluk Formation are generally very low and appear to be associated only with the chalcophile elements present in pyrite, except for the anomalous value within the tonstein zone at depth 66.2 m (sample 136_22Ee) where S is low (Fig. 6.1). The mode of occurrence of Mo in coals ranges from mostly organic to mostly inorganic, with varying proportions of each (Swaine, 1990). It may be, therefore, that Mo is associated with the organic material in the carbo-tonstein zone.

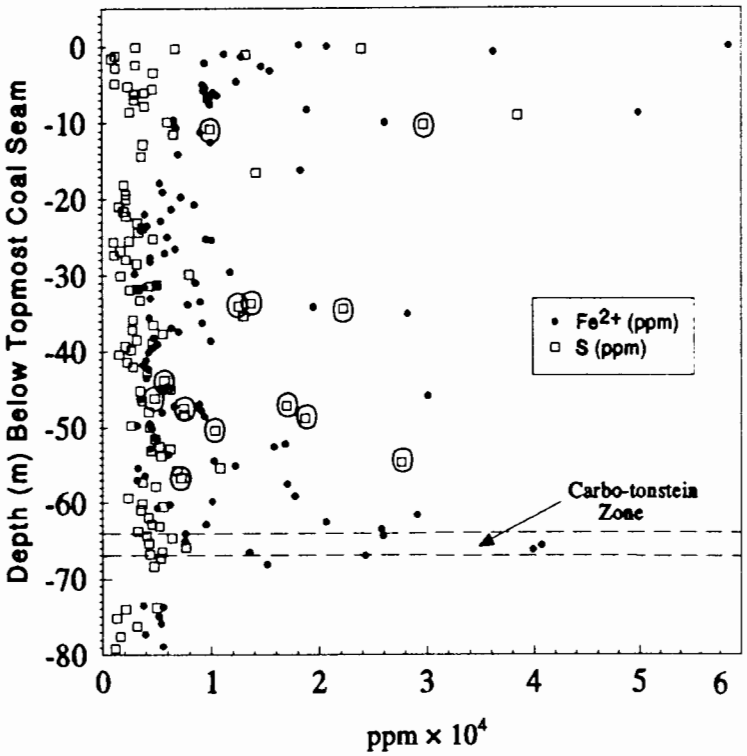

Figure 6.3. The variation plots with depth of Fe and S in the Grootegeluk Formation mudstones demonstrates that the concentration of Fe dominates over S especially in the lower portion of the Grootegeluk Formation from about 58 m to 68 m depth, and in the top 8 m of the formation. The "ringed" values are some of the samples that have a greater proportion of S which is assumed to be organic bound S because no other S-bearing minerals were identified.

The iron-sulphur ratios in the mudstones (Fig. 6.2) support the findings in Chapter 4 that the primary Fe-bearing mineral is siderite rather than pyrite. Figure 6.3 and Table II.3 (Appendix II) illustrate that the pyrite is present mainly in the mudstone samples that occur just above the topmost coal seam (137_0c), at depth 8.74 m (sample 136_2c), and at 33-35 m (samples 136_14a-e) in the middle part of the Grootegeluk Formation. The samples above the topmost coal seam and to a lesser extent the sample at depth 8.74 m, are also highly anomalous with respect to trace elements such as Co, As, Ni, Zn, Pb, U, Y and Se. Excess FeO (not enough S to form pyrite) occurs predominantly in samples in the lower half of the Grootegeluk Formation especially in the carbo-tonstein zone (~ 65 m; Fig. 6.3). Excess S, which occurs in a few samples, is assumed be organic-bound S.

Cobalt, As, Zn and S are the only trace elements that do not show any anomalous increase in concentrations within the carbo-tonstein zone.

6.2.1.4 FACTOR 4 **La, Ce, Nd,** and Y.

Lanthanum, Ce, and Nd are REE that comprise part of the lanthanide series, La-Lu. It was possible to analyse only three of the lanthanide series elements by XRF, but eleven

elements in the series have been analysed in selected samples by gradient ion chromatography and will be discussed separately. The REE behave as an unusually coherent group of elements (McLennan, 1989), an attribute that is also reflected in the samples analysed in this study (Fig. 6.1). In terms of geochemical behaviour, Y mirrors the heavy lanthanides Dy-Ho, and is typically included with them for discussion purposes (MacLennan, 1989). Yttrium is weakly positively loaded onto the "REE Factor", but its concentrations are highly variable (Fig. 6.1) and it is also positively loaded on Factor 1, indicating its association with more than one phase. The REE concentrations in the Grootegeluk Formation do not have any overall trend besides the abrupt increase at the base of the Grootegeluk Formation in the carbo-tonstein zone. It has been proposed in several studies that the REE are readily accommodated (adsorbed?) onto clay minerals (Cullers et al., 1979; Eskenazi, 1987a,b) but the overall trend of the REE in the Grootegeluk Formation does not correlate with any of the clay minerals (Fig. 6.1 and Table 6.2). It is therefore not possible even to speculate where the REE and Y predominantly reside in the mudstone samples. In the carbo-tonstein zone trace minerals such as xenotime (YPO_4), zircon ($Zr[SiO_4]$) and monazite ($[Ce,La,Th]PO_4$) may account for elevated REE and Y concentrations. Scandium behaves similarly to REE in low temperature sedimentary environments, in contrast to igneous processes where the REE are incompatible and Sc behaves as a compatible element, primarily because it has a much smaller cationic size (Puddephatt, 1972). Sc, however, is not loaded onto the "REE Factor" in the FA of the samples in this study, even though the variation diagram of Sc is similar to that of Y (Fig. 6.1).

Although it appears in Figure 6.1, because of the scale of the plots, that there is a fair degree of correspondence between the elements that have anomalous concentrations in the carbo-tonstein zone, the element distribution in fact does not overlap particularly closely. For example the REE peaks are at 64.36 m and 66.54 m depths (samples 136_22Eb and 136_22FSa); Sc and Y at 65.02 m and 66.54 m (samples 136_22Ec and 136_22FSa); Zr, Nb, Th, and V at 65.02 m and 67.0 m (samples 136_22Ec and 136_22FSb); Ni, W, and Cu at 65.62 m and 67.0 m (samples 136_22Ed and 136_22FSb); and Rb, Se, and Mo at 66.2 m depth (sample 136_22Ee).

6.2.1.5 FACTOR 5 **Sr, Ba,** and P_2O_5.

FACTOR 6 **CaO, Mn, P_2O_5,** FeO, and MgO

FACTOR 8 **P_2O_5, CaO,** MgO, -V, and -Cr

Several oxides are positively loaded on more than one of these Factors and therefore all three Factors, 5, 6 and 8 will be discussed together. The concentration of P_2O_5 in the Grootegeluk Formation is generally very low, expect in the samples at the base of the Grootegeluk Formation (Fig. 6.1). It has been established from mineralogical studies of the samples at the base of the Grootegeluk Formation (Chapter 4) that, in addition to high

proportions of kaolinite, they also contain variable amounts of siderite ($FeCO_3$), calcite ($CaCO_3$), apatite ($Ca_5(PO_4)_3F$), and small amounts of ankerite [$Ca(Mg,Fe,Mn)(CO_3)_2$].

An inspection of the overall Sr, Ba, and P_2O_5 variation (Fig. 6.1), shows that down to a depth of 64 m they have almost identical variations with depth in the formation, explaining why they are loaded together on Factor 5. A closer examination of the variation of these elements (Fig. 6.4) reveals why P_2O_5 is only weakly positively loaded on Factor 5. In Figure 6.4 strontium and Ba are perfectly correlated over the whole depth range whereas P_2O_5 only correlates well with Sr and Ba between 54 and 64 m depth. The sharp Sr and Ba peak (64.36 m - sample 136_22Eb) correlates with a relatively small P_2O_5 peak, whereas the major P_2O_5 peak (66.2 m - sample 136_22Ee) is associated with very low values of Sr and Ba. The samples between 54 and 64 m depths have high factor scores on Factor 5 and are associated with samples that have calcium phosphate mineral(s) that may or may not have minor amounts of Sr and Ba in its structure. The minerals goyazite and gorceixite (Sr and Ba aluminium phosphates) have been identified by Spears et al. (1988) in a tonstein, elsewhere in the Waterberg Basin, which is considered to be the stratigraphic equivalent of this carbo-tonstein (see Chapters 4 and 5).

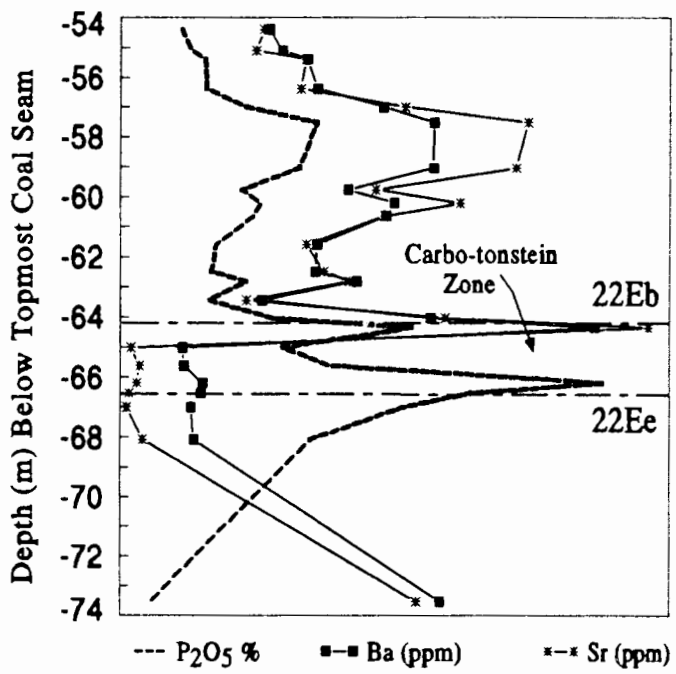

Figure 6.4. The variation of P_2O_5 (%) is compared to the variation of the trace elements Sr and Ba (ppm). There is an exceptionally good correlation between Sr and Ba and reasonably good correlation with P_2O_5 down to depths of 65 m. However, below 65 m depth there is no correlation. Samples 22Eb and 22Ee have been included in the carbo-tonstein zone, based on mineralogical textures.

Microprobe scanning of the samples between 54 and 64 m, however, revealed that Sr and Ba were not associated with apatite which occurred as alteration minerals in kaolinite grains or with the small (20 μm) anhedral apatite grains dispersed in the kaolinite and organic matrix. Strontium and Ba were detected by the microprobe scans of sample 136_22Eb, but was finely dispersed in the samples and not concentrated in any identifiable mineral or organic matter.

Examination of Figure 6.5 A, B reveals that samples below depths of approximately 61 m have excess CaO compared to P_2O_5. The additional CaO is contributed by calcite and ankerite which become more prominent in the lower part of the formation. It was established earlier (Factor 3) that the FeO in this part of the formation is contributed mainly by siderite and to a lesser extent ankerite. Thus the variables loaded onto Factor 6 are those associated

with the minerals apatite (no Sr or Ba), calcite, ankerite, and siderite at depths approximately between 61 and 68 m.

The strong positive loadings of P_2O_5, CaO (both second order - also loaded onto Factor 6) and weak positive loading of MgO on Factor 8 are indicative of apatite (± calcite) but the negative loadings of V and Cr are not as easily explained. In a plot of V, Cr and P_2O_5 concentrations of samples at the base of the Grootegeluk Formation and top of the Vryheid Formation, it is apparent that V and Cr do not vary much in the Grootegeluk Formation but concentrations increase slightly in the Vryheid Formation (Fig. 6.6; Fig. 6.1). It can only be

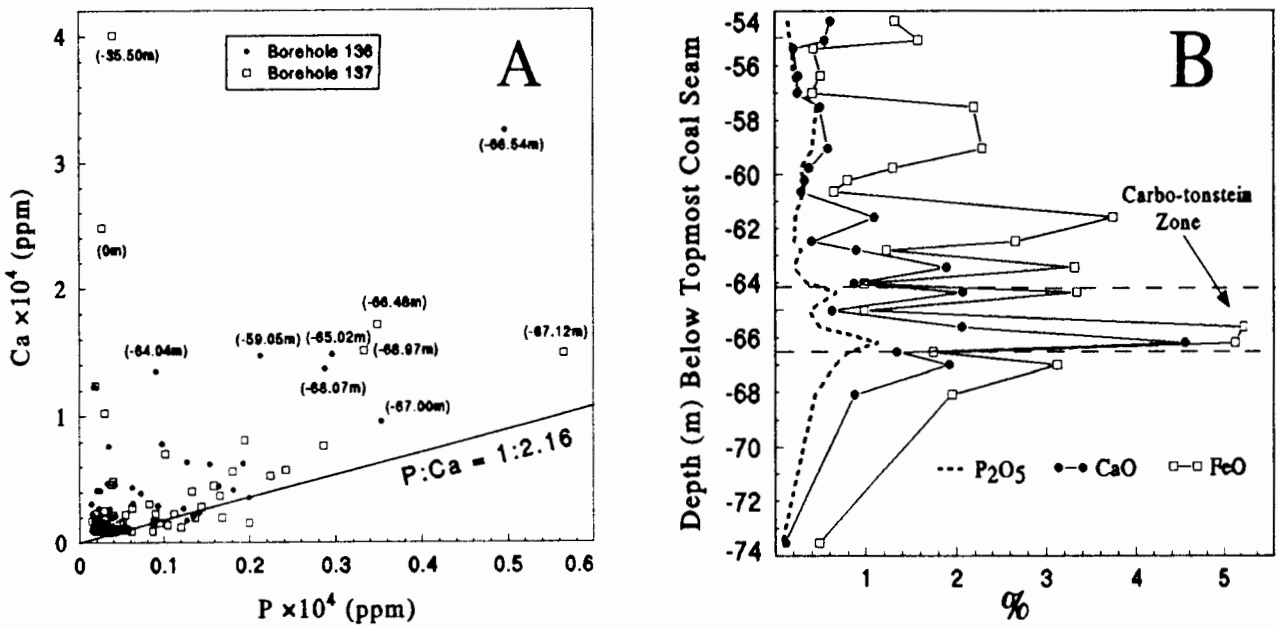

Figure 6.5 **A.** P vs. Ca plot of the mudstones displays the "apatite line" along which all whole-rock analyses would plot if the Ca and P were associated with apatite only. Selected samples which have Ca concentrations above the "apatite line", mostly from carbo-tonstein zone, are identified by their depths within the formation. **B.** This plot demonstrates the variation of P_2O_5, FeO, and CaO (borehole 136) in the basal portion of the Grootegeluk Formation. The Fe-bearing mineral in this part of the formation is predominantly siderite with minor amounts of ankerite which were identified in XRD analyses. The Ca-bearing phases are apatite and calcite.

speculated that the negative loading of V and Cr is as a result of a reverse trend with P_2O_5 and CaO at the Grootegeluk and Vryheid Formation contacts. Thin-section studies of the samples from the Vryheid Formation show that some samples have small scale planar and trough cross-bedding, in contrast to the Grootegeluk Formation and Beaufort Group mudstones which are massive. The concentrations in SiO_2 of samples from the Vryheid Formation are not higher than in any of the Grootegeluk Formation samples and therefore higher depositional environments in the Vryheid Formation are not considered to be the cause of an increase in concentration of Cr and V. It is possible that the dominant provenance of the Vryheid Formation samples was different to that of the overlying Grootegeluk Formation sediments and that the carbo-tonstein source rocks had relatively low concentrations of V and Cr compared to the Vryheid Formation source rocks.

In contrast to most other sedimentary geochemical investigations, Sr is not correlated with Ca (carbonates). The ionic radius of Sr^{2+} is between that of Ca^{2+} and Ba^{2+} and so Sr readily substitutes for these elements (Wedepohl, 1978). Barium is considered to be adsorbed from solution by clays, mainly illite, hydroxides and organic matter (Wedepohl, 1978; Nicholls and Loring, 1962). Wedepohl (1978) further suggested that Ba adsorption on clays is of less importance and that Ba enters the depositional basin as barytes. None of these modes of occurrence of Sr and Ba would appear to apply in the Grootegeluk Formation mudstones. Calcite is also present in predominantly coal samples but this was formed at very late-stages of diagenesis or during up-lift of the sediments in cleat (joint) structures (Chapter 4).

6.2.1.6 Trace Elements Not Included In the FA: Au, Cs, Se, Br, Ge, Mo, Pb and Bi

The Au concentrations of samples from borehole 136 were determined by Atomic Absorption Spectroscopy (Chapter 3). The carbonaceous mudstones have gold contents mostly below the LLD (~5 ppb), with only 13 samples above the detection limit (Fig. 6.7). The maximum Au value was 56 ppb and the rest of the values above the LLD were typically between 10 and 20 ppb.

Caesium was analysed in samples from only borehole 137. Figure 6.1. demonstrates that the Cs concentration is generally very low and highly variable with no specific trend. In the top 10 meters of the formation, however, the Cs concentration has an overall decreasing trend upwards in the formation, very similar to that of Na_2O (Fig. 6.1). It has been argued that Na_2O is associated with microcline in this part of the formation (Factor 2). It is not unexpected therefore that Cs should be associated with and substitutes for K which has a similar ionic size and charge to Cs. In the rest of the formation the highly erratic variation of Cs makes it impossible to speculate on any preferred association.

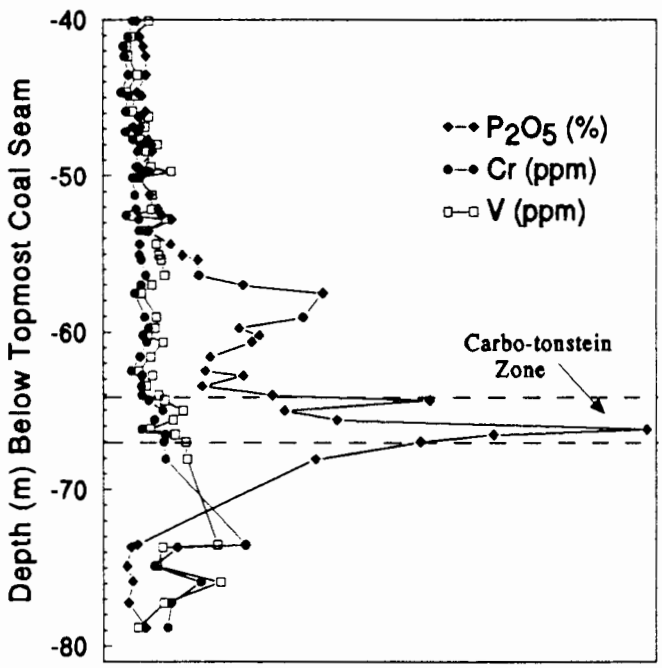

Figure 6.6. The relative variation of P_2O_5 (%), V (ppm) and Cr (ppm) concentrations in the lower half of borehole 136. The Cr and V increases in concentrations within the Vryheid Formation samples, whereas the P_2O_5 concentration decreases.

The selenium concentration of samples in the lower half of the formation and in the samples immediately above the topmost coal seam are generally above the LLD whereas in the remaining samples Se is not detectable by XRF spectrometry (Fig. 6.1). The two important

hosts of Se in coals are in pyrite (probably solid solution) and organic matter (Swaine, 1990). It has been demonstrated that the organic portion of the mudstones generally increases down the formation which may account for the Se being mostly above the LLD in the lower half of the formation. The Se peak at the very top of the formation is associated with high concentrations of pyrite which may be the host for small amounts of Se.

The Br distribution is similar to Se. Most of the values are below the LLD but in the lower half of the formation values are generally above the LLD and although variable, increase in concentration down the formation (Fig. 6.1). It is generally agreed that Br is predominantly associated with organic matter in coal, and that there is no direct evidence for the incorporation of Br into any mineral forms, although small amounts could be associated with iron oxides and clays (Swaine, 1990).

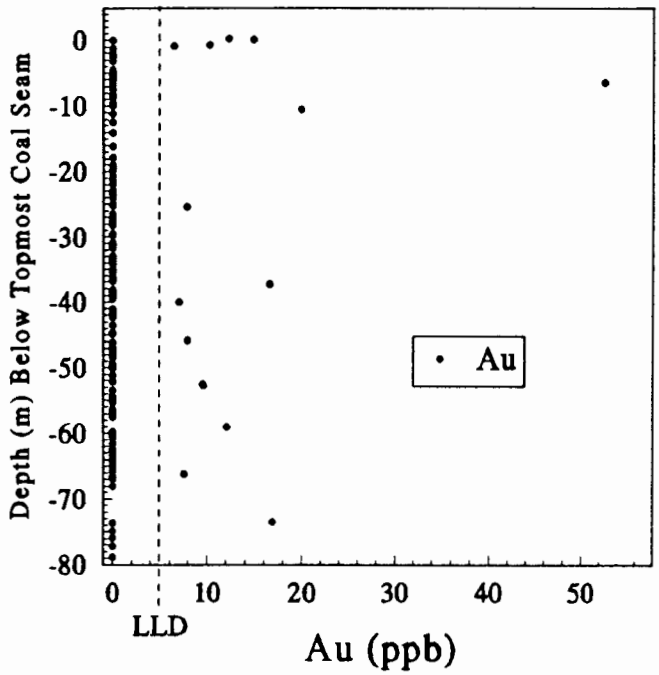

Figure 6.7. The Au concentrations, in the mudstones from borehole 136, were analyzed by A.A.S. at the Geological Survey in Pretoria. Most of the values are below the detection limit which was reported to be 5 ppb.

The Pb concentrations in samples from the two boreholes are not only highly variable, but the anomalies do not correlate between the two boreholes (Fig. 6.1). The absence of any coherence of Pb distribution in the samples is confirmed by the FA which assigned Pb, on its own, to a Factor which accounted for very little variance. It is suspected that Pb contamination occurred during the drilling of the cores (oil or diesel fuel?) and the values are therefore disregarded.

Bismuth concentrations in the mudstones are all below the LLD.

6.2.1.7 Comparison of Mean Chemical Compositions to Other Mudstones

The average composition of Post Australian Archaean Shales (PAAS; Taylor and McLennan, 1985) and world average shale (WAS; Turekian and Wedepohl, 1961; Levinson, 1974) are listed in Table 6.3 for comparison with the mean composition of all the mudstones analysed in this study. With respect to the major elements, the Grootegeluk Formation differs significantly (1 s.d.) from of PAAS and WAS. The Grootegeluk Formation mudstones have much higher Al_2O_3 concentrations and lower K_2O, Na_2O and CaO concentrations. A comparison of the trace elements show that the Grootegeluk Formation has higher Y, Zr, Th, W, U, La, Ce, Nd and lower Mn, Co, Cr, V, Zn, Cu, and Ni concentrations on average (1 s.d.) than the trace element compositions of PAAS and WAS. In comparison with typical acid (G-1)

Table 6.3 The mean (n=228) major and trace element concentrations of the mudstones analysed in this study are compared to the values of Post Archaean Australian Shales (PAAS; Taylor and MacLennan, 1985), World Average Shale (WAS; Turekian and Wedepohl, 1961 - major elements: Levinson, 1974 - trace elements), and G-1 and W-1 (Mason and Moore, 1982). The SiO_2 value of 15.6 % proposed by Turekian and Wedepohl (1961) is very low and may be a printing error. If the sum of the major elements (assuming an arbitrary LOI value of 3 %), excluding SiO_2, is subtracted from 100 % the difference is 64.9 % which is similar to the SiO_2 value of PAAS proposed by Taylor and MacLennan (1985).

wt. %	Grootegeluk	PAAS	WAS	G-1 (Granite)	W-1 (Diabase)
SiO_2 %	68.8	62.8	15.9 (64.9)	72.65	52.65
TiO_2 %	1.1	1.0	0.77	0.25	1.07
Al_2O_3 %	26.3	18.9	15.12	14.04	15.00
FeO %	1.5	6.5	6.1	1.76	9.98
MgO %	0.39	0.11	2.5	0.40	6.62
CaO %	0.39	2.2	3.1	1.39	10.96
Na_2O %	0.12	1.2	1.3	3.32	2.16
K_2O %	1.3	3.7	3.2	5.43	0.64
P_2O_5 %	0.14	0.16	0.16	0.09	0.14
LOI %	26.7	-	-	-	-
S	5720	-	2400	58	123
Sc	18.3	16	15	2.9	35
V	89	150	130	17	264
Cr	69	110	100	20	114
Mn	88	-	850	195	1280
Co	7.1	23	20	2.4	47
Ni	13.8	55	70	1	76
Cu	27	50	50	13	110
Zn	42	85	100	45	86
Ge	1.0	-	1.5	1.1	1.4
As	7.9	-	15	0.5	1.9
Se	1.8	-	0.6	0.007	0.3
Br	2.4	0.25	4	0.4	0.4
Rb	109	160	140	220	21
Sr	227	200	300	250	190
Y	61	27	25	13	25
Zr	349	210	160	210	105
Nb	35	19	20	24	9.5
Mo	2.2	1.0	3	6.5	0.57
Cs	11.1	15	5	1.5	0.9
Ba	593	650	700	1220	160
La	67	38	20	101	9.8
Ce	142	80	50	170	23
Nd	63	32	24	55	15
W	9.2	2.7	2	8.3	3.6
Pb	91	20	20	48	7.8
Bi	0.7	-	-	0.07	0.05
Th	38	14.6	12	50	2.4
U	9.0	3.1	4	3.4	0.58

and basic (W-1) rock compositions (Mason and Moore, 1982), the Grootegeluk Formation mudstones have higher concentrations of elements that are typically higher in acidic rocks, and lower concentrations of elements that are typically higher in basic rocks (Table 6.3).

6.3 LANTHANIDE ELEMENTS

Twelve REE from the lanthanide series were determined by gradient ion chromatography (GIC) in 17 selected samples (Chapter 3). It was, however, not possible to obtain data for Ho, due to interference by Y, or Lu which was not sufficiently well resolved from Yb.

6.3.1 RESULTS

The results of the mudstone analyses are presented in Table 6.4. Included in the 17 samples analysed for their REE composition was one sample from the Beaufort Group mudstones (sample 0b) and three samples from the Vryheid Formation (samples 23Asb, 23Asd and 23BSa). Individual and mean REE values will be compared and normalised to Chondrite (Sun and McDonough, 1989; Table 6.6), Post Archaean Australian Shale (PAAS; McLennan, 1989), and the North American Shale Composite (NASC; Haskin et al., 1968; Gromet et al., 1984) values, to assist in the interpretation of the REE data (Table 6.6).

6.3.2 GIC *vs.* XRF SPECTROMETRY REE RESULTS

The concentration of three REE (La, Ce and Nd) were determined by XRF spectrometry (see Section 6.2.1.4). It was previously argued that because the majority of elements (including REE) are mainly incorporated in the inorganic fraction, the mudstones, which have variable proportions of organic matter, can best be compared to one another if the results are calculated on a volatile-free basis. Analyses of the REE by GIC, which were done on volatile-free ashed samples, are compared to XRF spectrometry REE analyses, which were done on un-ashed samples recalculated to a volatile-free basis (Table 6.5). The GIC data correlates reasonably well with most of the normalised volatile-free XRF values, especially considering the relatively high analytical error for the REE (Table 3.2). However, the samples which have high proportions of organic matter (2c, 22Ae, 22Eb, 22Ee and 22Ed) have significantly higher concentrations of REE in the normalised XRF values, suggesting that some of the REE are associated (adsorbed or organic complexes?) with the organic matter and(or) may have been lost during the ashing processes.

Most studies of REE in coal, which usually have less than 15 weight % mineral matter, indicate that the predominant association of REE is with mineral matter. An inorganic association of REE is supported by the work of Zubovic (1966) and Filby et al. (1977). Bethell (1963) and Eskenazi (1987a,b) proposed that the REE are primarily chelated in clays, whereas

Table 6.4 The REE compositions (ppm) of selected mudstone samples from the Beaufort Group mudstones (0b), Grootegeluk Formation, and Vryheid Formation (23ASb, 23ASd and 23BSa). The samples are ordered according to their relative depth within the borehole.

Borehole 136	La	Ce	Pr	Nd	Sm	Eu	Gd	Tb	Dy	Er	Yb	La/Yb
0b	58.5	113	12.0	42.4	8.16	1.34	7.17	1.25	7.17	3.85	3.18	18.40
1Bd	40.8	84.0	9.30	34.6	6.66	1.00	5.06	0.74	4.02	2.21	2.18	18.72
2b	80.0	162	174	64.6	14.7	2.36	12.2	1.71	9.45	4.8	4.4	18.8
2c	61.9	121	16.7	55.9	10.4	1.62	9.81	1.69	10.9	7.39	7.47	8.29
8b	62.5	127	14.8	56.4	10.8	1.68	8.19	1.23	6.90	3.67	3.31	18.88
12b	69.1	135	15.17	59.11	12.07	1.81	8.98	1.36	6.90	3.08	2.51	27.53
19a	70.2	138	16.0	62.5	14.1	2.06	10.6	1.35	6.92	3.29	2.85	24.63
20a	81.7	156	18.0	62.4	10.3	1.40	7.43	1.12	6.80	3.82	3.45	23.68
21d	73.0	148	17.3	62.9	12.8	2.08	9.59	1.46	6.90	3.39	2.84	25.70
22Ae	63.0	125	14.8	54.1	11.0	1.96	9.09	1.35	7.99	4.63	4.51	13.97
22Eb	101	201	20.8	86.7	16.6	2.53	12.3	1.96	10.4	4.95	3.83	26.37
22Ee	50.8	112	12.77	45.0	8.57	1.18	6.54	1.04	6.27	3.52	3.36	15.12
22Ed	75.0	163	15.7	53.6	11.1	1.71	8.02	1.16	6.43	3.17	2.80	26.79
22FSa	116	232	24.7	93.1	19.3	3.49	14.9	2.17	10.9	4.58	3.54	32.77
23ASb	32.9	68.7	8.39	31.0	7.42	1.19	6.00	0.96	5.61	3.08	3.00	10.97
23ASd	36.9	69.7	9.4	42.3	14.9	2.82	13.8	2.41	13.4	7.01	6.13	6.02
23BSa	43.8	78.9	7.99	26.2	5.74	1.08	5.87	0.97	5.08	2.67	2.50	17.52

Table 6.5 A comparison of La, Ce and Nd values obtained from gradient ion chromatography (GIC) analyses and XRF values recalculated to a volatile-free, 100% major element composition. The La/Yb from GIC analyses, La/Y from XRF analyses, and the LOI proportions are also presented.

SAMPLE No.	GRADIENT ION CHROMATOGRAPHY			XRF RECALCULATED VOLATILE-FREE			LIGHT/HEAVY RATIO		LOI (WT %)
	La	Ce	Nd	La	Ce	Nd	La/Yb	La/Y	
0b	58.5	113	42.4	54	121	52	18.40	0.98	12
1Bd	40.8	84.0	34.6	42	82	38	18.72	1.02	13
2b	80.0	162	64.6	81	164	78	18.8	1.00	11
2c	61.9	121	55.9	73	136	65	8.29	0.64	49
8b	62.5	127	56.4	63	138	63	18.88	1.02	13
12b	69.1	135	59.11	70	143	63	27.53	1.13	18
19a	70.2	138	62.5	77	153	72	24.63	1.32	19
20a	81.7	156	62.4	84	175	74	23.68	1.29	31
21d	73.0	148	62.9	80	169	78	25.70	1.33	26
22Ae	63.0	125	54.1	71	147	70	13.97	0.97	54
22Eb	101	201	86.7	118	246	111	26.37	1.34	44
22Ee	50.8	112	45.0	65	135	57	15.12	0.63	33
22Ed	75.0	163	53.6	94	190	83	26.79	1.07	44
22FSa	116	232	93.1	119	247	103	32.77	0.89	43
23ASb	32.9	68.7	31.0	33	77	40	10.97	0.83	25
23ASd	36.9	69.7	42.3	33	82	48	6.02	0.45	33
23BSa	43.8	78.9	26.2	46	87	32	17.52	0.699	19

Finkelman (1981) suggested that the REE are primarily in rare earth phosphates. Goldschmidt and Peters (1933) who were the first to study REE in coal, however, concluded that inorganic processes were insufficient to account for the amount of REE in coal ash and that there must be some mode of biogenic accumulation.

Ridley et al. (1991) have demonstrated that the concentrations of light REE (LREE; La-Sm) in ashed coals were lower than those obtained using a microwave digestion technique, but that the heavy REE (HREE; Gd-Yb) were similar for both methods of preparation. Although REE are generally considered to be immobile and inert, and unfractionated during exogenous processes (Haskin et al., 1968) it is tentatively concluded here that LREE may be lost during high temperature ashing of organic-rich mudstones.

6.3.3 COMPARISON WITH CHONDRITE, PAAS AND NASC REE VALUES

6.3.3.1 Normalised REE Patterns

Chondrite normalised REE patterns in fine-grained sediments are likely to parallel primordial abundances in the solar nebula and also parallel bulk earth abundances (McLennan, 1989). The chondrite normalised REE values of the mudstones in Figure 6.8 demonstrate that they generally have enriched chondrite normalised LREE, flat chondrite normalised HREE patterns, and negative Eu-anomalies. The REE patterns and particularly the strong Eu-anomalies of the Grootegeluk Formation, reflect an average upper continental crust chondrite normalised REE pattern, associated with the production of granitic rocks (Taylor and McLennan, 1985; McLennan, 1989). Samples 136_2c and 23ASd, however, have chondrite normalised HREE enriched patterns which are distinctly unlike the REE patterns of the rest of the samples. In terms of geochemical behaviour Y mirrors the HREE, and in Table 6.5 the low La/Y correlates well with low La/Yb ratios which support a HREE enrichment of the two samples.

Comparison of the mean REE concentrations of the Grootegeluk Formation to PAAS and NASC (Table 6.6) show that the mudstones are enriched in the LREE compared to both PAAS and NASC and the HREE are higher than those of PAAS. The REE of samples from the Vryheid Formation mudstones have LREE compositions distinctly lower than the Grootegeluk Formation and very similar to those of PAAS and NASC. The one sample (0b) analysed from the Beaufort Formation is indistinguishable from the Grootegeluk Formation samples based on REE content. The PAAS normalised REE values in Figure 6.9 illustrate that the Grootegeluk Formation and carbo-tonstein mudstones are generally enriched in the LREE by a factor of 1.5-3 and in the HREE by about 1.2 to 1.8 times. The PAAS is a convenient reference material for normalising REE because the average shale is thought to be representative of the average upper continental crust in terms of REE (Taylor and McLennan, 1985). PAAS was considered by McLennan (1989) to be preferable to composite shales such

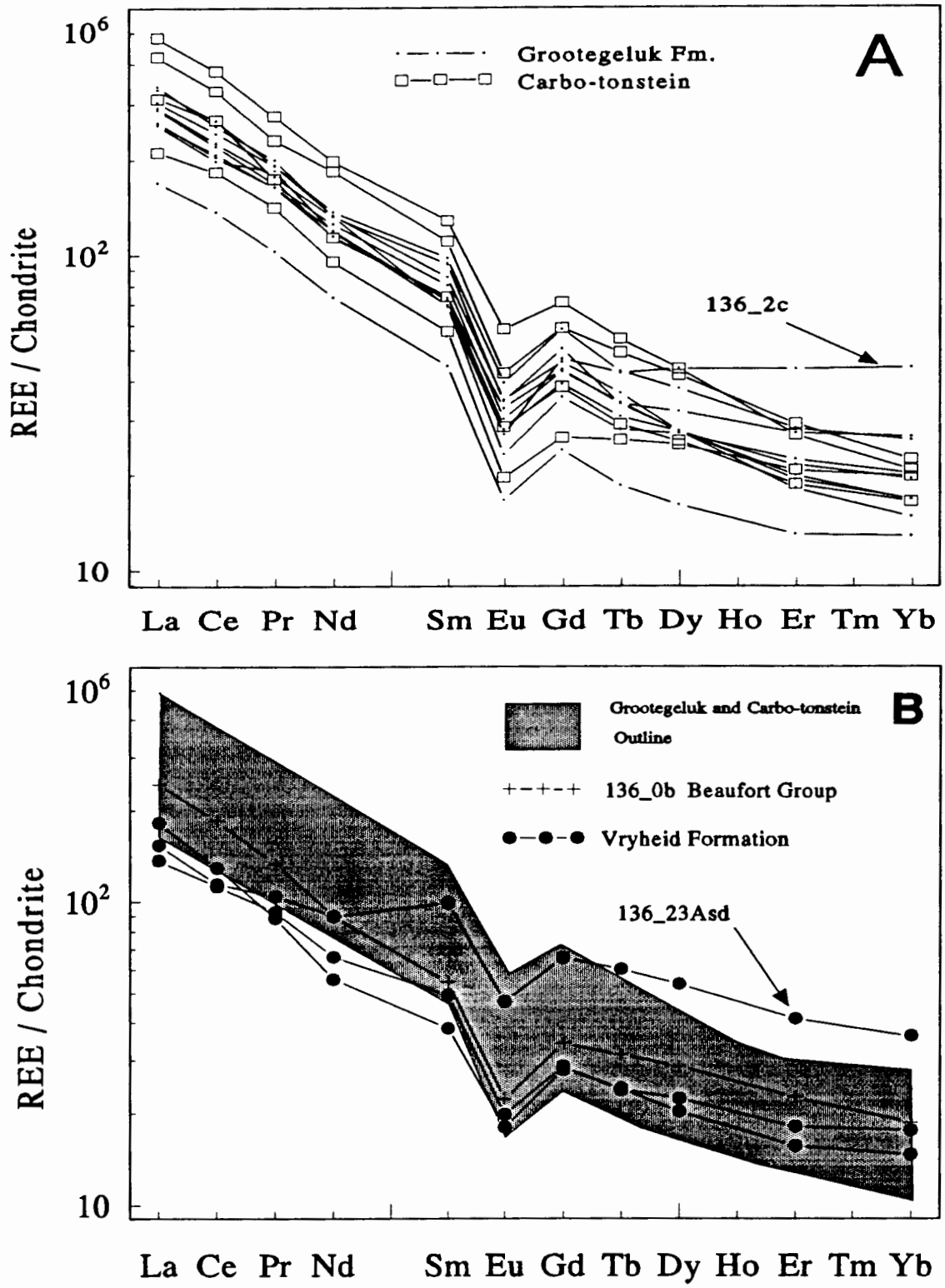

Figure 6.8. Chondrite normalised REE plots of selected mudstones, which were analyzed by gradient ion chromatography (GIC). (A) The Grootegeluk Formation and the carbo-tonstein samples from the base of the Grootegeluk Formation and (B) the Vryheid Formation and the Beaufort Group samples (Grootegeluk Formation and carbo-tonstein zone mudstones outlined). The mudstones have LREE-enriched, flat HREE patterns and strong negative Eu anomalies. Sample 136_2c (Fig. 6.8 A) and 136_23ASd (Fig. 6.8 B), however, have relatively HREE enriched patterns. Sample 0b from the Beaufort Group (Fig. 6.8 B), and the carbo-tonstein samples are indistinguishable from the Grootegeluk Formation REE patterns. The samples from the Vryheid Formation tend to have lower LREE normalised values than the rest of the mudstones.

Table 6.6 A comparison of the mean REE concentrations of the Grootegeluk Formation and Vryheid Formation mudstones to the values of PAAS (McLennan, 1989), NASC (Haskin et al., 1968; Gromet et al., 1984), Chondrite (Sun and McDonough, 1989), and G1 and W1 (Mason and Moore, 1982).

	Grootegeluk Fm. Mean	Grootegeluk Fm. (1 std. dev.)	Vryheid Fm.	PAAS	NASC	Chondrite	G1	W1
La	71.1	18.6	37.9	38.2	32	0.237	101	9.8
Ce	143.1	36.3	72.4	79.6	73	0.612	170	23
Pr	16.0	3.7	8.6	8.8	7.9	0.095	19	3.4
Nd	59.1	15.1	33.2	33.9	33	0.467	55	15
Sm	11.8	3.3	9.4	5.6	5.7	0.153	8.3	3.6
Eu	1.9	0.6	1.7	1.1	1.24	0.058	1.3	1.1
Gd	9.2	2.5	8.6	4.7	5.2	0.206	5.0	4
Tb	1.4	0.4	1.4	0.77	0.85	0.037	0.54	0.65
Dy	7.7	1.9	8.0	4.7	5.8	0.245	2.4	4
Er	4.0	1.2	4.3	2.9	3.4	0.166	1.2	2.4
Yb	3.2	0.6	2.9	2.8	3.1	0.170	1.1	2.1

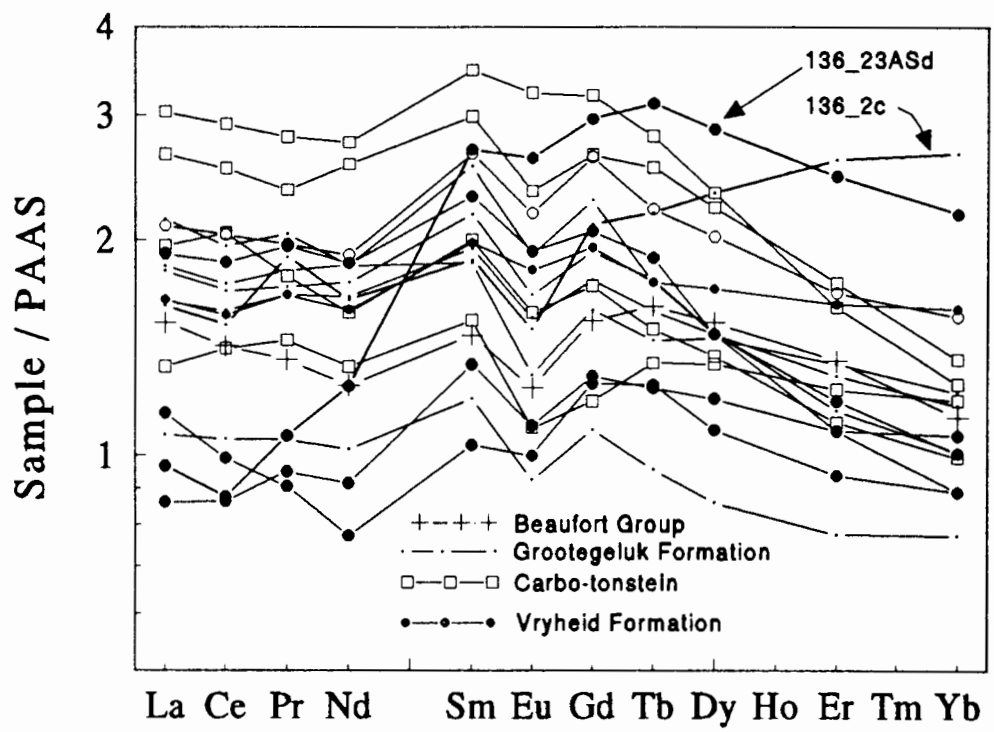

Figure 6.9 The PAAS normalised patterns of the mudstones demonstrate that the Grootegeluk Formation and the Beaufort Group mudstones are enriched in the LREE, have negative Eu anomalies, and are slightly less enriched in the HREE. The Vryheid Formation mudstones, except sample 23ASd which is enriched in the HREE, have approximately the same REE concentrations as PAAS. Sample 2c is also enriched in the HREE compared to PAAS.

as NASC "because there is always the potential for inclusion of aberrant material in a composite sample". Samples 136_2c and 136_23ASd normalised to PAAS, again, are anomalous with respect to their HREE values (Fig. 6.9).

6.3.3.2 Heavy Minerals and REE

According to McLennan (1989) the possibility of a dominating influence on REE compositions by heavy minerals in sedimentary rocks can be deduced in many cases by the examination of sedimentary REE patterns themselves. The enriched HREE patterns of samples 136_2c and _23ASd are therefore most likely to be as a result of an increased heavy mineral content, especially zircon which is highly enriched in the HREE (Gromet and Silver, 1983). Inspection of the whole-rock composition of these two samples reveals that they both have anomalous Zr concentrations with respect to the other mudstones (Fig. 6.1; Table II.3). If the increase of the HREE, Yb, was due solely to the increased concentration of zircon then it would be expected from stoichiometry that sample 136_2c (503 ppm Zr volatile-free), for example, should have 6099 ppm Zr (whole-rock) more than the adjacent sample 136_2b (351 ppm Zr volatile-free; assuming zircon has 253 ppm Yb - Gromet and Silver, 1983). However, sample 2c has only 152 ppm Zr more than sample 2b. It is difficult to account for the additional HREE in sample 2c, based on the whole-rock chemistry, because the only difference in mineralogy of this sample is a high proportion of pyrite that, however, does not normally host REE.

It was noted that even though the carbo-tonstein samples have the most anomalous high Zr values they do not have relatively enriched HREE concentrations (samples 22Ee, 22Ed and 22FSa; Table 6.4). A plot of Zr *vs.* La/Y demonstrates that the Grootegeluk Formation, the Vryheid Formation and the carbo-tonstein mudstones tend to plot in three groups (Fig. 6.10). It is expected that because zircon is enriched in HREE, the La/Y ratio should have an inverse relationship with Zr. This is broadly the case for the Vryheid and Grootegeluk Formation mudstones, but the carbo-tonstein samples which have high Zr values have average La/Y values (Fig. 6.10). There may be several reasons for the difference in the HREE proportion of the carbo-tonstein mudstones. One possible explanation may be that some of the Zr in the carbo-tonstein samples is not in zircon but adsorbed onto the clay fraction which is very high in these samples (~80% of the inorganic matter). Another reason for the differences may be that the mineral fraction in the carbo-tonstein samples has not been through the same sedimentological processes such as weathering, transport and deposition, and therefore has different chemical attributes.

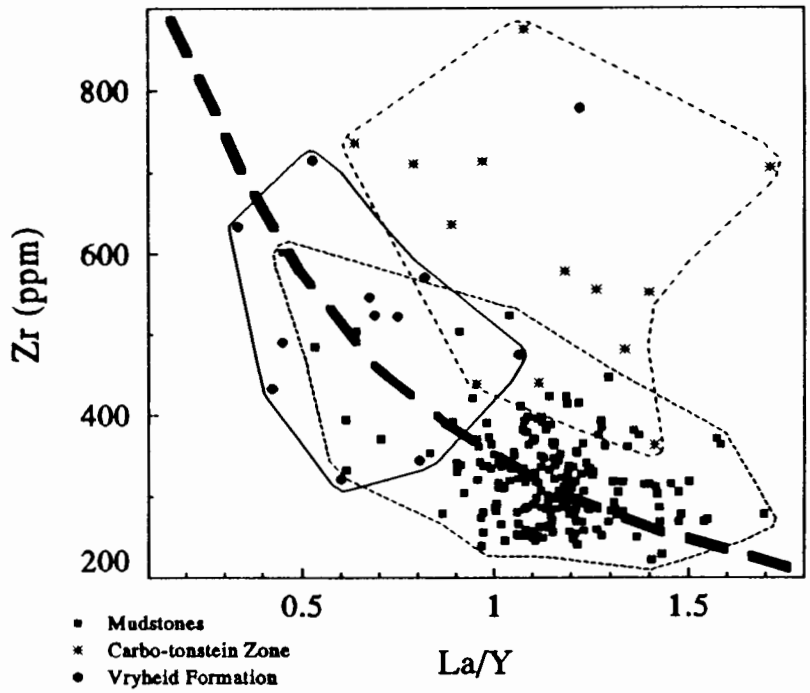

Figure 6.10 A plot of Zr vs. La/Y for all the mudstones in this study. There is a general inverse relationship between Zr and La/Y for the Grootegeluk and the Vryheid Formation samples. Zircon is highly HREE-enriched so it is to be expected that for increased proportions of zircon the La/Y ratio will decrease. This is, however, not the case for the carbo-tonstein samples which have some of the highest Zr concentrations but average La/Y.

6.3.3.3 Eliminating Quartz Dilution and Clay Mineral Concentration of REE

Nesbitt (1979) considered that REE are dominantly transported from the weathering profile by mechanical processes and are not significantly fractionated. Therefore, sedimentary REE patterns may provide an "index" to average provenance compositions (McLennan, 1989). A process that may fractionate REE is sedimentary sorting (Cullers et al., 1979; Reimer, 1985). Cullers et al. (1979) found that the REE reside in the silt and clay-size fraction, and that REE may readily be accommodated in most clay minerals. Quartz which has very low REE abundances is considered to have a REE diluting effect on sediments. Sedimentary sorting will also concentrate heavy minerals, such as sphene, zircon, allanite and monazite which are resistant to weathering. These minerals have high REE abundances that may have REE patterns very different to average source rock composition, and may therefore seriously affect the sedimentary REE pattern.

The REE data (Table 6.4) were recalculated to a quartz-free basis and normalised to an arbitrary kaolinite percentage of 35% to eliminate any increased concentration of REE as a result of greater amounts of clay minerals, or a decrease because of the diluting effect of quartz. The variation in the resultant REE patterns will therefore be independent of quartz and the clay mineral fraction. The quartz and clay contents of the samples were obtained from normative calculations based on the whole-rock chemical composition of the samples (discussed later in Section 6.4). The results of the normalising calculation show that the Grootegeluk

Formation samples have chondrite normalised REE curves that are slightly more closely spaced than in the un-normalised patterns, and also more distinct from those of the Vryheid Formation (Figs. 6.8 and 6.11). The one sample analysed from the Beaufort Formation is still indistinguishable from the Grootegeluk Formation samples after the quartz and clay mineral normalisation. The more compact grouping of the chondrite normalised REE curves suggest that the Grootegeluk Formation mudstones and Beaufort Group mudstone had a common provenance, but that the predominant source of sediments for the Vryheid Formation was different to that of the other samples. The carbo-tonstein samples, however, are indistinguishable from the other Grootegeluk Formation mudstones based on their REE concentrations.

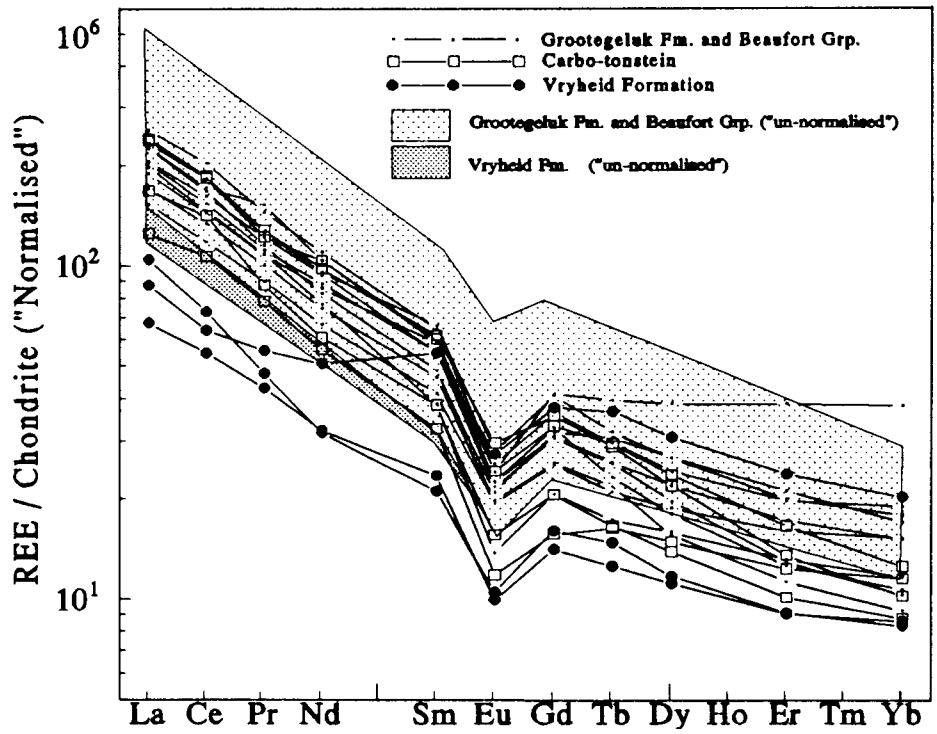

Figure 6.11. The REE plots of the mudstones that have been recalculated ("normalised") quartz-free and with kaolinite concentrations of 35 weight%, and normalised to chondrite. The recalculation minimises the REE dilution effect of quartz and the concentration effect of clay minerals, and therefore permits better comparison of the samples. The recalculation of the chondrite normalised REE data does not change the shape of the plots but the absolute concentrations. The REE curves of the Grootegeluk Formation and Beaufort Group mudstones are closer spaced than the "un-normalised" patterns (see shading), and the Vryheid Formation mudstones which overlap with the Grootegeluk Formation in the "un-normalised" patterns are more distinct from the other mudstones. The carbo-tonstein curves are less enriched in REE after the "normalisation" than the other mudstones because of their high kaolinite and low quartz concentrations.

6.3.3.4 Mudstone Provenance from REE

The chondrite normalised REE values of the granite (G1) and diabase (W1) standards (Mason and Moore, 1982; Table 6.6) are compared to the REE fields of the mudstones in this study (Fig. 6.12). The G1 values, indicative of granitoids, typically have LREE enriched and slightly depleted chondrite normalised HREE patterns with strong negative Eu anomalies. In

contrast W1 values, typical of basalts, have less-enriched LREE patterns, no negative Eu anomaly, and slightly more enriched chondrite normalised HREE patterns. The Grootegeluk Formation mudstones have REE patterns in-between these two standards, but more granitic than basaltic. The Vryheid Formation mudstones also have patterns in-between these two standards but more mafic than the Grootegeluk Formation mudstones. The carbo-tonstein samples are indistinguishable from the rest of the Grootegeluk Formation mudstones but tend to plot at the base of the Grootegeluk Formation field.

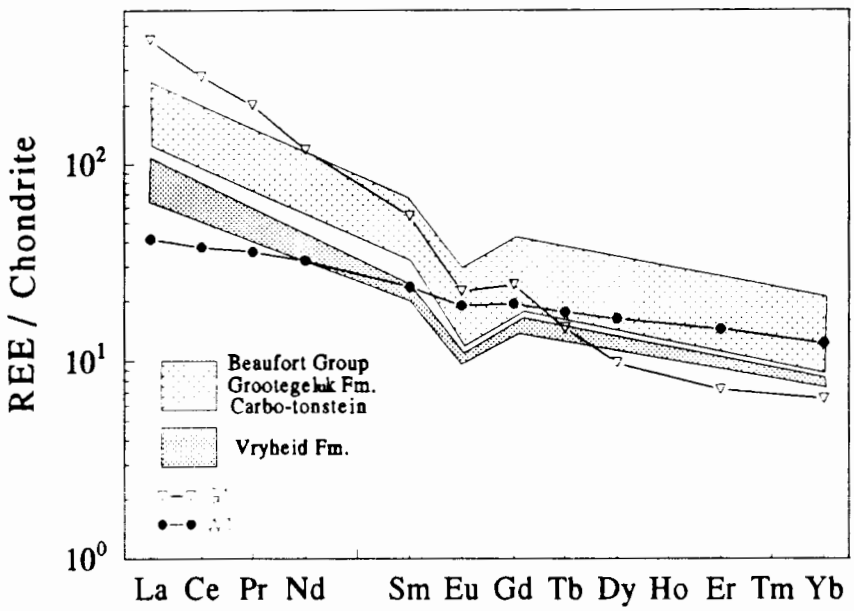

Figure 6.12 The chondrite normalised REE values of the granite (G1) and diabase (W1) standards (Mason and Moore, 1982) are compared to the chondrite normalised REE fields of the mudstones in this study which are normalised quartz-free and with a kaolinite concentration of 35 weight%. The G1 values typically have enriched LREE, strong negative Eu anomalies and slightly depleted HREE patterns. In contrast W1 has relatively smaller LREE-enriched values, no negative Eu anomaly and slightly enriched HREE patterns. The Grootegeluk Formation mudstones have REE patterns in-between these two standards, but closer to granitic than basaltic patterns. The Vryheid Formation mudstones have patterns in-between these two standards but slightly more mafic than the Grootegeluk Formation mudstones. The carbo-tonstein samples are indistinguishable from the rest of the Grootegeluk Formation mudstones but tend to plot at the base of the Grootegeluk Formation field.

6.4 NORMATIVE MINERAL CALCULATIONS

6.4.1 INTRODUCTION

Quantitative determination of mineral abundances in argillaceous sediments by point-counting techniques would be an extremely difficult if not impossible task. The irresolvable mineralogy of many lithic fragments and matrix components, especially in organic-rich mudstones, and the similarity between the optical properties of quartz, kaolinite, and feldspar are a major hindrance. X-ray diffraction methods are capable of identifying minerals present in a representative sample of rock powder, but variations in mineral crystallinity, mixed-layering in phyllosilicates, spectral interferences, high background counts in the case of organic-rich samples (low mass absorption coefficients) generally allow only limited use of XRD as a quantitative analytical method.

An alternative to these methods is the calculation of a normative mineral concentration, similar to CIPW norm calculations applied to igneous rocks. Normative methods for sedimentary rocks have been proposed by Nicholls (1962) and Garrels and Mackenzie (1971), and it is on the basis of their rationale, with a few modifications to suite the range of minerals observed in the Grootegeluk Formation, that a computer program was written to calculate the normative mineralogy of the mudrocks from whole-rock chemical compositions. The sequence of allocating elements to the various minerals is a function of observed sedimentary mineral assemblages, mineral stabilities in surficial environments, and the restriction of certain elements to specific minerals, for example phosphorous is completely contained in apatite. The program was designed to calculate normative compositions of minerals that occurred in major and minor proportions and(or) were important for the interpretation of palaeo-environment conditions. Elements have been assigned to minerals on the basis of data from XRD and optical petrology (Chapter 4). More complex normative programs have recently been published (Cohen and Ward, 1991; Merodio et al., 1992).

6.4.2 METHOD OF NORMATIVE CALCULATION

In deriving a sedimentary norm from oxide percentage data, the following principles or procedures have been applied:

1. Phosphorous is assumed to be present in apatite. Although a number of other phosphorous-bearing minerals such as goyazite-gorceixite and crandallite may be present, apatite is the dominant phosphate mineral in most types of sedimentary deposits. Excess P_2O_5 is assumed to be organic-bound phosphorus.
2. Calcium is assigned first to apatite and the remainder to calcite. Montmorillonite is not calculated because of the very low MgO (<0.75%) and Na_2O (usually <0.15%) concentrations in the samples. In addition the exact composition of montmorillonite, which probably occurs as a mixed-layer clay with illite, is not known and therefore the normative montmorillonite is highly dependent on an assumed Ca:Na ratio. Plagioclase was not detected in any of the samples.
3. Sulphur, if present, is assumed to occur as pyrite. No gypsum (calcium sulphate) was observed. In some samples there is an excess S and this is assumed to be organic-bound S.
4. Excess iron that remains after allocating S to Fe as pyrite, is assigned to siderite.
5. Although there are two K-bearing minerals (illite and microcline) in the Grootegeluk Formation only normative illite has been calculated. Microcline, which occurs within the same suite of samples as illite at the top of the sequence, was detected by XRD in only 3 samples from both boreholes. In the samples that do contain microcline the normative illite concentrations will be exaggerated. Microcline, however, is assumed to alter to a mixture of illite, smectite, kaolinite and quartz and therefore the normative illite concentration will be a good indicator of the degree of alteration of feldspars.

6. The Al and Si left over after calculation of the illite percentage are assigned to kaolinite, and any remaining SiO_2 is expressed as quartz. If Al_2O_3 rather than SiO_2 is left after the kaolinite calculation, it is expressed as gibbsite.
7. Carbon dioxide and H_2O^+ concentrations have not been determined. LOI data are available but contributions from organic carbon, carbonate mineral, sulphur oxidation, and water (H_2O^+) are unresolved. Because the mudstones are essentially clays, and excess CaO and FeO are predominantly associated with elevated concentrations of calcite and siderite, H_2O^+ and CO_2 are added to the calculations in surplus.

6.4.3 RESULTS

The results of the mineral calculations are presented in Figure 6.14A,B,C. The mineral data are expressed as volatile-free, recalculated to 100%. Before discussing the results of the mineral calculations of all the samples, the results from quantitative XRD analyses of selected samples are compared to the results obtained by the normative mineral program in this thesis and also to the results obtained by the normative mineral program of Cohen and Ward (1991). The quantitative XRD analyses were done by the Geological Survey in Pretoria (D. Bühmann analyst; Table 6.7). The Cohen and Ward (1991) program permits the choice of additional mineral types such as K-feldspar, smectite, anatase and dolomite not calculated in the program used in this study (Table 6.7).

6.4.4 XRD vs. NORMATIVE MINERAL PROPORTIONS

6.4.4.1 Quartz and Kaolinite

In the case of the major minerals, kaolinite and quartz, the XRD method estimated quartz to be higher in all samples by 9-19% than method A and B, and kaolinite to be slightly lower except in samples which had very high proportions of kaolinite, for example sample 136_22Ee where proportions differed by 13% between the two techniques (Table 6.7).

6.4.4.2 K-Bearing Minerals and Smectite

A comparison of the K-bearing minerals, illite and K-feldspar, and smectite (montmorillonite) results also revealed a poor correlation. Smectite was not reported in the XRD results and was not calculated in the program used in this study. The smectite proportion calculated in the Cohen and Ward (1991) program was as expected low, but dependent on the proportion of Ca and Na, and Fe and Mg selected in the options of the program. The proportions of microcline determined by XRD in samples 136_1Ca and _2b were lower than the K-feldspar proportions calculated in the Cohen and Ward (1991) program. The formula for K-feldspar used in the Cohen and Ward (1991) program does not include any Na, which is assigned to either halite, smectite or plagioclase. XRD analyses, however, indicate that microcline is present in some of the samples and that some solid solution between K and Na

is expected. The proportion of illite and K-feldspar calculated in the Cohen and Ward (1991) program is also, again, dependent on the options selected in distribution of K into illite and K-feldspar. The proportion of illite calculated in the program used in this study is exaggerated, especially in the samples which contain microcline, because all the K_2O is calculated as illite. The illite concentration calculated by the Cohen and Ward (1991) program is higher by about 7% for the samples which have relatively high K_2O concentrations than concentrations measured in the XRD analyses.

Table 6.7 Mineralogical results obtained from XRD (X) by the Geological Survey in Pretoria, the Cohen and Ward (1991) normative mineral program (A), and the normative mineral program used in this study (B). The Cohen and Ward (1991) program has the options of calculating a wider range of minerals than the program used in this study. The compositions of some of the minerals that occur only in minor quantities and in only a few samples are not known, and therefore assumptions have to be made which clearly can give extremely different results. Options selected in the Cohen and Ward (1991) program are: potassium distribution illite:K-feldspar = 1:1; smectite Ca:Na = 0:1, Mg:Fe = 1:1, and Mg initially into smectite then dolomite. The results from the quantitative XRD analyses were normalised to a 100%. The XRD analyst was not able to account for a 2.03Å peak in the samples, and the proportions from this peak are excluded from the normative calculation.

Sample Depth (m)	137_0c +0.1			136_1Ca -2.5			136_2b -8.2			137_7c -21.4			137_8b -22.7			136_22Eb -64.4			136_22Ee -66.2		
Method	X	A	B	X	A	B	X	A	B	X	A	B	X	A	B	X	A	B	X	A	B
Quartz	41	32	35	60	41	44	52	33	36	52	42	43	51	35	37	27	18	19	26	14	14
Kaolinite	20	17	15	27	30	14	29	28	21	37	42	35	43	50	44	59	64	64	50	63	63
Illite	5	4	10	7	15	40	7	14	39	7	7	20	3	7	18		3	8		3	6
Smectite		.6			1.4			2.2			2			1			2			2	
Fsp./Microcl.		2		2	8		3	8			4			4			2			1	
Siderite		26	20	4	3	3	5	4	3		1	.8		1	1	9	5	4	13	7	7
Pyrite	15	12	15		.2	.2		.3	.4		.5	.7		.2	.3		.7	1		.6	.9
Marcasite	20																				
Apatite		.1	.1		.2	.2		.2	.2		.1	.1		.1	.1		1.4	1.5		2.3	2.4
Calcite		5	5		.3	.3		.3	.3		.1	.1		.1	.1		2	2	4	5	5
Dolomite		1.9			1.3			1.1			.4			.5		4	1.6		4	1.5	
Anatase		.4			.7		4	.8		4	.8		2	1		5	1.1		4	1.5	
2.03Å not allocated	5			8			4			2						7			19		

6.4.4.3 Iron-Bearing Minerals

Determination of pyrite contents from the two techniques correlate reasonably well except for sample 137_0c which has major proportions of iron sulphide. The XRD report indicated that the sample had 35% sulphide (pyrite and marcasite) whereas the normative calculations indicate that it is chemically only possible to have 13-15% FeS_2. No siderite was reported in sample 137_0c in the quantitative XRD analyses but about 20% normative siderite

was calculated. Siderite was seen in a thin-section of this sample and XRD analyses done in this study confirmed the presence of siderite. Siderite concentrations estimated in both techniques correlate reasonably well in the other samples.

6.4.4.4 Apatite, Calcite and Anatase

Apatite was not reported in the XRD analyses but up to 2% apatite in sample 136_22Ee was calculated in the normative calculations. The normative mineral proportions are calculated on a volatile-free basis so the actual concentrations in the carbonaceous mudstones would be below the detection capabilities of the XRD spectrometer. XRD analyses only reported calcite in one of the samples (136_22Ee). Comparison of the calcite estimation by the two techniques was in good agreement in the one sample. Dolomite was reported in the XRD analyses for samples 136_22Eb and _22Ee but proportions suggested are higher by a factor of 3 than calculated in the Cohen and Ward (1991) program. Anatase was reported in five of the samples in the XRD report but as in the case of dolomite, estimation of anatase was higher by a factor of about 5 more than the whole-rock chemistry of the samples permitted.

6.4.4.5 Conclusion

The two techniques, XRD and normative mineralogy, used to estimate mineral proportions both have their short-comings. Overall there is a general agreement between the two methods concerning the relative changes in the proportions of the major minerals, i.e. that kaolinite increases and quartz decreases with depth, but not in the absolute concentrations. The XRD technique is not sensitive enough to identify and estimate the proportions of minor minerals that may be important for geological and palaeo-environmental interpretations, and in some cases incorrect identification of peaks and(or) peak interferences can give mineralogical results that are chemically impossible (e.g. sulphides in sample 137_0c). If minor minerals, such as anatase, do occur in high enough concentrations to be identified by XRD, the proportions are generally over estimated. Normative mineral calculations overcome most of the short-comings experienced by XRD, but normative results are often dependent on a choice of chemical options based on speculation. The calculation of mineral proportions is especially suitable, however, where a large number of samples are under investigation.

Reasonable mineral estimations, while perhaps not better than XRD values, can be obtained easily with substantial savings in time and money. To achieve meaningful results a reasonable knowledge of the sediments' mineralogy is required before applying normative calculations.

6.4.5 NORMATIVE MINERAL DISTRIBUTION

The normative mineral concentrations in the samples from borehole 136 have been plotted in Figure 6.13, and have been simplified in Figure 6.14. The distribution of the mineral proportions with depth are discussed below.

6.4.5.1 Quartz, Kaolinite and Illite

The plots of the major mineral variation demonstrates that the Grootegeluk and Vryheid Formation contact is characterised by an abrupt increase in the concentration of quartz in the Vryheid Formation samples (Figs. 6.13 and 6.14). The plots also demonstrate that the lower half of the borehole is dominated by kaolinite. Normative kaolinite decreases and normative quartz increases upwards in the Grootegeluk Formation. The quartz proportions in the Grootegeluk Formation generally vary in a very coherent manner except for the samples in the carbo-tonstein zone where the quartz contents abruptly decrease (Figs. 6.13 and 6.14). Above the 35 m depth, and up to the last mudstone band below the topmost coal seam, illite, and to a lesser extent smectite and the feldspar microcline, increase substantially. Above the topmost coal seam kaolinite increases at the expense of illite. As discussed above (Section 6.3.2), the illite concentration is exaggerated because the K_2O that is present in a few samples as microcline has also been calculated as illite, but the relative variation of the K-minerals and kaolinite is well illustrated.

6.4.5.2 Siderite and Pyrite

The mineral calculations confirm the findings in Chapter 4 that siderite is generally the dominant Fe-bearing mineral, especially within the carbo-tonstein zone. Normative siderite and pyrite also increase in the top 10 m of the Grootegeluk Formation and in the Beaufort Group mudstones, immediately above the topmost coal seam.

6.4.5.3 Calcite and Apatite

The normative calcite and apatite variations are as expected (see Section 6.2.1.5). The carbo-tonstein zone has both high apatite and calcite proportions, and a 10 m zone above the carbo-tonstein is dominated by apatite only (and high Sr and Ba). The calcite above the carbo-tonstein is present mainly as cleat-filling.

6.4.6 SUMMARY

The normative mineral distributions confirm the general mineral distributions proposed in Chapter 4, and permit a quick and inexpensive method of establishing mineral proportions for a large number of samples. An important advantage of normative calculations over quantitative XRD analyses is that the relative variation of minerals that are present below detection limits for XRD can easily be examined. The normative mineral proportions at best, however, probably only provide semi-quantitative results.

Figure 6.13 The normative mineral proportions of the mudstone samples, calculated from their major element compositions, are plotted against depth in the borehole (136) relative to the topmost coal seam in the Grootegeluk Formation. The mineral proportions are calculated on a volatile-free basis. The curves have been simplified and re-drawn in Figure 6.14.

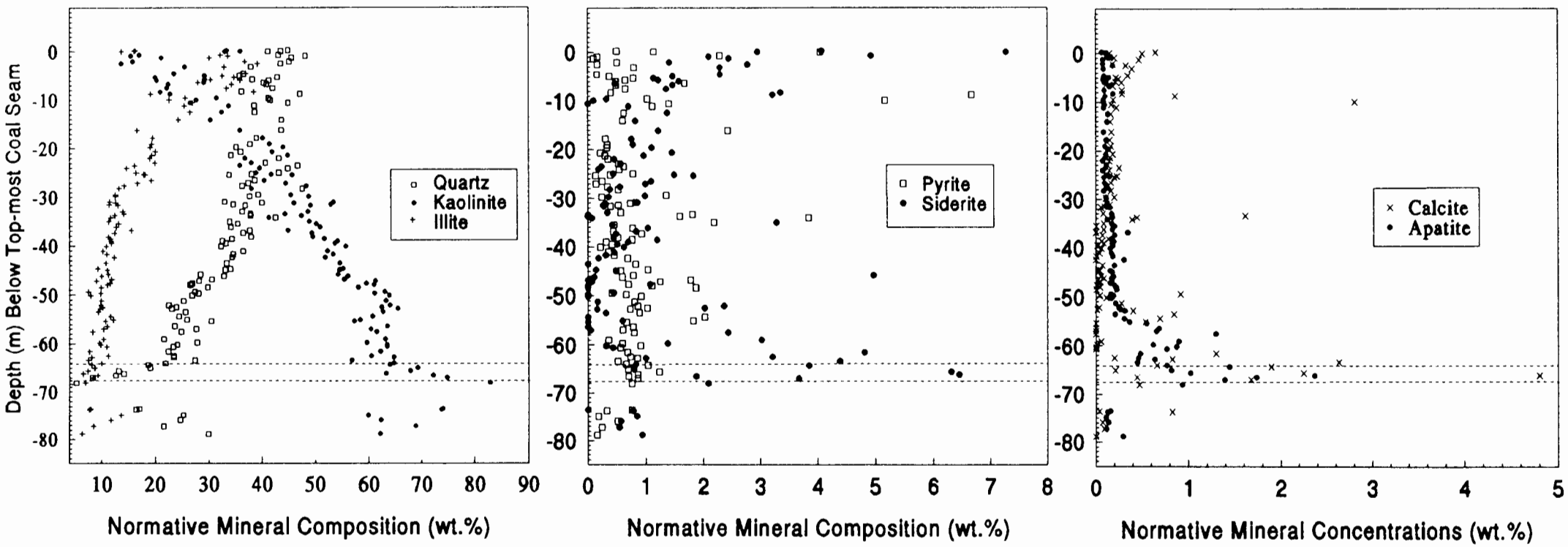

Figure 6.14 Generalised variation of the normative mineral concentrations based on curves in Figure 6.13.

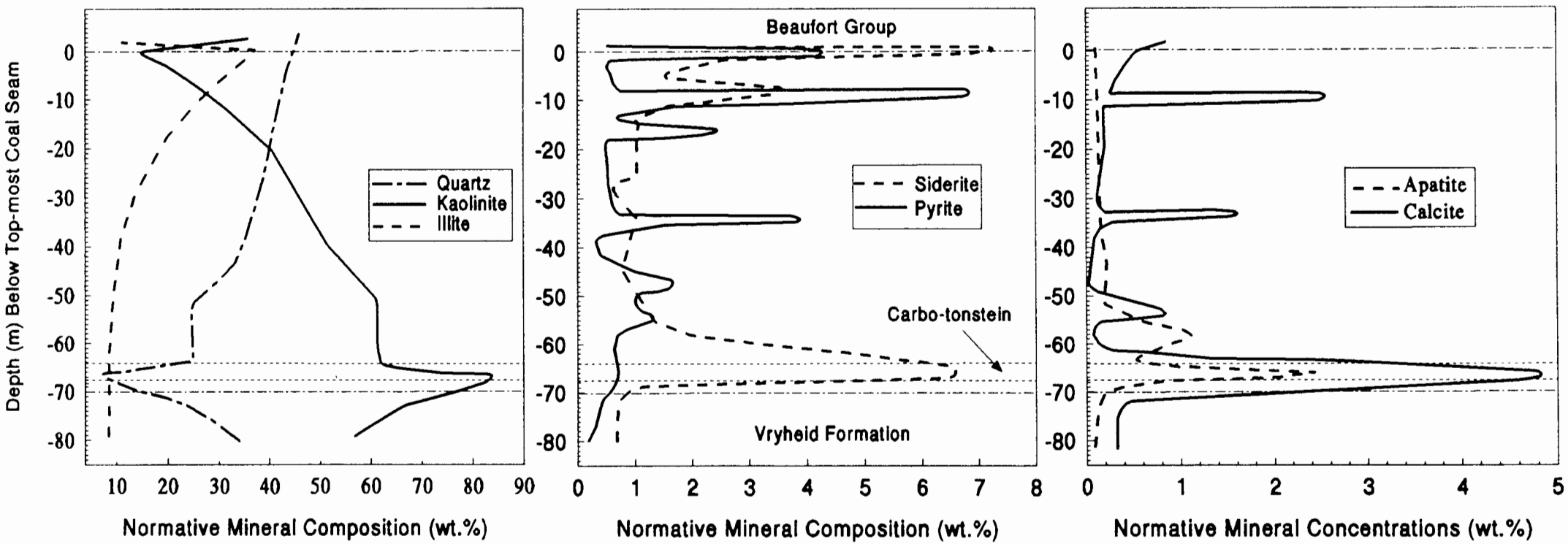

Deductions that can be made from the normative mineral variations are:

(1) The contact of the Grootegeluk Formation with the under-lying Vryheid Formation is characterised by a reversal of quartz and kaolinite concentrations.

(2) The carbo-tonstein zone is anomalous with respect to its normative kaolinite, siderite, apatite and calcite concentrations. A mineralogical investigation of the carbo-tonstein mudstones revealed that the kaolinite occurs as relatively large grains, the calcite is predominantly fine-grained and within the kaolinite matrix, and the apatite occurs both as an alteration mineral within the kaolinite and as small (about 20μm) anhedral grains (Chapter 4);

(3) Anomalous but smaller proportions of apatite occur immediately above the carbo-tonstein zone and are also correlated with anomalous concentrations of Ba and Sr. Kaolinite above the carbo-tonstein zone is generally micro-crystalline and does not exhibit the same textures as seen within the carbo-tonstein zone samples;

(4) The steady increase in quartz concentration upwards in the formation indicates a higher energy depositional environment or a region closer to the source of the sediments;

(5) The presence of microcline, and the increased proportion of the clay mineral illite (and smectite), at the expense of kaolinite, in the top of the Grootegeluk Formation is indicative of less chemical weathering of the mudstones; and

(6) The contact with the topmost coal-seam and the overlying grey massive mudstones is characterised by a rapid decrease in illite and a concomitant increase in kaolinite. The concentration of quartz increases steadily throughout the Grootegeluk Formation. The rapid variation in clay mineral proportion at the Grootegeluk Formation and Beaufort Group contact, without a substantial change of the energy in the depositional environment, suggests that chemical alteration in the depositional area rather than in the source area was the dominating factor.

6.5 CONTROLS ON THE CHEMICAL COMPOSITION OF THE MUDSTONES

6.5.1 INTRODUCTION

Although the chemical composition of mudstones may be used to constrain source-rock composition, the geochemistry of the mudstones can be controlled by several factors such as the influence of tectonics, degree of weathering (chemical or mechanical), transport and sedimentation, clay-mineral adsorption, organic adsorption and bonding, and effects of diagenesis. It is not always possible to distinguish the effect that each of the factors may have had on the eventual composition of the mudstones, but fortunately some elements are affected to different extents by these processes.

6.5.2 PROVENANCE

Considerable progress has been made in recent years in the use of bulk properties of fine-grained rocks for the purpose of provenance studies. Mudstones are very well suited for provenance studies of clastic sediments because of their relative homogeneity, their post-depositional impermeability, and because they dominate the sedimentary mass balance (Taylor and McLennan, 1985).

The composition of mudrocks is directly related to the composition of the parent material (Nesbitt et al., 1980; Nesbitt and Young, 1982). Secondary processes such as weathering, transport, sedimentation, diagenesis, etc. can have an effect on the composition of mudrocks, as discussed above, and therefore for provenance studies it is best to use elements that have little mobility under the expected geological conditions. Taylor and McLennan (1985) pointed out that such elements should possess very low partition coefficients between natural waters and upper crust and short oceanic residence times. Elements that meet these criteria are, for example, Al, Ti, Th, Sc and the REE (Taylor and McLennan, 1985). Of great importance was the observation by Taylor and McLennan (1985) that the ratios of these critical elements was not affected by weathering processes and that ratios can minimise the effect of mineral fractionation. Based on evidence from the REE concentration of the mudstones (section 6.3.3.3), and in following discussions (section 6.5.4), it is proposed that secondary processes in the mudstones were not significant enough to preclude the use of the elements proposed by Taylor and McLennan (1985) in predicting the composition of the source rock material.

Several major and trace element plots can be used to determine the composition of provenance rocks. The ratio of TiO_2 and Al_2O_3 has been used by McLennan et al. (1979), Amajor (1987) and Schreiber et al. (1992), and La-Th-Sc ternary diagrams by Taylor and McLennan (1985) and Wronkiewicz and Condie (1987) to distinguish between granitic and basaltic sources. The TiO_2 and Al_2O_3 plot of the mudstones in this study suggests that most of the Grootegeluk Formation samples had a similar origin (Fig. 6.15). According to the granitic and basaltic fields defined in the TiO_2 and Al_2O_3 plot, the average composition of the provenance area of the Grootegeluk Formation mudstones was greater then 80% granitic, slightly more granitic than PAAS, and close to the average crustal ratio. The presence of microcline in some of the less altered mudstones also suggests that the sources of those sediments were low temperature granitic or gneissic rocks. The TiO_2 and Al_2O_3 composition of the carbo-tonstein and the Vryheid Formation samples, however, suggest that the provenance compositions of these samples were more mafic than the Grootegeluk Formation. The anomalous concentrations of P_2O_5 and an array of anomalously high concentrations of trace elements suggest that the samples in the carbo-tonstein zone did not have the same source as the rest of the mudstones.

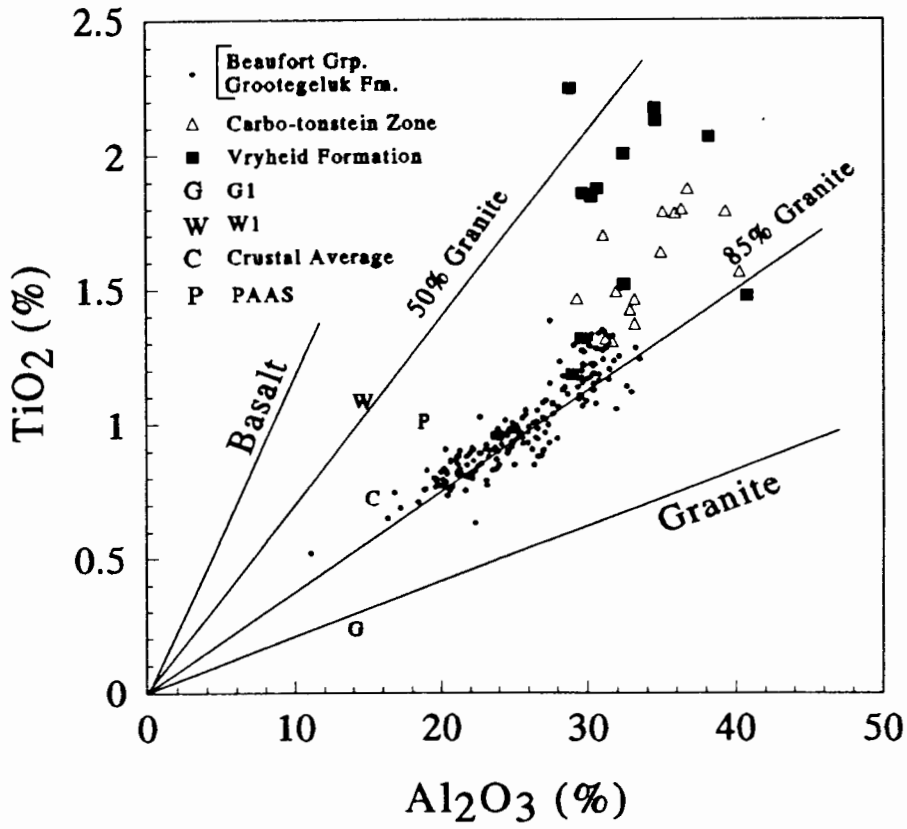

Figure 6.15. The TiO_2 and Al_2O_3 mudstone values are compared to the values of PAAS (Taylor and McLennan, 1985), the G1 (granite) and W1 (dolerite) standards and the crustal average (Mason and Moore, 1982). TiO_2 and Al_2O_3 compositions for typical basalts and granites are from Cox et al. (1979). The lines of constant ratio for different proportions of granite and basalt, based on Cox et al. (1979) compositions, are also presented.

The La-Th-Sc ternary diagram indicates a similar relationship between the sediments as the TiO_2 and Al_2O_3 plot (Fig. 6.16). The Grootegeluk Formation mudstones have a source which is more granitic than PAAS, whereas the Vryheid Formation samples have a source that is more mafic than either the Grootegeluk Formation or PAAS. The samples from the Beaufort Group are indistinguishable from the Grootegeluk Formation samples, and the carbo-tonstein zone samples overlap the compositions of the Grootegeluk and the Vryheid Formations.

6.5.3 WEATHERING IN THE SOURCE AREA OF THE MUDSTONES

A depletion in Na, Ca, and Sr observed in tropical rivers and the absence of any significant amounts of easily soluble cations in fine-grained sediments points to high rainfalls and concomitant intensive chemical weathering in the source areas (Barth, 1952; Martin and Maybeck, 1979; Nesbitt et al., 1980). Weathering conditions and climate have been inferred by application of a variety of chemical indices based on abundances of major elements (Englund and Jorgenson, 1973; Björlykke, 1974; Nesbitt and Young, 1982). The relative abundance of weathering products in sediments (or the relative proportion of primary minerals

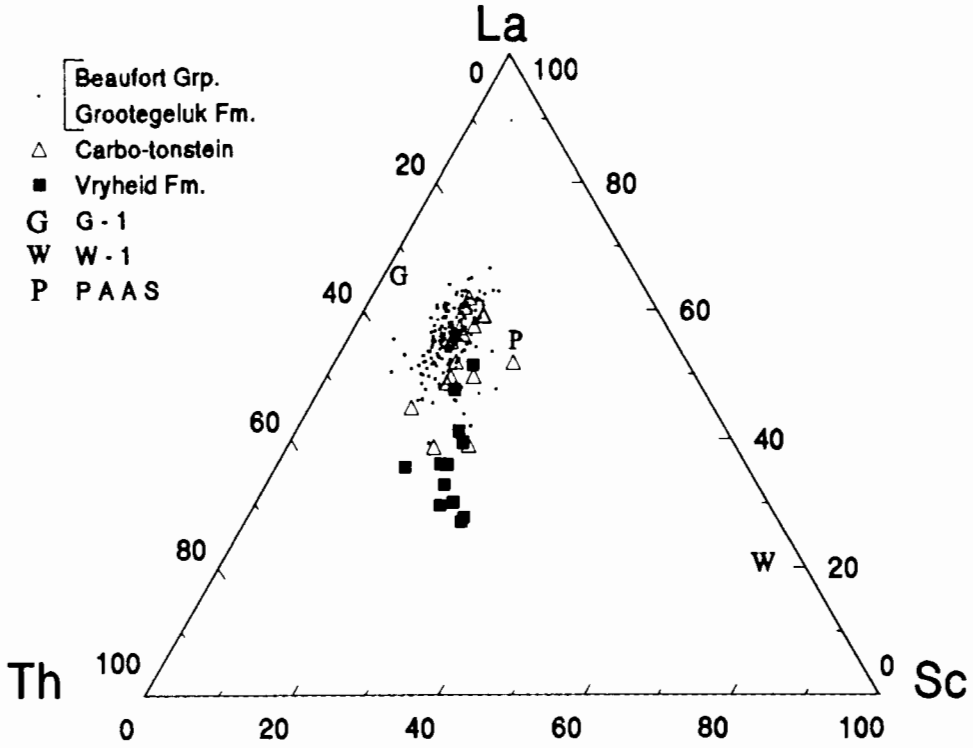

Figure 6.16. The ternary plot of La-Th-Sc. The mudstone values are compared to the values of PAAS (Taylor and McLennan, 1985), the granite (G1) and diabase (W1) standards (Mason and Moore, 1982).

and secondary weathering products) may be quantified using a chemical index of alteration (CIA; Nesbitt and Young, 1982), calculated from the following oxide concentrations:

$$CIA = \frac{Al_2O_3}{Al_2O_3+CaO+Na_2O+K_2O} \times 100\ \%$$

:where CaO represents Ca associated with silicate phases only

The CIA values have been calculated for the mudstones in this study and are plotted against their depth below the topmost coal seam in Figure 6.17A. Generally the proportions of calcite and ankerite in the mudstones are low, except in the carbo-tonstein zone. The correction for the CaO present in the carbonate minerals has not been made other than in the carbo-tonstein zone samples. The correction of Ca in apatite has been made based on the normative proportion of apatite in a sample. X-ray diffraction analyses, in this study and by the Geological Survey in Pretoria, did not detect any other CaO-bearing mineral other than Ca-carbonate and apatite. Based on these results the CaO concentrations of samples between 52 and 70 m were assumed to be within the carbonate and phosphate minerals. The CIA values of the rest of the samples are therefore minimum values because no correction has been made for CaO in carbonate minerals. A plot of the Al_2O_3 and Na_2O composition of these and other selected average mudstones are also presented in Figure 6.17B. The proportion of aluminium, which is a relatively immobile element, and Na, which is relatively soluble element, gives an

indication of the degree of chemical weathering in the source area, or the degree of alteration that has taken place after deposition of the mudstones.

The CIA values of the Grootegeluk Formation mudstones increase steadily with depth in the formation. As expected from mineralogical studies, the CIA values of the carbo-tonstein which is dominated by kaolinite are just less than 100. The relatively lower and decreasing CIA values of the samples in the upper portion of the formation, indicating less chemical alteration, are compatible with the presence of the feldspar microcline, and the clay minerals montmorillonite-illite which contain the relatively more soluble elements such as Ca, Na and K. The overall steady changes in CIA values of the Grootegeluk Formation are in contrast to the abrupt change in values at formation contacts. The CIA values of the Beaufort Group mudstone samples increase rapidly, immediately above the topmost coal seam, and the values in the samples immediately below the carbo-tonstein zone decrease to approximately the same values that were in the samples above the carbo-tonstein zone, and then increase again with depth.

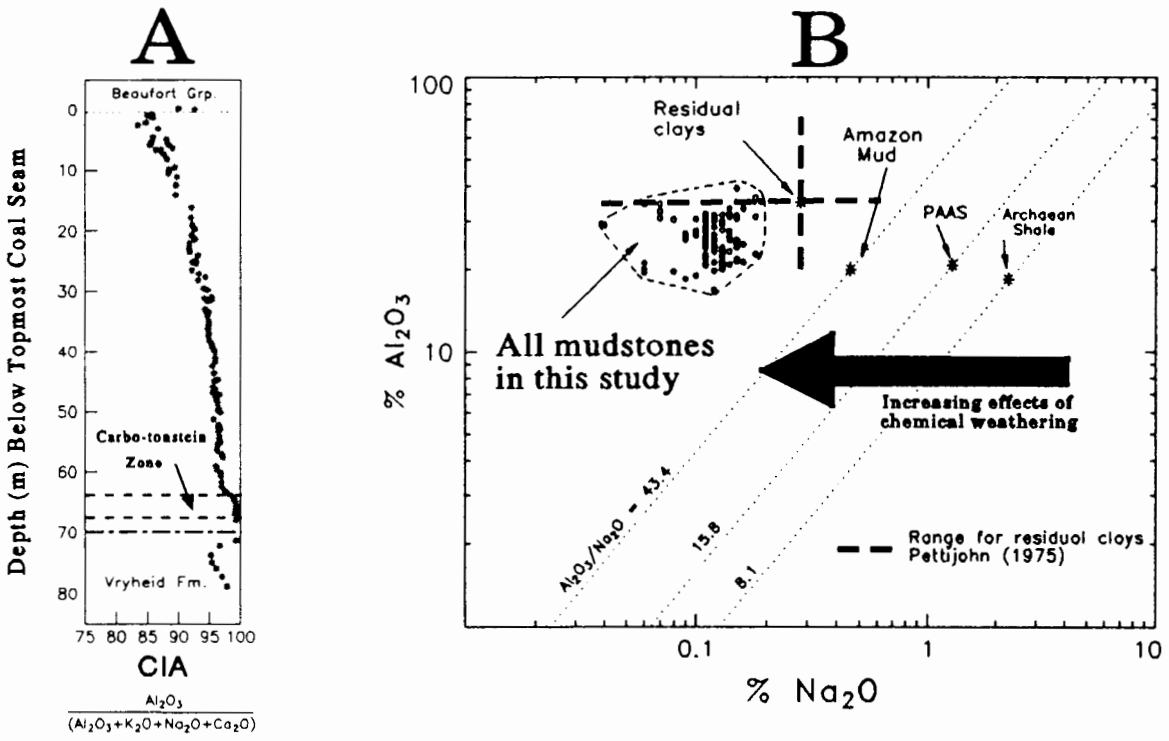

Figure 6.17. **A.** The CIA values of the mudstones plotted against depth below the top-most coal seam. The CIA values have been stoichiometrically corrected for Ca within apatite but not for Ca within carbonate minerals. The CIA values are therefore minimum values. Based on XRD and thin-section observations, Ca in the carbo-tonstein samples has been assumed to be all within calcite and ankerite. **B.** The Al_2O_3 and Na_2O values of the mudstones in this study are compared to the values of PAAS, average Archaean Shale (Taylor and McLennan, 1985), Amazon Cone muds (Kronberg et al., 1986), and the range of values for residual clays (Pettijohn, 1975).

Various investigators have utilized the CIA of Nesbitt and Young (1982) to evaluate the intensity of weathering in the source area of shales (Wronkiewicz and Condie, 1987). According to Wronkiewicz and Condie (1987) relatively consistent CIA values indicate little change in

palaeo-climate, as well as stable tectonic conditions within the source area. Abrupt decreases in the CIA values indicate climatic changes and greater tectonic instability. However, there is some uncertainty concerning the interpretation of CIA values because of possible post-depositional mobility of alkali and alkali earth elements. Sediment transport can also, via hydraulic sorting, lead to compositional fractionation as a result of change in sediment-size fractions (Nesbitt, 1979; Reimer, 1985; Cullers et al., 1987). It has been demonstrated in Chapter 4 and in the normative mineral calculations that the concentration of quartz, and quartz grain-size, also increase steadily upwards in the formation (Fig. 6.13; 6.14)). Therefore the lower CIA values in the upper part of the Grootegeluk Formation may result from changes in the energy or pH of the depositional environment or a progression of the shore-line, in addition to changes in the palaeo-climate of the source areas. The abrupt change of clay mineralogy and higher CIA values in the samples which overlie the upper-most coal seam in the Grootegeluk Formation may be an important clue to the demise of coal in these sediments.

The range of the CIA values (85-100) and the plot of the relatively immobile Al against the easily soluble Na (Fig. 6.17 A and B) demonstrate that the mudstones in this study are, as a whole, very depleted in the more soluble elements compared to the compositions of some other rocks such as PAAS and average Archaean shales (Taylor and McLennan, 1985), Amazon mud derived from highly weathered sources (Kronberg et al., 1986) and even residual clays (Pettijohn, 1975). Mudstone compositions (Pettijohn, 1975) typically have intermediate CIA values of about 72-75, indicating that weathering effects have not proceeded to the stage where alkali and alkaline earth elements are substantially removed from the clay minerals.

The overall high CIA values and the highly residual nature of all the mudstones illustrated in the Al_2O_3 vs. Na_2O plot can be interpreted in several ways. The plots could indicate that:

(1) these mudstones have under-gone a high degree of chemical weathering perhaps as a result of severely wet and humid palaeo-climatic conditions;

(2) that alteration during deposition or burial may have taken place because of the highly acidic pore-waters in the organic-rich sediments and(or);

(3) that the source of these sediments may have been high Al, and low alkaline and alkaline earth sediments or meta-sediments.

It is difficult to distinguish between the possible factors causing the residual nature of the mudstones, and inferring palaeo-climatic conditions based on the chemistry of the mudstones is not prudent. The anomalous character of the mudstones from the carbo-tonstein zone is again emphasized in Figure 6.17A.

6.5.4 TRANSPORT AND SEDIMENTATION

Although the composition of mudrocks is directly related to the composition of the parent material and the prevailing weathering regime in the source area (Nesbitt et al., 1980;

Nesbitt and Young, 1982) other processes such as transport and sedimentation can have an effect on the composition of mudrocks (Nesbitt, 1979; Reimer, 1985; Cullers et al., 1987; Wronkiewicz and Condie, 1987).

The chemical relationships for different sediments can be explained in most cases by the concentration of clay minerals at the expense of quartz and feldspar in the finer-grained fractions. This results in a decrease in silica and a corresponding increase in the abundances of most other elements. It has been demonstrated that the quartz:clay ratio of the mudstones in this study changes steadily with depth (Fig. 6.14). It has, however, also been demonstrated in the REE discussion (Section 6.2.3.3) that recalculating to a quartz-free and equal kaolinite concentration, the overall chondrite normalised REE do not change significantly, although the Grootegeluk Formation REE patterns are perhaps a little more coherent and the differences between the Vryheid Formation and the Grootegeluk Formation mudstones are enhanced.

The process of hydraulic sorting of minerals can concentrate minerals which have high specific gravities and are resistant to weathering. These minerals tend to be deposited in sediments with an overall larger grain size and higher quartz abundances. For example zircon because of its relatively high specific gravity (4.6-4.7) is more often concentrated in sandstones by hydrodynamic sorting rather than in low energy mudstone formations (Krauskopf, 1967). The Zr concentrations of the Grootegeluk Formation mudstones are generally constant. In a few samples such as at the base of the microcline-illite zone (depth 8.7 m, sample 2c) and in the carbo-tonstein zone the Zr concentration does increase relative to the other samples (Fig. 6.1). This increase in Zr concentration at the base of the microcline-illite zone, however, is not obviously related to hydraulic sorting processes because the quartz:clay ratio does not change significantly in these samples. The highly anomalous Zr concentration in the carbo-tonstein zone is very difficult to reconcile with a sedimentary sorting mechanism because the rocks are composed essentially of kaolinite. Thin-section studies of samples from the Vryheid Formation reveals that some samples do have fine sedimentary structures but, again, the relatively low quartz:clay ratio of these samples negates the possibility of heavy mineral concentration due to hydraulic sorting, as would be expected for quartzite.

Some elements have been found to be associated with and even concentrated by organic matter in highly carbonaceous sediments (Tourtelot, 1979). However, all the elements, except perhaps S, in the carbonaceous mudstones do not appear to be predominantly associated with the organic matter.

It is proposed therefore that the conditions during transport and deposition did not vary enough to cause significant changes in the concentration of immobile elements.

6.5.5 PALAEO-SALINITY CONDITIONS DURING DEPOSITION OF SEDIMENTS

Variation of clay type in sediments has been used with mixed success as an indicator of palaeo-environment in the absence of sedimentary structures and fossils. In view of some

of the difficulties associated with using clay type as a palaeo-environmental indicator, geochemical criteria have been used in an attempt to distinguish between different depositional environments. Bouska (1981) considered geochemical parameters as valuable in palaeo-environmental and palaeo-geographical studies, stating that: "Geochemical methods help in assessing only the substantial differences in the palaeo-salinity of sedimentary basins. They make it possible to readily distinguish between fresh-water and marine sediments, but the brackish environments are more difficult to define". Degens et al. (1957) pointed out that an effective geochemical parameter for indicating palaeo-salinity is required to have the following characteristics:

1. Affected markedly by salinity changes.
2. Sufficiently abundant to be precisely measured.
3. Relatively widespread.
4. Formed or concentrated in the shale itself.
5. Relatively unaffected by diagenetic changes.

Degens et al. (1957) further observed that, although the first characteristic is the most important, it is extremely difficult to find a critical indicator which is strongly affected by salinity changes. There is an abundance of literature with respect to trace elements, clay mineralogy, clay mineral ratios, whole-rock composition, isotope ratios, modified initial porosities, exchangeable cations, and other methods used in determining palaeo-salinities. So far, no one technique has proved to be an "ideal" indicator of palaeo-salinity (Walters et al., 1987).

Elements that have been considered to be important in a few selected studies are briefly discussed. Goldschmidt (1954), Degens et al. (1957), and Potter et al. (1963) selected twelve elements, namely V, Cr, Cu, Ni, Zn, Sr, Al, Fe, P, B, K and organic C, to indicate marine depositional environments for shales, because they had been found to be significant in previous studies. Schultz et al. (1980) found a similar pattern of enrichment in marine strata of the Pierre Shale of the northern Great Plains for Cr, Ni, Zn, Fe, and P as well as acid-soluble calcite and dolomite. The P in marine shales was thought to be largely due to the preservation of biogenic P in addition to the natural detrital apatite component. The trace elements V, Ni, Cu, Rb, and B were used by Zawada (1988) to indicate marine conditions in the mudstones in the Main Karoo Basin. Spears and Amin (1981) found that shales classified as marine, based on palaeontological evidence, were significantly enriched in the elements Pb, Cu, V, Ni, Sr and Zn. The use of Cu as a palaeo-environmental indicator is controversial because Curtis (1969) suggested that Cu behaves independently of clay minerals whereas Wedepohl (1978) and Hirst (1962) concluded that Cu is strongly associated with clay minerals. Degens et al. (1957) suggested Rb as a possible palaeo-environmental indicator, showing that Rb is concentrated in marine shales. Cambell and Williams (1965), working in shales of the Lower Cretaceous in Alberta, Canada, used K/Rb ratios as indices of palaeo-salinity. Ratios of approximately 250

were considered to be indicative of fresh to brackish conditions, whereas values of less than 165 indicated marine conditions. Wedepohl (1978), Potter et al. (1980), and Breit and Wanty (1991) suggested that V may be used as a possible palaeo-environmental indicator, stating that V is concentrated in marine sediments (> > 500 ppm) because of the relatively large amount of V provided by circulating ocean water compared to terrestrial run-off. Curtis (1969), however, concluded that V entered the basin of deposition firmly bound in the clay lattices and that initial concentrations were insignificantly augmented by adsorption from solution. According to Wedepohl (1978) Zn has a low mobility and adsorption capacity and it was found that its adsorption capacity was strongly temperature, pH, and salinity dependent.

Although the various studies discussed above propose several elements for palaeo-salinity identification, there nevertheless are some elements that consistently appear in these groups, for example V, Cu, Ni, and Zn. It was demonstrated in the comparison of the composition of the mudstones in this study with those of PAAS and NASC (section 6.2.1.7) that the mean concentrations of V, Cu, Ni, and Zn are significantly depleted, suggesting that the sediments were deposited in freshwater. This also agrees with the conclusion reached in the discussion of the mineralogy of the mudstones where a freshwater depository was proposed.

6.5.6 DIAGENESIS

Erosion and transport of sediment generally occurs under fairly oxidizing conditions at more or less constant pH, pressure and temperature. Upon deposition these parameters change drastically and thus influence the composition of the sediment (Price, 1976). As in the case of weathering, the more soluble alkali and alkaline earth elements are liable to movement and(or) redistribution, complicating interpretation of palaeo-climates and CIA values. The anoxic conditions under which many sediments are deposited can have significant consequences: for example Fe and Mn, which are generally insoluble at surface conditions, may change oxidation state and become readily soluble and mobilized. Elements such as Mn, Cu, Mo, Pb, Zn, S and C are clearly enriched in anoxic sediments, possibly as a result of incorporation in sulphide phases or adsorption on organic compounds (Tourtelot, 1979). Studies of the effects of diagenesis on the mobility of elements indicate, therefore, that some major and trace elements are subject to redistribution during diagenesis. Elements which are generally least susceptible to re-mobilisation during diagenesis (and metamorphism) are the REE, Y, Sc, and other high valency ions such as Th and Nb (Taylor and McLennan, 1985; Wronkiewicz and Condie, 1987).

Inspection of the variation in the distribution of the elements in Figure 6.1 reveals that there are only two mudstone horizons that could potentially have been altered as a result of diagenesis. They are the mudstones at the base of the Grootegeluk Formation, referred to in this study as the carbo-tonstein zone, and the mudstones from the Beaufort Group which overlie the topmost coal seams of the Grootegeluk Formation. The carbo-tonstein samples are

enriched mostly in the immobile elements that are unlikely to have been concentrated as a result of diagenesis.

Some of the Beaufort Group mudstones, however, have very high proportions of pyrite and associated anomalous concentrations of Mo, As, Pb, U, Zn and Ni. Pyrite is present in some of the Grootegeluk Formation samples but none of these samples have anomalous trace element concentrations. It has been proposed previously (Chapter 5) that the Beaufort Group mudstones which now do not contain any coal, may have been deposited with large proportions of organic matter that has subsequently been removed as a result of degradation after deposition. If this is the case then the break-down of the organic matter would have been a source of reduced S, and as demonstrated in Fig. 6.1, there was no shortage of Fe in the sediments to form pyrite. In the reducing conditions elements such as Mo, Cu, As, Zn, Pb, etc. would tend to be incorporated as S^{2-} minerals or as impurities in S^{2-} minerals.

6.6 SUMMARY and GENERAL DISCUSSION

The variations in the major element chemistry of the mudstones reflect the changing mineralogy and support the findings in Chapter 4. The samples from the Vryheid Formation and the lower half of the Grootegeluk Formation are dominated by kaolinite and lesser amounts of quartz. The contact of the Grootegeluk Formation with the under-lying Vryheid Formation is characterised by an increase in the concentration of quartz in the Vryheid Formation. The carbo-tonstein at the base of the Grootegeluk Formation is composed almost essentially of kaolinite with minor amounts of siderite, apatite, calcite, anatase and quartz. The samples approximately 5 m immediately above the carbo-tonstein contain minor amounts of siderite and apatite but no calcite. These samples are anomalous with respect to their Sr and Ba concentrations, but it was not possible to ascertain in which minerals, these elements are located. The kaolinite and quartz concentrations vary steadily but antipathetically within the Grootegeluk Formation. Quartz dominates the mudstones in the upper half of the Formation and illite (and smectite) rapidly increases in concentration with a concomitant decrease in the kaolinite concentration. Microcline is also present in some of the samples in the upper part of the formation. The samples which immediately over-lie the topmost coal seam have abrupt increases in kaolinite (at the expense of illite) and pyrite. The smooth upward increase in the quartz concentration and grain-size (Chapter 4) in the Grootegeluk Formation indicates that the energy of the depositional environment increased steadily upward in the Grootegeluk Formation or that the shore-line was more proximal. The mudstones up to the topmost coal seam underwent relatively less chemical alteration, either *in situ* or during erosion, than the rest of the mudstones. The mudstones immediately overlying the "illite-microcline mudstones" and the topmost coal seam, however, were subjected to increased chemical alteration, most likely *in situ*. The very uniform changes in the quartz content of the sediments negate against increased tectonic activity in the hinterland of the samples. As a whole, the mudstones analysed

in this study underwent very high degrees of chemical alteration, but to ascribe the high degree of alteration to palaeo-climatic conditions alone is extremely questionable. An alternative possibility may be that the source of the mudstones were igneous rocks or (meta)sediments that had very low concentrations of alkali and alkaline-earth elements. Alteration during deposition and diagenesis of especially the clay-rich mudstones in the lower half of the borehole cannot be discounted.

The variation of the trace element distribution in the mudstones is dominated by the abrupt increase in concentrations in the carbo-tonstein zone of all the elements except S, Co, As and Zn. Other notable trace element features are: (1) the relatively high concentration of Cr, V and to a lesser extent Zr in the Vryheid Formation; (2) the high Sr and Ba concentrations in samples within and immediately above the carbo-tonstein zone; (3) the excellent correlation of Rb (and Zn) with the K-bearing minerals and; (4) the increase of chalcophile trace elements in samples with high pyrite concentrations in the Beaufort Group mudstones. The trace elements in the carbonaceous mudstones are predominantly in the mineral fractions. It is possible that a small proportion of the elements are within the organic fraction (bonded or adsorbed?) of organic-rich mudstones.

In Chapter 4 it was pointed out that it was very difficult to identify the presence of the carbo-tonstein zone in hand-specimen because of the high organic content of the samples, and that the samples above and below the carbo-tonstein also had very high proportions of kaolinite. It is evident, however, that the chemical composition of the samples from the carbo-tonstein zone are highly anomalous compared to the chemical composition of the under- and over-lying mudstones. It was demonstrated (Chapter 4) that mineralogical textures and grain-sizes also differed from the other mudstones and that it was difficult to reconcile a detrital origin for these minerals. In Chapter 5 it was established that the carbo-tonstein zone had a high proportion of organic matter which was more oxidised or degraded than in the rest of the Grootegeluk Formation mudstones. It is conceivable that if volcanic ash was buried with the organic matter that the high temperature minerals would be very unstable in the acidic conditions produced during degradation of the organic matter. The acidic conditions would result in rapid break-down of the primary minerals and re-distribution of the major and trace elements into secondary minerals. There are several chemical anomalies in the carbo-tonstein zone which are difficult to explain if the mineral matter was introduced into the basin as detrital material. One of the problems is explaining the presence of fine-grained calcite and apatite in the matrix of these highly argillaceous mudstones that were deposited in acidic fresh-waters. The introduction of mineral matter such as volcanic ash which was unaltered and was deposited by wind or water in the coal forming basin is considered the most plausible way of introducing major elements such as Fe, Ca, and P, and most of the trace elements which occur in anomalous concentrations in the carbo-tonstein zone. The increase in degraded organic matter in the coal can also be as a result of the break-down of minerals which would increase

the Eh and pH, and therefore also make conditions more favourable for the precipitation of minerals such as calcite.

Based on the concentration and ratios of relatively immobile elements that have been shown to be directly related to their source rocks, the Grootegeluk Formation and Beaufort Group mudstones have the same predominant provenance. The average composition of the provenance area is dominantly "granitic", possibly close to a granodioritic composition. The provenances of the carbo-tonstein and Vryheid formation samples are more mafic than those of the Grootegeluk Formation samples.

The concentrations of trace elements considered to be good palaeo-salinity indicators suggest that the sediments were deposited in fresh rather than marine waters. This supports the findings in Chapter 4 and 5.

The very systematic change in major element chemistry (SiO_2 and Al_2O_3) and therefore in the mineralogy (kaolinite and quartz), and the good correlation between compositions of samples in different boreholes, makes whole-rock chemistry an ideal stratigraphic tool for the Grootegeluk Formation. The major element composition alone could potentially be a very useful method for determining the stratigraphic position of a mudstone layer. The anomalous concentrations of elements, such as Al, Ti, P, Zr, Nb, Sc, Th, Y, Cu, W, Ba, Sr, etc., in samples from the in carbo-tonstein zone, at the base of the Grootegeluk Formation, provide a valuable chemical-marker horizon for inter-basin stratigraphical correlation. Radiogenic isotope analyses of the carbo-tonstein (or tonstein elsewhere) may provide essential chronostratigraphic evidence for the age of the coal formations.

Presently, geologists working in the Grootegeluk Formation use the thicknesses of coal and mudstone beds and the ratio of coal-to-mudstone layers to determine the stratigraphic position of a coal or mudstone layer. This requires that one has good and plenty of exposure, above and below, so that stratigraphic columns can be constructed. The mapping method has the advantage of being relatively quick, inexpensive and suitable for opencast mining, but may not be possible if the coal-mudstones were to be mined underground and(or) if coal and mudstones layers change thickness laterally. Comparison of the trace (and major) element compositions and variations of these mudstones, to mudstones in other coal-bearing basins, such as the Limpopo Coal Field, may be useful in ascertaining the relative ages of the coal.

The analytical results from the mudstones, which had been sampled in detail from cores, did not reveal the presence of any strategic elements in concentrations that may be of economic interest. However, the carbo-tonstein zone may be of economic importance because of its high kaolinite (and organic) content if mined as a by-product of coal. The carbo-tonstein would be suitable for making bricks, tiles, etc.

7. ISOTOPE GEOCHEMISTRY

7.1 INTRODUCTION

The coal and carbonaceous mudstones of the Grootegeluk Formation contain carbonate minerals and organic matter which have been analysed for their carbon and oxygen isotope ratios. The stable isotope ratios provide information on the environment existing during the formation of the coal-basin and on diagenetic changes during burial of the sediments. The mudstones have also been analysed for their Sm/Nd ages that have provided important information on the mean age of the source rocks. Analytical techniques for the stable and radiogenic isotope determinations were described in Chapter 3.

7.2 CARBONATE C and O STABLE ISOTOPE GEOCHEMISTRY

7.2.1 INTRODUCTION

Four "types" of calcite have been identified in this study:

(1) Lenses of pure calcite, 10-20 cm thick and up to 50 m in length, occur predominantly in the upper half of the Grootegeluk Formation. The lenses are conformable with coal and mudstone beds and are considered to be syn-sedimentary.

(2) Calcite inclusions in some of the relatively large kaolinite crystals that occur in the carbo-tonstein.

(3) Calcite present as fine-grained crystals dispersed within the carbo-tonstein zone.

(4) Calcite as cleat(joint)-filling within the more carbonaceous seams. Cleats probably formed by loading and(or) unloading of the coal, but the calcite filling the cleats is probably a relatively late-stage mineral.

Siderite occurs predominantly as roughly spherical nodules or "spherulites", 1-5 mm in diameter. The siderite spherulites occur preferentially within the coal seams and to a lesser extent within the more carbonaceous mudstone layers. Siderite is also present as fine-grained granules (granular siderite), usually < 0.5 mm in diameter, commonly dispersed within the clay matrix of the less carbonaceous mudstones of the Grootegeluk Formation. Granular siderite has also been detected in the mudstones of the overlying Beaufort Group. The carbo-tonstein zone, however, contains both spherulitic and granular siderite. Ankerite has been identified in XRD analyses but has not been observed in petrographic studies. Where physical separation of the different forms of carbonate was not possible, the step-wise reaction procedure of Al-Aasm et al. (1990) was used to obtain the isotope ratios of the various carbonate phases (Chapter 3).

7.2.2 RESULTS

The results of the carbonate mineral stable isotope analyses are presented in Table 7.1 and Figure 7.1, and plotted against depth in the formation in Figures 7.2 and 7.3.

Table 7.1 Stable isotope analyses of calcite (cleat-filling and disseminated), calcite-lenses, ankerite and siderite. The $\delta^{18}O$ (V-SMOW) and $\delta^{13}C$ (PDB) values are in per mil. (‰) and depth is the depth in meters below the topmost coal seam of the Grootegeluk Formation. Samples which have positive depths are from the Beaufort Group mudstones which overly the Grootegeluk Formation. Only approximate depths of the calcite-lenses in the Grootegeluk Formation, and of siderite from samples in the Beaufort Group mudstones (positive depths greater than 3 m), are known because they were taken in the pit at the GCM. The rest of the analyses were samples taken from boreholes 136 and 137.

CALCITE			ANKERITE			SIDERITE			CALCITE LENS		
Depth	$\delta^{13}C$	$\delta^{18}O$	Depth	$\delta^{13}C$	$\delta^{18}O$	Depth	$\delta^{13}C$	$\delta^{18}O$	Depth	$\delta^{13}C$	$\delta^{18}O$
-1.84	-13.3	16.7	0	-14.2	7.7	+9	-15.1	22.0	-8	-13.4	16.2
-3.50	-13.2	16.3	-1.84	-13.9	19.7	+7	-14.8	21.7	-10	-11.8	19.4
-3.98	-13.4	19.3	-3.50	-13.4	20.0	+3	-14.6	21.9	-12	-11.6	19.0
-8.63	-12.2	18.6	-33.74	-8.1	9.3	0.5	-18.7	17.1	-14	-12.0	19.0
-10.41	-13.9	14.5	-34.06	-8.6	7.0	-0.74	-15.3	13.5	-17	-10.6	19.8
-33.41	-7.9	22.3	-34.93	+4.2	10.7	-1.84	-15.9	18.7	-33	-11.6	18.2
-34.06	-11.7	21.9	-38.91	-11.4	7.4	-3.50	-15.6	17.4			
-38.91	-11.6	13.5	-45.76	-3.5	11.1	-4.53	-14.6	16.0			
-39.67	-12.0	15.9	-51.13	-4.6	5.8	-20.69	-16.7	12.2			
-43.43	-12.7	17.4	-51.41	+4.6	12.0	-25.75	2.4	12.2			
-51.41	-11.2	18.4	-53.76	-9.3	7.0	-33.74	-2.8	14.7			
-53.76	-13.0	18.4	-58.94	-8.9	12.6	-34.06	0.8	10.0			
-55.28	-13.6	18.0	-61.48	-7.5	9.6	-34.93	-3.8	10.5			
-55.96	-12.3	15.8	-63.33	-9.5	12.1	-36.75	2.8	12.1			
-57.35	-12.5	17.3	-66.89	-12.4	6.7	-38.91	5.0	10.5			
-57.99	-11.9	17.0				-45.76	-3.7	10.6			
-58.44	-14.6	20.9				-51.13	7.0	11.1			
-58.94	-9.7	17.4				-51.41	4.8	13.3			
-61.48	-2.9	12.1				-52.24	8.1	12.3			
-63.33	-4.8	14.5				-58.94	-4.8	13.2			
-63.93	-8.7	15.3				-61.48	-10.0	11.2			
-65.70	-10.7	14.1				-66.09	-10.5	9.2			
-66.09	-5.6	14.4									
-66.89	-7.5	13.3									
-69.03	-12.1	12.5									
-75.34	-9.9	14.8									
-76.27	-8.1	18.1									

Siderite can be differentiated into two main groups (A and B) based on $\delta^{18}O$ and $\delta^{13}C$ values (Fig. 7.1). Group A spherulitic siderites have a narrow range of low $\delta^{18}O$ values (+9 to +15‰), and a high $\delta^{13}C$ range (-5 to +8‰; Fig. 7.1). Group B granular siderites have a narrow range of low $\delta^{13}C$ values (-19 to -14‰), and a high $\delta^{18}O$ range (+12 to +22‰; Fig. 7.1). However, siderites from two samples have $\delta^{18}O$ and $\delta^{13}C$ values which are in-between those of Group A and B, and are labelled Group AB (Fig. 7.1). These two samples occur within and very near the carbo-tonstein (Figs. 7.2 and 7.3).

Calcite lenses that occur predominantly in the upper half of the Grootegeluk Formation have a very narrow range of $\delta^{13}C$ values (~ −12‰) but a wider range of $\delta^{18}O$ values (+16 to +22‰).

Cleat-filling calcites show no systematic distribution in Figure 7.1 and generally plot in a $\delta^{13}C$ range of −15 to −7‰ and a $\delta^{18}O$ range of +12 to +22‰ (Fig. 7.1). Three samples, however, have calcite with $\delta^{13}C$ values between −6 and −3‰, slightly more positive than the other calcite $\delta^{13}C$ values, and $\delta^{18}O$ values that are indistinguishable from the other calcites (Fig. 7.1). The three samples are from the base of the Grootegeluk Formation, within and close to the carbo-tonstein (Fig. 7.3). It was not possible to separate calcite filling-cleat and fine-grained calcite disseminated in the matrix of the carbo-tonstein samples, and therefore the isotopic values from this zone are mixtures of the two types of calcite.

The ankerite has a wide range of $\delta^{13}C$ values (−19 to +5‰) and relatively low $\delta^{18}O$ values (< +13‰), except for two samples that have $\delta^{18}O$ values of about +20‰.

7.2.3 DISCUSSION

7.2.3.1 Maximum Temperature Constraints for the Grootegeluk Formation

A maximum temperature of formation can be inferred from the organic matter in the coal-mudstones that is independent of temperatures estimated from carbonate minerals. Results from the study of the organic matter in the Grootegeluk Formation (Chapter 5) do show a systematic, but small, increase of rank with depth ($\bar{R}_o$max range 0.52 to 1.06; Fig. 5.4). Evidence from palynological studies indicates that a maximum palynologic thermal alteration index (TAI) for the spores is 3,0 (MacRae, 1988). Based on the palynological TAI and the $\bar{R}_o$max % of vitrinite for coals, a maximum palaeo-temperature of ~100°C and a minimum of ~70°C is inferred for the Grootegeluk Formation (Fig. 5.2, 5.4).

7.2.3.2 $\delta^{18}O$ Value of Late Permian Meteoric Water

During the Permian southern Africa was at a latitude of approximately 55°S (Smith et al., 1981). The δD values measured in Permian coal at the same latitude in Australia, were in equilibrium with water of δD value −90‰ (Smith et al., 1983) that suggests that the meteoric water had a $\delta^{18}O$ value of about −13‰. It can therefore be assumed that early formed minerals such as the calcite in the syn-sedimentary calcite lenses and the spherulitic siderite precipitated in equilibrium with isotopically light Permian water. The $\delta^{18}O$ value of present day meteoric water is dependent on geographical parameters (latitude, height above sea-level) but is between approximately −2 and −4‰ (Sheppard, 1986). The temperature of crystallisation for the calcite lenses, using the O'Neil et al. (1969) calcite-H_2O fractionation factor and assuming a Late Permian $\delta^{18}O$ H_2O value of −13‰, is between +15 and +20°C, which is a reasonable temperature range expected for freshwater carbonates

(see Section 7.3.3.3 for palaeo-climatic interpretation based on palynological evidence), and therefore confirmation that the $\delta^{18}O$ value of Permian water of about −13‰ is correct.

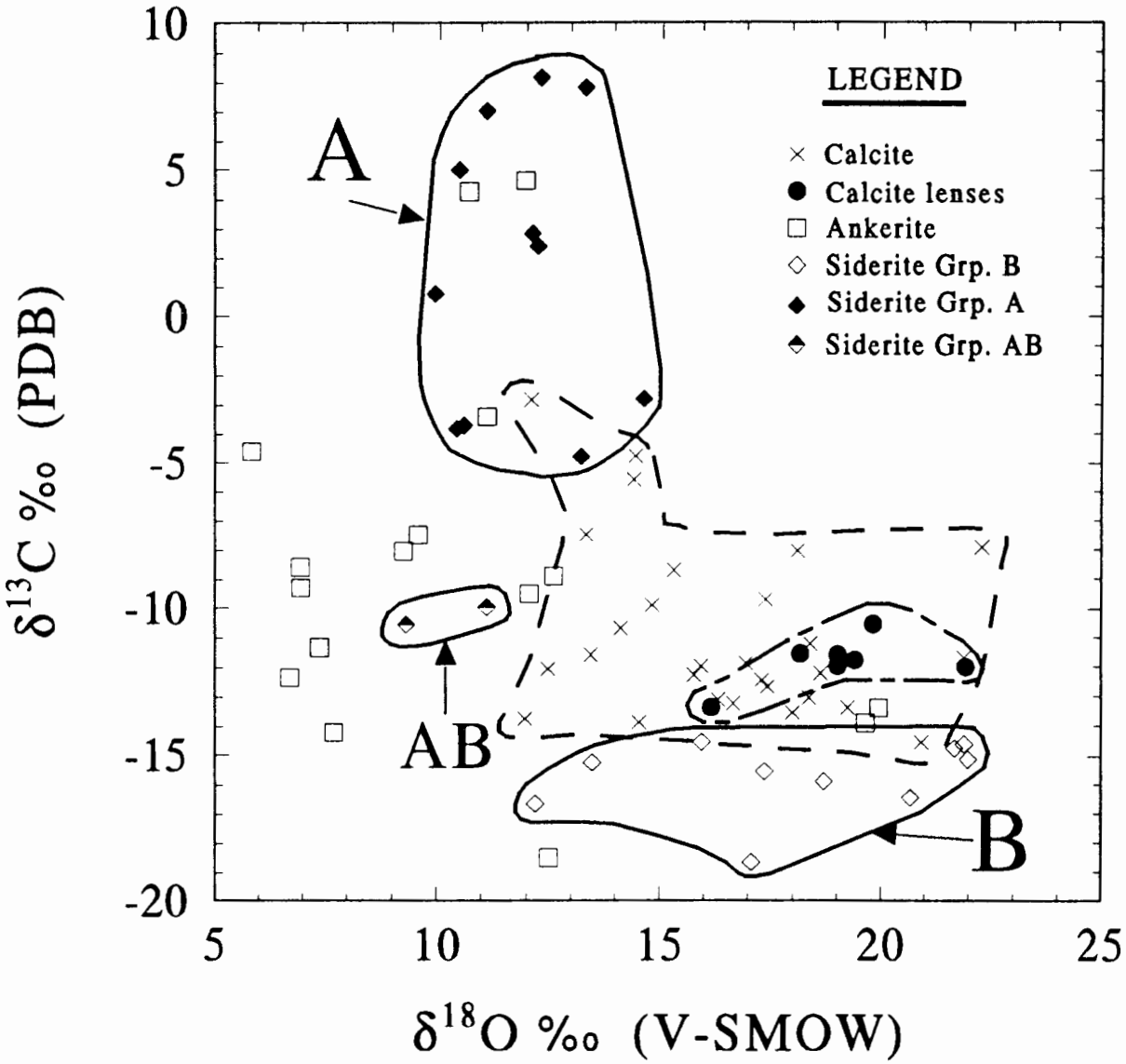

Figure 7.1 Plot of $\delta^{18}O$ vs. $\delta^{13}C$ for carbonate minerals in this study. The data are presented in Table 7.1. The siderite minerals can be differentiated into two groups (A & B). Group A has restricted $\delta^{18}O$ (+9 to +13‰) and large $\delta^{13}C$ (-19 to +9‰) range of values, and group B has low $\delta^{13}C$ (-19 to -14‰) and high $\delta^{18}O$ (+9 to +22‰) range of values. The syn-sedimentary calcite lenses which occur predominantly in the upper half of the Grootegeluk Formation have a very narrow range in $\delta^{13}C$ values (-11‰) and a wider range of $\delta^{18}O$ values (+16 to +22‰). Other calcite values have no general trend and plot in a relatively broad area in the centre of the scatter diagram. The ankerite values generally have relatively low $\delta^{18}O$ values (< +13‰) except for two samples that have values of about +20‰, and a wide range of $\delta^{13}C$ values (-19 to +5‰).

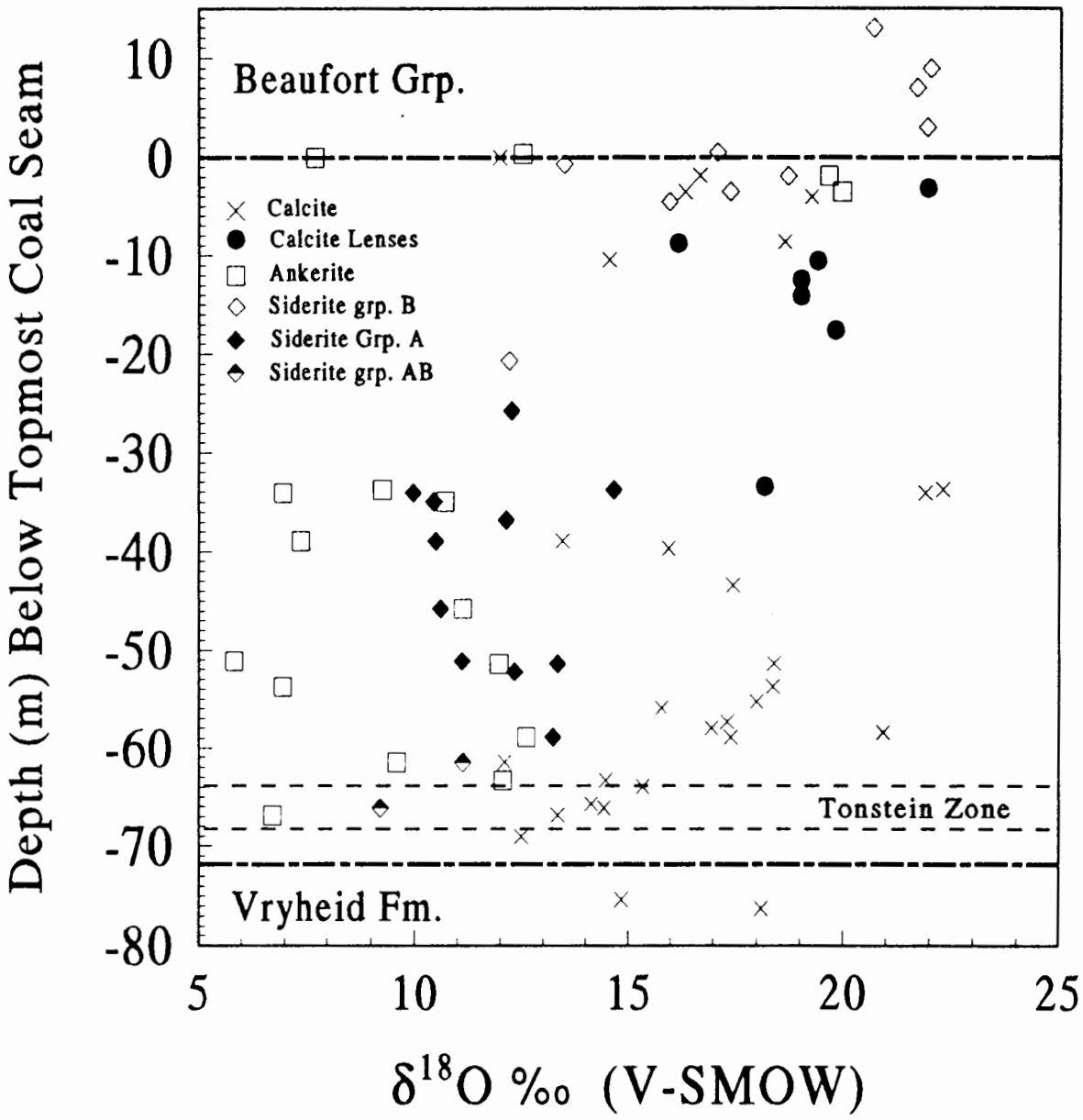

Figure 7.2 The $\delta^{18}O$ (V-SMOW) values of carbonate minerals plotted against depth below the top-most coal seam of the Grootegeluk Formation.

7.2.3.3 Siderite $\delta^{18}O$ and $\delta^{13}C$ Values

Using the siderite-H_2O oxygen isotope fractionation curve of Golyshev et al. (1981) a formation temperature between +35° and +60°C is calculated for the spherulitic siderite, assuming a mean $\delta^{18}O$ of −13‰ for Permian meteoric water. If a present day meteoric water $\delta^{18}O$ value (−3‰) is assumed, a formation temperature between +110° and +140°C is calculated. This is an unreasonably high temperature of formation, especially for the spherulitic siderite that is considered to be an early diagenetic mineral, and considering that the maximum temperature estimated from $\bar{R}_o max$ is ~100°C.

The granular siderites generally have a much higher and wider range of $\delta^{18}O$ values than the spherulitic siderites (Fig. 7.1 - Group B). Although a shift to lower latitudes will result in slightly higher $\delta^{18}O$ values, the abrupt and significant increase in $\delta^{18}O$ values at the top of the Grootegeluk Formation indicates that this was not an important influence (Fig. 7.2). Assuming therefore that the granular siderites crystallised during early diagenesis from Permian meteoric waters, temperatures between +6° and +50°C are calculated (using the Golyshev et al., 1981 equation).

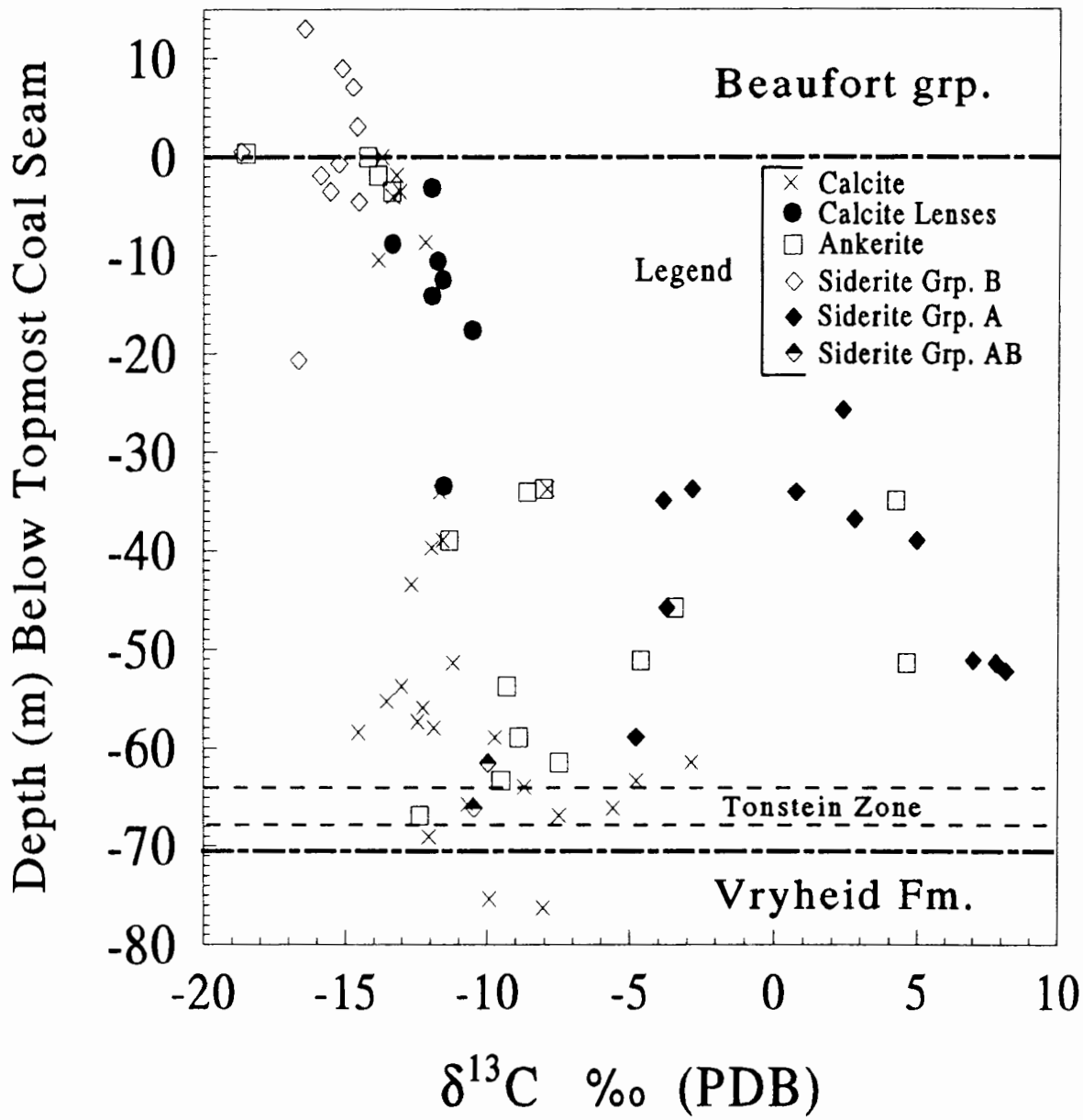

Figure 7.3 The $\delta^{13}C$ (PDB) values of carbonate minerals plotted against depth below the top-most coal seam of the Grootegeluk Formation.

The $^{13}C/^{12}C$ ratio of carbonates is not as sensitive to the temperature of crystallisation as is the $^{18}O/^{16}O$ ratio, and generally gives a better indication of their source material. The $\delta^{13}C$ values of spherulitic siderites (Group A) and some of the ankerites in the middle

portions of the formation are significantly more enriched in ^{13}C than the other carbonates (Figs. 7.1 and 7.3). It is generally accepted that anaerobic fermentation (microbial degradation) during eogenesis (low temperature diagenesis of organic matter) of peat produces CO_2, H_2O, CH_4 and NH_3 (Barnes et al. 1990). The isotopic exchange between CH_4 and carbonates and also between CH_4 and CO_2 results in the formation of "heavy" $\delta^{13}C$ carbonates (Irwin et al., 1977).

Granular siderite (Group B) which occurs preferentially in less carbonaceous shales from the top of the Grootegeluk Formation and the mudstones of the overlying Beaufort Group, have highly negative $\delta^{13}C$ values indicating a ^{12}C input as a result of organic degradation or oxidation (the organic matter is $< -20‰$ see Section 7.3.2; Figs. 7.1 and 7.3). The stability-field of siderite requires that conditions be reducing (Garrels and Christ, 1965; Fig. 4.10), but the presence of siderite does not mean that conditions could not initially have been oxidising in the mudstones from the top 20 m of the Grootegeluk Formation. The early formation of granular siderite (during organic oxidation) is consistent with the discussion above concerning the $\delta^{18}O$ values of the granular siderites that were thought to have precipitated at slightly lower temperatures from Permian meteoric fluids than the spherulitic siderites.

The carbo-tonstein horizon has both spherulitic and granular siderite that was not possible to separate for analysis. The $\delta^{13}C$ value of the whole-rock siderites from the carbo-tonstein zone have values that are in-between typical granular and spherulitic siderite, reflecting a mixture of the two types (Group AB; Fig. 7.3).

7.2.3.4 Ankerite $\delta^{18}O$ and $\delta^{13}C$ Values

It has been mentioned that the petrogenesis of the ankerite analysed in these samples is not known. The majority of the ankerite-bearing samples analysed have $\delta^{18}O$ values between +7 and +13‰ (Fig. 7.1). If the ankerite crystallised (early or late) at a temperature of say ~ +20°C it would have been in equilibrium with a meteoric fluid with a $\delta^{18}O$ value between −22 and −28‰ (using the Northrop and Clayton, 1966 dolomite equation), that is highly unlikely. Assuming equilibrium between ankerite and a meteoric fluid, it is more probable that the ankerite crystallised nearer to the maximum temperature to which the sediments were exposed, i.e. +90 - +100°C. For example, at +90°C the $\delta^{18}O$ of meteoric water in equilibrium with ankerite would have been between −15 and −10‰, which is much more realistic.

The ankerite $\delta^{13}C$ values have a wide range between −18 to +6‰. In the discussion above it was proposed that the ankerite precipitated generally later than the siderites and at higher temperatures. It is possible that some of the of the ankerite may have precipitated at the same time as siderite, depending on the availability of Fe^{2+}, the activity of Ca^{2+} and

Mg^{2+}, and the stability fields for ankerite. It is therefore also possible that some of the ankerites, like the spherulitic siderites, precipitated from ^{13}C-enriched bicarbonate derived during methanogenesis. However, biogenic decomposition reactions of organic matter give way to thermocatalytic reactions during burial diagenesis at temperatures of about +75°C (start of catagenesis; Fig. 5.2). During catagenesis, decarboxylation of organic acids produces CO_2 (Hesse, 1990) that could be a potential source of light $\delta^{13}C$ carbon for the precipitation of the ankerite, i.e. increased temperature of crystallisation results in decreased $\delta^{18}O$ and $\delta^{13}C$ values, as observed for most of the ankerites (Fig. 7.1).

7.2.3.5 $\delta^{18}O$ and $\delta^{13}C$ Values of Cleat-filling, Lens and Early Diagenetic Calcite

Cleat-filling calcite could have formed either during compaction or during uplift (more likely) of the coal-mudstone sequence (Chapter 4). The uniform, negative $\delta^{13}C$ values of the cleat calcites, except in the carbo-tonstein zone, indicate that organic matter was most probably the dominant source of carbon. The more positive $\delta^{13}C$ values of the calcite from the carbo-tonstein zone indicate that an additional source, besides the organic matter, must have provided carbon that had a higher $^{13}C/^{12}C$ ratio (Fig. 7.3).

The $\delta^{18}O$ values of the calcites, however, have a wide range of values (+12 to 22‰) and unlike the other carbonates do not show any correlation with $\delta^{13}C$ values or depth within the formation. It is therefore not possible, based on their $\delta^{18}O$ values, to predict whether the calcite precipitated predominantly during loading or un-loading of the sediments. The cleat-filling calcite may also have been dissolved and re-crystallised several times at different stages of burial and up-lift of the sediments and from different $\delta^{18}O$ meteoric fluids.

The calcite lenses also have highly negative $\delta^{13}C$ values indicative of the break-down of organic matter. Thin-section studies (Chapter 4) reveal root-hair trace-fossils in the calcite lenses that indicate shallow water levels. The shallow water levels at certain intervals during deposition in the later stages of the Grootegeluk Formation also imply that less organic matter accumulated and(or) was preserved, resulting in highly negative $\delta^{13}C$ values for the granular siderites within the mudstones in this part of the formation.

7.2.3.6 Palaeo-depositional Environment from Siderite $\delta^{18}O$ and $\delta^{13}C$ Values

Mozley and Wersin (1992) have recently proposed using the carbon and oxygen isotope composition of siderite as an indicator of palaeo-depositional environment. They compiled siderite stable isotope data and observed that continental sediments generally have higher $\delta^{13}C$ values than marine siderites, although there is significant overlap (Fig. 7.4). They proposed that siderites with $\delta^{13}C$ values < -8‰ (PDB) and $\delta^{18}O$ values $> +17$‰ (V-SMOW) are most likely of marine origin.

Comparison of the Grootegeluk Formation siderite values to the fields proposed by Mozley and Wersin (1992), demonstrate that spherulitic siderites (Group A) plot inside the

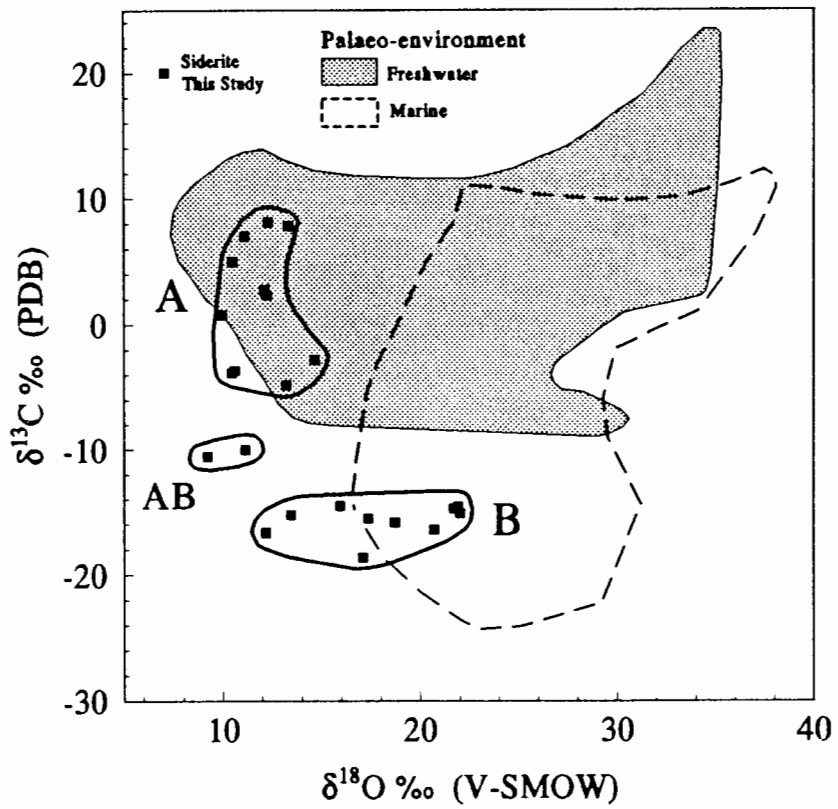

Figure 7.4 Plot of $\delta^{18}O$ (V-SMOW) vs. $\delta^{13}C$ (PDB) for siderites in this study compared to the siderite fields proposed by Mozley and Wersin (1992) to indicate terrestrial or marine depositional environments. The discrimination diagram suggests that the Group A (spherulitic) siderites were deposited in fresh water and the Group B (granulitic) siderites in marine water. However, evidence from sedimentological, palynological, and whole-rock chemistry studies of the Grootegeluk Formation sediments suggest that Group B siderites were deposited from fresh water and not marine. See text for discussion.

field of freshwater deposition, and the granular siderites (Group B) that occur in the top 20 m of the Grootegeluk Formation and the bottom 10 m of the overlying Beaufort Group, plot in the field indicating a marine palaeo-depositional environment. There is no evidence in this study, or from the palynology (MacRae, 1988) and sedimentology (Beukes, 1985; Siepker, 1986) of the mudstones, to suggest that the sediments were deposited in marine waters. For example, montmorillonite-illite (and microcline) which is commonly associated with marine environments, decrease rapidly in the Beaufort Group mudstones (Group B; Fig. 6.14). It has been demonstrated that the isotopic values of the granular siderites can satisfactorily be interpreted to have precipitated from Permian meteoric water. It was not possible to identify granular siderite in hand-specimen, and sometimes not even in thin-section. It is possible that the coarser siderite (nodular or spherulitic siderite), which is more common in organic rich-sediments or sediments that originally contained a high proportion of organic material which was not preserved, has been preferentially sampled and analysed. It is therefore suggested that the fields proposed by Mozley and Wersin (1992) are not

definitive enough, and that the siderite isotopic composition does not prove an unequivocal continental or marine palaeo-depositional environment. The fields proposed by Mozley and Wersin (1992) already have a considerable overlap and therefore the discrimination of palaeo-depositional environments, is unsound, based on carbon and oxygen isotopic composition alone.

7.2.4 CONCLUSION

The proposed sequence of mineral formation in the coal and mudstones (Figure 4.9) is augmented by the evidence from the carbonate stable isotope data, and presented in Figure 7.5.

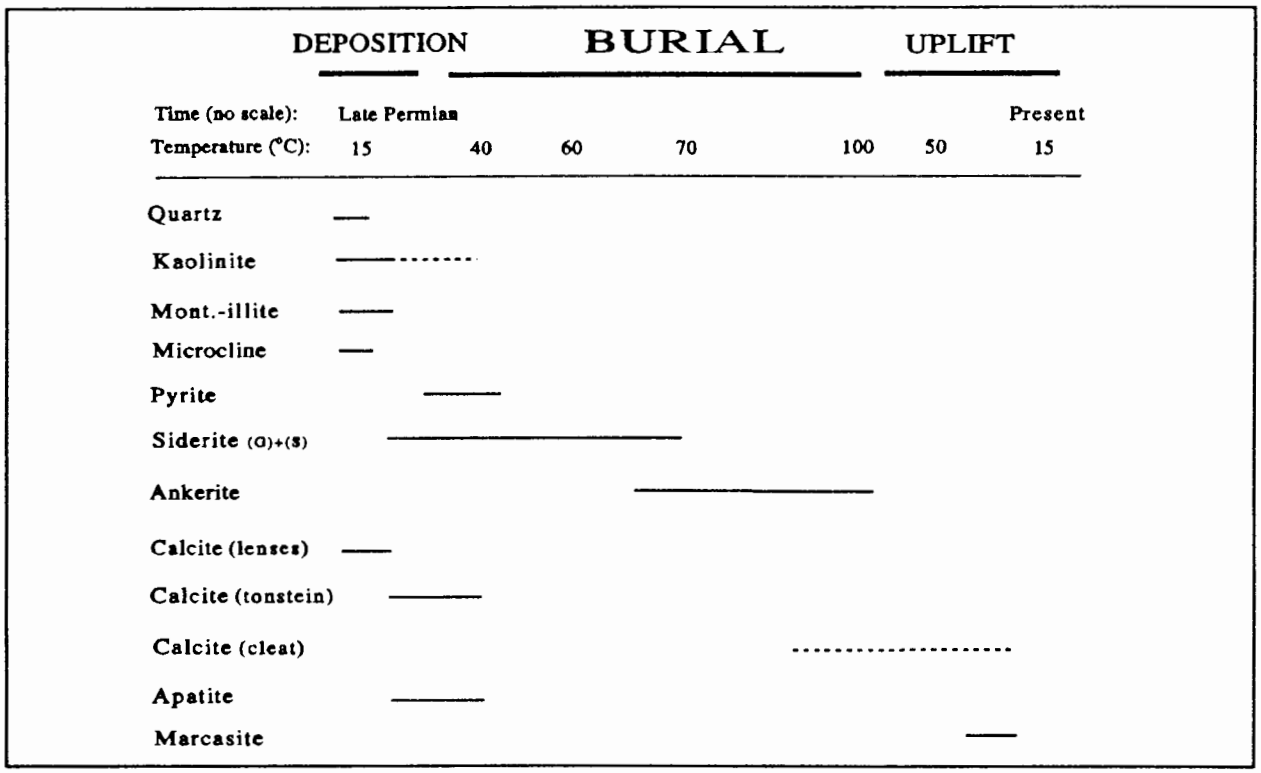

Figure 7.5. Diagram illustrating the relative timing of the formation of the minerals and proposed temperatures of formation, based on stable isotope data and mineralogical evidence (Chapter 4). Siderite (S) - spherulitic siderite and siderite (G) - granulitic siderite.

Evidence from petrography and carbon and oxygen isotope data suggest that syn-sedimentary calcite lenses precipitated in equilibrium with meteoric waters that had a $\delta^{18}O$ value of about −13‰. The spherulitic siderites, and some of the ankerite, formed from methane-bearing Permian meteoric water during early diagenesis of coal and the more carbonaceous mudstones at temperatures between +35° and +60°C. Carbon and oxygen stable isotope data are compatible with ankerite precipitating at temperatures generally higher than +70°C with an input of organic ^{12}C as a result of decarboxylation reactions of the organic matter. The stable isotope evidence is consistent with the proposal that granular siderite in the upper part of the Grootegeluk Formation and the lower Beaufort Group

crystallised at relatively low temperatures in equilibrium with Permian meteoric waters. The granular siderites have low ^{13}C values as a result of oxidisation of organic material during and(or) after deposition of the mudstones. It is not possible to establish whether cleat-filling calcite precipitated predominantly during burial or up-lift of the sediments but the consistently high negative $\delta^{13}C$ values point to an organic source for the carbon, and therefore favouring a later formation. The $\delta^{13}C$ values of calcite from the carbo-tonstein zone indicate that in addition to an organic carbon source, another (unidentified) source contributed ^{13}C for the calcite.

7.3 ORGANIC CARBON STABLE ISOTOPE GEOCHEMISTRY

7.3.1 INTRODUCTION

No $\delta^{13}C$ values of any southern Africa coals or organic matter in any southern African rocks, with ages ranging from the Upper Palaeozoic to the Mesozoic (410 - 65 Ma), have been published, and only a limited number of publications have reported ^{13}C isotopic compositions of coal elsewhere in the world. Craig (1953) was the first to determine the range of carbon isotopes on a limited number of coals of various ages and localities. Wickman (1953) presented data which indicated that $\delta^{13}C$ of different coals varied with age. He suggested that the shift was a response to changes in the atmospheric composition through geologic time. Compston (1960) measured the isotopic composition of lower and upper Permian Australian coals and related the differences to shifts in the $\delta^{13}C$ of plants as a result of late Permian glaciation. The $\delta^{13}C$ values of the organic fraction in coal can possibly provide valuable information on the palaeo-environment at the time of formation of the organic matter, even though very little research has been done in this regard.

Organic carbon stable isotope values have been determined from predominantly the carbonaceous mudstones of the Grootegeluk Formation, and also from a few selected samples in the remainder of the Ecca Group. On the basis of palynological evidence MacRae (1988) divided the Ecca Group rocks of the Waterberg Basin sediments into biozones (A-E) that will be compared with the variation of the organic $\delta^{13}C$ values. Although a reasonable number of samples have been analysed from the Grootegeluk Formation only a small number of samples have been analysed from the rest of the Ecca Group formations and this may prevent the observation of possible small-scale variations of organic $\delta^{13}C$ values.

7.3.2 RESULTS

The results of the organic $\delta^{13}C$ (PDB) analyses are presented in Table 7.2 and plotted against depth below the topmost coal seam in the Grootegeluk Formation in Figure 7.6. The

organic $\delta^{13}C$ values of the Waterberg Basin Ecca Group mudstones have a mean of $-22.6 \pm 2.0‰$ (3 s.d., n=22). Although the organic $\delta^{13}C$ values of the Ecca Group have a remarkably narrow range, the $\delta^{13}C$ values vary regularly within the MacRae (1988) biozones (Fig. 7.6).

Table 7.2 Carbon stable isotope analyses of organic matter in coal and carbonaceous mudstones of the Grootegeluk Formation. The $\delta^{13}C$ (PDB) values are in per mil. (‰) and "depth" is the depth in meters below the topmost coal seam of the Grootegeluk Formation in this study. Symbols indicate formation: P = Pietermaritzburg; V = Vryheid and; Grootegeluk Formations. Samples with depths between −92 to −210 m are from the Vryheid and Pietermaritzburg Formations and were supplied by C.S. MacRae (Geological Surv. Pretoria) and only the approximate depths below the top-most coal seam are known.

ORGANIC CARBON ISOTOPE VALUES		
Formation	Depth (m)	$\delta^{13}C$ (‰)
G	-3.5	-22.5
G	-7.53	-22.6
G	-12.46	-22.5
G	-16.16	-23.0
G	-23.48	-23.7
G	-31.68	-23.5
G	-36.19	-23.1
G	-45.76	-22.4
G	-49.73	-21.7
G	-55.96	-22.9
G	-60.21	-22.5
G	-61.48	-21.3
G	-66.09	-21.9
G	-66.89	-21.9
V	-73.69	-22.3
V	-78.84	-22.1
V	-92	-22.6
V	-102	-23.7
P	-130	-22.7
P	-160	-22.2
P	-190	-22.6
P	-210	-23.7

7.3.3 DISCUSSION

7.3.3.1 Primary $\delta^{13}C$ Values of Plants

Plants assimilate carbon from atmospheric CO_2 via one of three photosynthetic pathways (C_3, C_4 and CAM; O'Leary, 1988). The different pathways for fixing the CO_2 results in plants having different isotopic compositions. Plants from the Permian, however, used only the C_3 pathway of fixing atmospheric CO_2 (Ehleringer, 1991). The Grootegeluk organic matter $\delta^{13}C$ values fall within the $\delta^{13}C$ values for C_3 plants world-wide ($-26 \pm 7‰$; Schidlowski, 1988).

7.3.3.2 Effects of Diagenesis on the $\delta^{13}C$ of Peat

Degens (1969) noted that coals (humic, low H/C) show no evidence of isotopic fractionation during catagenesis. Laboratory coalification studies by Geissler and Belau (1971) and Chung and Sackett (1979) found no significant difference in $\delta^{13}C$ between the original material and the residual product. Even if an isotopic shift should occur during diagenesis only the absolute value will shift because the rank of the Waterberg coals does not change significantly with depth. Because only C_3 plants existed during the Permian, and no relative isotopic fractionation occurred during coalification, it can be assumed that isotopic shifts of the organic matter are largely due to primary effects such as plant species, pCO_2, climate, etc. Increased pCO_2 decreases $\delta^{13}C$ and increased dryness increases $\delta^{13}C$ of plants (Tieszen, 1991).

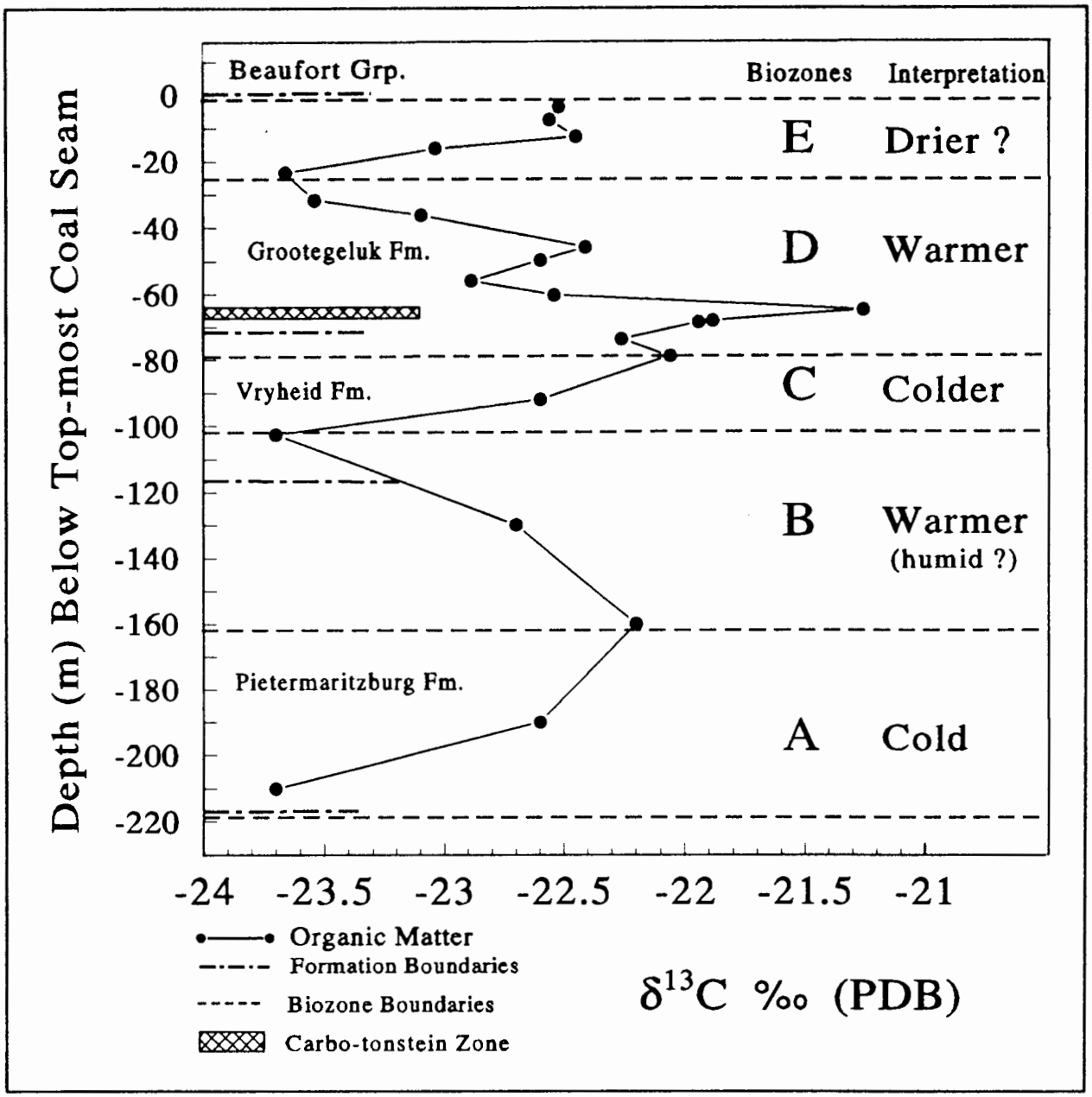

Figure 7.6 Plot of $\delta^{13}C$ values of organic matter from samples of the Ecca Group in the Waterberg Basin. The biozones have been proposed by MacRae (1988) on the basis of palynological evidence. Interpretation of biozones modified after MacRae (1988).

Numerous studies have demonstrated that the source of organic matter in sedimentary rocks can be differentiated on the basis of their $\delta^{13}C$ distribution (Sackett and Thompson, 1963; Kodina and Galimov, 1984; Golyshev et al., 1991). For example Golyshev et al. (1991) showed that in East and West Siberia the organic $\delta^{13}C$ values of marine and freshwater sediments ranges from −32 to −27‰ and from −28 to −23‰ respectively. These results, again, support a freshwater origin for the organic matter in the Waterberg Basin (−22.6 ±2‰).

7.3.3.3 Palynological Evidence

The biozones proposed by MacRae (1988), based on palynological evidence, are displayed in Figure 7.6. A synopsis of the findings and interpretations of the biozones by MacRae (1988) is presented:

(1) Biozone A. Monosaccites and Triletes taxa are abundant and are characteristic of Gondwana Carboniferous/Permian deposits. It was concluded that cold climatic conditions existed during this period.

(2) Biozone B. Abundant Monosaccites and Triletes taxa are present, but this zone is characterised quantitatively by an Aletes peak (floating colonial alga) indicating that warmer, milder and probably humid conditions prevailed during most of biozone B.

(3) Biozone C. Definite peak in Monosaccites and fairly abundant Triletes suggesting a return to cold conditions.

(4) Biozone D. Steady decline in Monosaccites and Triletes and a significant increase in Disacciatrileti and Straititi signifying a return to warm, humid and generally milder climatic conditions.

(5) Biozone E. Approximately equal proportions of Disacciatrileti and Straititi, and low abundance of Monosaccites. The characteristic of this zone is the distinct peak of the Zonotriltes. MacRae (1988) tentatively interprets the palynological evidence to manifest a drying-up or silting-up of the water body and that the distinct change in range and number of species at the biozone D and E boundary suggested some climatic change, not outwardly manifested in the lithology.

7.3.4 CONCLUSION

Comparison of the biozones of MacRae (1988) with the organic $\delta^{13}C$ values shows that the biozone boundaries coincide with "inflection-points" in the isotopic variations (Fig. 7.6) suggesting that some relationship does exist between the dominant type of plant-species and the organic $\delta^{13}C$ values of the carbonaceous mudstones. In Chapter 5 it was demonstrated that the coal quality in the Grootegeluk Formation varies with depth (Fig. 5.4). However, no apparent correlation between the coal quality (organic preservation conditions) and the organic $\delta^{13}C$ values exist and therefore the $\delta^{13}C$ variation of the organic matter does appear to be related to a primary source. Decreasing organic $\delta^{13}C$ values are associated with colder climates and increasing values with warmer climates. It is not clear, however, from the work of MacRae (1988) whether colder infers drier conditions and warmer assumes wetter conditions or if there is any relationship between these climatic conditions. Studies on the effects of environmental factors on the $\delta^{13}C$ of plants indicate that factors like water stress increase $\delta^{13}C$ values of C_3 plants (Tieszin, 1991). In the case of the Waterberg Basin, however, the co-variation of the organic $\delta^{13}C$ values with the changes in palynological data most probably reflect the change in the various species of plants as a

consequence of changing environments and resource (water and nutrients) availability. Two other points worthy of mention are: (1) The anomalously high organic $\delta^{13}C$ value of a sample in the carbo-tonstein zone (Fig. 7.6). Once again the carbo-tonstein zone is anomalous compared to all the other sediments, as it has been throughout this investigation; (2) The almost identical organic $\delta^{13}C$ values of samples from the top 10 m of the Grootegeluk Formation. The constant organic $\delta^{13}C$ values in the top 10 m of the Grootegeluk Formation give no indication of any major changes in climatic or atmospheric (pCO_2) conditions that point toward the pending demise of plants or the lack of preservation of peat to form coal.

7.4 Sm-Nd RADIOGENIC ISOTOPE GEOCHEMISTRY

7.4.1 INTRODUCTION

7.4.1.1 Background Information

Sedimentary formations are composites of older igneous, metamorphic, and sedimentary components exposed above sea level, usually characterized by different concentrations of Sm and Nd. The Sm-Nd isotopic ratios in a particular sedimentary formation are a function of the average Sm and Nd concentrations of the components at the time of deposition of the formation, the age of the formation, and the initial isotopic ratios of the components (Faure, 1977). It has been reasonably well established that Sm-Nd provenance ages for sediments provide a fair reflection of mean source region composition (McCullogh and Wasserberg, 1978; O'Nions et al., 1983; Nelson and DePaolo, 1988; Mearns, 1988, 1992). O'Nions (1984), Allègre and Rousseau (1984), Harris et al. (1987) and Dia et al. (1990) have applied Sm-Nd isotopic studies of sedimentary rocks to trace the average age of crust through time.

Van Berkel (1987) measured the concentrations of over thirty elements, including REEs, in several organic-rich shales and bituminous fractions derived from them. Kerogens associated with the shales had lower concentrations of REEs than the whole shales, but Sm/Nd ratios in the kerogens were not greatly different from those of their parent shales. In another study of the application of Sm and Nd in organic-rich rocks, Manning et al. (1991) have proposed that Nd isotope ratios may serve as a correlation tool in matching crude oils with their source rocks.

The isotopic evolution of Nd in the Earth is described in terms of a model called CHUR (CHondritic Uniform Reservoir; DePaolo and Wasserburg, 1976). This model assumes that terrestrial Nd has evolved in a uniform reservoir whose Sm/Nd ratio is equal to that of chondritic meteorites. The isotope ratios of Nd in a reservoir of chondritic composition at the present time enables us to calculate the $^{143}Nd/^{144}Nd$ at any time (t_{Nd}) in the past. Partial melting is the dominant process which fractionates Sm/Nd between mantle

and crust and typically leads to strong reduction in the Sm/Nd in the magma (destined to become crust) with corresponding increase in Sm/Nd in the residue (depleted mantle; Mearns, 1988). Since the REE are generally considered immobile (McLennan, 1989), the depleted mantle Nd model ages ($t_{Nd\text{-}DM}$) are therefore believed to record crust-mantle separation ("crustal residence ages" Faure, 1977), and are therefore also provenance ages for sediments (Mearns, 1988; Mearns, 1992).

DePaolo and Wasserburg (1976) introduced the "epsilon parameter" (ϵ_{Nd}) to compare the initial $^{143}Nd/^{144}Nd$ ratios of igneous and metamorphic rocks in the crust of the Earth with the corresponding $^{143}Nd/^{144}Nd$ ratios of CHUR at the time of crystallization of the rocks. A positive ϵ_{Nd} value indicates that the rocks were derived from residual solids in the reservoir after magma had been withdrawn at an earlier time. A negative ϵ_{Nd} value indicates that the rocks were derived from, or assimilated, old crustal rocks whose Sm/Nd had been lowered originally when they separated from CHUR. If an ϵ_{Nd} value is zero, then the isotopic composition of Nd in the rock is indistinguishable from that in the chondritic reservoir.

Dia et al. (1990) is the only published study of Sm-Nd isotope analyses of South African Phanerozoic sediments. Harris et al. (1987) reported Sm-Nd isotopic data for granite gneiss/greenstone terranes and granites and metasediments from the Zimbabwe and Kaapvaal cratons and Limpopo, Kalahari, Namaqualand and Damara mobile belts.

7.4.2 RESULTS

The results of the Sm-Nd isotopic analyses are presented in Table 7.3.

Table 7.3 The Sm and Nd concentrations (ppm) determined by isotope dilution, and the $^{147}Sm/^{144}Nd$ and $^{143}Nd/^{144}Nd$ ratios of selected mudstones. See Chapter 3 for analytical details. The Nd model ages are calculated assuming a depleted mantle ($t_{Nd\text{-}DM}$), and epsilon values (ϵ_{Nd}) are also presented.

SAMPLE	Sm (ppm)	Nd(ppm)	$^{147}Sm/^{144}Nd$	$^{143}Nd/^{144}Nd$	$t_{Nd\text{-}Dm}$	95% Confid.	ϵ_{Nd}
136_0b	8.56	47.40	0.109170	0.512190	1255.2	2.9	-6.00
136_1Bd	6.75	36.77	0.110840	0.512350	1039.6	14.3	-2.92
136_2c	10.62	56.21	0.114193	0.512175	1341.9	0.2	-6.44
136_8b	27.35	119.50	0.138506	0.512280	1567.5	35.6	-5.17
136_12b	5.72	60.16	0.057429	0.512183	849.2	13.1	-4.47
136_20a	11.49	65.98	0.105255	0.512186	1215.5	4.5	-5.94
136_22Eb	16.18	85.89	0.113895	0.512200	1299.5	0.9	-5.94
136_22Ee	8.39	45.20	0.112195	0.512314	1106.9	5.5	-3.66
137_22FSa	21.73	100.72	0.130400	0.512330	1319.5	45.6	-3.93
137_23BS	7.60	43.15	0.106462	0.511723	1898.0	9.7	-15.02
136_23BSa	6.21	30.02	0.124953	0.511699	2361.8	34.9	-16.08

7.4.3 DISCUSSION

7.4.3.1 Stratigraphic Variation of Sm-Nd Model Ages and ϵ_{Nd} Values

In Chapter 6 it was proposed, on the bases of whole-rock chemistry, that the Grootegeluk Formation and Beaufort Group mudstones had a common provenance and that the underlying Vryheid Formation had a different, relatively more mafic, provenance. The variation of the Sm-Nd model ages and ϵ_{Nd} values of the mudstones (Table 7.3 and Fig. 7.7) confirm the findings in Chapter 6. The Grootegeluk Formation and Beaufort Group have Sm-Nd model ages ("crustal resident ages"; $t_{Nd\text{-}DM}$) between 850 and 1570 Ma (mean 1222 Ma) and ϵ_{Nd} values between -6.4 and -2.9. The Vryheid Formation mudstones have much older model ages (1898 and 2362 Ma) and significantly different ϵ_{Nd} values (-15 and -16). The magnitude of the ϵ_{Nd} value is depended on the product of time and the chemical fractionation of Sm and Nd (DePaolo, 1988). The source of the Vryheid Formation mudstones are considered to have been more mafic (less fractionation) than the rest of the mudstones so the very low ϵ_{Nd} values must be as result of older crustal residence ages than the Grootegeluk Formation and Beaufort Group mudstone source rocks.

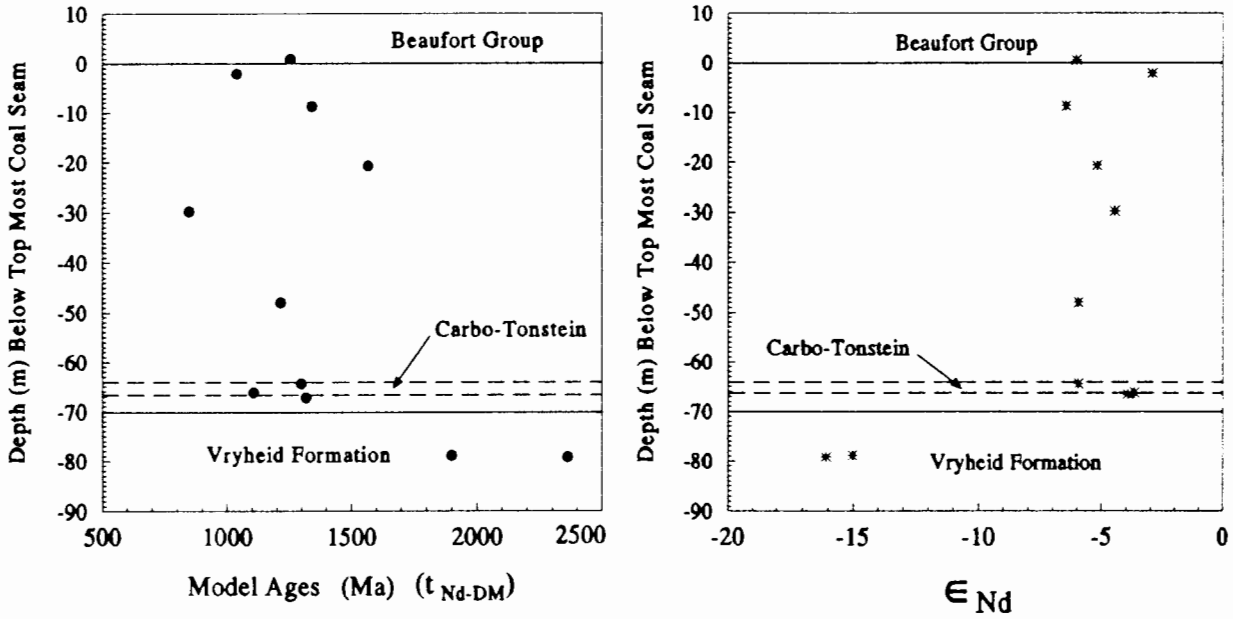

Figure 7.7 Model ages ($t_{Nd\text{-}DM}$) and ϵ_{Nd} values of the mudstones.

The Sm-Nd isotopic data from two of the carbo-tonstein samples are indistinguishable from the data of the rest of the Grootegeluk Formation mudstones. However, in a previous discussion it has been proposed that detrital matter had been washed into the basin with the tuffaceous sediments (Section 4.4). Even though the tuffaceous material may have been associated with eruptions at approximately the time of deposition of the carbo-tonstein zone, the Sm-Nd model age (crustal residence age) need not be the same as the depositional age.

7.4.3.2 Mudstone Provenances

Falcon (1986) considered that the source rocks of the Karoo strata were the ancient cratons that formed major areas of positive relief (Fig. 7.8). In the case of the Waterberg Basin, the sediments were considered to be deposited in localised cratonic grabens (Falcon, 1986). The ages of rocks from the Zimbabwe and the Kaapvaal cratons, however, have ages usually in excess of 2700 Ma and can therefore not be considered to be the predominant source rocks of the Grootegeluk Formation. The Sm-Nd model ages of the Grootegeluk Formation preclude a source from the ancient Limpopo Mobile Belt gneisses, the Zimbabwe or Kaapvaal Cratons.

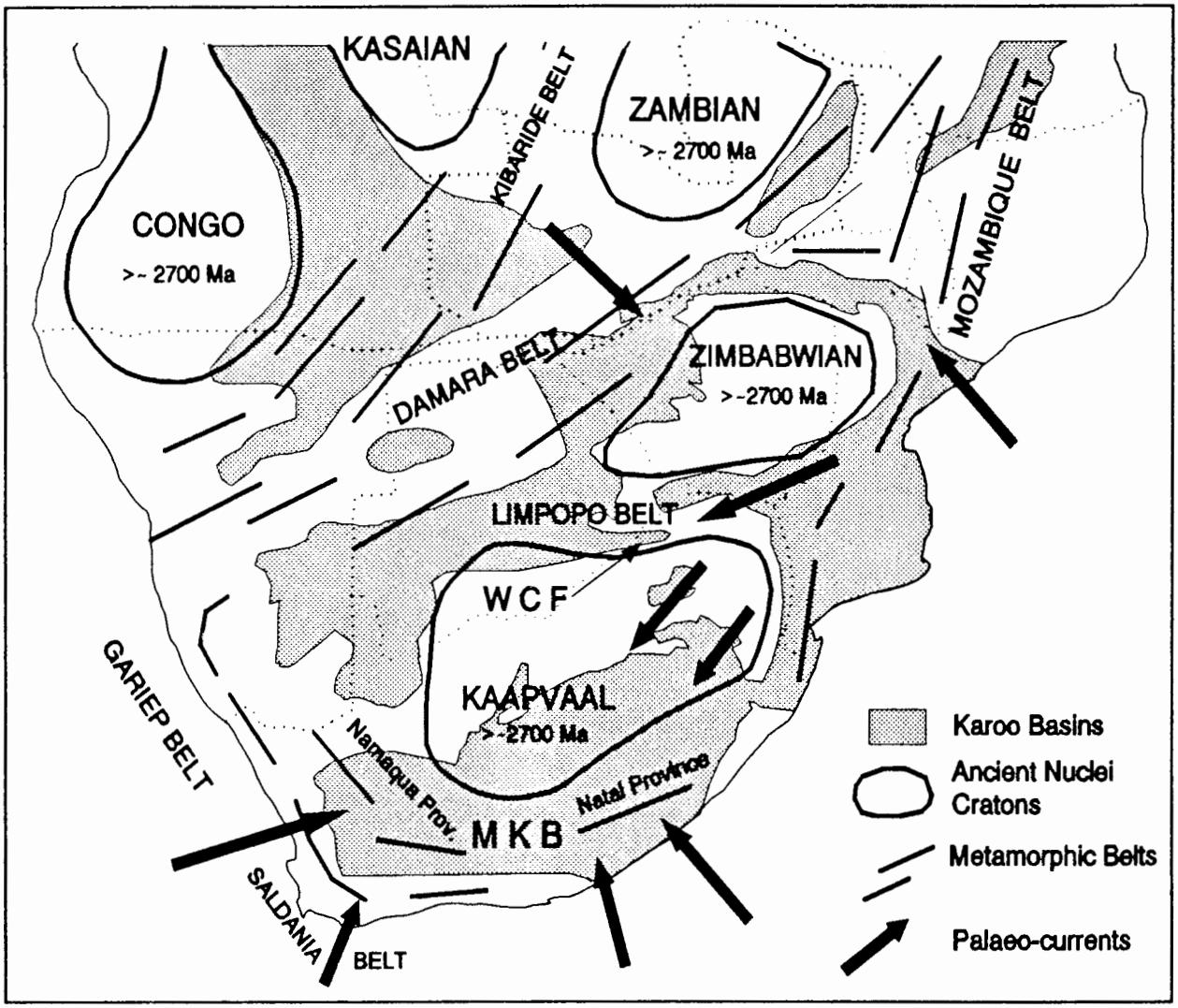

Figure 7.8 Distribution of the Karoo Sequence and a schematic representation of the metamorphic belts in southern Africa (modified from Falcon, 1986; Thomas et al., 1993). Palaeo-current directions of Late Permian Karoo Sequence sediments are from Ryan (1967), Turner (1991) and Smith et al. (1993).

Ryan (1967) proposed a source for the Waterberg Basin sediments from the north-east. Turner (1991) and Smith et al. (1993) proposed that the source of late Permian Ecca Group sediments in the northern MKB was also from the north-east, approximately in present day Mozambique (Fig. 7.8). The Waterberg Basin, however, is considered to be part

of the Kalahari Basin (Rust, 1975) and so it does not necessarily follow that the source of the Waterberg Basin sediments are the same as for the MKB.

Sedimentological studies of the sediments underlying the Grootegeluk Formation suggest that palaeo-currents and sandstone-channels were orientated east-west (Siepker, 1986). It has, however, been established that the provenances were different for the sediments underlying the Grootegeluk Formation and therefore the palaeo-current evidence may not apply to the Grootegeluk Formation. The Sm-Nd model ages of the Grootegeluk Formation indicate a provenance with a Late Proterozoic crustal resident age. The granitoids and metasediments from the Damara Belt (Fig. 7.8) have Sm-Nd depleted mantle model ages (1.0 to 2.0 Ga) that are comparable with those of the Grootegeluk Formation (Harris et al., 1987). No Sm-Nd model ages have been reported for rocks from the Mozambique Belt. The Vryheid Formation provenance had a predominantly Early Proterozoic crustal resident age.

7.4.3.3 Comparison of Sm-Nd Model Ages of WCF Basin Sediments with MKB Sediments

Dia et al. (1990) published Sm-Nd model ages for the Dwyka Formation and the Ecca Group in the northern MKB (Table 7.4). Unfortunately Dia et al. (1990) did not specify which Ecca Group formations in the northern MKB were sampled. The Ecca Group samples from the northern MKB have older model ages than the Grootegeluk Formation in the WCF but ages that are broadly comparable with those of the Vryheid Formation in the WCF, although slightly younger (Table 7.4). The ϵ_{Nd} values of the Ecca Group in the northern MKB are also comparable with those of the Vryheid Formation in the WCF. The Dwyka Formation (glacial sediments) samples have Sm-Nd model ages and ϵ_{Nd} values which are similar to those of the Grootegeluk Formation in the WCF. Siepker (1986), based on sedimentological studies, proposed that the Grootegeluk Formation mudstones may have been introduced from retreating glaciers to the north of the basin. The Sm-Nd isotopic data is consistent with this theory.

Table 7.4 Sm-Nd isotopic data of the Dwyka Formation and the Ecca Group in the northern Main Karoo Basin (Dia et al., 1990).

	Sample No.	Model Age ($t_{Nd\text{-}DM}$)	ϵ_{Nd}
Dwyka Formation	DW 1	0.99	-6.9
	DW 5	1.35	-8.8
	CV 86	1.44	-10.8
Ecca Group	BEC 4265	1.95	-14.4
	BEC 4287	1.88	-12.4
	GB 47/64/10	1.88	-14.4
	GB 48/65/9	1.86	-14.6

7.4.4 CONCLUSION

Sm-Nd isotopic studies confirm that the predominant provenance of the Grootegeluk Formation (and Lower Beaufort Group) mudstones in the WCF was fundamentally different to the provenance of the underlying Vryheid Formation. The provenance of the Grootegeluk Formation mudstones has Late Proterozoic crustal resident ages (mean 1.22 Ga) and relatively positive ϵ_{Nd} values compared to the Vryheid Formation. The provenance of the Vryheid formation has crustal resident ages of Early Proterozoic age. Although palaeo-current analyses of Ecca Group sediments in the WCF and the northern MKB indicate a provenance from the north-east (approximately present day Mozambique), the provenance of the Grootegeluk Formation mudstones may not necessarily be the same direction. Evidence for a provenance for the Grootegeluk Formation is not conclusive, but the Sm-Nd isotopic data are consistent with a source from the Damara Belt to the north-west of the basin and(or) sediments from northward retreating glaciers.

8. COAL, C-ISOTOPES, & THE PERMIAN-TRIASSIC BOUNDARY

8.1 INTRODUCTION

In Chapters 2 and 7 it was demonstrated that there still is considerable uncertainty concerning the relative and absolute ages of the South African coalfields. It was demonstrated in Chapter 7 that even though the range of the $\delta^{13}C$ organic values of the coal and carbonaceous mudstones in the Waterberg is remarkably small, the values nevertheless appear to correlate broadly with the palynological data. Whether the $\delta^{13}C$ organic values vary mainly in response to changing conditions or to changes in proportions of the different species that are suited to particular conditions, is uncertain. Nonetheless, the $\delta^{13}C$ organic values of coals in the different South African coalfields may be useful in supporting or challenging some of the hypotheses that have been made concerning at least the relative ages of the South African coalfields. Other topics on which $\delta^{13}C$ organic data may have some bearing are: the cause for the demise of coal that occurred almost simultaneously in many parts of Gondwana in the Tartarian stage of the Late Permian (Hobday, 1987; MacRae. 1988, 1989); the identification of the stratigraphic position of the Permian-Triassic boundary (P-T_R) in southern Africa; and P-T_R mass extinctions.

The $\delta^{13}C$ organic values were determined on Karoo coals that are considered to be from the oldest to the youngest in South Africa, i.e. Permian coals in the Main Karoo Basin (MKB), the Waterberg (also presented in Chapter 7) and Pafuri, and the Triassic coals in the Molteno Coalfield (Fig. 1.1). The $\delta^{13}C$ organic values of Early Permian particulate organic matter (not coal seams) in the Pietermaritzburg Formation of the Waterberg basin are also presented. Samples representative of five of the MKB coal seams were taken from the Vereeniging (Coalbrook Colliery - seams 1, 2 and 3) and Springs-Witbank (Navigation Colliery - seams 4 and 5) Coalfields. Samples from the Pafuri Coalfield were coal and particulate organic matter taken from a borehole drilled in the vicinity of the Thsikondeni Coal Mine near the Kruger National Park. Samples from the Molteno Coalfield were obtained from several boreholes that were sited over an extensive area in the north-eastern Cape Province.

8.2 RESULTS

The results of the stable isotope analyses of the organic matter are presented in Table 8.1, and plotted in Figures 8.1 and 8.2 according to approximate age. Estimates of the bio-stratigraphic positions for the Waterberg and Pafuri Coalfield formations in Figures 8.1 and 8.2 are from MacRae (1988), the MKB coal seams from Anderson (1977), and the coal in the Molteno Formation from Anderson (1974). Anderson (1974) considered the Molteno Formation to be of Carnian age (Late Triassic) but Plumstead (1969) and Keyser (1973) assigned a middle Triassic age to this unit.

The $\delta^{13}C$ organic values of the Permian coals and particulate matter range between −23.8 and −21.2‰ with a mean value of −22.7‰ (Table 8.1; Fig. 8.1). The range of the $\delta^{13}C$ organic values is exceptionally narrow considering that the ages of the Ecca Group rocks range from ~300 to ~250 Ma. The Triassic Molteno coals also have a remarkably narrow range of values from −24.4 to −24.0‰, considering that the Molteno coals vary in rank from sub-bituminous to anthracite across the coalfield (Christie, 1981), and that samples were from six different coal seams from boreholes up to 150 km apart.

Table 8.1 $\delta^{13}C$ values of organic matter in carbonaceous rocks from the Permian Witbank Coalfield in the northern MKB, the Pafuri and Waterberg Coalfield from the northern Karoo basins and the Triassic Molteno Coalfields in the MKB. The $\delta^{13}C$ (PDB) values are in per mil. (‰) and depth is in meters below the topmost coal seam in the Waterberg Basin. See Figure 8.1.

MOLTENO		PAFURI		WITBANK		WATERBERG	
$\delta^{13}C$	Depth	$\delta^{13}C$	Depth	$\delta^{13}C$	Depth	$\delta^{13}C$	Depth
-24.0	70	-23.1	+20	-22.3	-60	-22.5	-3.5
-24.4	67	-22.8	+10	-21.9	-65	-22.6	-7.53
-24.3	63	-22.9	-7.5	-22.4	-75	-22.5	-12.46
-24.2	60	-22.6	-13	-21.3	-90	-23.0	-16.16
-24.4	57	-23.8	-25	-23.6	-105	-23.7	-23.48
-24.3	55	-22.0	-75			-23.5	-31.68
						-23.1	-36.19
						-22.4	-45.76
						-21.7	-49.73
						-22.9	-55.96
						-22.5	-60.21
						-21.3	-61.48
						-21.9	-66.09
						-21.9	-66.89
						-22.3	-73.69
						-22.1	-78.84
						-22.6	-92
						-23.7	-102.
						-22.7	-130
						-22.2	-160
						-22.6	-190
						-23.7	-210

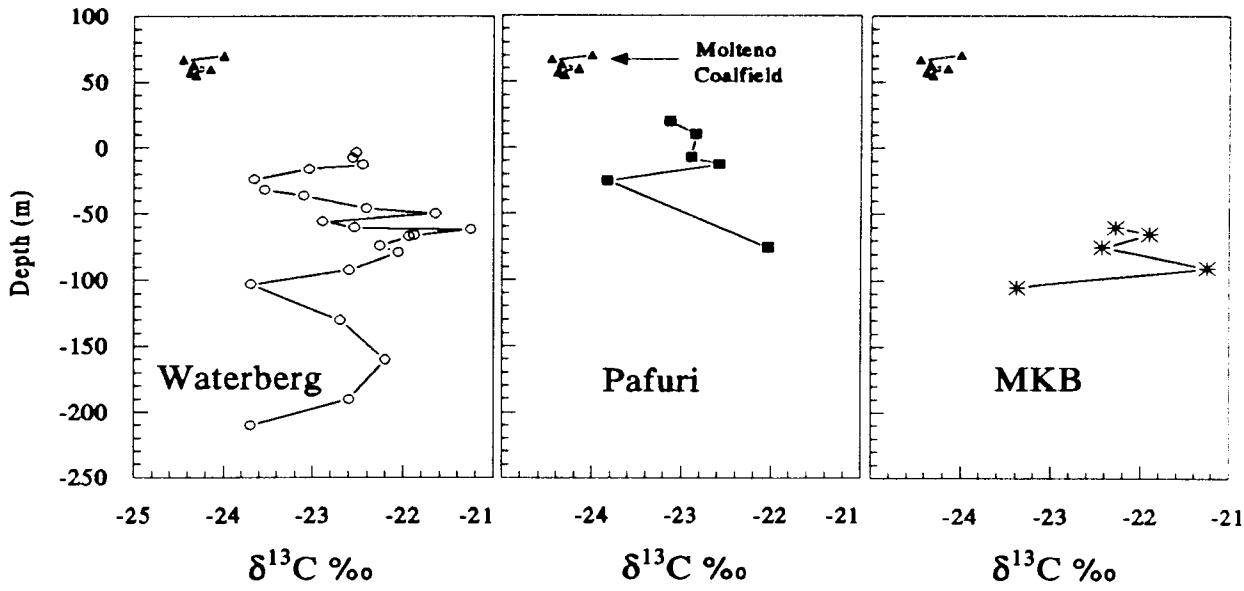

Figure 8.1 $\delta^{13}C$ values of Permian coal and organic matter from the Waterberg Basin, the Pafuri Coalfield and the MKB in the Witbank area, are compared to the $\delta^{13}C$ values of coal from the Triassic Molteno Coalfield. The variations of the organic $\delta^{13}C$ values are plotted against approximate depth below the topmost coal seam in the Waterberg Coalfield estimated from the literature (see Figure 8.2 for references).

8.3 DISCUSSION

8.3.1 ORGANIC $\delta^{13}C$ VALUES and CORRELATION OF SOME S.A. COALFIELDS

8.3.1.1 Permian Coalfields

The MKB coals that have been assigned to the Vryheid Formation are correlated with the four lower coal seams in the Waterberg Coalfield, based on sedimentological evidence (Beukes, 1985) and palynological data (Falcon, 1986; Fig. 2.4). Falcon (1986), however, considered that the 4 coal seams in the Waterberg Basin were formed slightly later than the MKB coal seams. Even though only a limited number of samples from the Permian coals have been analysed for their $\delta^{13}C$ organic values, some correlations are apparent (Figs. 8.1 and 8.2). The $\delta^{13}C$ organic values of coals and particulate organic matter in the Vryheid Formation of the Waterberg Basin and the coals in the Vryheid Formation of the MKB show good relative $\delta^{13}C$ organic correlation, but their peak values do not correlate. The correlation of $\delta^{13}C$ organic values of the coals from the stratigraphically related formations in different coalfields substantiate the idea that the coals in the different basins belong to the same stratigraphic horizon. The distinct decrease in $\delta^{13}C$ organic values at the base of the Vryheid Formation (Biozone C) at the two localities is particularly pronounced (Fig. 8.2). The very similar absolute $\delta^{13}C$ organic values, however, do not prove that these coal seams are also chrono-stratigraphic equivalents because micro-climates at similar times may have differed considerably in the two regions because of the relative positions of north-ward retreating glaciers.

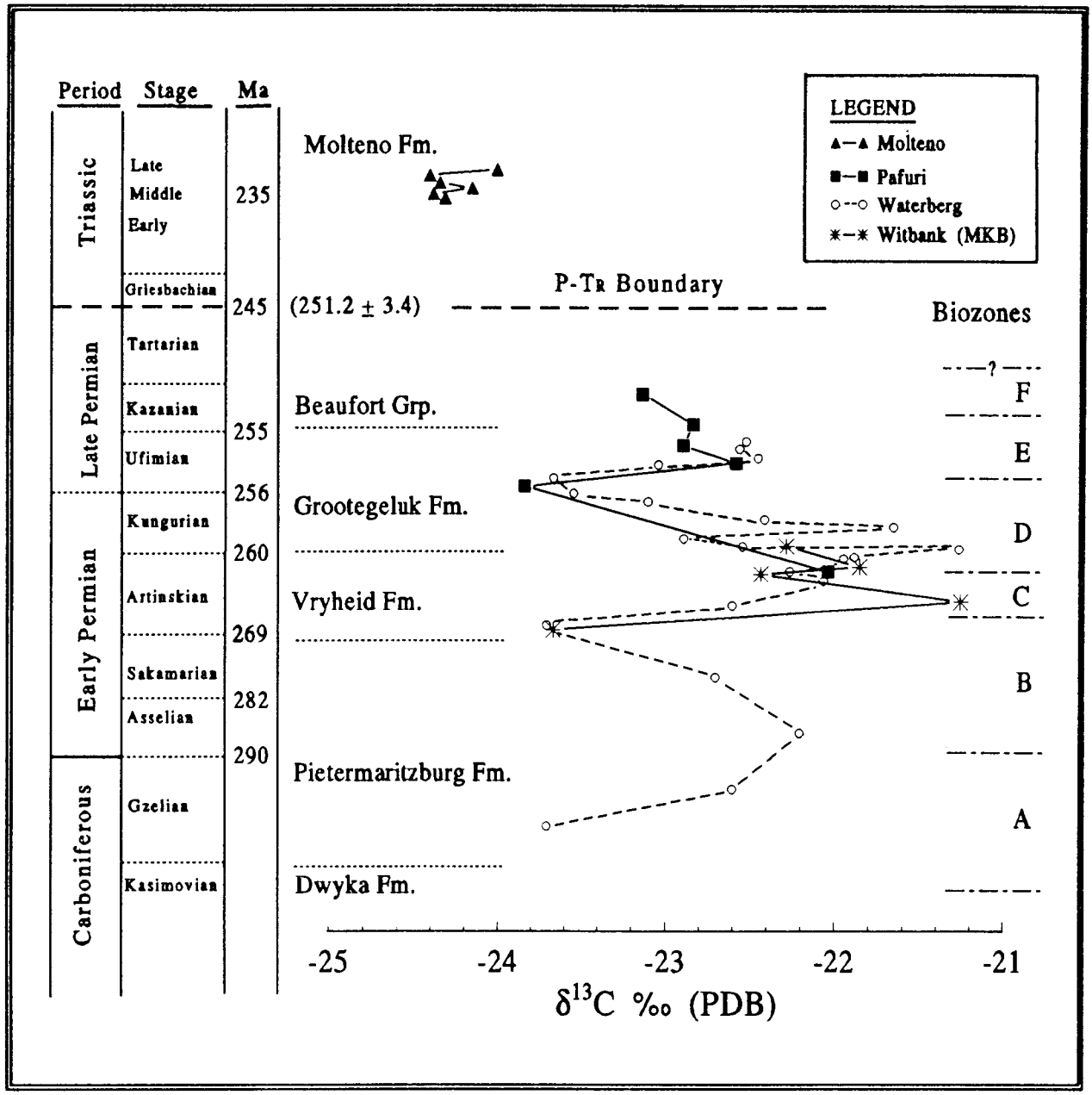

Figure 8.2 Plot of $\delta^{13}C$ values of coal and organic matter from the Waterberg Basin, and coal seams of the Main Karoo Basin in the Witbank area, the Pafuri Coalfield and the Molteno Coalfield. The relative ages of the different coalfields have been established. Estimations of the bio-stratigraphical correlations for the Waterberg and Pafuri Coalfield formations (and biozones) are from MacRae (1988), the Witbank coal seams from Anderson (1977), and the coal in the Molteno Formation from Anderson (1974).

Based on palynological evidence MacRae (1989) proposed that only Biozones D to F were present in the Pafuri coals in the northern portion of the Lebombo monocline (Fig. 8.2). Biozone D in the Pafuri coals is correlated with the upper portion of the Vryheid Formation in the Waterberg Basin, and Biozone F (not present in the Waterberg Basin) probably correlates with either the upper part of the Grootegeluk Formation or the base of the Beaufort Group in the Waterberg Basin. The general variation of the Pafuri $\delta^{13}C$ organic values compared to those from the Waterberg Basin, at the same stratigraphic horizon, is again remarkably similar. The topmost coals in the Waterberg Basin (Biozone E) have exceptionally consistent $\delta^{13}C$ organic values, unlike any of the other Permian

sediments except the upper Pafuri coals (although slightly displaced). The abrupt decrease in the $\delta^{13}C$ organic value at the base of Biozone E and the increase in values toward the base of Biozone D are also consistent with the variations observed in the same Biozones of the Waterberg sediments (Fig. 8.2).

8.3.1.2 Triassic Coalfield

No palynology and very little work on the coals of the Molteno Coalfield has been published. Most studies have considered mainly the stratigraphy, sedimentology and the economic potential of the Molteno coal seams (Turner, 1975; Christie, 1981). Samples from 6 coal seams of the Molteno Coalfield were obtained from various boreholes in the north-eastern Cape and analysed for their $\delta^{13}C$ organic values. The values from the seams are exceptionally uniform, indicating that climatic conditions or plant species did not vary much during this period. Even though only a few samples have been analysed from the Triassic coals it is evident that the $\delta^{13}C$ organic values are different to those of the coals analysed from the Permian coalfields. No coal or particulate organic matter analysed from the Permian rocks had a value lower than $-24‰$ whereas all the Triassic coals were consistently lower than $-24‰$.

Because of the lack of palynological data for the Molteno coals it is only possible to speculate on the reasons for the differences in the $\delta^{13}C$ organic values between the coals from the Permian and the Triassic. Whatever the reasons, they could be very important. They could help establish (1) the cause, which has not yet been satisfactorily resolved, for the global break in coal formation and(or) peat preservation during Permian-Triassic times and (2) the position of the P-T_R boundary which has not been established in South African stratigraphy.

8.3.2 MASS EXTINCTIONS and the PERMIAN-TRIASSIC BOUNDARY

8.3.2.1 Background Discussion

It is well known that many fossil groups have "disappeared" within relatively short periods of geological time at stratigraphic intervals such as Permian-Triassic (P-T_R), Cretaceous-Tertiary (K-T), Ordovician-Silurian and Frasnian-Famennian transitions (Hoffman, 1989). Mass extinctions have been studied for a very long time (Ager, 1973) but have recently become an important topic in Earth and Life Sciences due to the awareness of accelerated global warming, possibly because of anthropogenic pollution. The interest was also considerably enhanced by the proposal of Alverez et al. (1980) that a bolide impact was the primary cause of the K/T mass extinctions. The end of the Permian extinction has been considered to be the most comprehensive devastation of Phanerozoic life (Ager, 1973; Raup and Sepkoski, 1982). Many divergent reasons have been proposed for the P-T_R extinctions.

Some of the more recent postulations for the P-Tr mass extinctions, mainly involving marine invertebrates, include:

1. Maximal sea level regression (Valentine, 1973; Hallam, 1983; Holser and Magaritz, 1987);
2. Trace element poisoning (Waterhouse, 1973);
3. Increased cosmic radiation (Hatfield and Camp, 1970);
4. High temperatures (Waterhouse, 1973);
5. Low temperatures (Stanley, 1984, 1988);
6. Increased salinity (Bowen, 1968);
7. Reduced salinity (Stevens, 1977);
8. Anoxia - marine (Wignall and Hallam, 1992);
9. Oxygen low - continental (Budyko, 1986);
10. Meteorite impact (Hsü and McKenzie, 1990) and
11. Increased pCO_2 - continental (Thackeray, 1990).

Individually, none of these hypotheses can satisfactorily account for the relatively protracted P-Tr mass extinction that occurred ~ 250 Ma ago (Jablonski, 1986). This was the greatest crisis known to affect the Earths's biota, in which marine life was devastated, with a 57% reduction in the number of families (Sepkoski, 1986) and an estimated 96% extinction at the species level (Raup, 1979). Freshwater forms were similarly affected, with a 77% reduction in the number of tetrapod families (Maxwell and Benton, 1987). However, there has been a constant expression of doubt regarding the scale of the Permian extinction, especially in the freshwater realm. Three major factors that oppose the postulation of a catastrophic event that led to the simultaneous extinction of a significant proportion of life forms, especially during the P-Tr, are:

1. The presence of "Lazarus" taxa (Maxwell, 1989) i.e. taxa that re-appear in the Triassic.
2. Authors who have presented papers on "mass extinction" have little knowledge of fossils, *per se*, and have given equal weight to all taxa, be they families, genera or species (Teichert, 1990).
3. The incomplete stratigraphic record across the P-Tr boundary (Hoffman, 1989). There are only a few examples of complete marine stratigraphic records across the P-Tr boundary e.g., South China (Sheng et al., 1984), Pakistan (Teichert, 1990) and a recently identified locality at Gartnerkofel in the Austrian Alps (Holser et al., 1989; Magaritz and Holser, 1991; Magaritz et al., 1992).

8.3.2.2 Permian-Triassic Boundary and Mass Extinctions in Southern Africa

The P-Tr boundary in southern Africa occurs somewhere within the stratigraphic sequence of lacustrine and fluviatile sediments known as the Beaufort Group of the Karoo

Sequence (Tankard et al., 1982; Turner, 1991; Cole, 1992), but the exact position has not been located. The Karoo Sequence, in the MKB, is a well known source for gathering of data regarding the extinction of freshwater tetrapod families (King, 1990). However, episodes of maximum terrigenous influx were diachronous in different parts of the Karoo trough, so that correspondence between stratigraphic subdivisions in the Karoo basin is not always apparent (Tankard et al., 1982; Turner, 1991; Cole, 1992; Smith et al., 1993). Sedimentary reworking in many of the Beaufort Group strata also complicate the delineation of a P-Tr boundary (R.M.H. Smith pers. comm., 1992). Pitrat (1973) also suggested, that because of the changes in sedimentation in the Karoo Basin, the abruptness and magnitude of the freshwater extinctions may be exaggerated. Traditionally the systemic boundary is placed at the bottom of the *Lystrosaurus* Zone named after the therapsid genus that is widely distributed in the Gondwana area (not South America) and China (Teichert, 1990). Anderson and Cruickshank (1978) and Battail (1988), however, postulated a major stratigraphic break between the *Daptocephalus* zone and the *Lystrosaurus* zone, assigning the former to the Early Tartarian (~250 Ma, Harland et al., 1990) and the latter to the Early Griesbachian (~245 Ma, Harland et al., 1990; Fig. 8.2). The lack of known complete freshwater sections, therefore, is complicating interpretation of the extinction of non-marine forms and in establishing the P-Tr boundary.

8.3.3 PERMIAN-TRIASSIC COAL FORMATION

Coalfields of Permian age, such as the southern Africa coalfields, occur essentially in Gondwana basins (Chandra and Taylor, 1982; Frakes, 1979; Fig. 8.3). Palynological studies of southern Africa coals (MacRae, 1988, 1992) suggest that the Permian coals vary in age from late Sakamarian to mid-Tartarian (about 270 to 248 Ma, Harland et al., 1990; Fig. 8.3). Minimum age estimates of the Australian coalfields (Hobday, 1987) and bituminous black shales of the Irati Formation in Brazil (Daemon et al., 1991) also indicate an age of Mid-Tartarian. After a break in the formation or the preservation of coal during the P-Tr boundary times, coal re-appeared in South Africa in the Molteno Coalfields, which are either Middle or Late Triassic in age (235 to 220 Ma, Harland et al., 1990).

Very special conditions have to be maintained to preserve peat and thus to eventually produce coal with increased burial (Chapter 5). The formation of coal is dependent on several factors, e.g., the formation and type of plant community, climate, ecology, pH, Eh, and sedimentological conditions. Even though several criteria are required to preserve peat and to eventually form coal, it is still remarkable that no coal was formed and(or) preserved anywhere in the world at the P-Tr boundary (Fig. 8.4). This break in coal formation and(or) preservation during the Tartarian Stage was global and very abrupt.

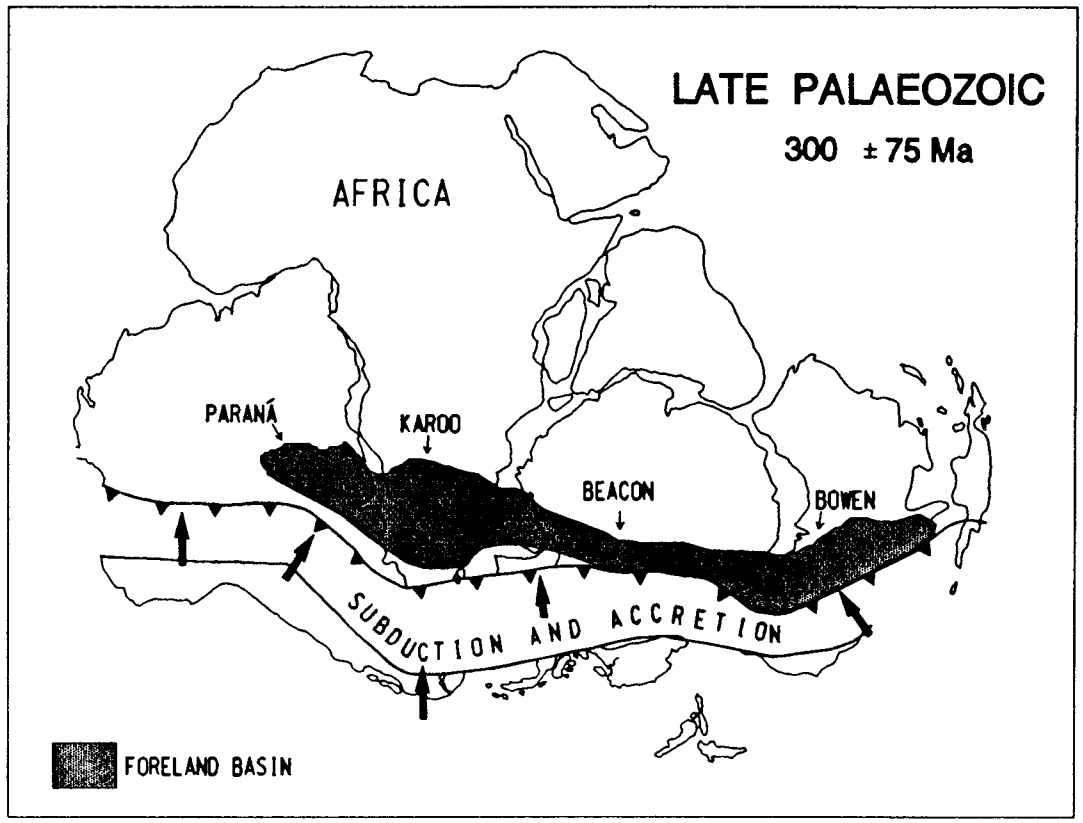

Figure 8.3 Schematic diagram showing the positions of the coal-bearing basins that formed during accretion tectonics along the southern margin of Gondwana during the late Palaeozoic (de Wit and Ransome, 1992). The distribution of coal deposits of Permian age (world-wide) occur predominantly in the regions delineated as foreland basins in Gondwana (Frakes, 1979).

The P-Tr boundary times are usually considered to be "dry and hot". Sedimentological studies of the Beaufort Group (Late Permian - Early Triassic), however, invariably describe environments that range from lacustrine deltas, estuaries with tidal flats, low to high sinuous rivers etc. (Smith, 1990; Stear, 1983; le Roux, 1992) and "flourishing vegetation on the channel banks" (Keyser, 1970). Although the palaeo-climate for this period has generally been interpreted as semi-arid to arid, Pretorius (1985) maintained that it was wet temperate. The evidence that Late Permian coals in southern Africa become more vitrinite-rich towards the top of the coal successions challenges the conjecture that conditions gradually became less favourable for the formation of coal as they are preserved today (Chapter 5). The paucity of coal in the P-Tr boundary times in Gondwana rocks do not represent a rapid migration towards lower latitudes because the migration only started after the Middle Triassic (Smith et al., 1981). The absence of coal in the rocks from the P-Tr therefore does not appear to be related to an extreme climatic change.

8.3.4 COAL FORMATION AND GONDWANA TECTONICS

Two of the most striking characteristics of the break in coal formation and(or) preservation at the end of the Permian, is the abruptness (Fig. 8.4) and regional extent (Gondwana scale) of the break. The common denominator of the vast majority of coal

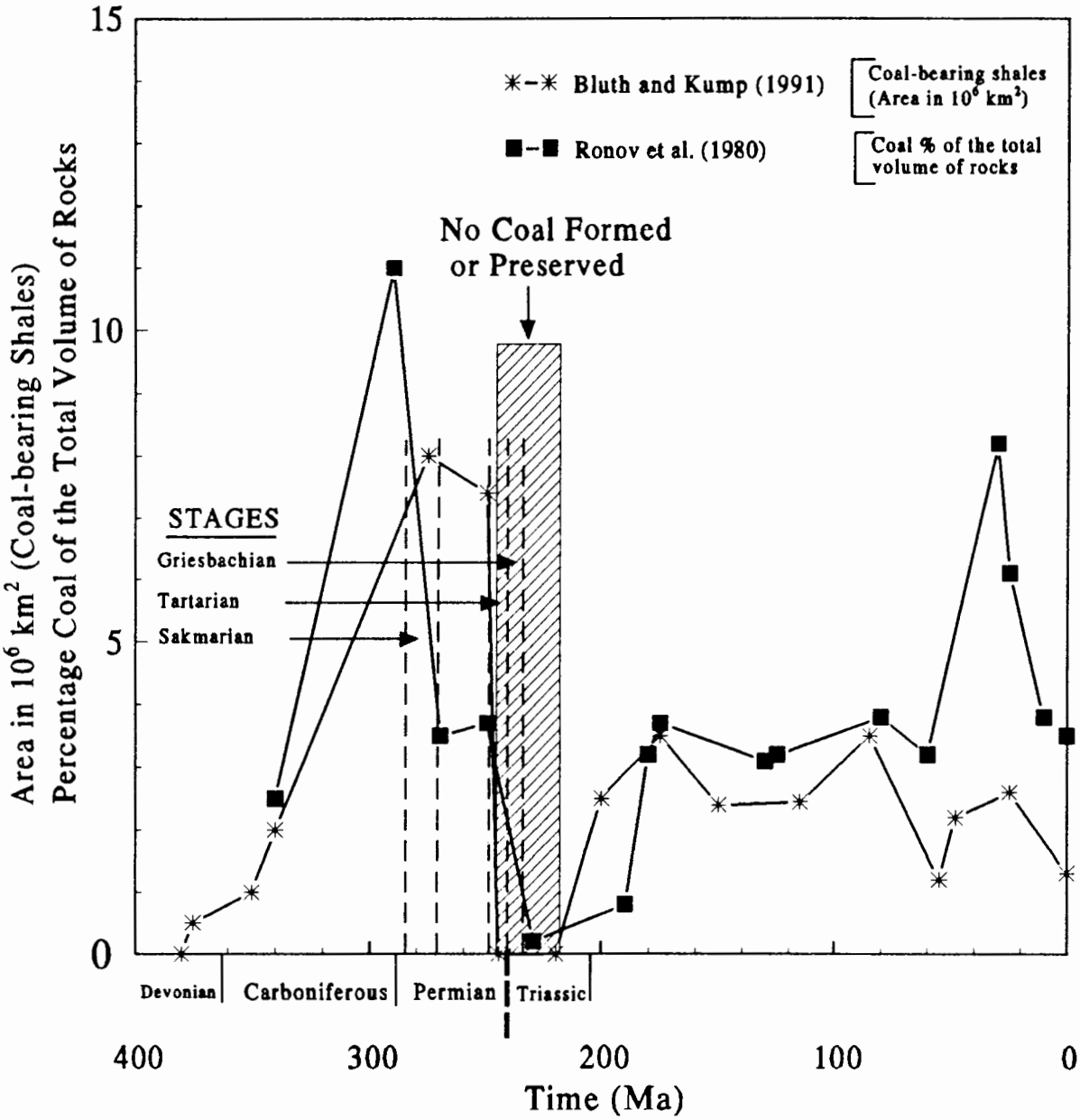

Figure 8.4 Plot of the abundances of coal-bearing sediments after Ronov et al. (1980; volume) and Bluth and Kump (1991; area) since the commencement of coal formations in the Devonian. The scale on the Y-axis is applicable for both estimations. The age of the P-Tr boundary, which is taken to be about 245 Ma, and the stage divisions are after Harland et al. (1990). The P-Tr boundary, however, has been estimated at 251.2 ±3.4 Ma by Claoué-Long et al. (1991), based on U-Pb ages of zircons in a P-Tr volcanic boundary clay in South China.

basins at the end of the Permian was that all were in Gondwana, and one of the most important events that was taking place throughout Gondwana at this time was large scale tectonism. It has now been reasonably well established that in the vicinity of southern Africa a series of about 6 episodic tectonic "paroxysms" (pulses) took place along the southern

margin of Gondwana (Hälbich et al., 1983; Gresse et al., 1992). As a result of "impact" tectonics along the southern margin of Gondwana, foreland basins such as the MKB formed in response to accretion. The effects of the accretion, however, are considered to have also resulted in large scale deformation over the whole of Gondwana (de Wit et al., 1988; Daly et al., 1991; de Wit and Ransome, 1992; Fig. 8.5). $^{40}Ar/^{39}Ar$ dating of the Cape Orogeny demonstrated that deformation resulting in the mega-folding in the Cape Fold Belt occurred sometime during the Late Permian (about 250 Ma; Hälbich et al., 1983; Gresse et al., 1992), and recent K/Ar biotite ages between 235-260Ma in the Elqui plutons, from the Chilean Gondwana margin, are considered to indicate uplift and collision related to subduction (Mpodozis and Kay, 1992). A similar sequence of deformation events and syn-collisional Late Permian granites have been postulated in the New England Fold belt of eastern Australia by Sylvester (1989).

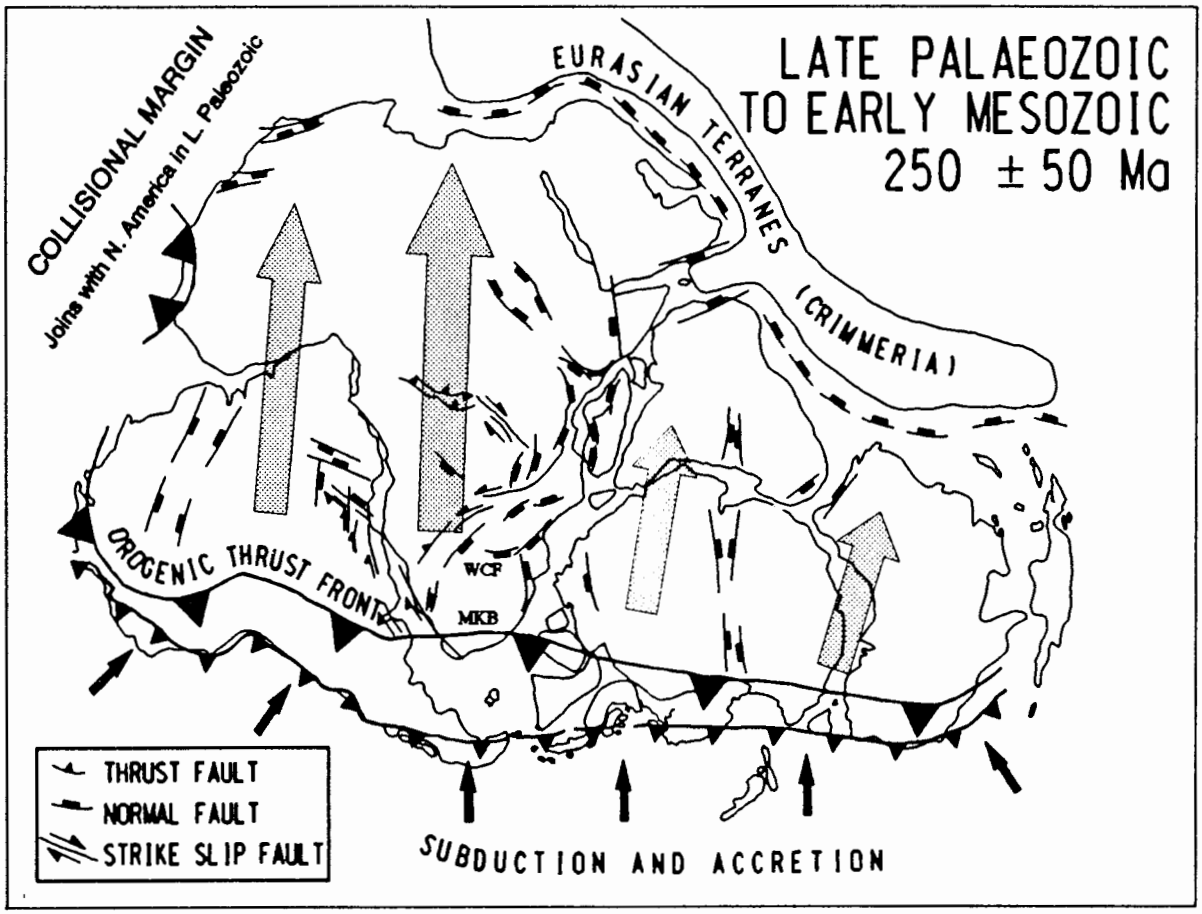

Figure 8.5 Schematic diagram showing large scale late Palaeozoic fracturing of the Gondwana lithosphere (Daly et al., 1991). The orientation of various fault systems are compatible with stress induced failure due to "impact" tectonics along the southern margin of Gondwana during terrane accretion. The assembly of Pangea and the formation of the Appalachian mountains in north America also occurred at this time. The arrows indicate the direction of continental scale stress transmission. The location of the MKB and the Waterberg Coalfield (WCF) are also shown. Diagram modified from de Wit and Ransome (1992).

The tectonic events described above are, as a whole, part of the global collisional assemblage of Pangea (Veevers, 1988). It has been demonstrated by Edmond (1992) that

the major positive oscillations in the $^{87}Sr/^{86}Sr$ isotope record in seawater can be caused only by continental collisions of the Himalayan type. One of the largest ^{87}Sr increases in seawater occurred at the Permian Triassic boundary. This probably records the assembly of Pangea and formation of associated Appalachian mountains (Fig. 8.5). The end of the Permian was also characterised by one of the strongest regressions of the sea in the entire Phanerozoic (Holser and Magaritz, 1987) and may have resulted in response to the assemblage of Pangea (c.f. Nance et al., 1988).

All these events approximately coincide or are slightly younger than the minimum ages of the Late Permian Gondwana coals. The collision tectonic event(s) along the margins of Gondwana may well have resulted in "fore-bulge" or uplift of the sediments containing shallow peat formations. Up-lift of peat formations buried to shallow depths, for example in the mudstones of the Beaufort Group in the Waterberg Basin, would have resulted in a profound drop of ground-water levels, and oxidation would have followed. Evidence for the previous existence of organic matter in the grey mudstones, overlying the vitrinite-rich mudstones to-day, is the presence of siderites with very low $\delta^{13}C$ values (– 18‰; Chapter 7). The absence of spherulitic siderite (positive $\delta^{13}C$ values) indicates that the burial of the organic matter did not reach the stage of methanogenesis and was therefore oxidized during relatively shallow burial depths. "Up-lift" that occurred subsequent to deposition of organic rich sediments would also account for other evidence from the Waterberg Coalfield: (1) the absence of any sedimentological breaks or changes at the top of the coal formation (Chapter 4 and 6); (2) the high vitrinite content of the topmost coals (Chapter 5); (3) the anomalous concentrations of pyrite and abrupt increase in kaolinite:illite ratio in the mudstones immediately above the topmost coals (Chapter 6) and; (4) the absence of any change in the $\delta^{13}C$ values of the organic matter in the upper Waterberg and Pafuri coals (Chapter 7).

8.3.5 "ISOTOPIC EVENTS" at the PERMIAN-TRIASSIC BOUNDARY

8.3.5.1 Evidence From Marine Carbonates

The carbon isotope composition of marine carbonate rocks show large variations through the geological record (Veizer et al., 1980). The large isotopic variations or "isotopic events" are beginning to be applied as time lines in stratigraphic correlation (Holser et al., 1986) and are also correlated with mass extinction events in the Earth's history. The $\delta^{13}C$ values of marine carbonates during the Permo-Carboniferous are characterised by relatively high values (5 to 7‰; Holser et al., 1986). $\delta^{13}C$ values of about +4‰ continued with only minor variations until very near the end of the Dorashamian and then declined sharply to values of or just below – 1‰ at the P-T_R boundary (Holser and Magaritz, 1987; Gruszczynski et al., 1989; Holser et al., 1989; Malkowski et al., 1989; Magaritz et al., 1992; Fig. 8.6). The sharp drop and a $\delta^{13}C$ minimum value at the P-T_R boundary is nearly universal throughout

the Tethyan Belt which crops out along the mountain chain from the Southern Alps to the Himalayas, and also in South China (Holser and Magaritz, 1992). In the Gartnerkofel in the Carnic Alps of Austria Holser et al. (1989) identified another $\delta^{13}C$ minimum in the Lower Triassic (Fig. 8.6). This upper minimum, however, has not been found elsewhere possibly because detailed sampling does not extend so far above the stratigraphy of the P-TR boundary (Holser and Magaritz, 1992).

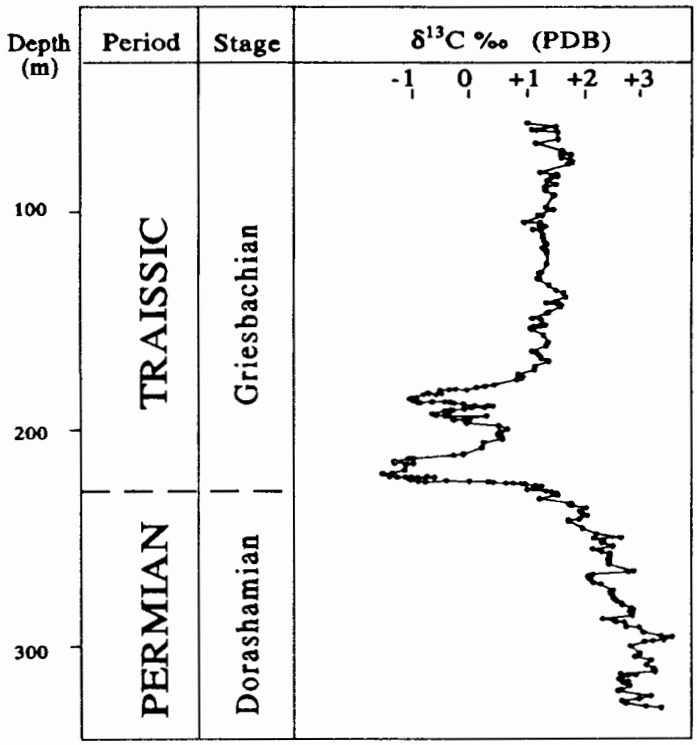

Figure 8.6 Marine carbonate $\delta^{13}C$ values in the borehole GK-1, drilled in the southern Alps of Austria (Holser et al., 1989). The distinct drop in the marine carbonate $\delta^{13}C$ values at the Permian-Triassic boundary has been verified on a global scale (Holser et al., 1986; Baud et al., 1989). The upper $\delta^{13}C$ minimum has, however, only been found in the GK-1 borehole (Holser et al., 1989; Holser and Magaritz, 1992).

The rise in $\delta^{13}C$ during the Permo-Carboniferous is thought to have been caused by a rapid and enormous removal from the ocean-atmospheric system of organic carbon. However, there is no evidence of where a massive (30 times total C presently in the biosphere; Gruszczynski et al., 1989; Malkowski et al., 1989) storage of organic carbon could have been. Berner (1990) suggested that the carbon was possibly stored in paralic (open to the sea) coal deposits. Paralic coals were being formed in Gondwana from the early-middle Permian in the MKB, but most of the late Permian coals that are present mainly in the northern Karoo basins have a freshwater origin. The subsequent decrease of the $\delta^{13}C$ of marine carbonates indicates that oxidation of organic matter must have occurred and that the ocean received 3 times more (Gruszczynski et al., 1989) organic carbon than it had previously lost.

8.3.5.2 Isotopic Variation of Permian-Triassic Freshwater Organic Matter

Regardless of the reason for the "isotopic events" of the marine carbonates, if the causes of the events were global then it is possible that the $\delta^{13}C$ value of freshwater organic matter also recorded these events. It has recently been demonstrated that the $\delta^{13}C$ marine organic values at the P-Tr boundary in the marine sediments at the Gartnerkofel site in the Austrian Alps (Magaritz et al., 1992) parallel the carbonate $\delta^{13}C$ values. No coal deposits are preserved across the P-Tr boundary but the $\delta^{13}C$ organic values presented in this study show that there is a distinct, albeit small, difference between the freshwater organic matter of the Permian and the Triassic Periods. It was also demonstrated that the differences in the $\delta^{13}C$ organic values persisted even in the particulate organic matter, and if a continuous sedimentary sequence was analysed for its $\delta^{13}C$ organic values then it may be possible to locate a freshwater P-Tr "isotopic event".

It has been discussed previously (Chapter 7) that a variety of factors influence the carbon isotopic composition of organic matter (O'Leary, 1988). Foremost among these is the different isotopic fractionation between C_3 and C_4 biosynthetic pathways (O'Leary, 1988). However, the oldest known fossil C_4 plants are late Miocene in age (about 10 Ma; Thomasson et al. 1986), and therefore the plants from the Permian used only the C_3 pathway of fixing atmospheric CO_2 (Ehleringer et al., 1991). High concentrations of CO_2 favour enzymatic rate control over diffusional rate control in isotopic fractionation, with the result that organic carbon synthesized under higher pCO_2 conditions is isotopically lighter (Deines, 1980; Popp et al., 1986; Rau et al. 1991). Rau et al. (1991) explained the decrease of 1 to 2‰ in $\delta^{13}C$ organic values across the last glacial-interglacial transition of the Quaternary as being due to the measured increase in $CO_2(aq)$ and pCO_2. Therefore, fluctuations in oceanic CO_2 or atmospheric pCO_2 concentrations could be represented in the Permian and Triassic organic matter isotopic record. Another cause for change in the $\delta^{13}C$ value of organic material is the effect of increased dryness but this has the effect of increasing $\delta^{13}C$ of plants (Tieszen, 1991).

The $\delta^{13}C$ values of organic matter (coal and particulate) that encompasses nearly the whole Permian up to the Tartarian stage show, in this study, that no *major* isotopic shifts occurred that would indicate major variations in the oxygen and CO_2 atmospheric concentrations during this period. The $\delta^{13}C$ organic values of the coal and organic matter in this study, however, do show an overall decrease between the Permian and the Triassic Period. Although no palynological work has been done on the Triassic coals it is considered that the plant material in the Molteno Coalfield had a freshwater origin (Christie, 1981). The freshwater origin of the organic matter is confirmed by $\delta^{13}C$ organic values which are typical of C_3 plants. Although it is not possible to estimate the absolute amount, it does appear that there was a relative increase in atmospheric pCO_2 over a period of about 10

million years from the Late Permian up to the Middle Triassic. The possibility of a worldwide shift of $\delta^{13}C$ organic values of freshwater vegetation (and $\delta^{13}C$ atmospheric), as measured in apatite of reptilian teeth, has also recently been proposed for the late Permian by Thackery et al. (1990).

8.3.6 TECTONICS, FRESHWATER CARBON and P-T_R MASS EXTINCTIONS

Even though there are problems in establishing the scale of the freshwater and marine P-T_R extinctions they nonetheless appear to have been real, as was the lack of coal formation (preservation). As discussed above, many theories have been proposed for P-T_R extinctions but no one theory satisfactorily accounts for the mass extinctions (Jablonski, 1986). It may be, however, that the reasons for extinction are dependent and interrelated to one another making it difficult to distinguish between cause and effect. For example, sea-level must have dropped substantially because of the formation of the Pangea mountains as a result of the "collision" of Gondwana with Laurasia. The whole southern margin of Gondwana also experienced collision and "uplift". Gondwana at this stage was predominantly covered by extensive shallow peat-bearing sequences (i.e. during deposition of rocks now termed lower Beaufort Group in the Waterberg Basin) that were oxidised because of this "up-lift"; this may have resulted in a significant lowering of atmospheric oxygen. Although the up-lift of continental areas occurred simultaneously with the drop in sea-level, the latter was not directly responsible for the oxidization of freshwater organic matter, or the P-T_R mass extinctions. Schopf (1974) proposed that sea-levels dropped as a result of sea-floor spreading, but increase in sea-floor spreading causes sea-levels to rise (Pitman, 1978). Sea-floor spreading rates, however, would have increased only during the subsequent break-up of Pangea, i.e. during the Triassic-Jurassic.

The oxidization of freshwater carbon would result in a decrease in $\delta^{13}C$ values in rivers flowing into the sea and therefore a decrease in marine carbonate $\delta^{13}C$ values (resulting in a carbon "isotopic event"). The oxidization of freshwater carbon results in an increase in atmospheric CO_2 causing a greenhouse effect, increasing atmospheric temperatures accompanied by continental aridity and decrease in worldwide organic matter burial. The increased atmospheric pCO_2, temperature, aridity, and marine regression would adversely affect freshwater and marine life causing either extinction or at least reduction in species.

It is not within the scope of this study to discuss the carbon cycle or how Earth is able to reverse a greenhouse climate or prevent a permanent ice-age. Nevertheless, the similar minimum biostratigraphic ages of the late Permian Gondwana coal formations correspond with the timing of regional collision tectonics and "up-lift" along the whole of the southern Gondwana margin. Up-lift resulted in oxidization of vast Gondwana peat

formations and affected atmospheric conditions and severally distressed freshwater and marine life. The end Permian extinctions may have resulted not necessarily from any one individual cause, but from several interrelated and inter-dependent events. Ultimately, it seems climate change due to collisions and amalgamation of Pangea was the driving force.

8.3.7 SUMMARY

Organic $\delta^{13}C$ values from coal and organic matter from selected South African coalfields support evidence, mainly from palynological studies, that the MKB coal seams were formed under different conditions and(or) at an earlier time than the coals from the northern Karoo basins. The isotopic data confirm the findings of MacRae (1988, 1989) that the Waterberg and Pafuri Coalfields from the northern Karoo basins can be correlated stratigraphically. The organic $\delta^{13}C$ values from the Triassic Molteno Coalfield are exceptionally constant and distinctly different from the values determined for Permian coals and mudstones. The results of the organic $\delta^{13}C$ analyses in coal and mudstones demonstrate a potentially useful method for establishing the P-Tr boundary in southern Africa, provided detailed sedimentology, palaeontology and palynology studies have been done on the rocks.

The $\delta^{13}C$ values of the Permian and Triassic freshwater organic matter suggest that there was a change in the atmospheric $^{13}C/^{12}C$ ratio during this time. The decrease in the ratio of atmospheric carbon is compatible with the input of negative $\delta^{13}C$ values resulting from the oxidisation of organic carbon. Studies of coal distribution have demonstrated that there was an abrupt and major decrease of coal formation and(or) preservation world-wide at the P-Tr boundary. During the Permian, coal formed predominantly in Gondwana which was at the time subjected to episodes of large scale tectonism as a result of collisions along the whole of its southern margin. The impact of the tectonism affected vast areas of land that were accumulating and burying organic matter. The uplift and oxidation of some of the shallow peat before further burial is consistent with evidence provided in this study. It is suggested, therefore, that the mass extinction which has been proposed for freshwater and marine species at the P-Tr boundary may directly or indirectly be related to a culmination of events that resulted from the P-Tr tectonism during the formation of Pangea.

9. COAL MINING DISCARDS - SIMULATED LEACHING TESTS

9.1 INTRODUCTION

The process of surface mining of fossil fuels disturbs vast land areas, and in the process, geological strata long buried are exposed to the atmosphere. Once exposed to air and water, the rocks start to "break-down" resulting in chemical reactions that may lead to environmental problems. The largest land disturbances and some of the worst environmental problems have been created by the surface mining of coal (Evangelou, 1983). Mechanisation of surface and underground coal-mining, and the ability of power stations to burn higher ash coals, have increased the proportion of discard material. It has been estimated that about 34 300 Mt and 52 300 Mt coal can potentially be produced from surface and underground mining respectively in the Waterberg Coalfield (Dreyer, 1991). If this is the case then approximately 146 000 Mt discard material will be produced assuming a 45% yield for surface and a 75% yield for underground mining.

Solid wastes produced by coal mining have acquired a variety of names in different countries. These include "waste", "refuse", "dirt", "slag", and "spoil". These names generally imply a valueless material, but the coal-mining industry is increasingly looking for ways of using this material for profit. Discard dumps now are becoming regarded rather as temporary stocking grounds of a raw material. The end result is that opencast workings, which produced very little discard material in the past because it was backfilled into pits after a relatively short period of time, now tend to "store" the discard material for longer periods on the surface. The coal-mining discard material (primarily carbonaceous mudstones) at Grootegeluk Coal Mine is presently placed onto dumps but will be back-filled into the mined-out pits after 15 years (J.C. Dreyer pers. comm., 1991).

The importance of establishing the mineralogy and chemistry of the geological strata that will be exposed in the Waterberg Coalfield is especially important because of the high coal reserves, the high proportion of discard material, and the customary use of groundwater from boreholes in the area. The difficulty of coal-mining and environmental damage control is that the environmental damage has often already started before steps are taken to minimise the harm. There are several environmental problems that result from opencast mining and coal discard disposal, such as acid mine drainage (AMD), erosion, air and groundwater contamination, combustion control, mine sealing, and reclamation (Sciulli et al., 1986). It is unfortunately outside the scope of this study to investigate all of these possible problems. This study has aimed only to try and establish whether solid discard products from coal mining could potentially be a source of toxic concentrations of trace elements either to the groundwater or if the discard material was used as a soil. The selected trace elements that have been analysed are elements that have been identified to be potentially harmful to life (Chapter 3).

Discard materials that have been tested in this study are the carbonaceous mudstones which interbed the coal seams, and also waste material produced from the incineration of coal (~ 35% ash) at the Matimba power station which receives its coal from the Grootegeluk Coal Mine. Fly ash is the particulate matter removed from the emissions resulting from combustion of pulverised coal in power stations by electrostatic precipitators. Bottom ash is the solid residue that remains at the base of furnaces after combustion of the coal. Bottom ash usually consists of sand-sized or coarser grains whereas fly ash are particles usually 10-20 μm in diameter (Bosch, 1990).

Laboratory leaching experiments were used to simulate natural leaching of selected elements, some potentially toxic, from discard dumps. After consideration of several leaching methods it was decided to use the ammonium nitrate leaching method of von Prüeß et al. (1991). The rational for using this method, the leaching procedure and the analysis of the leachates was described in Chapter 3.

9. 2 RESULTS

The elements that have been analysed in the leachates by ICP-OES were Na, Mg, Al, P, S, K, Ca, V, Cr, Fe, Ni and Zn. Boron, Be, Co, Cu, As, Mo, Cd, Sb, Ba, Tl, Bi, and U were analysed by ICP-MS. The full results are presented in Table II.5 (Appendix II) and are also plotted against depth below the topmost coal seam of the Grootegeluk Formation in Figure 9.1. Results of samples that were leached in duplicate and one in triplicate, were averaged and plotted on Figure 9.1 (Table II.4, Appendix II). If an element in one of duplicate leachates was below the lower limit of determination, then the value which was above the lower limit of determination was used in Figure 9.1. Values that were below the lower limit of determination are not plotted in Figure 9.1 and are designated as a negative number in Table II.5 (Appendix II). One fly ash and one bottom ash sample was leached in duplicate and the average results are reported in Table 9.1.

From the results plotted in Figure 9.1 it is apparent that the values generally are very low. Most of the results for Fe, B, Be Cu, As, Mo, Cd, and Bi are either below or have values close to the lower limit of determination. The most prominent exceptions are the values of samples that occur immediately above the topmost coal seam. The only elements which are not anomalous in these samples are Na, K, Ba, and Bi. Values of Mg, K and Na increase progressively in the upper 20 m of the Grootegeluk Formation and B concentrations also occur in anomalous concentrations in samples from the upper part of the formation. Barium and Sb values increase rapidly to anomalous concentrations in samples from the base of the Grootegeluk Formation.

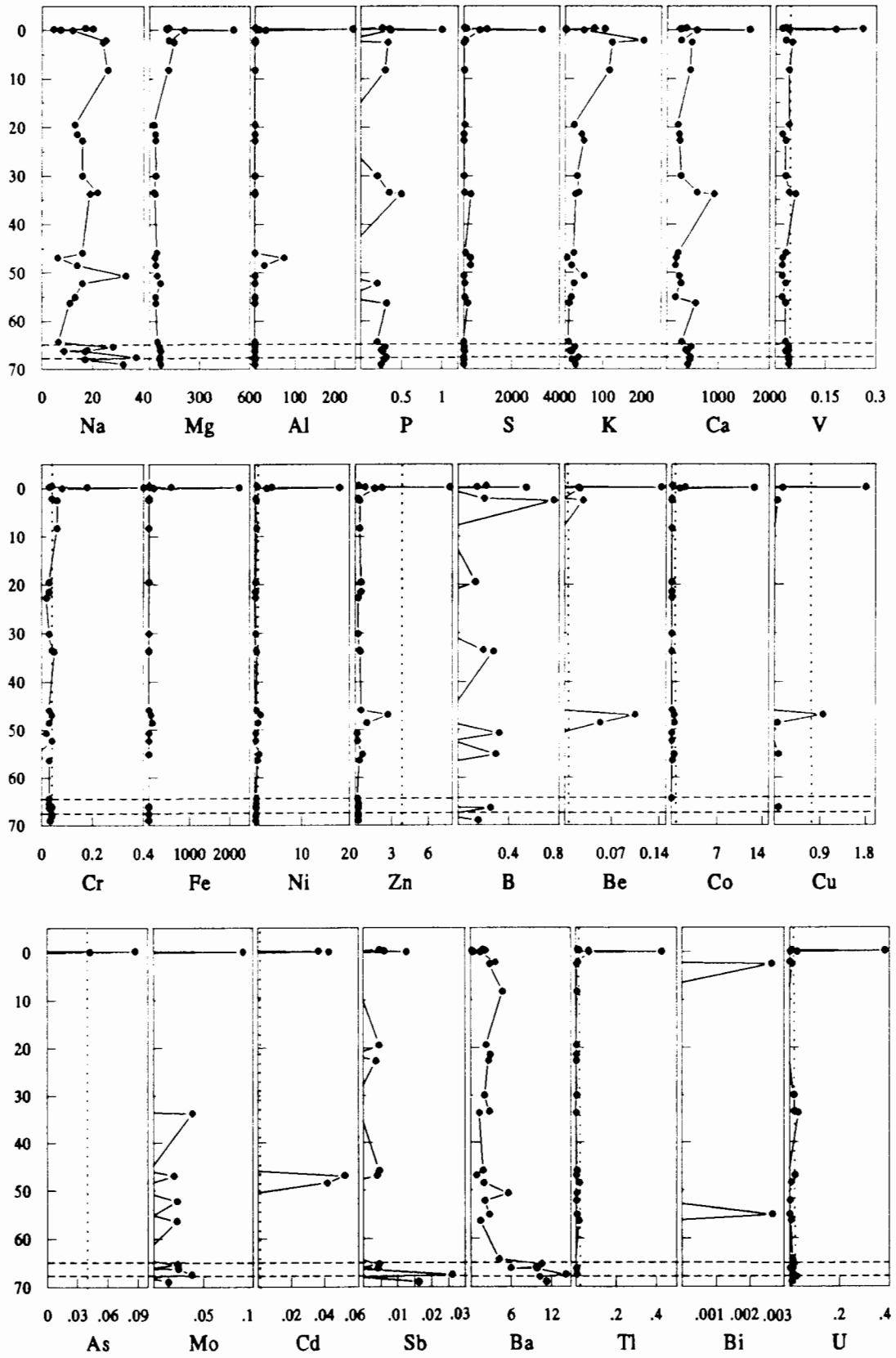

Figure 9.1 Concentration of elements (ppm) in ammonium nitrate leachates of samples from the Grootegeluk Formation. The leaching method used was that of von Prüeß et al. (1991). The samples are plotted according to depth below the topmost coal seam in the Grootegeluk Formation. Sodium to Zn were analysed by ICP-OES and B to U by ICP-MS. The vertical dotted lines indicate critical concentrations of trace elements, identified by von Prüeß et al. (1991), that could be harmful to the environment.

It is evident from Table 9.1 that the concentration of all of the elements in the leachate from the fly ash sample is substantially higher than in the bottom ash sample. The concentrations of P, Ca, V, Cr, and U, and particularly B, Mo, Sb and As are very high in the fly ash leachate compared to those from the mudstones.

Table 9.1 The concentrations (ppm) of elements in leachates of fly ash (FA) and bottom ash (BA) from the Matimba power station that receives its coal from the Grootegeluk Coal Mine. The elements from Na to Zn were analysed by ICP-OES, and B to U by ICP-MS. The ICP-MS data are analysed at the ppb level and are therefore reported to three significant figures in this Table. The results are averages of analyses of duplicate leachates, of the fly and bottom ash samples. Also included are the critical values for elements identified by von Prüeß et al. (1991) to be harmful to the environment. <lld = less lower limit of determination.

Element	Fly Ash	Bottom Ash	Critical Value	Element	Fly Ash	Bottom Ash	Critical Value
Na	24	21	-	B	18.61	0.472	-
Mg	111	25.5	-	Be	<lld	<lld	0.008
Al	0.4	<lld	-	Co	0.008	<lld	0.200
P	1.1	0.7	-	Cu	0.165	<lld	0.800
S	408	27	-	As	0.178	0.036	0.040
K	40	6	-	Mo	1.327	0.118	0.400
Ca	1270	243	-	Cd	0.016	<lld	0.008
V	0.4	0.1	0.040	Sb	0.256	<lld	0.400
Cr	2.1	0.03	0.040	Ba	2.231	2.158	-
Fe	3.5	0.02	-	Tl	0.006	<lld	0.012
Ni	0.62	0.17	0.400	Bi	<lld	<lld	0.040
Zn	0.67	0.18	4.000	U	0.201	0.007	0.016

9.3 DISCUSSION

9.3.1 MINERALOGY and CONCENTRATION of ELEMENTS in LEACHATES

In Chapter 6 it was concluded from the whole-rock geochemistry that the samples above the topmost coal seam have anomalous concentrations of pyrite and trace elements that are associated with pyrite. The Fe and S (and Ca) values in the leachates from samples above the topmost coal seam are much higher than those of other elements, and higher than leachates from the other mudstones. This suggests that the source of the Fe and S in the leachates is the pyrite in the samples. Concentrations of Mg, K and Na in the leachates increase progressively upward in the top 20 m of the Grootegeluk Formation and are most likely leached from the clay mineral montmorillonite-illite which was identified in this part of the formation (Chapter 4). Boron concentrations which are also relatively high in these samples are also most likely leached from the montmorillonite-illite.

In Chapters 4 and 6 it was established that apatite, Ba and Sr occurred in anomalous concentrations at the base of the Grootegeluk Formation (carbo-tonstein zone). However, neither P or Ca are anomalous in the leachates from samples in this part of the formation. Ba is anomalous and Sr was not determined. The mineralogical study of the carbo-tonstein mudstones (Chapter 4) demonstrated that the majority of the apatite occurred as an alteration mineral within kaolinite, and this may also be partly why the P and Ca concentrations do not increase in the leachates of these samples. The anomalous concentrations of Ba are significant because in Chapter 4 it was not possible to establish any mineralogical association for Ba (and Sr), even though a crandallite group association was proposed by Spears et al. (1988). An electron microprobe scan in this study established that Ba and Sr were in fact evenly dispersed in the carbonaceous-rich mudstones of the carbo-tonstein zone. The high concentration of Ba in the leachates of the samples at the base of the formation supports the suggestion that Ba (and Sr) are not bonded in any mineral but merely adsorbed onto the clay minerals and organic matter. The samples were not analysed for their antimony whole-rock concentrations and it is not clear why the concentrations of Sb in the leachates of the samples at the base of the Grootegeluk formation should be anomalous. The presence of Sb may be important in the interpretation of the origin of the carbo-tonstein because Sb has been detected in emissions from Hawaiian volcanoes (Cadle et al., 1973).

9.3.2 LEACHATES of GROOTEGELUK FORMATION MUDSTONES

Based on studies from 40 field sites and 400 soil and vegetation analyses, von Prüeß et al. (1991) established the leachable concentrations of selected elements that may be harmful to plants, animals and humans. The concentrations of the elements that are considered to pose a possible threat to the environment are listed in Table 9.2. It is evident from a comparison of the values in Figure 9.1 and Table 9.2 that the concentrations of leachable trace elements in the carbonaceous mudstones of the Grootegeluk Formation are not high enough to be of any environmental concern, according to the leaching method and critical values proposed by von Prüeß et al. (1991).

9.3.3 COAL MINING OVERBURDEN, and BENEFICATION DISCARDS

One of the biggest environmental problems associated with coal mining is that of acid mine drainage (AMD). The primary reactants that cause AMD are pyrite, water and oxygen, and bacteria which is an important catalyst in the reactions e.g. Thiobacillus ferrooxidans (Caruccio, 1975; Palmer, 1978; Stumm and Morgan, 1981; Heaton et al., 1982; Taylor et al., 1984). Not only does AMD deteriorate the quality of water by reducing the pH but most of the elements which are listed in Table 9.2 are generally also chalcophilic and will be

released during breakdown of the sulphide minerals. The decrease in pH will also augment the breakdown of other minerals and increase the concentration of potentially toxic trace elements. In general, coal deposits that were deposited in freshwater contain less pyrite (<1%) than those that were deposited in marine or brackish water (Chapter 4). Caruccio et al. (1978) also demonstrated that the frambroidal type of pyrite associated with coals deposited in the marine environment was highly reactive to oxidative weathering.

It has been established that the Grootegeluk Formation mudstones contain very little pyrite (Chapter 4 and 6), however, the coal seams which inter-bedded the mudstones tend to contain more pyrite that is removed during beneficiation and then stockpiled onto waste dumps. The addition of this pyrite onto discard dumps was not considered in the leaching experiments and may significantly increase concentrations of trace elements in water draining from the dumps. Spontaneous combustion has occurred in some of the discard dumps at Grootegeluk Coal Mine which suggests that pyrite oxidation, which is an exothermic reaction, and AMD is occurring in some dumps.

The Grootegeluk Formation mudstones yield leachable concentrations of elements that are much lower than those listed in Table 9.2. However, Beaufort Group mudstones immediately above the topmost coal seam of the Grootegeluk Formation have values for all elements, except Bi, Sb and Mo, much higher than those given in Table 9.2. Although the layer immediately above the coal seams may be only a fairly thin unit, it is part of the top-soil and over-burden that is stockpiled separately, and not mixed with other less harmful waste material. It must also be borne in mind that only mudstones from about one meter above the topmost coal seam have been analysed and that samples higher up in the formation may also have high concentrations of elements listed in Table 9.2. The overburden of the Grootegeluk Formation is potentially much more of a problem than the carbonaceous mudstones from the coal seams and deserves immediate further investigation.

9.3.4 LEACHATES of DISCARDS from COAL-FIRED POWER STATIONS

What is perhaps of even more concern than the mining wastes discussed so far, is the exceedingly high concentrations of extractable trace elements in the fly ash from the Matimba power station (Table 9.1). Elements such as As, Cd and Mo which are particularly toxic to humans, animals and plants are greater by factors of 5×, 2× and 3× respectively, than the critical concentrations recommended by von Prüeß et al. (1991). The ammonium nitrate leachate from the bottom ash sample on the other hand was extremely low in the elements analysed. Presently the fly ash from Matimba power station is discarded onto dumps near the power station but it still is not certain what eventually will be done with the majority of the fly ash. Some of the fly ash and bottom ash eventually may be used as backfill in the pits at the Grootegeluk Coal Mine (J.C. Dreyer, pers. comm., 1992). Should

this be the case then the results from this study should be kept in mind when deciding on the backfill procedure.

Table 9.2 The Table indicates the recommended maximum concentrations (critical concentrations; von Prüeß et al., 1991) of trace elements that should not be exceeded in leachates of soils, obtained according to the leaching of von Prüeß et al. (1991). The Table also indicates the soil functions that are most threatened by a critical concentration of an element, to indicate where countermeasures should be taken to minimise the threat. Abbreviations for the ranking of the problem if the critical concentrations are exceeded: PC - primary concern, C - concern, INV - further investigations needed to assess risk. A problem only if the critical concentrations are greatly exceeded: ⊗.

		SOIL FUNCTIONS AND RANKING OF CONCERNS				
	Critical concentrations in soil leachates (ppm)	Pollutant buffer with regard to plants for human consumption	Pollutant buffer with regard to plants for animal consumption	Habitat for plants	Habitat for soil organisms	Pollutant filter with regard to groundwater
As	0.040	PC	⊗	C	⊗	C
Be	0.008	⊗	⊗	⊗	⊗	INV
Bi	0.040	⊗	INV	⊗	⊗	⊗
Cd	0.008	PC	C	⊗	C	C
Co	0.200	⊗	C	C	⊗	⊗
Cr	0.040	⊗	⊗	⊗	PC	C
Cu	0.800	⊗	C	C	PC	C
Mo	0.400	⊗	PC	C	⊗	⊗
Ni	0.400	⊗	⊗	C	⊗	⊗
Pb	0.800	PC	C	⊗	C	C
Sb	0.400	⊗	⊗	⊗	⊗	C
Tl	0.012	PC	C	C	C	INV
U	0.016	⊗	⊗	⊗	⊗	INV
V	0.040	⊗	⊗	INV	⊗	⊗
Zn	4.000	⊗	⊗	C	⊗	⊗

South Africa is essentially dependent on electricity provided by coal-fired power stations, and the fly ash produced by all the power stations in S.A. account for 6% of the annual waste produced in the whole country (Willis et al., 1989). Although only 1.5% of this fly ash is used, mainly for active mine support and concrete and cement blends, other uses such as soil amelioration of acid soils in the maize producing area in the Transvaal are being investigated (Willis et al., 1989). It is recommended that the agricultural uses of fly ash be implemented cautiously based on the results of the leaching experiments which indicate that toxic concentrations of elements such as As, Cd, and Mo can easily be extracted and be available for plants growing in such a substrate.

9.3.5 LEACHATES from DISCARD DUMPS and GROUNDWATER QUALITY

Water that has flowed through a coal mining or power station discard dump or discards in a backfill will eventually enter the groundwater system. Two simple models which can be treated as the end members of all groundwater recharge systems are: (1) the conduit flow system (faults and fractures) and (2) the diffuse flow system (e.g. permeable rock formations; Wildeman, 1983). The formations that underlie the coal mining area consist predominantly of relatively impermeable lavas and sandstones. However, there are several major faults which transect the mining area and are probably the more important aquifers for recharging the groundwater system.

It is apparent from the comparison of the two types of aquifer (Table 9.3) that the water draining from coal mining or power station discard material should ideally not be close to a conduit aquifer system. The GCM is presently mining coal along the Daarby fault which is one of the major post-depositional faults in the Waterberg Basin (Fig. 2.1), and also have a well established discard dump near this fault. Should the discard dump or backfill be a source of contaminants, then groundwater flowing along conduit aquifers such as the Daarby fault will affect water quality of boreholes that may be exploiting this fault.

Coal mining in the Waterberg Basin is still in its infancy and because of its vast reserves and the increasing energy requirements by the people in southern Africa, it is important that a complete environmental investigation be done. Handling the environmental aspects of a coal mining operation can be very costly. However, once pollution occurs it is not easily stopped or corrected and but the control of a problem can be more costly and troublesome than planning to prevent the problem.

Table 9.3 Comparison of diffuse and conduit aquifer characteristics (Wildeman, 1983).

DIFFUSE AQUIFER (permeable rock formations)	CONDUIT AQUIFER (faults and fractures)
1. No response to climatological change.	1. Responds to climatological change.
2. Little fluctuation in flow.	2. Obvious fluctuations.
3. No suspended solids in the water.	3. Carries suspended solids at times of high runoff.
4. Water temperature may not change throughout the year.	4. Water temperature changes with the season.
5. Parameters indicative of concentration ions, such as conductivity and hardness, do not change with the climate.	5. Parameters indicative of concentration of ions, such as conductivity and hardness, show obvious changes with storms and runoff.
6. Specific concentrations of ions show little change with the climate.	6. Specific concentrations of ions show obvious changes with storms and runoff.
7. Residence time of months for the water aquifer.	7. Residence time of days for the water aquifer.

9.4 CONCLUSION

The results of leaching tests on the Grootegeluk Formation carbonaceous mudstones, which comprise the majority of the solid coal mining discards, indicate that the concentrations of trace elements which may be toxic to plants, animals or humans are too low to be of any concern. However, the mudstones that immediately overlie the coal-mudstones have concentrations that exceed the critical concentrations of elements believed to be harmful to the environment. Only the immediate over-burden of the coal seams was analysed in this study and it is recommended that overburden higher-up in the Beaufort Group should also be investigated for its extractable elements. Discards from the beneficiation of the coal have much higher proportions of pyrite than the carbonaceous mudstones and care should be taken during the disposal of this material. It is recommended that the overburden immediately above the coal formation be dispersed with the less problematic carbonaceous mudstones that interbed the coal seams, rather than on a separate dump. Only a few samples of fly ash and bottom ash from the Matimba power station were tested for their concentrations of extractable elements. It is evident that the fly ash has leachable concentration levels of elements such as As, Cd and Mo that are considered to be toxic according to von Prüeß et al. (1991). Fly ash from power stations should be used with caution, especially in agricultural applications. The concentrations of elements considered to be toxic by von Prüeß et al. (1991) are very low in leachates from bottom ash samples taken from Matimba power station. Disposal of discards and backfilling should not take place on top of or near major faults, because faults are efficient conduits for water drainage into the groundwater system.

10. SUMMARY and RECOMMENDED FUTURE WORK

10.1 SUMMARY

The Grootegeluk Formation in the Waterberg Coalfield consists of coal and mudstone layers that were deposited during the late Permian, in a basin that developed on the ancient Limpopo Mobile Belt. In the south-central part of the Waterberg Basin subsidence resulted in the formation of strata (~70 m thick) which consists of relatively thin coal beds that are interbedded with a multitude of mudstone and carbonaceous mudstone layers.

Field observations of the Grootegeluk Formation were done in an open-cast pit at the Grootegeluk Coal Mine, in the south-central Waterberg Basin. Samples from the Grootegeluk Formation, the underlying upper Vryheid Formation and the base of the overlying Beaufort Group mudstones were obtained predominantly from borehole cores. The methods of investigation entailed: thin-section petrography; mineralogy (X-ray diffraction); maceral composition and maximum vitrinite reflectivity of the organic matter and; geochemical analyses (X-ray fluorescence spectrometry, gradient ion chromatography, atomic absorption spectrometry, stable and radiogenic isotope geochemistry and inductively coupled plasma analyses). The aim of the thesis was to investigate: (1) the source of the sediments and the palaeo-environment of formation of the coal and mudstone layers; (2) the stratigraphical correlations of some South African coal formations and the formation of coal, on a continental scale, during the late Permian and Triassic times and; (3) the possibility of contamination to the environment by the waste products of coal-mining (carbonaceous mudstones) and coal-burning in the nearby Matimba power-station (fly ash and bottom ash).

The sequence and temperatures of mineral formation in the Grootegeluk Formation have been established. The lower portion of the Grootegeluk Formation is dominated by kaolinite, quartz and minor amounts of anatase, and the upper parts of by quartz, kaolinite and minor amounts of montmorillonite-illite and microcline. These minerals are predominantly allogenic. However, it is possible that some of the kaolinite may have formed as a result of *in situ* alteration of the montmorillonite-illite by acid pore-waters during burial. Mineralogical evidence from the mudstones suggests that the base of the Grootegeluk Formation was relatively more distal and the upper portions more proximal to the source of the sediments. The maceral variation of the coal seams and the organic matter in the mudstones reveal that conditions for the preservation of organic matter were more suitable during the deposition of the sediments in the upper (vitrinite-rich) rather than the lower (inertinite-rich) Grootegeluk Formation. The sedimentological conditions are considered to

have been instrumental in preserving peat that was subsequently converted to either inertinite- or vitrinite-rich coal.

At the base of the Grootegeluk Formation a 2 m thick carbo-tonstein occurs that is dominated by kaolinite, organic matter (~40 weight %) siderite, calcite and minor proportions of apatite. The carbo-tonstein has mineralogical, maceral and chemical characteristics distinctive from the other mudstones. At the base of the Grootegeluk Formation a 2 m thick carbonaceous mudstone zone occurs that is dominated by kaolinite and organic matter. The carbo-tonstein is considered to be the lateral equivalent of a 2 cm thick tonstein identified at Draai Om in the western portion of the Waterberg Coalfield (Spears et al., 1988). The carbo-tonstein differs substantially in appearance and thickness to the tonstein in the west Waterberg Basin mainly because it has a much higher proportion of organic matter than the west Waterberg tonstein. On the basis of the mineralogical and geochemical characteristics it is difficult to reconcile a detrital origin for some of the mineral matter in the carbo-tonstein zone. It is proposed that the origin of the inorganic fraction of the carbo-tonstein zone is a volcanic tuff that was deposited (wind or water) with organic material into a part of the Waterberg Basin that was subsiding relatively quickly. The thickness of the carbo-tonstein indicates that volcanic ash was deposited into this part of the basin over a period of time.

Syn-depositional calcite lenses are present sporadically in the upper-half of the Grootegeluk Formation. The calcite lenses precipitated from late Permian meteoric water which had a $\delta^{18}O$ value of about $-13‰$.

Globular pyrite in the coals and organic rich-mudstones formed at the sediment-water interface or during very early diagenesis. Globular pyrite in the organic-poor mudstones of the Beaufort Group that immediately overlie the topmost coal seam probably formed during early diagenesis. Spherulitic siderite, and some of the ankerite, formed from late Permian methane-bearing meteoric water during early diagenesis in coal and the more carbonaceous mudstones, at temperatures between 35°C and 60°C. Granular siderite, which occurs predominantly in organic-poor mudstones in the upper part of the Grootegeluk Formation and the overlying lower Beaufort Group mudstones, crystallised at similar temperatures as spherulitic siderite in equilibrium with late Permian meteoric waters. The granular siderites, however, have very low ^{13}C concentrations as a result of oxidation of organic matter that contributed ^{12}C to the meteoric fluids from which the granular siderites precipitated. Carbon and oxygen stable isotope data indicate that most of the ankerite precipitated at temperatures between 70°C and 100°C, with a ^{12}C input from the decarboxylation reactions of the organic matter. Marcasite sometimes occurs along bedding planes and probably formed during uplift. It was not possible to establish conclusively from oxygen stable isotope data whether cleat-filling calcite precipitated predominantly during burial or up-lift of the

sediments, but the consistently high negative $\delta^{13}C$ values point to an organic source for the carbon suggesting that the calcite precipitated during up-lift of the sediments.

The very smooth, systematic changes in the major element chemistry (SiO_2, Al_2O_3, TiO_2, K_2O) and mineralogy, and the good correlation of sample compositions within the same stratigraphic horizon, makes major element whole-rock chemistry an ideal stratigraphic-indicator tool for the Grootegeluk Formation. The normative mineral compositions of the mudstones were calculated from their major element compositions. The calculation of the normative mineral compositions of fine-grained sedimentary rocks provided a quick, semi-quantitative method of establishing the mineral concentrations in a large number of samples.

All the mudstones had very low concentrations of the alkali and alkaline-earth elements suggesting that the rocks had undergone very high degrees of chemical alteration. It was not certain whether the high degree of alteration could be ascribed to palaeo-climatic conditions and(or) alteration in an acidic depositional environment. An alternative possibility to palaeo-climate conditions or post-depositional alteration may be that the source of the mudstones were igneous rocks or (meta)sediments that had very low concentrations of alkali and alkaline-earth elements.

The trace elements in the carbonaceous mudstones are predominantly hosted in the mineral fraction. The trace element distributions in the mudstones are dominated by the abrupt increase to anomalously high concentrations of all the trace elements analysed except S, Co, As and Zn. The trace element concentrations, in addition to its mineralogical character, make the carbo-tonstein an important (chrono-)stratigraphic marker for local and intra-basinal correlation. Other notable trace element features are: (1) the relatively high concentration of V, Cr and to a lesser extent Zr in the underlying Vryheid Formation samples; (2) the excellent correlation of Rb and Zn with the K-bearing minerals and; (3) the increase of chalcophile trace elements in samples with high pyrite concentrations in the Beaufort Group mudstones. The concentrations of most of the immobile trace elements in the mudstones are not considered to have been altered by sedimentary or diagenetic processes. However, some of the chalcophile elements may have been concentrated as a result of diagenesis and(or) reduction-oxidation reactions in the mudstones (originally peat-bearing) of the Beaufort Group, which overlie the coal and mudstone layers.

Based on the concentrations and inter-element ratios of relatively immobile elements, that have been shown to be directly related to their source rocks, the Grootegeluk Formation and Beaufort Group mudstones analysed in this study have the same predominant provenance. A comparison of the immobile element concentrations in the mudstones to other typical and average rock types indicates that the average composition of the provenance area is dominantly "granitic", possibly granodioritic composition. The

Vryheid Formation samples have average provenances which are relatively more mafic than those of the Grootegeluk Formation samples.

Sm-Nd isotopic studies confirm that the predominant provenance of the Grootegeluk Formation (and Lower Beaufort Group) mudstones in the WCF was different to the provenance of the underlying Vryheid Formation. The provenance of the Grootegeluk Formation mudstones has Late Proterozoic crustal resident ages (mean 1.22 Ga) and relatively positive ϵ_{Nd} values compared to the Vryheid Formation. The provenance of the Vryheid formation has crustal resident ages of Early Proterozoic age. Although palaeo-current analyses of Ecca Group sediments in the WCF and the northern MKB indicate a provenance from the north-east (approximately present day Mozambique), the provenance of the Grootegeluk Formation mudstones may not necessarily be the same direction. Evidence for a provenance for the Grootegeluk Formation is not conclusive, but the Sm-Nd isotopic data are consistent with a source from the Damara Belt to the north-west of the basin and(or) sediments from northward retreating glaciers.

The concentration of trace elements considered to be good palaeo-salinity indicators, are in agreement with evidence from stable isotope data of syn-depositional and the early diagenetic minerals that these sediments were deposited in fresh rather than marine waters.

This is the first study to report $\delta^{13}C$ values of coal and Phanerozoic organic matter in southern African sediments. A comparison of the organic ^{13}C analyses with evidence from palynological studies of the Waterberg Coalfield and other coalfields in South Africa, indicate that $\delta^{13}C$ values can be used in stratigraphical correlations and as palaeo-ecological indicators. The stable isotope geochemistry of organic matter can be an important technique in identifying the Permo-Triassic boundary in freshwater sediments.

Organic $\delta^{13}C$ values from coal and organic matter from selected South African coalfields support evidence, mainly from palynological studies, that the MKB coal seams were formed under different conditions and(or) at an earlier time than the coals from the northern Karoo basins. The isotopic data confirm the findings of MacRae (1988, 1989) that the Waterberg and Pafuri Coalfields from the northern Karoo basins can be correlated stratigraphically. The organic $\delta^{13}C$ values from the Triassic Molteno Coalfield are exceptionally constant and distinctly different from the values determined for Permian coals and mudstones. The results of the organic $\delta^{13}C$ analyses in coal and mudstones demonstrate a potentially useful method for establishing the P-T_R boundary in southern Africa.

The $\delta^{13}C$ values of the Permian and Triassic freshwater organic matter suggest that there was a change in the atmospheric $^{13}C/^{12}C$ ratio during this time. The decrease in the ratio of atmospheric carbon is compatible with the input of negative $\delta^{13}C$ values resulting from the oxidisation of organic carbon. Studies of coal distribution have demonstrated that there was an abrupt and major decrease of coal formation and(or) preservation world-wide

at the P-Tr boundary. During the Permian, coal formed predominantly in Gondwana which was at the time subjected to episodes of large scale tectonism as a result of collisions along the whole of its southern margin. The impact of the tectonism affected vast areas of land that were accumulating and burying organic matter. The uplift and oxidation of some of the shallow peat before further burial is consistent with evidence provided in this study. It is suggested, therefore, that the mass extinction which has been proposed for freshwater and marine species at the P-Tr boundary may directly or indirectly be related to a culmination of events that resulted from the P-Tr tectonism during the formation of Pangea.

Mining, beneficiation and the burning of coal in power stations results in the production of vast amounts of discard material. Leaching experiments that were performed on the mudstones and carbonaceous mudstones, which comprise the majority of the solid coal mining discards, indicate that the concentrations of trace elements which may be toxic to plants, animals or humans are too low to be of any concern. However, the mudstones that immediately overlie the coal-mudstones have concentrations of elements that exceed the critical concentrations believed to be harmful to the environment. The results of leaching experiments done on a limited number of fly ash and bottom ash samples from the Matimba power station reveal that the fly ash has concentrations levels of leachable elements, such as As, Cd and Mo, that are toxic. Leachates of bottom ash samples from Matimba power station have very low concentrations of elements which are considered to be toxic.

10.1 SUGGESTED FUTURE WORK

The data and conclusions presented in this study provide a detailed mineralogical and geochemical account of the carbonaceous mudstones and mudstones of the Grootegeluk Formation in the south-central Waterberg Coalfield. The techniques used in this investigation differ from methods, such as sedimentology and palynology, that are usually applied to coal and sedimentary rock studies in southern Africa. This thesis therefore provides a framework for other similar studies. The following are some ideas for future work:

1. A detailed mineralogical and geochemical study should be done on the coals *and host sediments of coal formations* in other coalfields in southern Africa. It has been demonstrated that the whole-rock chemical profiles of the Waterberg Coalfield mudstones are very distinctive and provide a useful tool for stratigraphic correlation. The identification of tonsteins or carbo-tonsteins will be particularly important for stratigraphical correlations with other coalfields.
2. Investigation of the inorganic fraction is important in studies of coal formation. The variation in coal quality may be reflected in a mineralogical change of the sediments.
3. Research on mudstones and carbonaceous mudstones invariably does not include thin-section petrographic investigations. This study has demonstrated that, even

though mineral grain sizes in mudstones are generally assumed to be too small for thin-section observation, important information can sometimes still be obtained from this technique. Thin-sections should routinely be made, if possible, of all samples.

4. Radiogenic isotope analyses, such as single zircon U-Pb, should be done on the tonstein that occurs at the base of the Grootegeluk Formation. Tonstein samples, however, should be collected from the western portion of the Waterberg Basin because the tonstein is easier to identify and has less organic matter.
5. This is the first study to determine organic carbon stable isotope values of South African coals and Phanerozoic organic matter. The results from these analyses indicate that the $\delta^{13}C$ values of organic matter may be an important stratigraphical correlation tool and palaeo-ecological indicator. The $\delta^{13}C$ values of organic matter may be an important technique in studies attempting to identify the P-T_R boundary in freshwater (and marine) sediments.
6. A detailed investigation of the sediments, traditionally called the Beaufort Group mudstones, that overlie the Grootegeluk Formation mudstones must be done. This study demonstrates that no sedimentological break in the mudstones occurs between these two units. Results from a limited number of samples from the Beaufort Group mudstones suggest that peat accumulation did occur in the Beaufort mudstones but that post-depositional causes resulted in the break-down of the peat.
7. Only 0.5 m of the Beaufort Group mudstones, above the coal seams, were tested for concentrations of extractable elements. It is recommended that leaching experiments should also be done on the overburden higher-up in the Beaufort Group. Leaching experiments of coal discard material in other coalfields should be done to identify potentially hazardous material. This is especially important for coals that were deposited in a marine environment or overlain by sediments that were deposited in a marine environment.

REFERENCES

Ager D.V. (1973). The nature of the stratigraphical record. Macmillan, London, 114p.

Al-Aasm I.S., Taylor B.E. and South B. (1990). Stable isotope analysis of multiple carbonate samples using selective acid extraction. Chem. Geol. (Isotope Geoscience Section), 80, 119-125.

Alberts B.C. and Liebenberg B.F. (1982). The Geology and Mining of the Northern Transvaal Coal Deposits. In: Glen H.W. (Ed.). Proc., 12th CMMI congress, Johannesburg. 101-110.

Allègre C.J. and Rousseau D. (1984). The growth of the continent through time studied by Nd isotope analyses of shales. Earth Plan. Sci. Lett., 67, 19-34.

Alvarez L.W., Alvarez W., Asaro F. and Michel H.V. (1980). Mass extinctions caused by large bolide impacts. Physics Today, 40, (7), 24-33.

Amajor L.C. (1987). Major and trace element geochemistry of Alban and Turonian shales from the Southern Benue trough, Nigeria. J. Afr. Earth Sci.,6, 633-641.

Anderson H.M. (1974). A brief review of the flora of the Molteno "Formation" (Triassic), South Africa. Palaeont. Afr., 17, 1-10.

Anderson J.M. and Cruickshank A.R.I. (1978). The biostratigraphy of the Permian and the Triassic. Part 5. Review of the classification and distribution of Permo-Triassic tetrapods. Palaeontologia Africana, 21, 15-44.

Anderson J.M. and Anderson H.M. (1985). Paleoflora of Southern Africa-Prodromus of South African Megafloras of Devonian in the Lower Cretaceous. A.A. Balkema, Rotterdam, 52-55.

Anderson J.M. (1977). The biostratigraphy of the Permian and Triassic. Part 3. A review of Gondwana Permian palynology with particular reference to the northern Karoo Basin, South Africa. Mem. Bot. Surv. S. Afr., 41.

Bahrig B. (1988). Palaeoenvironment information from deep water siderite (Lake of Leach, W. Germany). In. Fleet A., Kelts K. and Talbot M. (Eds.). Lacustrine petroleum source rocks. Geol. Soc. London, Spec. Publ. 40. 153-158.

Baily S.W. (1966) The status of clay mineral structures. Proc. 14th Nat. Conf. on clays and clay minerals. Pergamon Pres. New York, 1-23.

Barker O.B. (1986). An overview of coal reserve position and certain technical development in South Africa. S.A. Mining World. November, 57-71.

Barnes M.A., Barnes W.C. and Bustin R.M. (1990). Chemistry and diagenesis of organic matter in sediments and fossil fuels: In McLlreath I.A. and Morrow D.W. (Eds.). Diagenesis. Geoscience Canada, reprint series 4, 189-204.

Barth T.F.W. (1952). Theoretical petrology. John Wiley, New York, 387p.

Battail B. (1988). Biostratigraphie des formations permo-triasiques continentales. Vertebres tetrapodes et biogeographie du Gondwanan. Soc. Geol. du Noord, Annales, 107, 37-44.

Baud A., Magaritz M. and Holser W.T. (1989). Permian-Triassic of the Tethys: Carbon isotope studies. Geolische Rundschau, 78, 649-687.

Bell P.R.F., Krol A.A. and Greenfield P.F. (1986). Factors controlling the leaching of major and minor constituents from processed Rundle oil shale. Water. Res., 20, No. 6, 741-750.

Bell P.R.F. and Krol A.A. (1990). Characterization of leachates from mine waste solids and shale ash from the Stuart resource and design of a retort water treatment cell. Fuel, 69, 1086-1090.

Berner R.A. (1981). A new geochemical classification of sedimentary environments. J. Sedimentary Pet., 51, 359-365.

Berner R.A. (1971). Principles of chemical sedimentology. McGraw-Hill Book Company, p240.

Berner R.A. (1990). Atmospheric carbon dioxide levels over Phanerozoic time. Science, 249, 1382-1386.

Bethell F.V. (1963). Progress review No. 55: The distribution and origin of minor elements in coal. J. Inst. Fuel, 36, 478-492.

Beukes N.J. (1985). Sedimentologie van die Ellisrassteenkoolveld. Finale verslag, WNNR. KWP, NGP: Steenkoolgeologieprojek. [Report to the C.S.I.R. (South Africa) Coal Project], p15.

Beukes N.J., Siepker E.H. and Naudé F. (1991). Genetic stratigraphy of the Waterberg coalfield. Extended Abstract: Conference on South Africa's coal resources, Witbank 6-9 Nov.

Björlykke K. (1974). Geochemical and mineralogical influence of Ordovician island arcs on epicontinental clastic sedimentation. A study of Lower Palaeozoic sedimentation in the Oslo region, Norway. Sedimentology, 33. 115-125.

Blatt H., Middleton G.V. and Murray R. (1980). Origin of sedimentary rocks. (2nd Ed.). Prentice-Hall. Englewood Cliffs. p782.

Bluth G.J.S. and Kump L.R (1991). Phanerozoic paleogeology. Am. J. Sci., 291, 284-308.

Bosch G.L. (1990). The mineralogy and chemistry of pulverised fuel ash produced by three South African coal-burning power stations. M.Sc. thesis, Univ. Cape Town, (unpublished), 189p.

Bostik N.H. (1979). Microscopic measurement of the level of catagenesis of solid organic matter in sedimentary rocks to aid exploration for petroleum and to determine former temperatures - a review. In: Schoelle P. and Schluger P.R. (Eds.). Aspects of diagenesis. Soc. of Economic Paleontol. and Mineral., Spec. Publ. No. 26, 17-43.

Botha P.A. (1984). Die Eienskappe van die Waterbergsteenkool met spesiale verwysing na stratigrafiese korrelasie. Unpublished. M.Sc., University of Pretoria. R.S.A.

Bouska V. (1981). Geochemistry of Coal. Elsevier, p284.

Bowen R.L. (1968). Palaeoclimatic and paleobiologic implications of Louaan salt deposition, Bull. Am. Assoc. of Petrol. Geol., 52 (9), 1833.

Breit G.N. and Wanty R.B. (1991). Vanadium accumulation in carbonaceous rocks: A review of geochemical controls during deposition and diagenesis. Chem. Geol., 91, 83-97.

Budyko M.I. (1986). The evolution of the biosphere. D.Reidel Publishing Company, Dodrecht. 423p.

Burger K., Zhou Y. and Tang D. (1990). Synsedimentary volcanic-ash-derived illite tonsteins in Late Permian coal-bearing formations of southwestern China. Int. Journ. Coal Geol., 15, 341-356.

Bustin R.M., Barnes M.A. and Barnes W.C. (1990). Determining levels of organic diagenesis in sediments and fossil fuels. : In McLlreath I.A. and Morrow D.W. (Eds.). Diagenesis. Geoscience Canada. reprint series 4. 205-226.

Burger K. (1985). Kohlentonsteine in Kohlenrevieren der Erde Erkkenntnisstand 1983. C.R. 10me Congr. Int. Stratigr. Geol. Carbonif. (Madrid 1983), 1. 155-174.

Cadle R.D., Wartburg A.P., Pollock W.H., Gandrud B.W. and Shedlovsky J.P. (1973). Trace constituents emitted to the atmosphere by Hawaiian volcanoes. Chemosphere, No. 6, 231-234.

Cairncross B. (1989). Palaeodepositional environments and tectonisedimentary controls of the post-glacial Permian coals, Karoo Basin, South Africa. Int. J. Coal Geol., 12, 365-380.

Cambell F.A. and Williams G.D. (1965). Chemical composition of shales of the Mannville Group (Lower Cretaceous) of central Alberta, Canada. Bull. Am. Ass. Petrol. Geol., 49, 81-87.

Caruccio F.T. (1975). Characterisation of strip mine drainage by pyrite grain size and chemical quality of existing groundwater. In: Hutnik R.J. and Davis G. (Eds.). Ecology and reclamation of devastated land. Gordon and Breach, New York.

Caruccio F.T. (1978). Depositional environment of carboniferous sediments-a predictor of coal mine problems. In: Goodman G.T. and Chadwick M.J. (Eds.). Environmental management of mineral wastes. Sijthoff and Noordhoff, Alphen aan den Rijn - Netherlands. 127-139

Castaño J.R. and Sparks D.M. (1974). Interpretation of vitrinite reflectance measurements in sedimentary rocks and determination of burial history using reflectance and authigenic minerals. In: Carbonaceous materials as indicators of metamorphism. Ed. Dutcher R.R., Geol. Soc. Amer. Spec. Pap. 153, 31-53.

Chadwick M.J. and Lindman N. (Eds.) (1982). Environmental implications of expanded coal utilization. Pergamon Press, p283.

Chandra D. and Taylor G.H. (1982). Gondwana coals. In Stach E. et al. (Eds.). Textbook of coal petrology. 2nd rev. Ed. Gebrüder Borntraeger, Berlin, 177-198.

Christie A.D.M. (1981). Stratigraphy and sedimentology of the Molteno Formation in the Elliot Indwe area, Cape Province. M.Sc. thesis (unpubl.), Univ. Natal, Durban.

Chung H.M. and Sackett W.M. (1979). Uses of stable carbon isotope compositions of pyrolytically derived methane as maturity indices for carbonaceous materials. Geochim. et Cosmo. Acta, 43, 1979-1988.

Cillié J.F. (1957). Waterberg Coalfields: Records of boreholes 101-143. Bull. Geol. Surv. South Africa. 23. 276p.

Cillié J.F. and Visser H.N. (1946). Waterberg Coalfield: Records of boreholes 21-40. Bull. Geol. Surv. South Africa, 16. 132p.

Cillié J.F. (1951). Waterberg Coalfields: Records of boreholes 41-100. Bull. Geol. Surv. South Africa, 21. 381p

Claoué-Long J.C., Zichao Z., Guogan M.and Shaohua D., (1991). The age of the Permian-Triassic boundary. Earth Plan. Sci. Lett., 105, 182-190.

Clarke W.P., Krol A.A. and Bell P.R.F.(1990). Simulation of leachate quality from Rundle spent shale. Fuel, 69, 1095-1098.

Clarke T.H. (1954). Shale: a case study of nomenclature. Trans. Roy. Soc. Canada, 48, ser 3, (4), 1-7.

Clymo R.S. (1987). Rainwater-fed peat as a precursor of coal. In: Coal and Coal-bearing Strata: Recent Advances. Ed. Scott A.C. Geol. Soc. Spec. Publ. No. 32, 17-34.

Cohen D. and Ward C.R. (1991). Sednorm - a program to calculate a normative mineralogy for sedimentary rocks based on chemical analyses. Computers & Geosci., *17*, 9, 1235-1253.

Cole D.I. (1992). Evolution and development of the Karoo Basin. In: de Wit and Ransome I.G.D. (Eds.), Inversion tectonics of the Cape Fold Belt, Karoo and Cretaceous basins of southern Africa. Balkema, Rotterdam. 87-99.

Compston W. (1960). The carbon isotopic compositions of certain marine invertebrates and coals from the Australian Permian. Geochim. et Cosmochim. Acta, 18, 1-22.

Cox K.G., Bell J.D., and Pankhurst R.J. (1979). Interpretation of igneous rocks. George Allen & Unwin, London, 450p.

Craig H. (1953). The geochemistry of the stable carbon isotopes. Geochim. et Cosmochim. Acta, 3(1), p53.

Crockett R.N. and Jones M.T. (1975). Some aspects of the geology of the Waterberg System in eastern Botswana. Trans. geol. Soc. S. Afr., 74, 211-235.

Cullers R.L., Barrett T., Carlson R. and Robinson B. (1987). REE and mineralogical changes in Holocene soil and stream sediment: a case study in the Wet Mountains, Colorado, U.S.A. Chem Geol, 63, (3-4), 275-297.

Cullers R.L., Chaudhuri S., Kilbane N. and Koch R. (1979). Rare earths in size fractions and sedimentary rocks of the Pennsylvanian-Permian age from the mid-content of the U.S.A. Geochim. et Cosmo. Acta, 43, 1285-1302.

Curtis C.D. (1969). Trace-element distribution in some British Carboniferous sediments. Geochim. et Cosmochim. Acta., 33, 519-523.

Curtis C.D. and Spears D.A. (1971). Diagenetic development of kaolinite. Clays Clay Minerals, 19, 219-227.

Curtis C.D. and Coleman M.L. (1986). Controls on the precipitation of early diagenetic calcite, dolomite and sideritic concretions in complex depositional sequences. Roles of organic material in sediment diagenesis SEPM special publ. 38, 23-33.

Curtis C.D. (1983). Geochemistry of porosity enhancement and reduction in clastic sediments: In Brooks J. (Ed.). Petroleum geochemistry and exploration of Europe. The Geol. Soc. Blackwell, London, 113-125.

Daemon R.F., Casaletti P. and Ciguel J.H.G. (1991). Biopaleogeografia da Bacia do Paraná. Curitiba: PETROBRÁS internal report.

Daly M.C., Lawrence S.R., Kimuna D., and Binga M. (1991). Late Palaeozoic deformation in central Africa: a result of distant collision? Nature, 35, 605-607.

de Jager F.S.J. (1983). Coal reserves of the Republic of South Africa - an evaluation at the end of 1982. Rep. geol. Surv. S. Afr., Bull. 74, 17p.

de Jager F.S. (1976). Coal. In: Coetzee C.B. (Compiler). Mineral Resources of South Africa. Geol. Surv. S.A., 5th Ed. 289-330.

de Jager F.S.J. (1986). Coal occurrences of the central, north-western, northern, and eastern transvaal. In: Mineral and Deposits of Southern Africa. Anhaeusser C.R. and Maske S. (Eds.). Vols I and II. Geol. Soc. S. Afr., Johannesburg. 2047-2056.

de Witt M.J. and Ransome I.G.D. (1992). Regional inversion tectonics along the southern margin of Gondwana. Tectonic inversion and radiometric resetting of the basement in the Cape Fold Belt. In: de Wit M.J. and Ransome I.G.D. (Eds.). Inversion tectonics of the Cape Fold Belt, Karoo and Cretaceous Basins of southern Africa. Balkema, Rotterdam, 217-228.

de Witt M.J., Jeffery M., Nicolaysen L.O.N., and Bergh H. (1988). Explanatory notes on the Geologic Map of Gondwana. Am. Assoc. Petrol. Geol. Tulsa.

Deer W.A, Howie R.A, and Zussman J. (1966). An introduction to the rock-forming minerals. Longman, London, 528p.

Degens E.T, Williams E.G., Keith M.L. (1957). Environmental studies of Carboniferous sediments, Part I. Geochemical criteria for differentiating marine and fresh-water shales. Am. Assoc. Petroleum Geologists Bull., 41, 2427-2455.

Degens E.T. (1969). Biogeochemistry of stable carbon isotopes. In: Eglinton G. and Murphy M.T.J. (Eds.), Organic Geochemistry, New York, Springer. 304-356.

Deines P. (1980). The isotopic composition of reduced organic carbon. In: Fritz P. and Fontes J.Ch. (Eds.). Handbook of environmental isotope geochemistry. Vol. 1., Elsevier Scientific Publ., Amsterdam. 329-406.

DePaolo D.J. (1988). Neodymium isotope geochemistry. Springer-Verlag. Berlin. 187p.

DePaolo D.J. and Wasserburg G.J. (1976). Nd isotopic variations and petrogenetic models. Geophys. Res. Lett., 249-252.

Dia A., Allégre C.J. and Erlank A.J. (1990). The development of continental crust through geological time: the South African case. Earth and Plan. Sci. Lett., 98, 74-89.

DIN V 19730 (1993): Ammoniumextraktion zur bestimmung mobiler spurenelemente in mineralböden. Preliminary German norm, printed by and to be purchased from: Beuth Verlag GmbH, Burghafenstr. 6, 1000 Berlin 30.

Dreyer J.C. and Roux L. (1991). Geophysics for grade control at Grootegeluk Coal Mine. Abstract. Conference on South Africa's coal resources, Geol. Soc. S.A. Witbank, 6-9 Nov.

Dreyer J.C. (1991). Waterberg Coalfield: Geology, resources, mining and products. Abstract. Conference on South Africa's coal resources, Geol. Soc. S.A. Witbank, 6-9 Nov.

Duncan A.R., Erlank A.J. and Marsh J.S. (1984). Analytical techniques and database description. In: Erlank A.J. (Ed.). Petrogenesis of the volcanic rocks of the Karoo Province. National Geodynamics Program. Geol. Soc. S.A., Spec. Publ. No. 13, 389-395.

Durand B. (1980). Sedimentary organic matter and kerogen. Definition and quantitative importance of kerogen. In: Durand B. (Ed.). Kerogen insoluble organic matter from sedimentary rocks, 13-34.

Edmond J.M. (1992). Himalayan tectonics, weathering processes, and the strontium isotope record in marine limestones. Science, 258, 1594-1597.

Edzwald J.K and O'Melia C.R.C (1975). Clay distribution in recent estuarine sediments. Clays Clay Mineral., 23, 39-44.

Eglington B.M and Harmer R.E (1991). GEODATE: a program for the processing and regression of isotope data using IBM-compatible microcomputers. CSIR Manual EMA-H8901, C.S.I.R., Pretoria, 57p.

Ehleringer J.R., Sage R.F., Flanagan L.B. and Pearcy R.W. (1991). Climate change and the evolution of C_4 photosynthesis. Trends in Ecol. and Evoln., 6, no. 3, 95-99.

Englund J.-O. and Jorgensen P. (1973). A chemical classification system for argillaceous sediments and factors affecting their composition. Geol. Föreningens i Stockholm Föhandlingar, 95, 87-97.

EPA (1980). Toxicity extraction procedure (EP). US EPA Federal Register, 45(98) 33121-33133 (May 19, 1980), ISSN 0097-6326.

EPA (1990). Toxicity characteristic leaching procedure (TCLP), US Govt. Documents, 40 CFR Ch. 1 (7-1-90 Edition), Part 261, App. II.

Eskenazi G.M. (1987a). Rare earth elements in a sampled coal from the Pirin deposit, Bulgaria. Int. Jour. of Coal Geol., 7, 301-314.

Eskenazi G.M. (1987b). Rare earth elements and yttrium in lithotypes of Bulgarian coals. Org. Geochem., 11, 83-89.

Evangelou V.P. (1983). Pyritic coal spoils: their chemistry and water interactions. In: Leaching and diffusion in rocks and their products: Ed. S.S. Augustithis. Theophratus Publ. S.A., Athens, 75-227.

Falcon R.M.S. (1986). A brief review of the origin, formation, and distribution of coal in southern Africa. In: Mineral and Deposits of Southern Africa. Anhaeusser C.R. and Maske S. (Eds.). Vols I and II. Geol. Soc. S. Afr., Johannesburg. 1879-1898.

Falcon R.M.S. and Snyman C.P. (1986). An introduction to coal petrography: atlas of petrographic constituents in bituminous coals of southern Africa. Geol. Soc. S.A. Review Paper No 2.

Falcon R.M.S. (1977). Coal in South Africa, Part I: The quality of South African coal in relation to it's uses and world energy resources. Mins. Sci. Engng., 9, No. 4, 198-217.

Faure G. (1977). Principles of isotope geology. 2nd Ed. John Wiley and Sons, N.Y. 589p.

Filby R.H., Shah K.R. and Sautter C.A. (1977). A study of trace element distribution in the solvent refined coal (SRC) process using neutron activation analysis. J. Radioanal. Chem., 37, 693-704.

Finkelman R.B. (1981). Modes of occurrence of trace elements in coal. US Geol. Surv. Open-File Rep., Np. OFR-81-99, 301p.

Frakes L.A. (1979). Climates throughout geologic time. Elsevier Sci. Publ. Co., Amsterdam, 310p

Fullard H. (Ed.) (1967). Philips' college atlas for southern Africa. George Philip and Son Ltd., London.

Garrels R.M. and MacKenzie F.T. (1971). Evolution of sedimentary rocks. Norton, 397.

Garrels R.M. and Christ C.L. (1965). Solutions, minerals and equilibria. Freeman, Cooper and Co., San Francisco. 405p.

Geissler C. and Belau L. (1971). Zum verhalten der stabilen kohlenstoff-isotopes bei der ibkohlung. Z. Angew. Geol. 7(1), p13.

Goldschmidt V.M. and Peters C. (1933). The enrichment of rare elements in hard coals. Nachr. Ges. Wiss. Goettingen, Math.-Phys. Kl., Fachgruppe IV, 371-386.

Goldschmidt V.M. (Muir A.) (1954). Geochemistry. Claredon Press, Oxford, 730p.

Golyshev S.I., Verkhovskaya N.A., Burkova V.N. and Matis E.Y. (1991). Stable carbon isotopes in source-bed organic matter of West and East Siberia. Org. Geoch., 17, No. 3, 277-291.

Golyshev S.I, Padalko N.L. and Pechenkin S.A. (1981). Fractionation of stable oxygen and carbon isotopes in carbonate systems. Geochem. Intl., 18, 85-99.

Green D, Crockett R.N. and Jones M.T. (1980). Tectonic control of Karoo sedimentation in mid-eastern Botswana. Trans. geol. Soc. S. Afr., 83, 213-219.

Gresse P.G., Theron J.N., Fitch F.J., and Miller J.A. (1992). Tectonic inversion and radiometric resetting of the basement in the Cape Fold Belt. In: de Wit M.J. and Ransome I.R. (Eds.). Inversion tectonics of the Cape Fold Belt, Karoo and Cretaceous Basins of southern Africa. Balkema, Rotterdam, 217-228.

Gromet L.P and Silver L.T (1983). Rare earth element distributions among minerals in a granodiorite and their petrogenetic implications. Geochim. et Cosmo. Acta, 47, 925-939.

Gromet L.P., Dymek R.F., Haskin L.A. and Korotev R.L. (1984). The "North American Shale Composite": Its Compilation, Mayor and Trace Element Characteristics. Geochim. et Cosmochim. Acta, 48, 2469-2482.

Gruszyński M., Halas S., Hoffman A. and Malkowski K. (1989). A brachiopod calcite record of the oceanic carbon and oxygen isotopic shift at the Permo/Triassic transition, Nature, 337, 64-68.

Hälbich I.W., Fitch F.J., and Miller J.A. (1983). Dating the Cape orogeny. In: Söhnge A.P.G. and Hälbich I.W. (Eds.). Geodynamics of the Cape Fold Belt. Geol. Soc. of S.A. Spec. Publ., 12, 149-164.

Hallam A. (1983). Plate tectonics and evolution. In Bendall D.S. (Ed.). Evolution from molecules to men. Cambridge Univ. Press, Cambridge, 367-386.

Hangari K.M., Ahmad S.N., and Perry Jr. E.C. (1980). Carbon and oxygen isotope ratios in diagenetic siderite and magnetite from upper Devonian ironstone, Wadi Shatti, Libya. Econ. Geol., 75, 538-545.

Harland W.B., Armstrong R.L., Cox, A.V., Craig, L.E., Smith, A.G. and Smith D.G. (1990). A geologic time scale 1989. Cambridge Univ. Press, Cambridge, p127.

Haskin L.A., Haskin M.A., Frey F.A., and Wildman R.T. (1968). Relative and absolute terrestrial abundances of rare earths. In: Ahrens L.H. (Ed.). Origin and distribution of the elements. Pergamon, New York, 889-912.

Hassett D.J. (1987). A generic test of leachability: The synthetic groundwater leaching method. Conference Proc. Waste management of the energy industries, 30-39, Univ. of North Dakota, Grand Forks, North Dakota.

Hatfield C.B. and Camp M.J. (1970). Mass extinctions correlated with periodic galactic events. Bull. Geol. Soc. of Am., 81, (3), 911-914.

Haughton S.H. (1969). Geological history of southern Africa. Geol. Soc. S. Afr. 528p.

Heaton R.C., Williams J.M., Bertino J.P., Wangen L.E., Nyitray A.M. Jones M.M., Wanek P.L. and Wagner P. (1982). Leaching behaviours of high-sulphur coal wastes from two Appalachian coal preparation plants. Los Alamos National Laboratory, Los Alamos, New Mexico 87545. LA-9356-MS

Heaton R.C., Wanek P.L, Thode E.F, Cokal E.J and Wagner P. (1981). Leaching experiments on coal preparation wastes: comparisons of the EPA extraction procedure with other methods. Los Alamos National Laboratory, Los Alamos, New Mexico 87545. EPA-600/7-81-072.

Heaton R.C. and Wagner P. (1983). Trace-element characterisation of coal-preparation wastes. Final Program Report (LA-9626). Los Alamos National Laboratory.

Heinrich K.F.J. (1986). Mass absorbtion coefficients for electron probe microanalysis. Proc. of the 11th Intern. Congress on X-ray Optics and Microanalysis, Univ. Ontario, London, Ontario, Canada, (August 4-8), 67-119.

Heinrichs H., Schulz-Dobrick B. and Wedepohl K.H. (1980). Terrestrial geochemistry of Cd, Bi, Tl, Pb, Zn, and Rb. Geochim et Cosmochim. Acta, 44, 1519-1533.

Hemely J.J. (1959). Some mineralogical equilibria in the system (K_2O-Al_2O_3-SiO_2-H_2). Am. J. of Sci., 257, 241-270.

Hesse R. (1990). Early diagenetic pore water/sediment interaction: modern offshore basins. In: McLlreath I.A. and Morrow D.W. (Eds). Diagenesis. Geoscience Canada, reprint series 4, 277-316.

Hill P.A. (1988). Tonsteins of Hat Creek, British Columbia: a preliminary study. Int. Journ. Coal Geol., 10, 155-175.

Hirst D.M. (1962). The geochemistry of modern sediments from the Gulf of Paria-II: The location and distribution of trace elements. Geochim et Cosmochim. Acta, 26, 1147-1187.

Hobday D.K. (1987). Gondwana Coal Basins of Australia and South Africa: Tectonic Setting Depositional Systems and Resources. In: Coal and Coal-bearing Strata: Recent Advances. Ed. Scott A.C. Geol. Soc. Spec. Publ. No. 32, 219-213.

Hoffman A. (1989). Changing palaeotological views on mass extinction phenomena. Donovan S.K. (Ed.) Mass extinctions: Processes and evidence. Belhaven Press, London, 1-18.

Hoffmann H and Jenker A. (1932). Neue erkenntnisse über die vorgänge der Flözbildung. Bergbau,7, 89-94.

Hofmeyr P.K. (1971). The abundances and distribution of some trace elements in some selected South African shales. Ph.D. thesis Univ. of Cape Town (unpubl).

Holser W.T., Schönlaub H-P., Attrep M. Jr., Boeckelmann K., Jenny C., Kralik M., Mauritsch H., Pak E., Schramm J-M., Statteger K. and Schmöller R. (1989). A unique geochemical record at the Permian/Triassic boundary. Nature, 337, No. 6202, 39-44.

Holser W.T., Magaritz M. and Clark (1986). Carbon-isotope stratigraphic correlations in the Late Permian. Am. J. Sci., 286, 390-402.

Holser W.T and Magaritz M. (1987). Events near the Permian-Triassic boundary. Modern Geology, 11, (2), 155-179.

Hower J. (1981). Shale diagenesis. In: Longstaffe F.J., Ed., Clays and resource geologist. Min. Assoc. of Canada, Short Course Handb., 7, 60-80.

Hsü K.J. and McKenzie J.A. (1990). Carbon-isotope anomalies at era boundaries; Global catastrophes and their ultimate cause: In Sharpton V.L. and Ward P.D. (Eds.), Global catastrophes in Earth history; An interdisciplinary conference on impacts, volcanism, and mass mortality. Geol. Soc. of Am., Spec. Pap. 247, 61-70.

Hunt J.M. (1979). Petroleum geochemistry and geology. Freeman, San Francisco.

Ingram R.L. (1953). Fissility of mudrocks. Geol. Soc. Am. Bull., 65, 869-878.

Irwin H., Curtis C and Coleman M (1977). Isotopic evidence for source of diagenetic carbonates formed during burial of organic-rich sediments. Nature, 269, 209-213.

Jablonski D. (1986). Causes and consequences of mass extinctions: a comparative approach. In Elliot D.K (Ed.). Dynamics of extinction, Wiley and Sons, NY, 183-229.

Keyser A.W. (1973). A preliminary study of the type area of the Cistecephalus zone of the Beaufort Series, and a revision of the Anomodont family Cistecephalidae. Mem. Geol. surv. S. Afr., 62, 1-71.

Keyser A.W. (1970). Some ecological aspects of the Cistecephalus zone of the Beaufort Series of South Africa. In: Haughton S.H. (Ed.). 2nd symposium on Gondwana stratigraphy and palaeontology, Pretoria. 653-657.

King G.M. (1990). Life and death in the Permo-Triassic: The fortunes of the Dicynodont mammal-like reptiles. Sidney Haughton Memorial Lecture 3. South African Museum, Cape Town. 17p.

Kodina L.A. and Galimov E.M. (1984). The organic carbon isotopic composition of "humic" and "sapropelic" types forming in marine sediments. Geochemistry, 11, 1742-1756.

Krauskopf K.B. (1967). Introduction to geochemistry. McGraw-Hill Book Company. New York, p721.

Kronberg B.I., Nesbitt H. W. and Lam W.W. (1986). Upper Pleistocene Amazon deep-sea fan muds reflect intense chemical weathering of their mountainous source lands. Chem. Geol., 54, 283-294.

le Roux J.P. (1992). Palaeoenvironment interpretation of tabular sandstones in the Beaufort Group of the Karoo Basin, South Africa. S. Afr. J. Geol., 95, (5/6), 171-180.

le Roux A.P. and Watkins R.T. (1990). Analysis of rare earth elements in geological samples by gradient ion chromatography: An alternative to ICP and INAA. Chem. Geol., 88, 151-162.

Levinson A.A. (1974). Introduction to exploration geochemistry. Applied Publ. Ltd., Illinois, p614.

Lewan M. (1978). Laboratory classification of very fine-grained sedimentary rocks. Geology, 6, 745-748.

MacRae C.S.(1992). Age of the Whitehill Formation in the Hopetown area, northeastern Cape Province. Abstr. 7th Conf. Palaeont. Soc. S. Afr., Johannesburg. 29.

MacRae C.S.(1991). Carboniferous sediments in the Waterberg Basin, South Africa, and identification of the Carboniferous/Permian boundary. S. Afr. J. of Sci., 87, 381-387.

MacRae C.S. (1989). Palynostratigraphic identification of an unconformity in borehole KNP 7 from the north-eastern part of the Soutpansberg Coalfield (Permian Period), South Africa. S. Afr. J. Geol., 92, 3, 261-271.

MacRae C.S. (1988). Palynostratigraphic correlation between the lower Karoo sequence of the Waterberg and Pafuri coal-bearing basins and the Hammanskraal plant macrofossil locality, Republic of South Africa. Geol. Surv. Mem. 75.

Magaritz M., Krishnamurthy R.V., and Holser W.T. (1992). Parallel trends in organic and inorganic carbon isotopes across the Permian/Triassic boundary. Am. J. of Sci., 292, 727-739.

Magaritz M. and Holser W.T. (1991). The Permian-Triassic of Gartnerkofel-1 core (Carnic Alps, Austria): Carbon and oxygen isotope variations. Abhandl. Geol. Bundesanst., 45, 149-163.

Malkowski K., Gruszczynski M., Hoffman A., and Halas S. (1989). Oceanic stable isotope composition and a scenario for the Permo-Triassic crisis. Histor. Biol., 2, 289-309.

Manning L.K., Frost C.D. and Branthaver J.F. (1991). A neodymium isotopic study of crude oils and source rocks: potential applications for petroleum exploration. Chem. Geol, 91, 125-138.

Martin J.M. and Meybeck M. (1979). Elemental mass-balance of material carried by major world rivers. Mar. Chem., 7, 375-388.

Mason B. and Moore C.B. (1982). Principles of geochemistry. Fourth Edition. John Wiley & Sons New York, p350.

Matsumoto R. and Iijima A. (1981). Origin and diagenetic evolution of Ca-Mg-Fe carbonates in some coalfields of Japan. Sediment., 28, 239-259.

Maxwell W.D. (1989). The end Permian mass extinction. Donovan S.K. (Ed.) Mass extinctions: Processes and evidence. Belhaven Press, London, 152-173.

Maxwell W.D. and Benton M.J. (1987). Mass extinctions and data bases: changes in the interpretation of tetrapod mass extinction over the past 20 years. In: Currie P.J. and Koster E.H (Eds.). 4th Symposium on Mesozoic Terrestrial Ecosystems, occasional paper of the Tyrell Museum of Palaeontology, Alberta, 3, 156-160.

McCabe P.J. (1991). Geology of coal; Environments of deposition. In: Gluskoter H.J, Rice D.D. and Taylor R.B. (Eds.). The geology of North America, v. P-2, Economic Geol. U.S. The Geol. Soc. of Am., 469-482.

McCrea J.M. (1950). On the isotopic chemistry of carbonates and palaeo-temperature scale. Journ. Chem. Phys., 18, 849-857.

McCulloch M.T. and Wasserburg G.J. (1978). Sm-Nd and Rb-Sr chronology of continental crust formation. Science, 200, 1003-1011.

McDowell S.D. and Elders W.A. (1980). Authigenic layer silicate minerals in borehole Elmore 1, Salton Sea geothermal field, California, U.S.A., Contrib. Min. and Pet., 74, 293-310.

McLennan S.M., Taylor S.R. and Eriksson K.A. (1983b). Geochemistry of Archaean shales from the Pilbara Supergroup, Western Australia. Geochim. Cosmochim. Acta, 47, 1211-1222

McLennan S.M. (1989). Rare Earth Elements in sedimentary rocks: Influence of provenance and sedimentary processes. In: Lipin B.R. and McKay G.A. (Eds.). Geochemistry and mineralogy of rare earth elements. Mineral. Soc. of Am., Rev. in Mineralogy, 21, 169-200.

McLennan S.M., Taylor S.R. and Kröner A. (1983a). Geochemical evolution of Archaean shales from South Africa. I. The Swaziland and Pongola Supergroups. Precam. Res., 22, 93-124

McLennan S.M., Fryer B.J. and Young G.M. (1979). Rare earth elements in Huronian (Lower Paleozoic) sedimentary rocks: composition and evolution of the post-Kenoran upper crust. Geochim. et Cosmo. Acta, 43, 375-388.

Mearns E.W. (1992). Samarium-neodymium isotopic constraints on the provenance of the Brent Group. In: Haszeldine A.C., Giles R.S. and Brown S. (Eds.). Geology of the Brent Group. Geol. Soc. Spec. Publ. No. 61, 213-225.

Mearns E.W. (1988). A samarium-neodymium isotopic survey of modern river sediments from Northern Britian. Chem. Geol. (Iso. Geosci. Sectn.), 73, 1-13.

Merodio J.C., Spallletti L.A. and Bertone L.M. (1992). A fortran program for calculation of normative composition of clay minerals and pelitic rocks. Computers and Geosc., 18, 1, 47-61.

Mozley P.S. and Wersin P. (1992). Isotopic composition of siderites as an indicator of depositional environment. Geology, 20, 817-820.

Mpodozis C and Kay A.M (1992). Late Palaeozoic to Triassic evolution of the Gondwana margin: Evidence from Chilean Frontal Cordilleran batholiths (28°S to 31°S). Geol. Soc. Am. Bull., 104, 999-1014.

Murchison D.G. (1987). Recent advances in organic petrology and organic geochemistry: an overview with some reference to "oil from coal". In: Scott A.C. (Ed.). Coal and Coal-bearing Strata: Recent Advances. Geol. Soc. Spec. Blackwell Scientific Published. Publ. No. 32, 257-302.

Nance R.D., Worsley T.R. and Moody J.B (1988). The supercontinent cycle. Scientific American, July, 44-51.

Nelson B.K. and DePaolo (1988). Application of Sm-Nd and Rb-Sr isotope systematics to studies of provenance and basin analysis. J. Sediment. Petrol., 58, 348-357.

Nesbitt H.W. and Young G.M. (1982). Early Proterozoic climates and plate motions inferred from major element chemistry of lutites. Nature, 299, 715-717.

Nesbitt H.W., Markovics G. and Price R.C. (1980). Chemical processes affecting alkalis and alkaline earths during continental weathering. Geochim. et Cosmochim. Acta, 44, 1659-1666.

Nesbitt H.W. (1979). Mobility and fractionation of rare elements during weathering of granodiorite. Nature, 279, 206.

Nicholls G.D. (1962). A scheme for recalculating the chemical analyses of argillaceous rocks for comparative purposes. Am. Mineralogist, 47, 34-46.

Nicholls G.D. and Loring D.H. (1962). The geochemistry of some British carboniferous sediments. Geochim. et Cosmochim. Acta, 26, 181-223.

Norrish K. and Hutton J.T. (1969). An accurate X-ray spectrographic method for the analysis of a wide range of geological samples. Geochim. et Cosmochim. Acta, 33, 431-453.

Northrop D.A. and Clayton R.N. (1966). Oxygen isotope fractionations in systems containing dolomite. J. of Geology, 74, 174-196.

O'Leary M (1988). Carbon Isotopes in photosynthesis. BioScience, 38, No. 5, 328-336.

O'Neil J.R., Clayton R.N. and Mayeda T.K. (1969) Oxygen isotope fractionation in divalent mineral carbonates. J. Chem. Physics, 51, 5547-5558.

O'Nions R.K., Hamilton P.J. and Hooker P.J. (1983). A Nd isotope investigation of sediments related to crustal development in the British Isles. Earth and Plan. Sci. Lett., 63. 229-240.

O'Nions R.K (1984). Isotopic abundances relevant to the identification of magma sources. Philos. Trans. R. Soc. Lond. Matm. Phys. Sci., 310, 591-603.

Oremland R.S. and Kvenvolden K.A. (1981). Microbial formation of ethane in anoxic estuarine sediments. Applied and Env. Microbio., 42, 122-129.

Palmer M.E. (1978). Acidity and nutrient availability in colliery spoil. In: Environmental management of mineral wastes. (Eds.), Goodman G.T. and Chadwick M.J. Sijthoff and Noordhoff, Alphen aan den Rijn - Netherlands. 85-126

Pettijohn F.J. (1975). Sedimentary Rocks (3rd Ed.) Harper and Row, 628.

Pevear D.R., Williams V.E. and Mustoe G.E. (1980). Kaolinite, smectite, and K-rectorite in bentonites: relation to coal rank at Tulameen, British Columbia. Clays and Clay Mins., 28, No.4, 241-254.

Picard M.D. (1971). Classification of fine-grained sedimentary rocks. Journ. Sed. Petrol., 41, 179-195.

Pinna P., Jourde G., Calvez J.Y., Mroz J.P. and Marques J.M. (1993). The Mozambique Belt in the northern Mozambique: Neo-proterozoic (1100-850) crustal growth and tectogensis, amd superimposed Pan-African (800-550) tectonism. Precam. Res., 62, 1-59.

Pitman W.C. III (1978). Geol. Soc. Am. Bull., 89, 1389.

Pitrat C.W. (1973). Vertebrates and the Permo-Triassic extinctions. Palaeo. Palaeo. Palaeo., 14(4), 249-264.

Plumstead E.P (1969). Three thousand million years of plant life in Africa. Geol. Soc. Afr. Trans., 72 (Annex).

Popp B.N., Anderson F.T., and Sandberg P.A. (1986). Brachiopods as indicators of original isotopic composition of limestones. Geol. of Am. Bull., 97, 1262-1269.

Potter P.E., Shimp N.F. and Witters J. (1963). Trace elements in marine and fresh-water argillaceous sediments. Geochim. et Cosmochim. Acta, 27, 669-694.

Powell T.G. and Snowdon L.R. (1983). A composite hydrocarbon generation model: Implications for evaluation of basins for oil and gas. Erdöl unde Kohle-Rdgas-Petrch., 36, 163-170.

Powell T.G., Foscolos A.E., Gunther P.R. and Snowdon L.R. (1978). Diagenesis of organic matter and fine-clay minerals: a comparative study. Geochim. et Cosmo. Acta, 42, 1181-1197.

Pretorius L.E. (1985). Stable isotope, sedimentological and chemical aspects of the lower Beaufort group uranium province in the southwestern Karoo basin, South Africa. Ph.D. thesis (unpubl.) Univ. Queensland, 233p.

Price N.B. and Duff P.McL.D. (1969). Mineralogy and chemistry of tonsteins from carboniferous sequences in Great Britain. Sedimentology, 13, 45-69.

Price N.J. (1966). Fault and joint development in brittle and semi-brittle rock. Pergamon Press, New York.

Price N.P. (1976). Chemical diagenesis in sediments. In: Riley J.P. and Chester R. (Eds.). Chemical Oceanography, Vol 6, Chapter 30, 2nd Ed., Academic Press, London.

Puddephatt R.J. (1972). The Periodic Table of elements, Oxford Univ. Press, Oxford. 84p.

Pye K., Dickson J.A.D., Schiavon N, Coleman M.L. and Cox M. (1990). Formation of siderite-Mg-calcite-iron sulphide concretions in intertidal marsh and sandflat sediments, north Norfolk, England. Sedimentology, 37, 325-343.

Rau G.H., Froelich P.N., Takahashi T., and Des Marais D.J. (1991). Does sedimentary organic $\delta^{13}C$ record variations in quaternary ocean[CO_2(aq)]. Palaeo-oceanography, 6, 335-347.

Raup D.M. and Sepkoski J.J., Jr. (1982). Mass extinctions in the marine fossil record. Science, 215 (4539), 1501-1503.

Raup D.M. (1979). Size of the Permo-Triassic bottleneck and its evolutionary implications. Science, 206 (4415), 217-218.

Reimer T.O. (1985). Rare earth elements and the suitability of shales as indicators for the composition of the Archaean continental crust. Neues Jahrbuch Miner. Abh., 152, 2, 211-223.

Renton J.J.(1982). Mineral matter in coal. In: Meyers R.A. (Ed.). Coal structure. Academic Press, London, 283-326.

Ridley M.K., Watkins R.T. and Willis J.P. (1991). Determination of rare earth elements in whole coal and pulverized fuel ash by gradient ion chromatography. In: Vourvopoulos G. (Ed.). Elemental analysis of coal and its by-products. World Scientific, London, 49-74.

Ronov A.B., Khain V.E., Balukhovsky and Seslavinsky K.B. (1980). Quantitative analysis of Phanerozoic sedimentation. Sedimentary Geol., 25, 311-325.

Rosenbaum J. and Sheppard S.M.F. (1986). An isotopic study of siderites, dolomites and ankerites at high temperatures. Geochim. et Cosmo. Acta , 50, 1147-1150.

Rust I.C. (1975). The sedimentary and tectonic framework of Gondwana basins in southern Africa. In: Campbell K.S.W. (Ed.). Gondwana geology: papers from the 3rd Gondwana Symposium, Canberra, Australia. A.N.U. Press, 537-564.

Ryan P.J. (1966). The basin analysis of the Waterberg Coalfield. Geol. Surv. S.A. (Unpubl. Report). 59p.

Ryan P.J. (1967). Stratigraphic and paleocurrent analysis of the Ecca Series and the lowermost Beaufort beds in the Karroo Basin of South Africa. Ph.D. thesis, Univ. Witwatersrand, 210p. (unpubl.)

Sackett W.M. and Thompson R.R. (1963). Isotopic organic carbon composition of recent continental derived clastic sediments of eastern Gulf Coast, Gulf of Mexico. Am. Assoc. Pet. Geol. Bull., 47, 525-531.

Schidlowski M. (1988). A 3,800-million-year isotopic record of life from carbon in sedimentary rocks. Nature, 333, 313-318.

Schopf T.J.M. (1974). The Permo-Triassic extinction: relation to sea-floor spreading. J. of Geology, 82 (2), 129-143.

Schreiber U.M., Eriksson P.G. and Snyman C.P. (1992). Mudrock geochemistry of the Proterozoic Pretoria Group, Transvaal Sequence (South Africa): geological implications. J. Afr. Earth Sciences, 14 , No. 2, 393-409.

Schultz L.G., Tourtelot H.A., Gill J.R. and Boerngen J.G. (1980). Composition and properties of the Pierre Shale and equivalent rocks, northern great plains region. U.S. Geol. Surv. Professional Paper, 1064-B. 114p.

Sciulli A.G., Ballock G.P. and Wu K.K. (1986). Environmental approach to coal refuse disposal. Mining Engineering, March, 181-186

Sepkoski J.J, Jr. (1986). Global bioevents and the question of periodicity. In: Walliser O.H. (Ed.). Global bio-events, Springer, Berlin, 47-61.

Sheng J., Chen C., Wang Y., Rui L., Liao Z., Bando Y. Ishii K., Nakazawa K., and Nakamura K. (1984). Permian-Triassic boundary in middle and eastern Tethys. J. Fac. Sci. Hokkaido Univ. (Ser. 4), 21, 133-181.

Sheppard S.M.F. (1986). Characterization and isotopic variations in natural waters. In: Valley J.W., Taylor H.P., O'Neil J.R. (Eds.) Stable isotopes in high temperature geological processes. Mineral. Soc. Am., Rev. in Mineral., 16, 165-181.

Siepker E.H. (1986). Genetiese stratigrafie en sedimentologie van die opeenvolging Karoo in die westelike en noordelike deel van die Waterbergsteenkoolveld., M.Sc.(unpubl.) Randse Afrikaanse Universiteit.

Smith R.M.H. (1990). Alluvial paleosols and pedofacies sequences in the Permian Lower Beaufort of the southwestern Karoo Basin. J. Sedimentary Petrology, 60, No. 2, 258-276.

Smith J.W., Rigby D., Schmidt P.W. and Clark D.A. (1983). D/H ratios of coals and the palaeolatitude of their deposition. Nature, 302, 322-323.

Smith R.M.H., Eriksson P.G. and Botha W.J. (1993). A review of the stratigraphy and sedimentary environments of the Karoo-aged basins of southern Africa. J. of Afr. Earth Sci., 16, No. 1/2, 143-169.

Smith A.G., Hurly A.M. and Briden J.C. (1981). Phanerozoic palaeocontinental world maps. Cambridge Univ. Press, p122.

Smyth M. and Mastalerz M. (1991). Organic petrological composition of Triassic source rocks and their clastic depositional environments in some Australian sedimentary basins. Int. J. Coal Geol., 18, 165-186.

Snyman C. (1976). Die petrografiese samestelling en die onstaan van steenkool, veral met verwysing na Suid-Afrikaansw steenkool. Trans. Geol. Soc. S. Afr., 79, 2, 242-252.

South African Committee for Stratigraphy (S.A.C.S) (1980). Stratigraphy of South Africa. Part 1 (Comp. Kent L.E.). Lithostratigraphy of the Republic of South Africa, South West Africa/Namibia, and Republics of Bophuthatswana, Transkei and Venda: Handb. Geol. Surv. S.A., 8. 690p.

Spears D.A. and Caswell S.A. (1986). Mineral matter in coals: cleat minerals and their origin in some coals from the English Midlands. Int. Journ. of Coal Geol., 6, 107-125.

Spears D.A., Duff P.McL.D. and Caine P.M. (1988). The West Waterberg tonstein, South Africa. Int. J. of Coal Geol., 9, 221-233.

Spears D.A. and Duff P.McL. D. (1984). Kaolinite and mixed-layer-smectite in Lower Cretaceous bentonites from Peace River coalfield, British Columbia. Can. J. Earth Sci., 21, 465-476.

Spears D.A. and Amin M.A. (1981). Geochemistry and mineralogy of marine and non-marine Namurian black shales from the Tansley Borehole, Derbyshire. Sedimentology, 28, 407-417.

Spears D.A. (1987). Mineral matter in coals, with special reference to the Pennine Coalfields. In: Scott A.C. (Ed.). Coal and coal-bearing strata: recent advances. Geol. Soc. Spec. Publ. No. 32, Blackwell Scientific Publ., London, 171-186.

Stanley S.M. (1988). Palaeozoic mass extinctions: shared patterns suggest global cooling as a common cause. Am. J. of Science, 288, (4), 334-352.

Stanley S.M. (1984). Marine mass extinctions: a dominant role for temperature. In Nitecki M.H. (Ed.). Extinctions. Univ. Chicago Press, Chigaco. 69-117.

Stapleton R.P. (1977). Carboniferous unconformity in Southern Africa. Nature, 268, 222-223.

Staplin F.L. (1969). Sedimentary organic matter, organic metamorphism, oil and gas occurrences. Bull. Canadian Petrol. Geol., 17, 47-56.

Stear W.M. (1983). Morphological characteristics of ephemeral stream channel and overbank splay sandstone bodies in the Permian Lower Beaufort Group, Karoo Basin, South Africa. In: Collinson J.D. and Lewin J. (Eds.). Modern and ancient fluvial systems. Spec. Publ. Intern. Assoc. Sediment., 6, 405-420.

Stevens C.H. (1977). Was brackish oceans a factor in Permian extinctions? Bull. Geol. Soc. of Am., 88 (1), 133-138.

Stumm W. and Morgan J.J. (1981). Aquatic chemistry (2nd Ed.). Wiley, New York. 780p.

Sun S.-s. and McDonough W.F. (1989). Chemical and isotopic systematics of oceanic basalts: implications for mantle composition and processes. In: Saunders A.D. and Norry M.J. (Eds.). Magmatism in the ocean basins. Geol. Soc. Spec., 42, 313-345.

Swaine D.J. (1990). Trace elements in coal. Butterworths, London, 278p.

Sylvester P.J. (1989). Post-collisional alkaline granites. J. of Geol., 145, 251-280.

Tankard A.J., Jackson M.P.A., Eriksson K.A., Hobday D.K., and Minter W.E.L. (1982). Crustal evolution of Southern Africa - 3.8 billion years of earth history. Springer-Verlag, New York, 523p.

Taylor S.R. and McLennan (1985). The continental crust: It's composition and evolution. Blackwell Scientific Publications, p312.

Taylor R.K. and Smith T.J. (1986). The engineering geology of clay minerals: swelling, shrinking and mudrock breakdown. Clay Minerals, 21, 235-260.

Taylor B.E., Wheeler M.C. and Nordstrom D.K (1984). Stable isotope geochemistry of acid mine drainage: Experimental oxidation of pyrite. Geochim. et Cosmochim. Acta, 48, 269-678.

Teichert C. (1990). The Permian-Triassic boundary revisited. In: Kauffman E.G and Walliser O.H. Extinction events in Earth History. Springer-Verlag. Berlin, 199-238.

Teichmüller M. and Teichmüller R. (1975). Fundamentals of coal petrology. : In Stach E. (Ed.) Coal Petrography, 2nd Ed. Gebruder Borntraeger, Berlin, 5-174.

Teichmüller M. (1975). Origin of the petrographic constituents of coal: In Stach E. (Ed.) Coal Petrography, 2nd Ed. Gebruder Borntraeger, Berlin, 176-238.

Teichmüller M. (1987). Recent advances in coalification studies and their application to geology. In: Coal and Coal-bearing Strata: Recent Advances. Ed. Scott A.C. Geol. Soc. Spec. Blackwell Scientific Published. Publ. No. 32, 127-170.

Thackery J.F., van der Merwe N.J., Lee-Thorpe J.A., Sillen A., Lanham J.L., Smith R., Keyser A. and Monteiro P.M.E. (1990). Carbon isotopic evidence from late Permian Therapsids teeth, for a progressive change in atmospheric CO_2 composition, Nature, 347, 751-753.

Thomas R.J., von Vey M.W. and McCourt S. (1993). The tectonic evolution of southern Africa: an overview. J. of Afr. Earth Sci., 16, No. 1/2, 5-24.

Thomasson J.R., Nelson M.E., and Zakrezewski R.J. (1986). A fossil grass (Gramineae: Chloridoideae) from the Miocene with Kranz anatomy. Science, 233, 876-878.

Thornton, I. (1983). Applied environmental geochemistry, London, 495p.

Tieszen L.J. (1991). Natural variations in the carbon isotope values of plants: Implications for archaeology, ecology, and paleoecology. Journ. of Archaeological Sci., 18, 227-248.

Ting F.T.C (1977). Origin and spacing of cleats in coal beds. J. Pressure Vessel Technol., Trans. ASME, 99, 624-626.

Tissot B and Welte D.H. (1984). Petroleum formation and occurrence: a new approach to oil and gas exploration. 2nd Ed., Springer-Verlag, Berlin, 538p.

Torrey S. (Ed.) (1978). Trace Contaminants from Coal Preparation Waste and Ash Disposal. In: Trace Contaminants from Coal Pollution Technology, Review No. 50. Noyes Data Corp., New Jersey. 229-292.

Tourtelot H.A. (1979). Black shale - its deposition and diagenesis. Clays and Clay Mins., 27, No.5, 313-321.

Triplehorn D.M. and Bohor B.F. (1983). Goyazite in kaolinitic altered tuff beds of cretaceous age near Denver, Colorado. Clays and Clay Mins., 31, 4, 299-304.

Triplehorn D.M. (1990). Applications of tonsteins to coal geology: some examples from western United States. Int. Journ. Coal Geol., 16, 157-160.

Tucker M.E. (1981). Sedimentary petrology an introduction. Blackwell Scientific Publ., London, p243.

Turekian K.K. and Wedepohl K.H. (1961). Distribution of elements in some major rock units of the Earth's crust. Bull. Geol. Soc. Amer., 72, 175-192.

Turner B.R. (1991). Southern Africa. In: Moullade M. and Nairn A.E.M. (Eds.). The Phanerozoic geology of the world: I the Palaeozoic. Elsevier, Amsterdam. 1-70.

Turner B.R. (1975). The stratigraphy and sedimentary history of the Molteno Formation in the Main Karoo Basin of South Africa and Lesotho. Ph.D. thesis, Univ. Witwatersrand, Johannesburg. (unpubl.)

Valentine J.W. (1973). Evolutionary palaeoecology of the marine biosphere. Prentice Hall, Englewood Cliffs, NY.

Valkovic V. (1983). Trace elements in coal. CRC Press, Boca Ranton. Vol I, 210p, Vol II, 281p.

van Krevelen D.W. (1961). Coal. Elsevier, Amsterdam.

van Berkel G.J. (1987). The role of kerogen in the origin and evolution of nickel and vanadyl geoporphyrins. Ph.D. thesis, Washington State Univ., Pullman, Wash., 246p. (unpubl.)

Veizer J., Holser W.T., and Wilgus C.K. (1980). Correlation of $^{13}C/^{12}C$ and $^{34}S/^{32}S$ secular variations. Geochim. et Cosmochim. Acta, 44, 579-587.

Venter F.A. (1944). Waterberg coalfield: records of boreholes 1-20. Bull Geol. Surv. S.A., 15. 106p.

Venter P.E. and van Loggerenberg C. (1992). Modifications to the coal-preparation circuit at the Grootegeluk Coal Mine to improve its efficiency. J. S. Afr. Inst. Min. Metall., 92, No. 2, 53-61.

Veveers J.J. (1988). Gondwana facies started when Gondwanaland merged in Pangea. Geology, 16, 732-734.

Visser J.N.J. (1990). The age of the late Palaeozoic glacigene deposits in southern Africa. S. Afr. J. Geol., 93(2), 366-375.

Visser H.N. (1961). Karoo sequence in the Northern Transvaal. 4th C.C.T.A., Southern Regional Comm. Geol., 115-123.

Visser H.N. (1953). The geology of the Koedoesrand area, northern Transvaal: Expl. Shts. Geol. Surv. S.A., 35 and 36 (Koedoesrand). 110p.

von Prüeß, A., Turian, G., and Schweikle, V. (1991). Ableitung kritischer Gehalte an NH_4NO_3-extrahierbaren ökotoxikologisch relevanten Spurenelementen in Böden SW-Deutschlands, Mitt. Dtsch. Bodenkundl. Gesellsch., 66,I:385-88.

von Prüeß, A. (1992). Vorsorgewerte und Prüfwerte für mobile und mobilisierbare, potentiell ökotoxische Spurenelemente in Böden. Verlag Ulrich E. Grauer Wendlingen.

Walters L.J. JR., Owen D.E., Henley A.L., Winsten M.S. and Valek K.W. (1987). Depositional environments of the Dakota sandstone and adjacent units in the San Juan Basin utilizing discriminant analysis of trace elements in shales. J. of Sed. Pet., 57, No. 2, 265-277.

Ward C.R. (1984). Coal Geology and Coal Technology. Blackwell Sci. Publ., London.

Waterhouse J.B. (1973). The Permian-Triassic boundary in New Zealand and New Caledonia and its relationship to world climatic changes and extinction of Permian life. In Logan A. and Hills L.V. (Eds.). The Permian and Triassic Systems and their mutual boundary. Mem. of the Canadian Soc. of Petroleum Geol., 2, 445-464.

Weaver C.E. (1960). Possible uses of clay minerals in search for oil. Am. Assoc. Petr. Geol. Bull., 44, 1505-1578.

Wedepohl K.H. (1978). Handbook of geochemistry. Vols. I-V. Springer-Verlag, New York.

Wickman F. (1953). Wird das haufigkeitsverhaltnis der kohlenstoffisotopen bei der inkohlung verandert? Geochim. et Cosmochim. Acta, 3(2), p244.

Wignal P.B. and Hallam A. (1992). Anoxia as a cause of the Permian/Triassic mass extinction: facies evidence from northern Italy and the western United States. Palaeo. Palaeo. Palaeo., 93, 21-46.

Wildeman T.R. (1983). Chemistry of the Argo Tunnel. Quarterly of the Colorado School of Mines, 78, No. 4, 31-37.

Williamson I.A. (1970). Tonsteins - their nature, origins and uses. Mining Magazine, 122, No. 2, 119-125; No. 3, 203-211.

Willis J.P. (1989). Compton scatter and matrix correction for trace elements analysis of geological materials. In: Ahmedali S.T. (Ed.). X-ray Fluorescence analysis in the geological sciences. Advances in methodology. Geol. Assoc. of Canada. 91-119.

Willis J.P., Bosch G.L. and Kruger R.A. (1989). The Chemical and Mineralogical Composition and Utilization of South African Fly Ash. In: H.M Hess (Ed.). Proc. of the Fifteenth Biennial Low-Rank Fuels Symposium, Mannesota. U.S. Dept. of Energy. 577-591

Wnuk C. and Pfefferkorn H.W. (1987). A Pennsylvanian age terrestrial storm deposit: using plant fossils to characterize the history and process of sediment accumulation: J. Sed. Pet., 57, 212-221.

Wronkiewicz D.J. and Condie K.C. (1987). Geochemistry of Archaean Shales from the Witwatersrand Supergroup, South Africa: Source-area Weathering and Provenance. Geochim. Cosmochim. Acta, 51, 2401-2416.

Wyberg W.L. (1928). The coal resources of the Union of South Africa. Mem. Geol. Surv. S.A., 19(3). 181p.

Zawada P.K. (1988). Trace elements as possible palaeosalinity indicators for the Ecca and Beaufort Group mudrocks in the southwestern Orange Free State. S. Afr. J. Geol., 91, No. 1, 18-26.

Zubovic P., Stadnichenko T. and Sheffey N.B. (1966). Distribution of minor elements in coal beds of the Eastern Interior region. US Geol. Surv. Bull., No. 1117-C. 3p.

APPENDIX I. SAMPLING PROCEDURE and SAMPLE NUMBERING

Two boreholes (LQ 136 and 137) were drilled by ISCOR in the confines of the Grootegeluk Coal Mine (GCM) and intersected the whole of the Grootegeluk Formation. Only carbonaceous mudstones (approximately > 60% inorganic matter) were made available for this study. The core was first logged by the Chief Geologist, Claris Dreyer, before the samples were collected under supervision.

As a result of the relatively persistent nature of the coal and shale beds and closely spaced drilling (300 m by 300 m) within the confines of the GCM, the mine geologists have been able to further subdivide the eleven coal zones (numbered from bottom up) into "samples" (numbered from top down) to assist with stratigraphic correlation and grade control (Fig. 2.3). Sampling in this project has conformed to the existent sampling number system as used at GCM and further division of these units ("samples") by the author is indicated by an additional alphabetic suffix to the "sample" number. For example, samples from borehole 136 in "sample" 22E are numbered 136_22Ea, 136_22Eb, 136_22Ec, etc. It was not possible in Figure 2.3 to indicate the position of every sample taken in this study because of the scale of the diagram and the small sampling widths. Figure I.1 below is an enlarged section from borehole 136 that demonstrates the sample numbering that was used in this study and also illustrates the small sampling widths. The exact co-ordinates for the boreholes can be obtained from the Geological Department at the GCM.

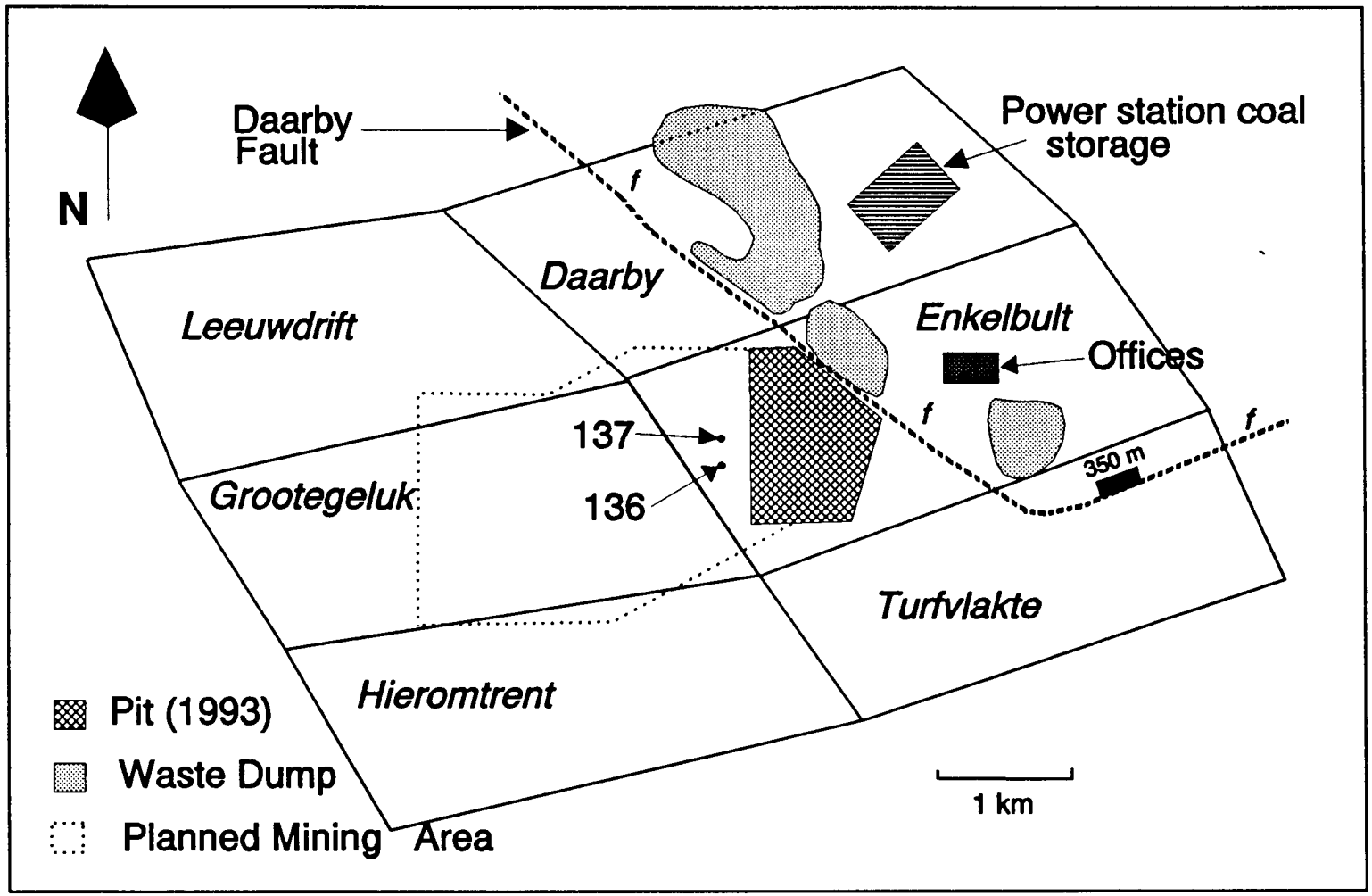

Figure I.1. Map showing the location of boreholes 136 and 137, farm boundaries and Grootegeluk Coal Mine pit. The discard and storage dumps and mine offices have been established to the north of the Daarby fault which has been down thrown by 350 to the north.

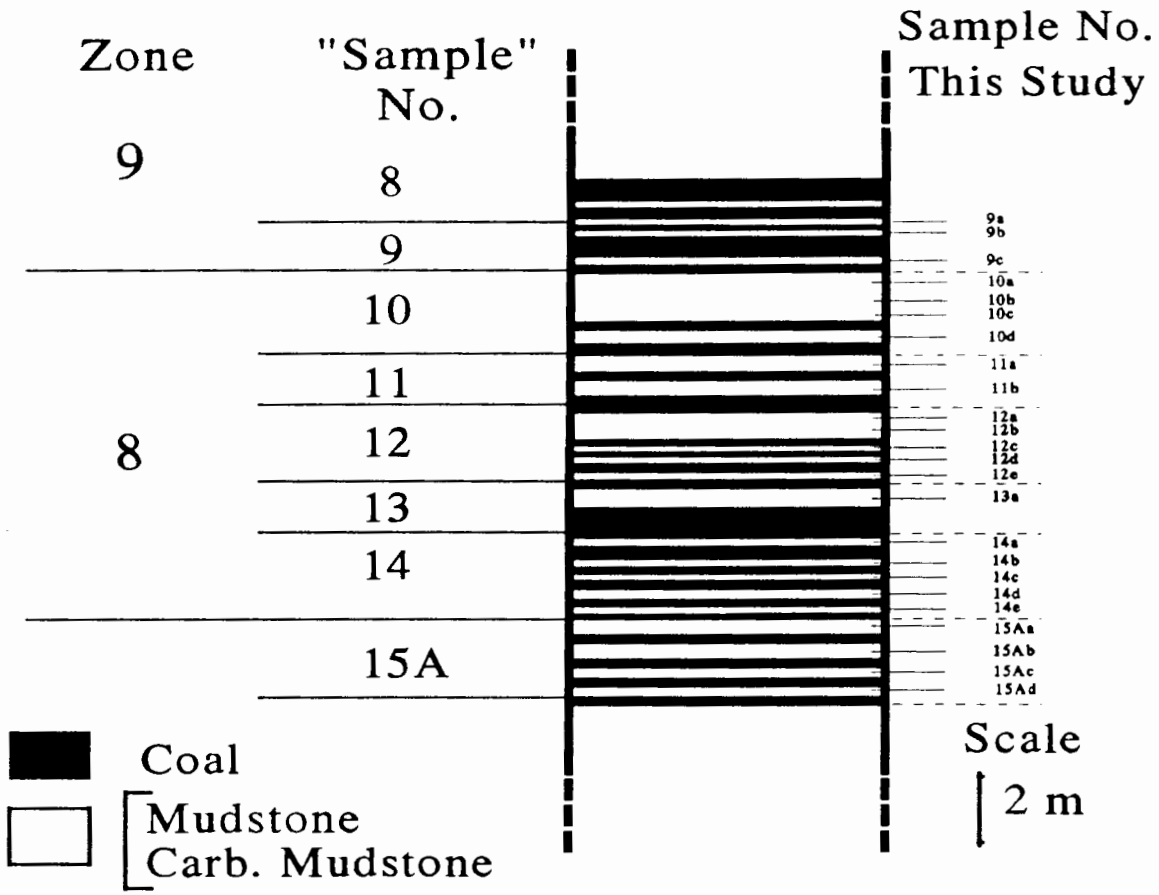

Figure I.2. The diagram illustrates the numbering scheme used by the GCM geological department (on the left side of diagram) and is also used in this study (right side of diagram). In most cases several mudstone samples were taken from a GCM "sample" and an additional alphabetic suffix is added to the "sample" number.

Table II.1 Results of petrographic analyses of samples that consist predominantly of coal. The coal samples were separated into different relative densities (RD) before the analyses. Maceral proportions in % were recalculated to 100% without the mineral fraction. The analyses were done by ISCOR's Department of Material Research, in Pretoria. Results of petrographic analyses of samples that consist predominantly of mudstone are given in the Table on the next page.

Coal RD 1.35					Coal RD 1.80					Coal RD 2.00				
Vitrin.	Exin.	RSF	Inert.	$\bar{R}_o$max	Vitrin.	Exin.	RSF	Inert	$\bar{R}_o$max	Vitrin.	Exin.	RSF	Inert.	$\bar{R}_o$max
97.4	1.4	0.4	0.8	0.6	87.2	2.0	3.0	7.8	0.7	58.7	2.3	5.0	33.9	0.8
94.0	1.6	1.5	2.9	0.7	68.0	0.8	10.0	21.2	0.7	68.1	7.5	2.3	22.2	0.7
94.3	0.9	1.5	3.2	0.7	62.7	1.9	16.3	19.1	0.7	67.0	4.7	2.1	26.1	0.9
96.8	0.9	0.5	1.8	0.7	64.6	4.7	13.4	17.2	0.7	72.9	3.3	8.2	15.6	0.7
95.4	1.1	0.8	2.6	0.7	78.4	1.8	8.4	11.4	0.7	78.8	2.5	6.3	12.4	0.7
94.3	1.3	1.4	3.1	0.7	73.9	1.4	9.7	15.0	0.6	61.7	2.6	15.6	20.2	0.6
94.1	1.0	1.3	3.6	0.6	70.7	3.0	9.8	16.6	0.6	80.0	2.5	6.3	11.2	0.6
96.7	1.0	0.4	1.9	0.7	69.4	1.7	10.0	18.9	0.6	73.5	1.9	7.6	17.0	0.6
95.6	1.5	0.5	2.4	0.8	58.9	6.7	15.6	18.8	0.7	74.5	2.2	8.8	14.5	0.7
96.5	1.1	0.7	1.6	0.8	80.6	4.4	6.0	9.0	0.7	59.1	2.2	18.3	20.5	0.6
99.0	0.8	0.1	0.1	0.7	74.6	1.5	8.4	15.6	0.7	87.1	1.9	3.8	7.2	0.6
93.6	0.6	0.3	5.5	0.7	78.7	3.0	1.4	17.0	0.7	86.7	2.9	4.4	6.1	0.6
94.8	0.5	2.1	2.6	0.7	68.9	1.3	12.6	17.2	0.7	71.5	1.6	8.6	18.3	0.7
96.7	0.1	0.9	2.3	0.7	72.0	0.3	12.4	15.3	0.7	76.9	2.3	8.1	12.6	0.6
93.9	0.1	1.9	4.1	0.7	63.8	2.3	14.3	19.6	0.7	75.3	5.0	8.4	11.3	0.7
94.1	1.5	1.5	3.0	0.8	61.1	1.1	15.6	22.3	0.7	52.1	0.6	21.6	25.8	0.7
94.4	3.3	0.6	1.6	0.8	57.9	1.5	20.1	20.6	0.7	66.3	2.3	13.5	17.9	0.8
96.8	1.0	0.0	2.2	0.8	58.1	1.5	15.9	24.5	0.7	68.9	1.1	9.6	20.3	0.7
94.8	1.7	0.0	3.5	0.7	47.4	3.2	23.6	25.8	0.7	38.4	0.9	21.0	39.7	0.7
95.0	1.4	1.5	2.1	0.7	44.3	3.6	28.9	23.2	0.7	36.1	0.6	29.4	33.9	0.7
90.2	4.4	2.3	3.1	0.8	49.0	3.4	25.6	22.0	0.7	44.3	1.1	5.2	49.4	0.7
93.5	2.2	0.7	3.6	0.8	63.7	2.6	17.0	16.6	0.7	28.3	1.9	37.9	31.9	0.8
91.3	1.8	1.2	5.7	0.7	33.7	4.0	31.9	30.4	0.7	11.1	3.6	37.9	47.4	0.8
92.8	2.2	1.3	3.8	0.7	52.8	3.4	23.0	20.7	0.7	33.9	0.7	31.4	33.9	0.8
87.3	2.0	3.0	7.7	0.7	32.5	0.8	30.3	36.4	0.8	11.5	2.0	31.8	54.7	0.8
86.2	3.8	2.5	7.5	0.8	24.5	2.7	30.2	42.5	0.8	10.0	1.1	41.8	47.1	0.8
85.3	1.6	2.8	10.3	0.7	50.8	1.7	16.4	31.1	0.8					
95.6	1.0	0.5	2.8	0.8	30.9	1.3	35.4	32.4	0.8					
75.4	3.9	6.7	14.0	0.8	4.9	1.0	62.4	31.6	1.0					
57.5	3.2	16.9	22.4	0.8	7.2	0.6	22.4	69.8	0.9					
73.2	3.8	7.6	15.4	0.7										
71.2	2.6	10.2	16.0	0.9										

Table II.1 continued.....

Mudstone RD 1.50					Mudstone RD 1.8					Mudstone RD 1.9				
Vitrin.	Exin.	RSF	Inert.	$\bar{R}_o$max	Vitrin.	Exin.	RSF	Inert.	$\bar{R}_o$max	Vitrin.	Exin.	RSF	Inert.	$\bar{R}_o$max
96.4	0.0	0.8	2.8	0.8	77.8	1.5	9.3	11.3	0.6	66.1	1.1	13.5	19.4	0.6
91.4	0.2	1.8	6.6	0.8	72.1	1.0	12.0	15.0	0.6	55.7	0.9	20.8	22.6	0.5
93.5	0.2	1.8	4.5	0.8	69.2	1.8	10.9	18.1	0.6	68.3	0.7	14.0	16.9	0.6
89.7	0.1	3.4	6.8	0.7	78.9	1.8	8.1	11.2	0.7	58.1	1.9	25.6	14.3	0.7
92.1	0.6	2.0	5.3	0.8	67.4	0.0	16.4	16.2	0.7	52.5	3.9	19.1	24.5	0.6
92.1	0.0	2.1	5.8	0.8	69.0	0.0	11.4	19.6	0.7	57.6	1.2	21.4	19.8	0.6
95.9	1.0	1.5	1.5	0.7	69.9	0.4	10.6	19.1	0.8	51.7	1.7	21.8	24.7	0.7
94.2	1.5	1.3	2.9	0.7	56.2	0.8	19.2	23.9	0.7	56.1	1.3	16.1	26.5	0.6
92.5	0.4	1.2	5.8	0.8	72.9	1.5	10.9	14.7	0.7	33.5	1.7	26.9	38.0	0.7
88.0	0.4	3.6	8.0	0.8	64.3	1.8	12.7	21.2	0.5	65.7	0.8	14.5	19.0	0.6
89.9	0.6	2.4	7.2	0.7	60.3	2.7	14.1	22.9	0.6	56.9	2.6	18.2	22.4	0.6
97.6	0.0	0.4	1.9	0.7	65.8	1.0	13.6	19.7	0.6	61.9	3.4	18.7	16.1	0.7
96.1	0.5	0.4	3.0	0.8	57.1	0.4	23.3	19.1	0.7	48.1	2.7	29.0	20.1	0.7
85.5	0.7	3.0	10.9	0.7	63.0	0.1	20.5	16.3	0.6	45.8	5.2	25.3	23.7	0.7
81.5	3.3	4.6	10.5	0.8	61.0	2.9	19.0	17.1	0.7	53.7	6.3	22.9	17.1	0.6
86.9	1.8	3.5	7.8	0.7	59.1	6.3	12.8	21.7	0.6	50.9	3.4	24.9	20.7	0.7
82.4	1.3	2.1	14.2	0.8	52.8	1.0	19.6	26.5	0.6	42.0	5.1	24.8	28.1	0.7
70.8	1.5	11.3	16.4	0.7	55.7	0.9	18.3	25.0	0.6	23.4	0.0	31.2	45.5	0.7
72.4	0.5	9.6	17.5	0.8	57.0	5.6	17.3	20.0	0.6	35.3	0.6	37.8	26.3	0.8
87.7	1.5	1.6	9.1	0.8	48.6	3.1	26.6	21.7	0.6	43.7	4.6	29.8	21.8	0.7
80.7	0.9	7.8	10.6	0.8	54.3	1.1	24.7	19.9	0.6	29.5	0.9	33.0	36.6	0.6
70.4	1.1	10.5	18.0	0.9	27.8	1.7	30.3	40.2	0.8	28.2	7.6	28.6	35.5	0.8
57.8	3.8	19.8	18.5	0.8	26.6	7.5	24.8	41.1	0.7	25.9	5.0	29.9	39.2	0.7
					35.1	0.4	32.5	32.0	0.7	23.3	2.9	28.9	44.9	0.6
					37.9	1.9	32.6	27.6	0.8	29.4	4.0	29.7	36.9	0.8
					37.1	0.3	35.0	27.6	0.8	25.8	1.4	33.0	39.9	0.7
					19.8	3.1	31.7	45.3	0.8	12.0	2.2	19.6	66.2	0.8
					14.1	2.1	23.7	60.2	0.9	8.9	2.3	14.7	74.1	0.8
					7.2	0.6	22.4	69.8	0.9	11.1	3.7	18.4	66.8	0.8

Table II.2 Whole-rock major and trace element compositions of mudstones and carbonaceous mudstones from borehole 136 and 137. Majors are reported in weight % oxide and trace elements in ppm. All Fe is calculated as FeO. Analytical conditions and statistics are reported in Chapter 3 (< indicates less than lower limit of detection). D = depth (m) with respect to the topmost coal seam in the Grootegeluk Fm (negative value below and positive above). Sample numbering and position in boreholes are explained in Appendix I.

136	0a	0b	0c	1ba	1bb	1bc	1bd	1ca	1cb	1cc	1cd	1ce	1da	1db	1dc	1dd	2a	2b	2c
SiO_2	66.00	64.13	58.28	63.17	70.03	68.56	64.08	66.40	54.48	61.73	58.50	54.75	55.19	60.76	48.37	61.41	55.64	61.52	37.08
TiO_2	0.74	0.75	0.66	0.66	0.66	0.70	0.68	0.71	0.65	0.69	0.70	0.57	0.60	0.70	0.42	0.68	0.67	0.79	0.38
Al_2O_3	17.90	18.33	16.17	16.54	16.97	18.00	16.86	17.80	17.30	20.25	19.93	15.42	17.84	17.74	14.88	18.27	16.06	19.94	8.50
FeO	2.68	2.32	6.28	4.08	1.33	1.51	1.04	1.70	1.52	1.39	0.98	0.91	0.92	1.09	0.91	1.05	0.97	2.14	3.25
MgO	0.75	0.38	0.40	0.49	0.54	0.57	0.43	0.66	0.47	0.52	0.42	0.38	0.36	0.42	0.27	0.38	0.35	0.61	0.25
CaO	0.38	0.14	0.31	0.16	0.18	0.29	0.13	0.27	0.22	0.23	0.18	0.14	0.15	0.18	0.11	0.17	0.17	0.24	0.29
Na_2O	0.05	0.05	0.05	0.09	0.08	0.08	0.10	0.11	0.08	0.12	0.10	0.10	0.09	0.13	0.08	0.13	0.12	0.16	0.06
K_2O	1.19	1.14	0.95	2.28	2.46	2.20	2.50	2.80	2.03	2.59	2.18	2.05	1.88	2.38	1.50	2.31	2.02	2.71	0.80
P_2O_5	0.03	0.04	0.04	0.06	0.06	0.03	0.03	0.07	0.03	0.04	0.05	0.03	0.04	0.03	0.05	0.05	0.03	0.07	0.02
H_2O^-	0.91	0.81	0.29	0.75	1.02	0.98	0.92	1.13	0.90	0.88	0.85	0.80	0.77	1.08	0.79	1.16	1.08	0.86	0.73
LOI	9.33	11.93	14.85	11.05	6.47	7.18	13.30	8.30	22.51	11.27	16.13	24.71	22.10	15.43	32.63	14.42	23.09	11.10	48.71
Total	99.97	100.02	98.28	99.32	99.80	100.10	100.06	99.96	100.19	99.71	100.02	99.85	99.93	99.94	100.01	100.02	100.19	100.15	100.08
Mn	68.4	37.0	50.5	37.7	32.2	50.3	29.4	51.6	68.7	57.3	44.0	46.0	50.9	54.9	31.5	42.7	50.3	105.7	58.1
S	2508.1	5621.5	19625.8	11282.0	828.2	507.5	2378.3	821.6	3388.7	768.5	1715.0	3223.6	2767.0	2215.1	6271.4	2245.1	2731.1	1968.1	19335.4
Ba	222.8	212.2	196.9	340.8	324.6	308.2	560.1	396.4	315.6	385.9	339.8	328.2	312.6	399.2	287.6	369.5	358.3	572.9	163.7
Sc	15.6	14.7	13.6	12.8	15.5	11.8	9.7	14.2	10.4	13.0	11.0	10.1	10.5	13.0	7.8	11.0	10.1	15.8	9.4
Rb	112.9	104.0	81.2	156.0	188.6	149.1	150.0	191.5	131.3	174.5	146.2	138.3	130.6	160.8	95.8	145.3	141.4	179.7	65.2
Sr	88.0	118.6	97.7	253.2	218.0	126.4	116.8	297.1	118.6	139.2	186.4	108.4	138.1	129.0	205.7	199.5	109.4	244.5	68.8
Y	45.2	47.7	42.5	51.1	47.1	39.1	35.0	52.4	36.2	38.1	43.9	36.0	44.8	42.7	37.2	44.2	36.3	71.2	57.7
Zr	332.0	324.9	258.6	239.8	351.7	282.2	211.0	289.5	218.0	231.9	206.8	190.4	191.4	226.3	147.8	212.9	226.5	309.8	254.7
Nb	31.0	32.1	26.2	25.7	28.6	28.7	22.4	28.6	20.4	26.5	21.5	16.4	17.5	24.9	8.5	21.0	22.1	25.0	10.3
Mo	3.2	7.6	15.1	8.5	1.7	1.9	1.4	1.7	2.0	1.4	0.8	1.1	1.2	1.6	0.8	1.1	1.2	1.3	4.2
Co	7.2	5.9	13.7	14.4	4.5	1.9	2.4	2.9	9.1	2.0	2.1	3.2	<1.6	3.3	5.3	2.2	5.0	4.9	9.0
Cr	57.4	62.0	51.9	42.3	51.6	44.5	38.2	48.6	37.2	42.2	35.8	36.9	35.7	43.1	27.0	40.9	44.4	58.2	29.3
V	100.9	119.4	68.5	61.9	68.9	63.7	42.7	88.3	48.4	51.9	48.5	51.9	41.3	52.1	30.6	45.3	57.3	80.6	51.7
Zn	89.5	61.2	66.0	87.8	50.9	33.5	32.8	80.4	51.7	49.1	30.7	47.3	41.2	45.5	39.4	33.2	53.7	70.7	48.4
Cu	16.5	20.3	21.1	35.1	17.9	5.7	14.6	30.2	11.4	20.7	9.8	16.1	13.3	13.8	16.6	15.8	17.1	53.1	9.5
Ni	9.8	13.7	26.1	26.3	6.8	4.1	5.7	6.9	13.9	5.1	3.8	5.4	6.7	6.8	7.3	7.5	8.8	16.2	10.1
Ge	<0.9	<0.9	<0.9	<.0.91	<0.9	<0.9	<0.9	<0.9	<0.9	<0.8	<0.9	<0.8	<0.8	<0.8	<0.8	<0.7	<0.8	<0.9	2.2
W	5.2	8.8	8.8	6.6	7.4	4.4	7.8	6.3	3.6	5.2	5.8	6.3	6.2	9.7	1.2	8.0	7.3	10.2	5.4
U	21.9	45.7	21.9	6.1	4.3	5.2	3.7	8.5	4.4	4.4	5.7	3.5	7.0	4.1	3.3	4.7	4.6	6.9	3.9
Th	24.8	25.6	25.2	25.9	22.6	23.3	21.2	27.8	24.5	26.8	34.4	21.1	30.9	23.8	21.3	24.2	21.6	30.8	12.2
Pb	537.2	39.5	57.8	671.0	22.0	214.2	11.6	123.2	73.0	19.7	73.3	17.6	25.1	25.6	33.4	18.2	15.6	35.4	54.7
As	14.0	13.0	66.7	25.5	2.2	2.6	3.0	0.6	4.6	1.5	0.5	1.2	6.2	2.2	2.1	3.3	5.0	3.5	6.5
Se	2.2	5.6	6.6	1.7	<0.9	<0.9	<0.8	<0.9	1.2	<0.8	<0.8	<0.7	<0.8	<0.8	<0.7	<0.8	<0.8	<0.9	1.1
Bi	<3.2	<3.1	<3.6	<3.5	<3.1	3	<2.9	<3.1	<2.7	<3.	<2.8	<2.6	<2.6	<2.8	<2.4	<2.9	<2.6	<3.1	<2.5
Br	<1.1	<1.1	<1.3	<1.2	<1.1	<1.1	<1.0	<1.1	<1.0	<1.1	<1.0	<.9	<1.0	<.9	<.9	<1.0	<.9	<1.1	<1.1
La	31.8	47.1	42.9	49.3	63.9	43.9	35.9	62.3	43.8	43.7	48.3	41.5	53.9	49.1	52.3	47.0	42.2	71.2	36.8
Ce	69.9	106.0	88.4	103.1	136.7	87.7	70.3	132.9	85.6	91.9	97.1	86.5	115.4	103.6	106.2	95.1	89.2	144.9	69.0
Nd	31.8	45.6	40.5	53.0	53.1	33.8	32.6	63.3	38.0	42.2	43.8	39.2	54.3	47.8	51.0	45.0	37.9	68.6	33.0
D	0.23	0.04	0.00	-0.74	-0.89	-1.30	-2.10	-2.50	-3.15	-4.53	-4.92	-5.27	-5.73	-5.90	-6.38	-6.69	-7.53	-8.24	-8.74

136	2d	2e	3a	3b	4	5	6	7a	7b	8a	8b	8c	8d	8e	9a	9b	9c	10a	10b
SiO_2	52.19	32.42	48.77	55.18	61.08	60.59	48.68	61.57	59.40	57.50	60.72	57.74	61.91	59.11	57.74	55.51	59.54	60.88	62.08
TiO_2	0.59	0.35	0.49	0.69	0.79	0.73	0.54	0.82	0.80	0.79	0.86	0.80	0.76	0.73	0.58	0.63	0.69	0.82	0.83
Al_2O_3	15.92	9.11	13.44	17.91	19.68	17.37	13.95	20.31	20.19	20.78	21.37	21.40	18.43	18.67	15.78	16.08	17.81	20.44	23.14
FeO	0.61	1.53	0.57	0.89	1.09	0.73	1.55	0.58	0.60	0.76	0.94	0.68	0.42	0.57	0.41	0.34	0.62	1.04	1.15
MgO	0.28	0.54	0.27	0.32	0.35	0.30	0.19	0.28	0.26	0.29	0.32	0.28	0.24	0.28	0.22	0.18	0.22	0.35	0.34
CaO	0.12	0.79	0.10	0.14	0.15	0.13	0.10	0.13	0.13	0.14	0.15	0.13	0.11	0.12	0.16	0.10	0.12	0.19	0.16
Na_2O	0.09	0.06	0.09	0.10	0.11	0.11	0.08	0.11	0.10	0.09	0.11	0.09	0.10	0.10	0.08	0.08	0.09	0.10	0.11
K_2O	1.47	0.84	1.40	1.57	1.81	1.58	0.89	1.34	1.30	1.26	1.40	1.30	1.27	1.30	0.99	0.87	1.06	1.23	1.32
P_2O_5	0.03	0.02	0.03	0.03	0.05	0.04	0.03	0.04	0.04	0.05	0.04	0.04	0.03	0.04	0.04	0.03	0.05	0.06	0.04
H_2O^-	0.78	0.66	0.78	1.14	1.11	1.02	0.82	0.88	0.86	0.87	0.74	0.45	0.38	0.16	0.82	0.88	0.77	0.78	1.02
LOI	27.98	53.73	34.02	22.03	13.95	17.14	33.25	14.08	16.38	17.15	13.41	17.73	16.10	19.03	22.98	25.19	19.18	14.14	9.89
Total	100.06	100.06	99.94	100.01	100.16	99.76	100.07	100.14	100.04	99.70	100.07	100.63	99.74	100.11	99.79	99.87	100.15	100.03	100.07
Mn	33.1	87.9	31.0	52.4	55.0	54.7	23.8	30.6	33.0	81.7	113.3	43.2	24.2	30.4	26.6	21.6	26.7	73.8	72.6
S	4094.5	13415.2	6253.4	4792.5	2951.6	2701.0	9109.9	1459.3	1549.5	1523.9	1021.4	1380.9	1588.0	2376.7	2620.5	2244.0	3500.0	1855.8	671.1
Ba	240.4	169.3	226.2	259.7	290.9	358.6	184.5	619.9	259.9	307.4	523.3	244.5	250.7	269.4	192.4	182.4	225.9	275.0	360.5
Sc	9.1	7.6	8.6	12.5	14.6	10.9	7.8	13.7	12.2	17.0	16.9	14.6	8.0	8.7	7.7	6.5	10.2	15.4	16.4
Rb	104.7	59.7	97.3	117.0	135.2	121.7	82.3	111.5	108.6	105.9	115.6	108.9	99.0	112.2	74.1	72.6	87.7	107.6	111.3
Sr	83.6	81.7	96.5	97.9	129.4	137.4	79.5	106.3	81.8	104.7	93.4	74.8	68.4	130.5	119.0	65.7	111.7	153.2	78.4
Y	31.4	23.8	31.7	41.3	49.2	38.8	29.4	43.9	44.7	58.4	53.7	56.5	36.7	34.2	30.2	26.3	39.6	52.3	47.7
Zr	178.3	135.7	175.5	227.2	265.7	231.3	177.8	262.0	236.9	268.5	293.5	261.5	213.3	218.2	174.0	183.9	264.6	353.1	327.0
Nb	16.5	10.4	13.1	21.7	28.6	23.1	14.2	29.4	28.3	30.1	33.2	29.3	21.2	24.5	15.6	17.2	21.1	31.4	33.0
Mo	0.9	1.2	0.7	0.7	1.5	1.4	1.3	1.1	1.3	1.1	2.1	1.7	1.1	1.2	0.7	0.7	1.8	3.0	1.3
Co	3.0	7.2	5.2	4.7	2.3	2.7	3.0	2.4	2.9	3.7	3.7	3.4	2.5	2.1	1.7	3.5	7.0	3.3	7.5
Cr	35.5	26.1	35.5	45.7	56.2	44.4	30.9	53.2	51.2	56.3	63.9	61.2	33.4	40.8	28.5	26.9	38.5	56.9	58.7
V	43.3	43.9	53.1	63.3	71.5	49.6	36.6	70.9	65.5	83.9	90.3	81.8	35.1	46.6	34.0	29.2	57.0	87.6	81.6
Zn	27.8	38.9	26.4	35.8	43.6	31.4	20.9	43.1	34.7	56.1	51.2	47.2	21.5	27.6	28.8	14.9	41.1	54.5	58.2
Cu	11.5	10.7	16.4	17.3	26.1	18.7	8.9	19.5	18.8	26.7	26.4	17.9	13.3	14.5	22.0	10.6	26.7	26.1	27.8
Ni	5.0	7.5	5.2	8.0	10.4	6.1	6.2	6.3	6.9	9.8	13.9	11.9	4.2	3.7	.1	6.6	10.7	11.7	26.2
Ge	<.7	<.6	<.7	<.8	<0.9	<0.8	<0.7	<0.8	<0.8	<0.8	<0.8	<0.8	<0.8	<0.8	<0.8	<0.7	<1.2	<0.8	<0.4
W	3.2	2.4	4.4	6.1	13.9	7.9	3.4	6.2	6.7	10.2	12.6	9.7	4.6	6.3	4.1	3.9	6.5	6.4	11.2
U	4.3	2.8	4.5	6.0	5.9	5.5	4.8	6.4	5.8	8.1	6.2	7.2	4.3	4.4	4.6	4.0	7.0	8.5	6.9
Th	25.2	12.1	19.4	23.0	29.6	26.4	20.5	27.6	24.9	29.5	29.8	28.5	19.9	28.1	20.6	19.8	26.4	30.2	37.4
Pb	39.1	20.5	70.7	49.4	35.4	28.1	90.9	72.1	26.5	49.3	48.6	44.2	34.9	40.0	43.1	111.2	47.1	102.2	42.9
As	1.6	3.8	0.8	1.2	1.9	0.4	6.9	1.4	5.3	2.9	2.7	1.9	1.0	1.5	1.1	1.4	2.5	3.4	4.3
Se	<0.7	<0.6	<0.6	<0.7	<0.7	<0.7	<0.7	<0.7	<0.7	<0.7	<0.7	1.2	<0.7	<0.7	<0.7	<0.7	1.7	2.0	0.8
Bi	<2.5	<2.2	<2.4	<2.6	<2.8	<2.7	<3	<2.8	<2.7	<2.7	<2.7	<2.8	<2.7	<2.7	<2.5	<2.5	<2.5	<2.8	<2.9
Br	<.9	<.8	<.8	<.9	<1.0	<1.0	<.9	<1.0	<1.0	<1.0	<1.0	<1.0	<.9	<.9	<.9	<.9	<.9	<1.0	<1.0
La	42.9	27.1	38.9	47.0	58.1	48.4	43.3	51.3	44.7	69.6	54.4	61.0	35.7	52.6	43.3	29.7	49.7	63.7	45.3
Ce	92.7	54.0	83.2	99.8	126.6	103.5	85.6	105.2	95.4	146.5	118.6	122.1	72.9	113.3	93.3	62.2	107.6	129.5	86.4
Nd	41.5	25.2	36.3	45.6	57.8	47.8	35.4	46.8	40.4	65.3	53.8	55.0	29.7	49.3	40.3	25.9	48.2	62.6	41.9
D	-9.60	-9.94	-10.52	-11.14	-12.46	-14.06	-16.16	-17.83	-19.05	-19.69	-20.69	-21.34	-22.00	-22.89	-23.48	-24.04	-24.93	-25.21	-25.37

136	10c	10d	11a	11b	12a	12b	12c	12d	12e	13a	14a	14b	14c	14d	14e	15aa	15ab	15ac	15ad
SiO_2	59.37	61.88	56.68	58.05	50.54	58.76	49.90	46.55	50.52	54.58	50.72	32.44	31.89	27.48	33.21	52.58	46.99	55.83	47.14
TiO_2	0.80	0.85	0.74	0.65	0.67	0.79	0.65	0.63	0.68	0.74	0.73	0.41	0.40	0.33	0.46	0.74	0.57	0.76	0.62
Al_2O_3	19.70	21.38	20.37	15.64	16.65	20.51	19.41	15.28	19.07	19.42	18.21	10.93	10.95	8.17	12.19	19.31	17.71	19.14	16.85
FeO	0.72	0.64	0.46	0.44	1.06	0.31	0.79	0.42	0.36	0.33	0.41	0.53	0.45	0.94	1.76	0.42	0.79	0.64	0.68
MgO	0.29	0.28	0.23	0.18	0.17	0.19	0.18	0.16	0.16	0.19	0.20	0.23	0.15	0.12	0.13	0.19	0.18	0.24	0.18
CaO	0.13	0.13	0.11	0.11	0.13	0.11	0.11	0.11	0.09	0.10	0.11	0.49	0.17	0.12	0.08	0.09	0.11	0.10	0.11
Na_2O	0.09	0.09	0.07	0.08	0.09	0.09	0.07	0.08	0.08	0.10	0.11	0.07	0.07	0.06	0.07	0.11	0.10	0.12	0.08
K_2O	1.28	1.17	0.92	0.81	0.72	0.84	0.68	0.66	0.67	0.81	0.81	0.53	0.45	0.36	0.45	0.80	0.70	0.99	0.67
P_2O_5	0.04	0.05	0.04	0.03	0.04	0.04	0.04	0.04	0.04	0.05	0.05	0.04	0.04	0.02	0.04	0.07	0.05	0.09	0.06
H_2O^-	1.00	0.75	0.73	0.73	0.73	0.69	0.65	1.04	0.86	0.61	1.10	0.92	0.12	0.08	0.88	0.86	0.92	0.89	0.83
LOI	16.78	12.99	20.02	23.33	29.18	17.81	27.67	35.15	27.22	23.15	26.95	53.29	54.42	62.43	50.66	24.80	32.39	21.21	32.82
Total	100.20	100.21	100.37	100.05	99.98	100.14	100.14	100.10	99.75	100.07	99.38	99.86	99.10	100.01	99.93	99.95	100.52	100.00	99.98
Mn	48.3	57.0	46.2	24.5	23.7	18.4	18.9	34.3	27.8	17.2	21.2	51.7	32.6	33.4	209.1	27.9	84.6	39.7	55.3
S	1129.3	694.2	1499.1	2211.2	5383.4	1107.6	3411.6	2620.0	2122.2	1691.2	2273.2	6114.1	5449.7	8249.4	6131.8	1897.1	2955.6	1913.7	3487.8
Ba	286.4	357.9	200.8	260.4	193.8	228.2	204.7	185.6	208.8	285.9	300.0	216.4	207.8	118.2	215.0	424.7	330.5	526.1	352.2
Sc	16.6	14.4	12.1	10.1	11.5	13.9	8.3	8.3	7.5	9.7	9.6	10.9	8.6	6.4	7.2	10.1	8.4	10.0	10.4
Rb	113.0	96.1	78.3	71.7	66.9	76.8	68.0	63.8	60.1	75.2	80.1	50.6	44.6	37.1	46.7	76.1	64.6	85.0	62.8
Sr	54.4	96.8	98.9	73.1	84.5	95.9	107.7	100.1	97.4	132.3	130.5	110.6	100.0	65.9	98.2	150.1	121.8	173.4	135.7
Y	66.8	49.0	45.5	43.9	46.7	51.0	35.6	35.0	33.8	38.2	34.9	35.1	27.7	24.5	26.9	36.5	35.3	37.8	39.5
Zr	304.9	278.5	246.7	196.7	267.6	283.5	193.4	180.3	204.5	223.1	224.3	158.7	141.9	118.3	147.6	209.8	173.3	196.3	192.5
Nb	32.2	30.1	27.2	19.0	22.4	31.5	20.1	15.2	17.4	23.5	23.2	9.7	9.0	7.0	8.5	23.3	15.9	22.9	16.9
Mo	1.8	0.9	0.7	1.1	1.5	0.9	0.7	0.9	1.0	< 0.5	0.6	1.1	0.8	1.0	1.0	1.2	0.9	1.1	0.8
Co	< 1.6	2.3	1.9	3.2	5.9	1.6	2.8	4.1	1.7	2.2	2.2	5.6	5.5	10.5	5.7	2.7	3.9	3.9	4.7
Cr	55.2	50.5	46.8	34.6	48.2	50.4	33.6	32.6	30.4	38.9	45.6	29.7	29.2	22.8	28.6	38.4	31.9	38.5	35.3
V	74.5	67.4	67.4	35.9	64.9	70.4	38.7	39.4	32.6	46.8	54.1	42.0	39.1	28.8	40.8	44.8	37.1	39.5	45.2
Zn	52.4	40.3	42.9	31.8	24.0	19.3	23.1	28.5	13.9	15.3	18.1	25.2	15.1	19.7	16.6	13.8	24.9	21.3	33.1
Cu	16.9	23.9	18.3	13.8	17.3	17.0	10.3	14.5	10.1	16.8	15.7	10.9	11.2	5.5	15.8	17.4	11.3	18.3	16.2
Ni	8.2	6.5	6.5	10.1	8.9	5.1	5.0	7.8	3.8	4.3	6.5	7.8	6.9	10.8	6.8	7.0	7.1	10.5	10.8
Ge	< 0.8	< 0.8	< 0.8	< 0.7	< 0.7	< 0.8	< 0.7	< 0.7	< 0.7	< 0.7	< 0.7	< 0.7	< 0.7	< 0.7	< 0.6	< 0.6	< 0.6	< 0.6	< 0.7
W	10.3	7.3	5.9	6.9	8.4	4.6	4.0	6.9	3.4	4.5	6.6	5.4	3.9	3.5	5.5	6.7	5.5	7.5	4.2
U	8.8	6.4	7.1	4.2	6.1	6.6	5.9	4.4	4.6	5.7	6.5	2.9	2.3	1.9	3.7	5.0	4.0	5.2	4.3
Th	34.8	28.6	28.9	19.1	29.3	33.8	25.1	19.1	36.1	25.0	23.9	12.9	12.2	13.7	14.2	20.4	22.0	26.1	20.8
Pb	46.9	104.8	67.0	24.0	40.3	53.3	45.8	21.2	20.7	57.5	30.7	14.9	12.0	17.4	13.9	26.3	19.0	27.1	75.5
As	1.4	2.2	2.4	3.4	5.4	2.3	7.2	3.5	1.4	1.3	2.7	3.3	2.3	5.3	1.9	4.0	4.7	11.5	10.3
Se	< 0.7	< 0.7	< 0.7	0.7	0.8	0.8	2.0	< 0.6	< 0.6	< 0.7	< 0.6	< 0.6	< 0.6	< 0.6	< 0.6	< 0.7	< 0.6	0.9	0.7
Bi	1.4	1.4	1.3	1.3	1.2	1.3	1.2	1.1	1.2	2.9	1.2	1.0	1.0	0.9	1.1	1.2	1.2	1.3	2.9
Br	< 1.0	< 1.0	< .9	< .9	< .9	< .9	< .9	< .8	< .9	< .9	< .9	< .7	< .7	< .7	< .8	< .9	< .9	< .9	< .8
La	63.8	52.0	54.7	47.5	52.9	57.5	50.9	46.7	44.4	50.0	48.4	40.6	41.6	34.3	39.7	47.5	43.5	48.3	43.5
Ce	126.0	111.4	117.3	94.9	112.0	116.8	107.1	99.1	97.3	104.5	102.5	85.8	84.7	69.3	82.1	100.5	88.4	100.9	95.4
Nd	59.4	50.4	49.7	40.5	53.9	51.2	42.5	42.7	45.1	44.8	41.6	40.0	35.5	31.1	32.5	42.0	40.3	48.0	43.2
D	-26.51	-27.08	-27.63	-28.22	-29.53	-29.77	-30.95	-31.14	-31.49	-31.68	-32.99	-33.42	-33.77	-34.17	-35.04	-35.5	-36.19	-36.86	-37.36

136	15ba	15bb	15bc	15bd	16a	16b	17a	17b	17c	17d	18	19a	19b	19c	19d	19e	20a	20b	21a
SiO_2	53.14	46.77	55.61	54.64	59.20	56.59	56.64	53.00	48.36	48.40	55.64	50.07	52.15	39.38	50.59	51.97	45.08	32.14	53.59
TiO_2	0.74	0.61	0.80	0.76	0.92	0.83	0.84	0.76	0.70	0.61	0.87	0.79	0.86	0.61	0.83	0.95	0.80	0.54	1.02
Al_2O_3	18.45	17.55	21.89	21.24	23.56	20.46	21.36	19.99	18.78	18.57	21.71	21.04	20.58	16.18	22.24	23.28	20.47	13.50	23.95
FeO	0.45	0.86	0.53	0.47	0.47	0.41	0.39	0.42	0.36	0.53	0.54	2.95	0.34	0.66	0.64	0.91	0.48	0.57	0.45
MgO	0.20	0.19	0.22	0.19	0.20	0.18	0.17	0.18	0.17	0.14	0.18	0.23	0.17	0.14	0.14	0.19	0.16	0.10	0.30
CaO	0.13	0.10	0.13	0.10	0.11	0.10	0.09	0.09	0.11	0.08	0.10	0.12	0.12	0.08	0.09	0.10	0.11	0.07	0.53
Na_2O	0.09	0.07	0.09	0.09	0.08	0.07	0.07	0.08	0.07	0.06	0.09	0.10	0.08	0.06	0.09	0.10	0.08	0.05	0.11
K_2O	0.67	0.64	0.77	0.76	0.76	0.66	0.72	0.76	0.61	0.53	0.72	0.71	0.62	0.57	0.56	0.75	0.62	0.39	0.52
P_2O_5	0.05	0.06	0.07	0.07	0.06	0.06	0.07	0.07	0.06	0.05	0.07	0.07	0.06	0.05	0.06	0.07	0.07	0.05	0.06
H_2O^-	0.74	0.68	0.65	0.60	0.63	0.60	0.93	1.03	1.07	0.88	0.83	0.84	0.93	0.96	0.56	0.67	0.77	0.87	0.74
LOI	25.24	32.53	19.26	21.10	14.06	20.34	18.67	23.46	29.61	29.90	18.49	23.01	24.01	41.14	24.21	20.98	31.14	51.56	18.58
Total	99.91	100.05	100.00	100.01	100.04	100.31	99.96	99.82	99.91	99.75	99.23	99.94	99.91	99.83	100.01	99.98	99.77	99.84	99.83
Mn	37.9	106.9	42.2	31.3	17.3	30.9	15.5	19.6	22.6	16.0	21.2	237.9	22.3	31.1	23.1	47.8	20.2	24.8	53.6
S	2140.7	2900.8	1443.7	1838.6	1069.1	1585.7	2049.6	2917.5	3775.2	4108.9	2564.2	3454.6	2534.7	9636.9	5433.5	3152.2	4911.5	8721.7	1888.3
Ba	310.6	320.5	371.2	359.9	330.1	340.7	389.8	404.7	323.3	256.2	367.6	320.4	291.3	242.0	288.9	387.1	345.5	208.7	364.6
Sc	14.2	11.9	12.5	12.9	14.1	9.5	10.4	10.4	11.9	10.4	11.8	11.0	14.8	12.6	12.0	13.8	15.3	11.3	13.5
Rb	70.7	62.9	77.2	70.3	79.3	72.1	68.7	77.9	67.7	53.4	79.1	71.9	62.5	65.9	58.5	84.1	67.5	51.6	56.7
Sr	111.0	121.6	120.9	123.1	91.4	113.6	116.2	138.0	117.8	91.9	122.2	142.3	114.3	84.5	98.3	132.1	130.2	109.0	103.9
Y	49.8	43.1	46.5	51.2	46.6	35.9	41.2	37.0	38.3	36.9	37.9	44.3	44.8	47.1	39.2	44.1	44.4	45.7	42.3
Zr	249.6	200.6	255.5	228.5	300.4	227.3	214.1	195.4	199.0	175.8	239.0	211.0	244.5	177.4	220.5	253.4	261.2	181.3	293.0
Nb	27.5	19.3	31.5	24.1	34.1	26.9	27.3	20.9	19.1	14.7	27.8	25.6	30.8	16.3	27.9	33.3	29.5	14.1	35.7
Mo	1.0	0.8	1.0	0.6	1.2	0.7	1.2	1.0	1.1	1.2	1.2	1.2	1.6	1.5	1.1	0.9	1.6	2.0	1.4
Co	3.7	3.9	2.3	2.5	2.6	2.6	3.2	6.2	5.2	2.6	2.4	4.6	3.1	5.9	3.2	3.2	3.8	6.6	3.7
Cr	45.7	33.9	46.8	36.4	53.4	40.8	33.7	33.4	36.4	26.2	41.4	35.7	55.9	36.1	35.0	48.6	54.2	34.1	55.6
V	74.3	52.8	66.0	45.6	80.8	46.5	38.9	39.2	49.4	33.3	52.8	46.4	71.8	50.5	42.8	60.2	77.7	42.6	80.0
Zn	24.1	31.0	20.0	19.2	16.1	18.3	27.2	18.1	33.4	10.5	15.8	54.0	20.8	18.0	23.3	23.7	19.0	35.7	11.1
Cu	17.5	13.4	20.3	18.5	18.4	20.7	24.4	20.0	20.9	13.8	24.6	27.1	27.6	17.2	19.0	26.6	25.7	13.0	28.1
Ni	8.0	10.4	5.9	8.6	6.0	10.1	8.3	11.7	11.3	7.0	9.5	12.2	10.1	9.0	8.3	12.1	12.7	11.2	11.9
Ge	< 0.7	< 0.7	< 0.8	< 0.8	< 0.8	< 0.8	< 0.8	< 0.8	< 0.7	< 0.7	< 0.8	< 0.9 <	< 0.7	< 0.6	< 0.8	< 0.8	< 0.7	< 0.6	< .8
W	6.0	5.7	7.0	6.4	5.8	5.6	8.0	5.6	5.3	3.9	6.9	7.3	6.2	5.9	7.2	6.0	6.0	5.7	6.9
U	6.0	5.1	7.7	6.8	7.4	7.2	5.9	6.1	5.8	5.9	6.7	7.4	7.5	5.1	7.6	7.8	7.8	5.5	8.7
Th	23.3	18.7	35.8	28.8	34.4	26.6	30.0	22.1	23.3	18.7	33.3	28.1	28.2	20.1	30.6	28.6	30.4	24.7	35.4
Pb	71.3	63.3	58.3	51.6	49.7	40.0	27.8	68.7	36.4	43.5	36.0	34.2	39.1	41.7	33.0	49.6	37.0	32.8	48.3
As	6.0	11.0	4.9	9.7	2.8	7.1	8.0	15.2	9.6	7.0	4.7	13.1	5.9	6.8	5.7	11.5	11.4	5.7	8.5
Se	< 0.7	< 0.6	< 0.7	1.1	< 0.7	< 0.7	< 0.7	0.8	< 0.6	< 0.6	< 0.7	1.6	0.7	0.7	1.4	1.3	2.3	1.1	1.4
Bi	< 2.5	< 2.4	< 2.6	< 2.5	< 2.7	< 2.6	3	< 2.5	3	< 2.4	< 2.6	< 2.8	3	< 2.2	3	3	3	< 2.0	3
Br	< .9	< .9	< .9	< .9	< 1.0	< .9	< .9	< .9	< .9	< .9	< .9	< 1.0	< .9	< .8	< .9	< .9	< .9	< .7	< .9
La	48.4	49.3	55.8	51.5	54.7	44.6	43.8	46.8	46.4	44.6	45.1	58.3	56.2	55.8	46.2	51.8	56.7	49.1	42.0
Ce	100.8	104.8	114.5	105.5	121.8	91.5	97.0	96.8	97.4	93.9	92.6	116.7	120.6	111.7	98.5	108.5	118.5	100.7	88.6
Nd	46.4	43.0	47.1	50.9	54.2	38.7	45.7	39.9	45.0	41.4	44.0	54.6	52.9	48.1	42.1	49.4	50.3	49.5	39.3
D	-38.17	-38.6	-39.02	-39.5	-40.09	-41.09	-41.72	-42.34	-43.54	-44.66	-44.88	-45.87	-46.2	-46.87	-47.17	-47.68	-47.99	-48.46	-49.43

136	21b	21c	21d	22aa	22ab	22ac	22ad	22ae	22ba	22bb	22bc	22bd	22be	22ca	22cb	22cc	22da	22db	22dc
SiO_2	48.59	39.62	48.01	46.66	47.23	46.99	46.97	29.63	42.62	44.64	38.45	46.11	41.25	46.78	44.61	39.21	43.37	38.08	40.71
TiO_2	0.88	0.67	0.98	0.85	0.87	0.90	0.82	0.54	0.78	0.77	0.71	0.79	0.75	0.96	0.87	0.81	0.89	0.79	0.72
Al_2O_3	21.43	18.03	22.42	22.99	22.54	23.11	21.74	13.93	19.31	18.50	18.59	20.43	19.13	23.27	19.51	18.70	21.04	18.43	19.43
FeO	0.30	0.35	0.46	1.59	1.49	0.42	0.56	0.60	1.03	0.28	0.30	0.29	1.40	1.70	0.87	0.48	0.44	2.29	1.70
MgO	0.16	0.12	0.21	0.20	0.20	0.26	0.30	0.13	0.29	0.17	0.17	0.18	0.20	0.32	0.23	0.17	0.20	0.30	0.28
CaO	0.10	0.10	0.22	0.13	0.13	0.32	0.46	0.28	0.36	0.13	0.15	0.17	0.32	0.43	0.25	0.20	0.20	0.67	0.26
Na_2O	0.08	0.06	0.08	0.09	0.09	0.08	0.08	0.07	0.08	0.08	0.08	0.08	0.08	0.09	0.09	0.08	0.08	0.07	0.07
K_2O	0.59	0.40	0.60	0.60	0.62	0.59	0.56	0.44	0.66	0.57	0.54	0.59	0.45	0.65	0.53	0.49	0.61	0.40	0.60
P_2O_5	0.06	0.05	0.07	0.08	0.09	0.11	0.07	0.07	0.11	0.13	0.12	0.20	0.29	0.31	0.19	0.20	0.21	0.14	0.14
H_2O^-	0.85	0.72	0.69	0.67	0.56	0.54	0.48	0.38	0.44	0.59	0.54	0.52	0.55	0.96	0.92	0.82	0.77	0.67	0.88
LOI	26.79	39.75	25.63	26.09	26.01	26.46	27.75	53.85	34.15	33.90	40.10	30.44	35.39	24.26	31.73	38.74	32.22	38.35	35.19
Total	99.83	99.87	99.36	99.96	99.83	99.76	99.79	99.91	99.82	99.76	99.75	99.79	99.82	99.75	99.81	99.91	100.02	100.21	99.99
Mn	15.6	15.4	36.5	110.1	94.5	39.2	42.4	29.6	53.1	18.4	17.1	18.6	116.1	151.4	71.3	42.7	33.0	265.1	160.2
S	2956.6	5957.8	3363.8	3672.5	4365.7	3056.3	3680.0	12498.5	6863.7	4280.6	4100.3	2369.5	2996.8	1532.7	2285.8	3201.0	2175.8	2429.5	2730.9
Ba	285.8	202.1	343.3	375.8	401.1	438.7	304.5	302.4	471.3	544.8	520.3	809.1	897.0	1044	683.5	739.4	797.2	537.6	556.8
Sc	19.2	11.2	12.9	13.9	12.9	18.5	19.5	10.1	19.5	14.6	13.7	16.5	11.6	16.5	16.7	12.5	16.3	11.8	11.1
Rb	61.5	40.1	60.0	64.8	67.2	61.7	59.4	48.3	64.6	59.2	51.1	65.8	44.3	66.4	50.9	53.1	60.4	39.4	62.8
Sr	101.9	83.1	141.1	151.9	167.6	190.6	113.4	124.9	171.0	223.0	196.8	344.5	446.6	506.9	304.9	355.9	314.2	209.5	236.6
Y	54.2	39.5	43.6	39.6	47.1	53.9	54.2	33.3	43.6	46.4	38.2	36.5	37.4	42.9	44.0	39.4	43.4	29.2	24.4
Zr	283.8	217.6	263.9	232.6	205.9	289.0	271.5	178.2	224.1	253.5	223.9	258.2	205.4	279.7	263.4	203.0	277.4	186.6	178.2
Nb	30.6	17.8	30.4	26.0	22.5	29.3	25.2	13.8	23.9	25.7	21.3	26.7	21.9	31.0	26.1	21.2	29.4	21.8	19.4
Mo	1.6	1.4	1.3	1.7	2.2	1.9	1.6	2.6	1.5	1.5	1.1	1.1	1.3	1.1	1.1	1.4	0.9	1.2	1.4
Co	2.8	4.3	4.6	4.4	10.2	3.9	4.6	15.3	4.1	5.1	4.2	2.0	2.9	2.6	3.3	4.3	2.7	3.2	2.4
Cr	69.5	36.4	48.4	50.4	35.1	53.7	53.3	34.8	49.0	51.5	52.1	54.0	41.8	64.0	63.4	49.8	60.7	46.7	37.3
V	102.7	44.5	75.1	73.6	44.8	95.2	65.4	50.8	75.7	79.5	76.1	69.8	50.4	82.9	72.5	55.4	83.8	60.5	47.1
Zn	15.8	24.0	15.9	35.2	53.7	24.6	22.5	31.8	26.9	15.5	15.2	9.7	14.6	24.0	17.9	23.9	16.1	24.9	16.0
Cu	28.3	17.2	33.4	29.5	24.3	31.5	25.5	18.6	19.2	23.2	14.8	16.7	18.3	26.1	15.0	18.7	22.5	20.8	17.5
Ni	11.6	9.8	11.4	11.8	21.4	16.0	16.7	17.8	16.4	15.0	10.6	7.9	9.5	11.9	12.4	12.5	8.3	10.3	6.2
Ge	< 0.7	0.7	< 0.7	< 0.8	< 0.8	< 0.7	< 0.7	< 0.6	< 0.7	< 0.7	< 0.6	< 0.7	< 0.7	< 0.7	< 0.7	0.8	< 0.7	< 0.8	< 0.7
W	9.2	6.0	6.7	6.3	8.4	8.4	7.2	3.9	6.4	6.6	6.5	4.5	6.6	6.6	6.2	5.1	7.4	4.5	5.0
U	8.3	6.7	7.8	7.6	6.7	7.7	7.5	4.6	7.0	7.1	6.0	6.9	5.7	7.0	6.6	6.0	6.8	5.2	4.6
Th	30.7	27.4	34.7	30.2	25.5	31.6	29.8	16.6	24.4	30.4	25.8	36.6	28.8	33.7	29.4	23.0	30.6	23.5	23.7
Pb	43.7	27.7	29.6	47.0	47.5	34.8	32.1	45.3	23.5	30.4	29.0	42.9	26.3	37.6	22.8	27.9	34.1	87.2	15.8
As	6.7	4.9	8.5	9.9	22.1	14.1	10.5	14.4	16.3	13.7	4.9	3.8	3.1	3.9	2.4	2.7	0.8	2.7	1.9
Se	1.6	1.0	2.0	2.6	12.5	2.2	2.6	1.7	1.3	1.6	1.0	< 0.7	1.1	1.2	0.3	1.0	< 0.7	0.8	< 0.7
Bi	4.3	< 2.2	< 2.7	< 2.6	< 2.6	< 2.5	< 2.5	< 2.0	< 2.4	< 2.3	< 2.2	< 2.4	< 2.4	3	2.4	3	< 2.4	3	< 2.4
Br	< .9	< .8	< .9	< .9	< .9	< .9	< .9	< .7	< .9	< .8	< .8	< .9	< .9	< 1.0	< .9	< .9	< .8	< .9	< .9
La	69.1	45.5	58.6	52.8	49.8	60.5	58.5	32.6	50.8	53.2	41.4	50.1	43.2	54.4	39.2	44.1	51.5	38.5	41.5
Ce	142.4	92.6	123.5	108.7	103.7	131.3	115.5	67.0	106.6	112.2	90.7	110.5	93.8	114.4	90.5	93.5	99.5	74.5	80.7
Nd	63.8	43.9	56.9	49.6	48.8	62.2	55.0	32.0	48.8	53.5	40.8	44.7	43.2	50.4	37.1	44.4	38.7	30.9	29.8
D	-49.73	-50.15	-51.24	-52.15	-52.53	-52.8	-53.52	-54.39	-55.09	-55.39	-56.38	-57	-57.53	-59.05	-59.77	-60.21	-60.64	-61.59	-62.49

136	22dd	22de	22ea	22eb	22ec	22ed	22ee	22fsa	22fsb	22fsc	23asa	23asb	23asc	23asd	23ase	23bsa	0a	0b	0c
SiO_2	39.53	43.89	41.46	32.80	37.11	30.40	36.28	32.15	27.52	29.75	36.55	44.95	52.30	42.91	49.09	54.77	62.83	53.99	25.38
TiO_2	0.79	0.94	0.85	0.72	0.87	0.75	1.13	0.99	0.91	0.98	1.26	1.60	1.47	1.23	1.54	0.95	0.76	0.57	0.23
Al_2O_3	19.15	18.72	20.69	17.19	19.82	18.02	20.56	19.49	18.32	21.45	20.46	25.40	24.12	20.15	24.87	23.26	17.07	15.36	4.92
FeO	0.76	2.26	0.64	1.84	0.59	2.85	3.40	0.97	1.58	1.07	0.29	0.54	0.54	0.46	0.39	0.58	1.96	3.55	11.18
MgO	0.32	0.50	0.31	0.54	0.26	0.52	0.66	0.29	0.39	0.26	0.15	0.22	0.29	0.22	0.21	0.13	0.35	0.28	0.65
CaO	0.55	1.29	0.57	1.14	0.37	1.12	3.02	0.75	0.97	0.48	0.07	0.43	0.11	0.08	0.10	0.09	0.11	0.11	1.54
Na_2O	0.07	0.10	0.09	0.08	0.08	0.09	0.12	0.11	0.09	0.08	0.04	0.05	0.07	0.05	0.05	0.03	0.05	0.04	0.03
K_2O	0.42	0.43	0.54	0.38	0.43	0.35	0.38	0.44	0.36	0.33	0.39	0.47	0.89	0.63	0.54	0.42	1.06	0.83	0.39
P_2O_5	0.18	0.14	0.23	0.37	0.23	0.26	0.75	0.45	0.33	0.24	0.04	0.04	0.04	0.04	0.04	0.07	0.04	0.04	0.03
H_2O^-	0.88	0.89	1.00	1.16	1.18	1.33	0.98	1.47	1.40	1.37	1.35	1.10	1.07	1.10	1.03	0.45	1.06	0.86	0.89
LOI	37.39	30.96	33.70	43.91	39.05	44.43	32.75	42.83	48.24	44.04	39.46	25.17	19.14	33.08	22.06	19.07	12.64	22.91	51.84
Total	100.05	100.15	100.09	100.16	99.99	100.13	100.08	99.94	100.12	100.04	100.04	99.98	100.01	99.95	99.92	99.83	97.93	98.55	96.09
Mn	66.4	286.9	47.5	177.0	44.2	247.7	437.6	86.2	157.3	94.9	16.9	40.9	28.3	26.4	19.7	36.2	32.5	48.1	77.4
S	3071.0	2037.3	2495.4	3369.3	2402.7	4011.4	3456.2	2293.3	2584.6	2448.5	2796.6	1355.2	797.2	1920.4	1028.8	704.7	10040.0	15966.0	53681.0
Ba	652.9	433.0	908.2	1178	169.0	155.3	246.0	201.1	160.5	181.3	848.0	11078	496.6	1160	1147	884.0	236.7	216.4	253.3
Sc	12.6	14.6	15.1	14.5	34.9	16.0	22.3	31.1	21.5	13.8	18.1	17.8	16.0	18.4	19.6	22.7	14.6	11.3	6.0
Rb	34.7	35.0	50.2	34.9	31.8	38.6	96.1	52.9	35.1	25.6	36.7	32.3	26.8	39.4	36.9	33.0	98.9	74.3	29.8
Sr	254.5	168.9	369.7	497.3	37.8	41.7	47.6	33.3	28.2	44.7	307.7	394.9	247.3	458.8	430.3	360.9	116.0	97.0	95.1
Y	34.3	36.5	35.3	48.7	70.4	47.7	68.0	74.6	55.4	31.2	40.5	29.9	41.2	47.8	51.8	53.6	53.5	56.3	52.7
Zr	224.4	241.2	242.3	264.4	424.8	475.4	488.1	354.0	360.2	385.8	309.0	253.5	256.2	321.7	332.0	420.0	297.2	233.0	266.9
Nb	25.6	27.9	26.0	24.6	42.6	50.8	56.8	38.5	39.9	22.5	27.9	26.2	28.4	32.3	33.9	41.3	32.1	19.4	9.4
Mo	1.1	1.1	1.0	1.0	3.7	4.1	6.9	4.0	3.5	1.0	0.6	1.1	1.3	1.2	1.6	1.0	7.6	3.4	5.9
Co	4.4	3.9	3.9	3.1	2.9	4.2	4.8	2.7	4.7	3.9	4.5	5.6	4.0	2.4	6.2	15.2	22.9	8.4	48.2
Cr	49.6	54.1	52.4	52.4	74.5	58.1	53.5	72.6	64.1	71.6	176.1	114.6	84.9	134.2	109.3	108.9	59.9	46.5	27.2
V	63.3	61.3	76.3	70.9	100.1	80.0	64.7	84.0	87.2	96.1	141.4	91.3	90.0	160.7	97.4	57.4	99.0	69.4	63.7
Zn	16.9	19.4	15.5	21.0	11.8	23.3	16.5	9.9	12.8	24.6	13.6	18.7	12.0	13.3	15.6	16.2	80.5	80.6	46.5
Cu	14.9	17.8	23.3	16.8	25.3	41.5	31.2	17.9	25.4	18.1	20.2	16.9	27.1	25.2	21.5	30.3	19.5	17.2	9.3
Ni	12.7	16.1	12.5	10.9	19.6	38.7	20.6	19.3	27.1	27.7	13.0	18.5	21.9	19.2	19.1	3.3	30.0	8.7	71.2
Ge	< 0.7	< 0.8	< 0.7	< 0.7	2	1	2	1	2	2	0.8	< 0.6	< 0.7	0.9	0.8	0.8	< 0.9	< 0.9	26
W	6.2	7.0	5.9	6.4	9.5	12.7	15.8	8.0	10.8	3.9	5.6	6.5	7.4	7.8	7.0	11.3	6.6	6.0	6.7
U	5.8	6.3	6.8	8.4	8.3	8.9	8.4	7.2	6.1	5.2	6.3	7.0	7.7	9.3	8.7	10.5	22.9	8.5	3.9
Th	26.0	31.8	28.0	27.9	51.2	46.7	45.6	30.3	32.4	29.5	28.1	31.0	27.9	32.5	31.0	42.2	27.5	22.4	8.9
Pb	26.0	22.4	35.8	41.5	43.0	50.0	45.5	33.5	20.6	21.4	40.6	38.1	31.3	41.1	46.0	61.1	113.9	77.0	33.4
As	1.5	1.4	1.8	1.2	1.7	2.3	4.2	1.7	2.2	4.5	1.6	2.3	3.9	2.2	1.9	2.2	29.6	31.5	108.7
Se	1.0	0.8	< 0.7	1.3	3.0	5.5	3.2	2.4	2.1	2.4	1.8	1.0	0.8	1.6	1.5	2.3	3.2	1.0	1.7
Bi	< 2.3	< 2.6	< 2.4	< 2.4	3	4	5	2	3	< 2.1	2	< 2.5	< 2.5	4	4	4	< 3.1	< 3.1	< 3.7
Br	< .8	< .9	< .9	< .9	< .8	< .9	< 1.1	< .8	< .8	< .7	< .8	< .9	< .9	< .9	< .9	< 1.0	< 1.1	< 1.1	< 1.3
La	39.6	30.3	55.5	65.1	55.4	51.3	43.1	66.2	53.6	53.4	30.2	24.0	24.7	21.5	21.9	36.8	65.0	57.7	23.7
Ce	80.9	63.3	116.4	135.4	116.3	103.0	89.5	137.7	112.2	110.1	89.9	57.1	53.3	53.9	49.3	69.7	154.3	117.1	46.8
Nd	36.2	27.4	49.1	61.3	51.5	45.0	38.0	57.1	46.5	45.7	44.5	29.3	31.4	31.7	27.8	25.4	62.3	52.5	19.3
Cs																	8.2	4.2	1.5
D	-62.8	-63.44	-64.04	-64.36	-65.02	-65.62	-66.2	-66.54	-67	-68.07	-73.53	-73.69	-74.89	-75.89	-77.23	-78.84	0.35	0.12	0

Samples 137_0a, _0b and _0c are on bottom of previous page.

137	1Ba	1Bb	1Bc	1Bd	1Be	1Ca	1Cb	1Cc	1Cd	1Ce	1Cf	1Cg	1Da	1Db	1Dc	1Dd	2a	2b	2c
SiO_2	63.47	68.65	63.20	57.38	60.20	65.99	62.15	57.50	60.16	58.37	56.42	49.58	60.59	52.42	60.45	56.95	59.58	64.42	59.53
TiO_2	0.71	0.68	0.57	0.79	0.65	0.62	0.70	0.64	0.69	0.68	0.58	0.51	0.68	0.61	0.68	0.67	0.73	0.74	0.71
Al_2O_3	17.62	16.94	14.40	19.62	16.37	15.53	16.91	17.85	18.59	19.42	16.81	13.54	17.66	15.04	17.70	15.99	20.71	18.29	17.23
FeO	1.96	0.98	5.02	1.04	1.26	2.90	0.85	1.48	1.34	1.03	0.98	0.85	1.16	0.84	1.00	1.05	2.23	2.63	0.92
MgO	0.46	0.45	1.69	0.48	0.47	1.23	0.48	0.40	0.52	0.45	0.40	0.34	0.43	0.27	0.42	0.41	0.58	0.66	0.38
CaO	0.18	0.19	1.53	0.16	0.15	1.29	0.15	0.14	0.21	0.16	0.15	0.15	0.18	0.12	0.18	0.25	0.27	0.32	0.20
Na_2O	0.07	0.07	0.07	0.06	0.08	0.10	0.09	0.10	0.11	0.09	0.09	0.08	0.12	0.10	0.12	0.12	0.16	0.19	0.12
K_2O	1.88	1.88	1.67	1.81	2.23	2.45	2.43	2.40	2.52	2.23	2.15	1.64	2.40	1.73	2.35	2.04	2.54	2.78	2.05
P_2O_5	0.09	0.06	0.04	0.05	0.04	0.06	0.04	0.03	0.04	0.05	0.03	0.04	0.04	0.05	0.07	0.04	0.11	0.06	0.03
H_2O^-	1.22	1.10	0.95	1.42	1.01	1.00	1.14	1.12	1.22	1.09	1.11	1.34	1.08	0.98	0.97	1.06	1.25	1.01	0.86
LOI	10.93	7.72	10.26	15.68	16.73	8.41	14.26	16.84	13.41	14.90	20.22	31.34	14.58	27.10	15.58	20.22	10.29	7.94	16.83
Total	98.58	98.72	99.42	98.51	99.17	99.57	99.18	98.52	98.81	98.49	98.94	99.41	98.92	99.25	99.53	98.79	98.43	99.05	98.85
Mn	35.1	25.4	110.0	22.6	44.3	110.2	27.8	29.3	56.7	48.4	46.4	45.1	44.5	26.9	49.9	53.1	67.3	125.6	43.2
S	5483.6	998.2	1189.2	3565.1	2714.2	539.0	1818.9	3934.8	1396.5	1249.8	2832.5	5559.9	2789.3	5651.4	2122.8	2773.4	2687.4	1843.5	1708.5
Ba	503.8	312.1	292.4	246.0	368.4	395.8	373.5	485.9	405.1	363.7	419.1	292.0	509.4	387.8	406.3	353.7	447.7	458.0	351.3
Sc	13.6	10.8	13.9	10.8	9.7	12.4	13.3	10.2	12.5	10.6	9.9	11.0	11.9	7.4	10.3	9.5	15.0	20.1	13.7
Rb	136.6	154.1	132.9	128.4	142.4	164.8	164.7	153.3	168.0	151.6	144.3	115.5	170.0	110.3	148.2	147.1	175.0	181.4	137.9
Sr	294.2	206.3	141.1	143.7	134.4	278.5	124.3	122.6	142.5	212.0	118.6	130.7	133.6	165.0	227.3	128.0	357.8	154.2	69.9
Y	54.6	42.2	40.6	28.2	32.7	48.3	48.5	37.4	41.4	50.8	38.7	46.0	41.2	35.3	43.0	37.5	78.2	80.7	55.7
Zr	263.0	280.8	293.0	243.8	209.4	304.5	280.4	223.1	240.8	197.4	190.9	199.0	239.3	186.5	208.9	222.0	294.1	436.2	320.0
Nb	28.0	28.0	23.7	34.8	20.7	25.6	26.3	21.5	25.4	23.1	17.7	16.0	26.2	13.3	19.7	23.1	26.2	31.1	25.1
Mo	3.4	1.3	1.5	3.1	1.0	1.3	1.4	1.0	1.5	1.5	0.6	1.4	1.5	0.6	0.8	1.1	1.3	1.1	1.7
Co	23.2	4.5	4.7	4.6	3.7	4.0	2.7	3.6	2.6	1.8	<1.6	3.0	2.6	5.6	4.1	3.5	4.0	16.7	4.2
Cr	48.9	47.8	43.1	51.8	44.0	45.4	50.6	39.0	43.1	35.0	37.0	36.1	41.7	33.9	41.2	39.0	53.7	53.2	51.3
V	66.9	67.2	53.2	87.9	45.7	58.4	69.7	43.8	53.2	49.3	48.3	53.1	56.2	37.3	49.3	48.7	70.3	89.6	74.3
Zn	75.5	80.4	56.8	45.5	39.0	46.8	66.8	48.4	51.8	45.1	43.3	46.2	43.1	42.7	50.5	39.4	69.0	53.4	49.6
Cu	32.4	16.9	14.4	12.0	23.5	14.2	8.4	10.1	17.0	10.1	14.6	16.8	10.0	12.7	19.3	9.3	49.4	24.2	13.3
Ni	20.8	4.4	3.4	<1.1	2.1	3.5	1.4	2.5	1.2	<1.1	<1.1	2.0	2.0	2.4	3.7	4.1	13.0	34.5	<1.1
Ge	<0.9	<0.9	<1.0	<0.8	<0.9	<1.0	<0.9	<0.9	<0.9	<0.8	<0.7	<0.7	<0.9	<0.8	<0.8	<0.8	<0.9	<1.0	<0.8
W	6.2	5.2	5.8	6.2	6.7	6.7	5.7	6.9	6.0	5.8	5.4	4.8	<2.9	3.2	3.3	5.4	9.5	10.5	6.4
U	6.1	7.0	4.8	10.0	4.6	6.3	6.2	4.4	5.4	8.8	5.0	6.3	4.7	4.3	5.1	5.0	8.8	7.5	6.7
Th	26.4	25.1	20.4	33.4	23.1	22.0	21.5	24.5	25.6	36.6	24.1	22.8	24.3	19.1	24.2	19.9	30.6	28.1	23.1
Pb	68.0	35.8	45.3	14.5	14.9	23.5	27.3	12.5	14.6	21.0	20.8	24.1	24.3	24.2	21.1	15.7	40.7	44.9	26.6
As	10.3	3.7	4.0	2.3	4.6	3.0	2.1	2.0	1.6	1.5	1.3	2.1	3.4	2.5	2.7	3.9	4.0	10.5	1.8
Se	1.7	<0.9	<1.0	<0.9	<0.9	<1.0	<0.9	<0.9	<0.9	<0.9	<0.9	<0.7	<0.9	<0.9	<0.9	<0.9	<0.9	<1.0	<0.9
Bi	3	<3.0	<3.5	<2.8	<2.8	<2.8	<3.3	<2.9	<2.9	<2.8	<2.7	3	<2.9	<2.5	<2.8	<2.7	<3.1	<3.2	<2.8
Br	<1.1	<1.1	<1.2	<1.0	<1.0	<1.2	<1.0	<1.0	<1.0	<1.0	<1.0	<.9	<1.0	<.9	<1.	<1.0	<1.1	<1.1	<1.0
La	50.3	59.8	24.9	68.8	39.0	55.9	52.2	42.9	44.8	49.2	42.8	55.9	44.8	39.9	47.8	44.4	71.3	42.9	34.1
Ce	109.2	125.5	57.8	137.9	85.9	123.7	114.4	89.3	102.1	101.9	93.4	114.2	96.7	84.4	100.8	93.8	153.4	99.1	75.3
Nd	54.2	55.0	23.4	31.0	37.1	50.1	50.9	37.4	44.7	44.7	41.9	52.9	44.4	39.8	47.3	40.0	80.8	45.9	34.3
Cs	5.6	8.3	9.1	11.2	6.3	9.2	13.2	9.9	11.3	11.5	11.7	8.9	11.4	7.8	5.7	11.0	7.3	9.0	8.7
D	-0.85	-1.07	-1.84	-2.38	-2.7	-3.5	-3.98	-4.54	-4.89	-5.3	-5.66	-6.13	-6.28	-6.74	-7.09	-7.37	-8	-8.58	-9.16

137	2d	2e	3a	3b	4	5	6a	7a	7b	7c	8a	8b	8c	8d	8e	9a	9b	9c	10a
SiO_2	48.34	37.91	55.16	55.85	59.73	60.52	41.38	59.71	60.07	54.26	59.81	57.77	57.64	52.36	59.03	61.22	52.03	52.25	63.56
TiO_2	0.53	0.37	0.61	0.68	0.76	0.74	0.44	0.79	0.80	0.65	0.80	0.75	0.72	0.56	0.71	0.75	0.56	0.67	0.84
Al_2O_3	13.73	10.31	15.61	18.63	19.78	18.90	12.11	20.09	19.56	16.04	19.64	20.22	19.74	12.85	18.85	18.32	14.78	17.68	20.78
FeO	0.77	0.46	0.64	0.82	0.96	0.74	0.37	0.66	0.67	0.52	1.02	0.76	0.75	0.45	0.62	0.52	0.80	1.99	1.00
MgO	0.27	0.20	0.30	0.32	0.36	0.32	0.15	0.27	0.26	0.23	0.34	0.27	0.22	0.18	0.26	0.23	0.17	0.22	0.30
CaO	0.15	0.11	0.12	0.16	0.16	0.15	0.10	0.14	0.13	0.11	0.16	0.12	0.11	0.09	0.11	0.12	0.09	0.12	0.16
Na_2O	0.09	0.07	0.10	0.10	0.11	0.11	0.07	0.10	0.10	0.09	0.10	0.09	0.09	0.09	0.09	0.10	0.08	0.10	0.12
K_2O	1.38	0.98	1.66	1.61	1.82	1.66	0.68	1.33	1.31	1.16	1.37	1.18	1.12	1.00	1.24	1.19	0.89	1.09	1.35
P_2O_5	0.03	0.03	0.04	0.04	0.04	0.06	0.02	0.04	0.04	0.05	0.06	0.05	0.04	0.03	0.04	0.04	0.04	0.08	0.04
H_2O^-	0.87	0.80	0.63	0.86	0.63	0.45	1.31	0.78	0.74	0.64	0.65	0.52	0.65	0.63	0.57	0.26	0.37	0.24	0.39
LOI	33.02	48.34	24.21	20.30	14.89	15.29	42.85	15.44	15.88	25.32	14.62	17.49	16.97	29.96	18.18	15.59	29.21	24.71	9.67
Total	99.17	99.58	99.07	99.36	99.24	98.92	99.49	99.34	99.58	99.05	98.60	99.24	98.06	98.20	99.69	98.34	99.01	99.18	98.20
Mn	29.4	26.7	33.5	38.9	47.1	41.4	22.1	109.9	82.5	35.5	197.4	175.3	161.5	29.8	30.0	27.5	24.2	312.5	41.3
S	5887.3	7685.2	3070.5	3334.3	3279.9	2451.2	6041.1	1518.0	2003.8	2916.5	1209.0	1469.9	1392.1	3547.7	1862.0	1418.3	4900.3	3785.6	621.8
Ba	244.9	200.0	281.1	278.8	296.1	301.6	157.7	508.5	267.3	239.4	345.8	257.9	248.1	218.8	473.3	415.8	240.3	713.2	274.1
Sc	8.4	6.6	9.7	11.4	12.7	11.3	5.6	12.9	12.8	9.4	16.6	25.7	12.0	8.1	8.2	9.6	6.6	5.6	12.9
Rb	97.9	71.9	116.7	117.6	134.9	128.1	67.2	107.9	108.0	92.7	120.8	95.0	109.4	88.4	98.2	94.4	80.2	86.4	117.2
Sr	93.7	74.7	102.2	108.8	110.8	169.9	71.9	84.5	85.7	121.3	135.8	105.5	91.4	83.5	96.7	101.7	67.3	176.1	58.1
Y	27.5	23.1	35.6	40.7	42.2	39.5	20.9	48.9	52.1	40.1	58.4	53.3	53.8	34.5	41.0	38.6	33.2	26.6	42.7
Zr	181.7	135.9	178.6	223.1	247.9	239.0	150.6	265.4	274.0	193.1	281.3	259.9	254.8	174.2	205.0	219.4	174.6	211.6	294.6
Nb	13.8	8.4	16.9	23.2	26.6	24.6	9.4	29.3	29.4	18.7	29.1	26.7	26.1	14.0	23.1	25.9	13.9	18.2	31.0
Mo	0.8	0.8	0.8	1.0	0.8	1.1	0.8	1.2	1.4	0.7	1.6	1.2	1.2	0.8	0.9	0.8	1.6	1.0	2.0
Co	4.5	5.9	3.1	4.6	3.4	2.3	2.6	3.2	4.3	3.0	3.0	<1.5	1.5	4.8	1.7	2.3	4.2	4.7	4.3
Cr	38.7	27.2	38.5	43.8	48.7	47.1	27.5	53.3	50.7	37.8	56.8	47.0	45.0	32.4	35.7	44.2	25.8	35.0	53.0
V	47.7	37.9	44.4	61.3	60.0	57.7	37.2	78.2	81.5	44.5	75.6	68.8	51.7	35.7	37.6	52.1	27.4	35.7	74.1
Zn	29.4	26.4	23.9	34.3	43.2	32.2	24.8	42.7	32.3	40.0	50.4	45.8	37.0	27.0	21.1	22.2	19.1	33.2	31.2
Cu	14.5	10.5	13.4	18.9	20.5	14.9	10.4	20.7	17.8	16.4	21.8	20.0	10.4	13.5	23.2	17.9	11.9	20.6	13.8
Ni	2.2	1.9	2.5	3.6	5.6	1.5	<0.8	<1.7	2.7	1.2	3.4	1.8	<1.1	<1.1	<1.1	<1.1	4.3	4.1	8.1
Ge	<0.7	<0.6	<0.8	<0.8	<0.8	<1.2	<0.8	<0.8	<0.9	<0.8	<0.8	<0.8	<0.9	<0.7	<0.8	<0.8	<0.7	<0.8	<0.9
W	4.2	3.9	7.4	5.6	4.5	4.5	2.4	6.4	7.0	4.9	8.5	7.0	5.4	5.1	7.3	6.6	5.6	7.2	7.6
U	3.9	3.2	4.7	5.7	6.7	4.6	3.7	6.1	6.3	5.0	6.9	6.5	5.5	3.9	5.8	5.9	4.8	3.5	7.9
Th	23.6	12.4	22.3	24.9	26.9	24.9	15.2	24.6	27.3	24.8	31.4	30.0	34.8	16.5	23.8	25.7	16.5	23.5	30.5
Pb	18.4	8.8	18.3	21.6	58.5	109.9	53.1	85.4	57.5	51.8	51.3	44.5	0.2	14.2	19.3	21.0	17.8	10.7	29.9
As	1.3	1.4	<0.8	2.4	5.8	3.5	1.8	2.4	3.1	1.6	2.0	1.3	18.4	1.0	1.6	1.2	2.4	3.8	3.9
Se	<0.7	<0.7	<0.8	<0.8	<0.8	<0.8	<0.7	<0.8	<0.8	<0.8	<0.8	<0.8	<0.8	<0.7	<0.8	<0.8	<0.8	1.1	2.2
Bi	<2.4	<2.0	<2.7	<2.7	<2.8	<2.8	1.1	2.8	<2.8	<2.7	<2.8	<2.7	<2.8	<2.4	<2.7	<2.8	<2.4	<2.8	3.7
Br	<.9	<.7	<.9	<.9	<1.0	<1.0	<.8	<1.5	<1.0	<1.0	<1.0	<.9	<1.0	<1.0	<1.0	<.9	<1.0	<.9	<1.
La	40.7	30.0	43.3	46.8	50.4	46.9	32.3	50.8	47.1	45.7	69.7	51.0	54.4	38.0	43.5	39.3	36.0	33.0	42.3
Ce	88.1	67.3	92.1	106.9	109.7	101.8	67.5	106.6	102.8	97.1	154.5	110.2	116.7	78.9	96.7	85.6	75.1	70.8	94.4
Nd	38.1	29.6	43.2	48.0	48.4	48.3	29.0	46.1	46.3	48.4	74.4	51.2	53.9	37.4	41.4	37.9	31.1	30.7	39.6
Cs	7.6	5.1	8.6	8.7	10.1	8.7	7.4	8.9	9.5	6.6	9.7	5.7	11.3	6.7	7.2	7.3	5.5	6.5	7.8
D	-10.11	-10.48	-11.13	-11.77	-13.24	-14.70	-17.15	-19.46	-20.22	-21.43	-21.88	-22.72	-22.88	-23.19	-24.22	-24.71	-25.23	-25.75	-26.38

137	10b	10c	10d	11a	11b	12a	12b	12c	12d	12e	13	14a	14b	14c	14d	14e	15Aa	15Ab	15Ac
SiO_2	62.64	59.18	58.70	54.48	57.87	55.75	55.36	40.38	46.06	47.10	49.69	51.80	28.58	33.06	47.47	29.60	47.00	49.99	47.68
TiO_2	0.86	0.75	0.77	0.71	0.66	0.73	0.76	0.51	0.59	0.63	0.68	0.72	0.38	0.42	0.66	0.36	0.63	0.68	0.65
Al_2O_3	22.02	22.56	19.42	18.89	17.66	18.84	19.48	13.18	15.40	18.62	17.56	18.27	9.68	11.45	14.49	10.71	16.90	18.87	16.36
FeO	1.09	0.62	0.54	0.41	0.31	0.31	0.31	0.56	0.63	0.41	0.35	0.41	5.46	0.36	0.34	1.32	0.37	0.56	0.75
MgO	0.31	0.26	0.24	0.19	0.16	0.18	0.18	0.16	0.15	0.17	0.17	0.20	0.36	0.12	0.16	0.15	0.20	0.21	0.22
CaO	0.16	0.13	0.12	0.10	0.11	0.12	0.10	0.12	0.10	0.14	0.09	0.10	2.68	0.06	0.10	0.13	0.11	0.09	0.11
Na_2O	0.11	0.08	0.09	0.07	0.08	0.09	0.08	0.07	0.09	0.08	0.10	0.11	0.07	0.06	0.09	0.06	0.09	0.09	0.08
K_2O	1.34	1.18	1.14	0.87	0.74	0.72	0.82	0.60	0.65	0.73	0.76	0.85	0.49	0.51	0.58	0.45	0.77	0.84	0.83
P_2O_5	0.04	0.05	0.07	0.05	0.04	0.03	0.04	0.03	0.03	0.05	0.05	0.06	0.04	0.04	0.04	0.04	0.06	0.07	0.07
H_2O^-	0.95	0.85	0.82	0.92	0.74	0.76	0.70	0.91	0.59	0.52	0.50	0.49	0.51	0.58	1.06	1.39	1.15	1.04	1.05
LOI	9.12	13.55	16.53	21.90	20.81	21.01	20.94	42.81	34.50	30.29	29.40	25.50	50.65	52.77	33.68	55.09	31.89	26.03	30.41
Total	98.64	99.20	98.43	98.59	99.18	98.53	98.77	99.31	98.79	98.74	99.34	98.51	99.00	99.42	98.66	99.31	99.16	98.46	98.85
Mn	49.1	34.8	31.9	25.3	19.0	18.6	15.7	25.5	21.0	21.8	19.0	19.7	912.6	27.3	22.1	192.2	26.8	32.8	62.5
S	987.0	849.6	1522.7	2130.8	2139.8	1831.1	1785.7	5162.3	3944.6	2398.3	2926.5	2276.2	12920.0	5354.7	2874.3	7754.1	3444.3	2876.0	4757.8
Ba	269.4	228.0	278.8	212.2	179.1	201.8	241.1	177.6	195.4	227.4	267.9	312.0	212.7	212.5	224.2	219.5	342.0	419.7	454.3
Sc	14.3	12.1	12.6	11.1	9.3	9.3	12.0	9.4	7.6	9.5	8.8	10.0	7.7	7.9	8.6	6.5	10.3	8.7	9.5
Rb	110.1	95.1	95.7	74.8	64.3	64.9	74.3	61.8	65.2	62.9	71.4	78.0	50.6	48.3	63.0	43.2	73.9	76.3	75.2
Sr	65.5	51.9	103.0	103.7	70.0	56.4	84.4	66.9	87.1	96.1	112.2	114.0	114.2	82.5	87.3	93.2	119.2	127.9	141.9
Y	42.7	48.5	48.1	46.8	37.1	32.1	45.1	33.7	34.7	34.5	39.3	35.3	38.2	29.9	40.3	26.1	37.0	36.1	35.9
Zr	299.4	268.7	270.9	253.0	231.4	231.7	256.7	194.7	177.2	194.7	221.2	231.0	133.1	139.7	218.7	141.6	210.5	192.7	191.6
Nb	34.6	31.2	27.3	25.2	22.7	24.1	28.1	14.6	16.1	18.6	20.8	24.8	8.3	8.0	20.1	10.2	19.4	20.7	18.7
Mo	2.6	1.6	1.1	0.8	1.0	0.8	1.0	0.7	1.1	0.7	0.6	0.7	1.9	0.6	1.1	0.8	0.8	1.0	0.9
Co	8.4	2.6	2.8	2.3	1.5	1.8	2.6	5.1	2.7	2.6	1.9	2.6	7.3	7.9	3.6	5.7	3.4	4.6	5.6
Cr	56.5	45.0	51.6	42.1	35.5	35.9	45.6	34.0	34.2	33.8	45.3	40.6	25.4	26.5	33.5	26.5	39.0	34.5	36.5
V	84.1	66.1	75.4	60.1	48.2	44.4	64.6	52.8	39.8	35.2	52.2	56.0	34.0	33.9	45.0	43.7	51.1	35.3	45.5
Zn	42.1	33.9	45.9	37.3	21.4	14.3	21.7	20.9	21.9	23.7	22.4	19.8	35.9	16.4	13.8	15.5	17.2	26.3	66.1
Cu	16.1	7.1	22.1	17.5	12.3	11.3	17.9	10.7	11.6	12.6	18.9	14.9	10.7	9.3	10.2	9.9	13.2	13.2	16.7
Ni	26.4	1.6	2.1	0.5	0.5	0.5	0.5	1.7	1.3	0.5	1.0	1.3	5.0	2.3	1.1	3.4	1.7	3.8	8.2
Ge	< 0.9	< 0.8	< 0.8	< 0.8	< 0.8	< 0.8	< 0.8	< 0.6	< 0.7	< 0.7	< 0.7	< 0.8	< 0.7	< 0.7	< 0.8	< 0.7	< 0.7	< 0.7	< 0.7
W	8.3	8.1	7.6	6.7	6.0	5.1	4.8	2.8	5.3	5.9	4.7	7.4	4.9	4.3	5.8	1.0	3.6	5.4	4.3
U	8.1	7.7	7.0	6.9	5.1	5.5	7.1	3.7	4.9	5.9	5.4	5.5	3.7	4.0	5.2	3.3	5.2	5.9	5.2
Th	31.2	33.4	28.0	27.9	22.5	27.0	35.5	19.8	21.7	23.4	23.7	22.2	12.6	14.8	23.7	14.8	26.0	24.5	23.7
Pb	49.0	40.1	33.6	832.8	205.7	179.8	185.1	114.1	24.2	28.5	26.8	29.2	30.7	11.7	15.4	86.6	397.9	244.5	207.3
As	6.4	2.1	2.2	10.4	2.4	1.6	1.4	4.0	3.5	4.6	2.3	2.5	5.9	1.1	1.7	2.9	8.0	10.6	7.1
Se	4.8	< 0.8	< 0.8	< 0.8	< 0.8	< 0.8	< 0.8	< 0.7	< 0.7	0.9	< 0.7	< 0.8	< 0.8	< 0.7	< 0.8	< 0.7	< 0.7	< 0.8	< 0.7
Bi	< 2.9	< 2.7	< 2.7	< 2.6	< 2.5	< 2.5	< 2.5	< 2.1	< 2.3	< 2.3	< 2.4	< 2.8	< 2.8	< 1.9	< 2.5	< 2.0	< 2.3	< 2.5	< 2.4
Br	< 1.0	< 1.0	< .9	< .9	< .9	< .9	< .9	< .8	< .8	< .8	< .8	< .9	< 1.0	< .7	< .9	< .7	< .8	< .9	< .9
La	41.8	54.1	50.2	55.8	41.1	36.6	51.5	37.8	41.6	49.2	51.4	39.0	33.0	42.4	38.8	32.6	44.8	43.7	40.7
Ce	91.6	111.8	111.8	116.3	88.0	78.5	114.5	79.4	92.2	104.4	109.7	83.4	70.6	90.3	88.1	70.0	96.7	96.8	85.3
Nd	38.2	48.0	50.3	47.1	37.1	32.3	53.5	34.7	41.5	41.7	47.0	35.2	32.7	37.3	37.5	31.7	41.5	39.9	36.3
Cs	8.0	7.8	7.8	5.3	6.4	11.1	8.3	10.3	7.0	7.3	5.9	6.4	3.5	6.0	13.7	5.1	7.9	6.7	7.4
D	-26.55	-27.28	-27.81	-28.43	-29.21	-29.92	-30.39	-31.32	-31.52	-31.91	-32.18	-33.46	-33.74	-34.26	-34.43	-35.32	-36.02	-36.72	-37.42

137	15Ad	15Ba	15Bb	15Bc	15Bd	16a	16b	17a	17b	17c	17d	18	19a	19b	19c	19d	19e	20a	20b
SiO_2	51.63	52.04	52.21	53.51	53.00	58.27	54.99	52.90	50.85	48.90	43.41	56.12	54.06	51.70	31.82	47.10	44.06	46.78	34.88
TiO_2	0.68	0.73	0.68	0.75	0.72	0.90	0.80	0.75	0.73	0.72	0.60	0.88	0.89	0.85	0.52	0.75	0.72	0.84	0.57
Al_2O_3	17.03	17.53	18.01	20.26	18.31	22.49	19.87	19.66	18.26	18.83	17.74	22.46	23.60	21.27	13.86	20.89	21.81	19.25	15.78
FeO	0.44	0.42	0.64	0.56	0.54	0.47	0.39	0.35	0.36	0.43	0.79	0.70	0.47	0.33	0.25	0.84	0.79	0.45	1.72
MgO	0.20	0.19	0.17	0.19	0.18	0.21	0.17	0.18	0.19	0.17	0.17	0.21	0.21	0.18	0.13	0.16	0.17	0.20	0.22
CaO	0.09	0.10	0.09	0.13	0.09	0.11	0.10	0.09	0.10	0.09	0.10	0.10	0.10	0.09	0.06	0.08	0.09	0.10	0.08
Na_2O	0.08	0.08	0.08	0.08	0.08	0.08	0.07	0.07	0.07	0.07	0.06	0.09	0.08	0.07	0.05	0.08	0.06	0.08	0.05
K_2O	0.79	0.71	0.69	0.66	0.69	0.76	0.62	0.71	0.72	0.60	0.58	0.70	0.76	0.64	0.45	0.57	0.57	0.70	0.39
P_2O_5	0.06	0.05	0.06	0.06	0.06	0.06	0.06	0.06	0.06	0.05	0.05	0.06	0.08	0.06	0.05	0.06	0.07	0.08	0.05
H_2O^-	1.02	1.07	0.72	0.59	0.60	0.71	0.66	0.59	0.59	0.94	0.91	0.78	0.78	0.83	0.62	0.77	0.80	0.81	0.88
LOI	27.09	25.72	25.56	22.37	24.50	14.46	21.19	23.97	26.68	28.20	34.83	16.61	17.81	22.50	51.63	27.63	30.05	29.94	45.57
Total	99.11	98.64	98.91	99.15	98.77	98.52	98.90	99.32	98.60	99.01	99.24	98.69	98.83	98.53	99.44	98.92	99.18	99.22	99.23
Mn	34.0	30.0	62.6	51.2	42.3	19.5	22.2	17.5	18.9	20.1	35.6	54.4	27.6	18.7	14.1	16.7	41.7	31.0	23.2
S	3200.3	2403.3	2381.8	2009.2	2005.5	992.0	1861.9	2663.4	3076.0	4044.8	5644.2	1366.6	1489.4	1954.7	7580.4	4605.3	3786.3	3009.2	10771.3
Ba	364.1	342.5	355.6	323.5	327.9	355.5	342.2	355.5	373.6	327.0	300.3	377.2	428.5	321.8	257.8	313.9	357.3	415.7	258.2
Sc	10.6	12.2	10.0	13.8	12.3	13.2	10.9	10.1	11.0	11.2	12.7	10.5	13.8	13.7	12.1	10.5	12.6	15.7	10.2
Rb	74.0	73.2	66.5	63.0	66.7	78.6	66.1	71.7	75.8	64.6	58.5	79.1	80.1	65.7	54.9	60.9	63.0	76.3	43.5
Sr	119.2	104.9	128.3	108.1	95.9	94.0	102.7	108.5	109.2	101.1	89.6	107.2	128.4	100.7	69.7	103.1	120.9	125.8	106.1
Y	43.2	45.7	46.6	50.7	49.0	47.6	37.9	37.6	39.4	38.0	42.9	36.0	42.7	46.9	48.4	38.1	42.0	51.2	41.8
Zr	200.2	244.8	204.2	259.5	228.3	291.6	219.6	213.6	187.8	195.0	180.5	233.1	273.4	250.8	170.4	202.9	223.8	250.5	187.3
Nb	19.5	26.2	21.6	27.2	24.6	33.1	26.6	23.4	20.4	20.1	13.9	28.6	33.3	31.7	12.7	23.6	27.6	28.3	16.3
Mo	0.7	1.1	1.1	1.1	0.8	0.9	0.7	0.7	0.9	0.9	1.1	0.8	1.3	1.3	1.5	1.4	1.4	1.5	2.7
Co	5.4	3.4	5.0	3.5	3.8	3.3	3.3	3.4	4.3	2.8	6.5	2.5	3.1	2.3	12.6	3.8	4.5	4.8	7.6
Cr	36.2	49.0	37.8	42.3	43.1	50.5	45.8	37.5	33.0	31.6	29.1	35.6	45.6	50.8	34.4	31.2	41.1	54.2	32.1
V	42.3	61.9	49.4	65.8	59.1	69.9	52.7	43.5	41.4	41.9	35.8	46.1	65.9	77.8	49.2	36.3	53.3	78.6	43.8
Zn	18.0	21.5	26.1	32.1	27.9	16.7	18.8	18.2	17.5	14.1	25.0	17.1	23.6	20.6	20.8	31.4	29.2	17.6	23.6
Cu	16.4	16.8	17.6	19.8	16.7	17.0	18.0	16.9	17.9	15.9	15.3	19.1	24.6	21.8	16.1	21.1	23.1	26.6	16.2
Ni	4.9	4.1	7.5	2.8	4.8	1.7	3.7	4.1	5.3	3.5	6.5	2.8	5.7	5.0	8.1	5.3	7.5	10.1	8.3
Ge	< 0.7	< 0.7	< 0.7	< 0.7	< 0.7	< 0.7	< 0.7	< 0.7	< 0.7	< 0.7	< 0.7	< 0.7	< 0.7	< 0.7	< 0.7	< 0.7	< 0.7	< 0.7	< 0.7
W	5.3	7.4	8.4	9.1	6.9	8.6	6.2	5.3	5.7	5.1	3.8	6.0	8.0	7.6	4.8	6.1	7.0	5.0	5.3
U	4.6	5.4	5.3	7.6	6.0	7.2	5.7	5.7	5.3	5.2	4.7	6.3	8.0	7.6	5.3	6.2	7.3	7.6	4.3
Th	22.7	22.2	22.7	36.0	25.5	31.8	27.5	25.8	23.3	20.9	20.8	27.3	35.2	31.3	17.8	23.8	33.7	25.7	22.5
Pb	200.1	32.9	28.5	36.1	33.2	40.0	163.4	99.4	97.2	113.1	99.3	122.8	136.9	39.3	26.2	31.1	36.6	33.4	31.1
As	6.1	4.9	10.7	2.9	5.9	< 0.8	< 0.9	2.6	2.3	< 0.8	2.2	< 0.9	< 0.9	3.3	4.1	4.0	9.0	11.9	15.4
Se	< 0.7	< 0.7	< 0.7	1.1	1.4	1.7	1.4	1.5	0.9	1.8	0.7	1.3	1.8	1.1	0.9	1.4	1.7	1.1	2.1
Bi	< 2.4	< 2.4	< 2.4	< 2.4	< 2.4	3	< 2.4	3	< 2.3	3	< 2.2	< 2.5	4	3	< 1.8	2	< 2.3	< 2.3	2
Br	< .9	< .9	< .9	< .9	< .9	< 1.0	< .9	< .9	< .9	< .9	< .8	< .9	< .9	< .9	< .7	< .9	< .9	< .9	< .8
La	43.4	46.3	45.3	45.6	50.2	50.1	44.0	45.6	44.0	45.9	46.2	40.5	52.8	49.8	46.4	45.0	51.5	59.1	43.8
Ce	91.4	97.4	99.8	102.2	110.2	111.6	97.5	99.7	94.4	99.5	96.2	89.3	114.1	107.7	98.0	100.3	111.8	125.5	90.2
Nd	41.1	40.9	41.5	47.0	48.8	51.1	41.6	42.9	39.1	40.2	42.9	37.6	49.5	46.6	44.6	40.1	48.5	53.5	42.8
Cs	6.8	8.1	4.8	5.4	7.0	6.8	7.8	8.7	6.9	8.0	6.5	9.2	6.6	9.5	11.2	6.4	5.7	11.4	8.5
D	-37.92	-38.76	-39.22	-39.67	-40.2	-40.84	-41.85	-42.46	-43.11	-44.21	-45.38	-45.58	-46.52	-47.27	-47.82	-48.13	-48.67	-49.18	-49.52

137	21a	21b	21c	21d	21e	22Aa	22Ab	22Ac	22Ad	22Ae	22Ba	22Bb	22Bc	22Bd	22Be	22Bf	22Ca	22Cb	22Cc
SiO_2	52.26	52.92	43.52	40.45	43.54	48.20	44.42	51.70	39.30	38.81	45.37	39.30	39.53	47.67	40.49	43.78	48.13	43.69	45.13
TiO_2	1.02	1.00	0.71	0.72	0.81	0.99	0.87	1.00	0.66	0.73	0.80	0.73	0.69	0.84	0.72	0.86	0.99	0.85	0.98
Al_2O_3	22.85	23.26	20.06	20.51	20.08	22.94	23.47	34.38	17.10	18.14	23.43	18.01	17.39	22.15	18.10	21.97	23.62	21.34	20.54
FeO	0.31	0.32	0.58	0.45	2.29	0.48	0.36	0.41	0.41	0.66	0.41	0.52	0.29	0.26	1.03	0.55	0.45	1.29	0.28
MgO	0.17	0.19	0.14	0.13	0.22	0.18	0.17	0.21	0.14	0.20	0.20	0.19	0.15	0.20	0.23	0.17	0.19	0.32	0.17
CaO	0.11	0.10	0.08	0.08	0.11	0.11	0.09	0.11	0.08	0.26	0.09	0.19	0.13	0.14	0.32	0.15	0.21	0.43	0.12
Na_2O	0.09	0.08	0.05	0.05	0.07	0.07	0.06	0.08	0.07	0.07	0.06	0.06	0.06	0.07	0.07	0.07	0.08	0.07	0.07
K_2O	0.59	0.68	0.46	0.46	0.62	0.62	0.55	0.70	0.46	0.59	0.72	0.50	0.44	0.58	0.42	0.55	0.64	0.50	0.49
P_2O_5	0.07	0.07	0.05	0.06	0.08	0.10	0.10	0.08	0.07	0.11	0.14	0.12	0.13	0.17	0.23	0.31	0.29	0.25	0.19
H_2O^-	0.61	0.63	0.61	0.50	0.74	0.81	0.68	0.73	0.66	0.61	0.64	0.60	0.50	0.48	0.51	0.51	0.62	0.37	1.15
LOI	20.78	20.07	32.68	35.61	30.55	24.30	28.08	19.66	40.01	38.93	27.48	38.09	39.75	25.72	36.90	29.59	23.36	29.95	29.17
Total	98.87	99.31	98.93	99.01	99.13	98.80	98.83	99.07	98.95	99.11	99.35	98.32	99.05	98.27	99.03	98.51	98.56	99.07	98.20
Mn	17.3	19.1	40.3	25.4	183.7	34.5	27.7	22.8	19.9	35.6	15.7	64.1	20.1	15.4	110.9	39.7	31.3	135.4	18.5
S	1464.9	1359.0	3212.2	3976.4	3754.3	2109.0	2403.8	1669.2	5777.8	6829.6	2622.8	4084.1	4050.0	1877.9	3279.9	2151.1	1458.0	1805.0	1663.0
Ba	164.5	316.0	260.3	268.4	380.0	460.3	429.6	462.3	288.2	547.9	718.9	562.3	598.6	761.4	951.3	1293	1025	964.9	745.1
Sc	5.4	13.8	9.7	9.6	10.5	15.2	16.5	17.9	13.4	14.0	13.2	13.8	12.7	13.1	11.7	13.3	15.2	17.4	16.1
Rb	63.5	69.5	47.7	43.7	68.0	63.9	57.2	75.5	49.2	62.8	71.4	51.5	43.1	65.1	41.0	55.3	56.3	35.5	39.4
Sr	109.6	95.8	81.2	101.9	150.4	157.0	171.1	113.9	125.2	185.9	227.7	209.8	205.2	283.7	421.3	547.3	306.1	251.7	302.9
Y	43.7	49.3	38.7	36.3	41.0	50.5	56.4	54.2	46.6	45.5	42.6	46.2	37.7	32.7	35.5	30.5	41.9	38.4	37.9
Zr	285.4	285.9	216.3	198.6	208.0	289.5	296.2	312.9	206.9	220.9	239.3	233.4	232.9	261.2	206.1	248.6	306.6	251.0	228.5
Nb	36.2	35.8	19.6	20.0	21.5	31.9	30.8	33.0	17.8	21.6	27.5	23.1	21.9	30.5	21.0	29.7	32.8	28.9	24.4
Mo	1.5	1.7	1.3	1.3	1.5	1.8	1.3	1.1	1.1	1.8	1.2	1.8	1.0	1.0	1.1	1.0	1.2	1.0	0.7
Co	3.1	1.8	4.5	6.6	12.3	4.8	5.4	4.1	10.2	8.4	4.3	4.8	6.9	1.9	4.4	3.4	3.0	2.8	3.6
Cr	57.9	58.7	29.2	38.2	40.6	57.2	54.4	70.5	44.6	46.9	48.1	51.6	48.8	46.5	44.2	55.8	66.0	65.4	64.6
V	91.4	93.1	37.5	52.7	51.4	97.4	89.0	97.2	52.3	71.1	73.6	79.6	76.8	57.4	56.7	74.0	89.9	88.7	68.5
Zn	11.2	9.6	14.9	28.5	44.6	24.5	32.5	21.1	38.2	32.4	16.6	22.2	17.1	9.0	16.6	17.5	13.6	20.5	20.2
Cu	26.5	33.4	15.3	24.7	21.6	32.5	30.4	32.5	17.9	22.8	29.3	23.2	15.9	17.5	14.8	21.1	20.0	24.4	19.8
Ni	8.2	6.3	5.4	8.7	14.9	11.3	13.7	10.9	15.9	13.5	10.5	9.7	11.2	3.3	5.1	4.1	6.9	13.2	9.0
Ge	< 0.7	< 0.7	0.9	< 0.8	0.7	0.9	1	0.9	1.1	< 0.8	< 0.8	0.7	< 0.6	< 0.8	0.9	< 0.8	0.8	0.8	< 0.8
W	10.5	7.4	8.7	6.3	7.9	8.1	7.7	7.0	8.0	6.7	6.2	6.0	5.7	7.5	5.3	5.4	7.9	5.5	5.5
U	9.2	6.4	5.5	6.2	6.1	7.7	7.8	7.8	5.0	5.1	8.2	5.4	5.8	6.9	6.0	5.4	6.2	5.6	5.8
Th	33.0	31.4	27.3	25.0	29.8	31.8	35.5	37.2	22.0	21.2	36.3	26.7	26.3	36.2	26.3	32.4	33.0	31.9	29.1
Pb	43.0	38.2	22.7	27.4	40.4	35.8	42.0	204.7	112.1	98.6	33.7	109.9	93.4	63.2	42.3	47.8	38.0	407.6	425.8
As	6.8	4.1	5.3	7.2	12.5	7.6	9.8	< 1.0	10.9	14.5	13.4	4.4	3.1	1.7	1.6	2.0	< 0.7	< 1.2	< 1.2
Se	2.3	1.8	1.4	2.3	9.7	2.3	2.6	5.7	3.2	1.7	1.7	1.4	1.4	1.6	1.4	1.4	1.7	1.9	1.2
Bi	3	3	< 2.2	< 2.1	< 2.5	< 2.4	< 2.3	< 2.5	< 2.1	< 2.2	< 2.3	< 2.2	< 2.1	< 2.3	< 2.2	< 2.3	2	3	< 2.3
Br	< .9	< .9	< .8	< .8	< .9	< .9	< .9	< .9	< .8	< .8	< .9	< .8	< .8	< .9	< .8	< .9	< .9	< .9	< .9
La	48.1	53.7	42.8	52.7	50.5	54.4	64.5	58.9	56.4	50.2	51.4	51.9	41.9	42.0	44.3	48.3	44.7	47.2	38.5
Ce	100.9	116.9	93.2	112.4	105.8	116.0	135.2	130.9	116.9	105.2	103.9	107.0	92.1	87.2	97.9	99.4	100.4	105.7	91.9
Nd	42.7	50.6	41.5	45.7	48.0	50.3	60.9	57.6	52.5	48.8	49.1	46.2	39.4	36.0	45.1	41.2	42.5	48.9	40.5
Cs	10.2	10.4	6.0	5.7	9.8	9.9	7.4	7.9	6.5	6.0	5.1	7.6	9.3	10.6	5.1	7.2	7.7	8.2	7.3
D	-50.65	-50.92	-51.41	-52.24	-53.12	-53.76	-53.98	-54.31	-55.09	-55.96	-56.39	-56.56	-57.35	-57.99	-58.44	-59.51	-59.98	-60.38	-60.84

137	22Da	22Db	22Dc	22Dd	22De	22Ea	22Eb	22Ec	22Ed	22Ee	22FSa	22FSb	22FSc	23ASa	23ASb	23ASc	23ASd	23ASe	23BS
SiO_2	35.37	37.71	38.87	47.06	42.07	36.16	36.91	36.42	31.03	35.67	28.26	25.95	30.07	46.24	38.57	42.46	46.39	49.19	54.08
TiO_2	0.66	0.73	0.70	0.92	0.86	0.76	0.82	0.85	0.82	1.03	0.89	0.90	0.87	1.22	1.38	1.23	1.11	1.65	1.06
Al_2O_3	16.76	18.15	18.07	21.92	19.76	19.80	16.37	19.62	17.50	21.87	17.91	17.64	22.35	33.79	25.47	19.66	23.79	21.15	23.68
FeO	1.15	2.03	3.52	0.42	1.51	1.25	0.67	1.34	2.83	1.09	1.19	1.33	0.69	0.33	0.50	1.39	0.73	0.42	0.47
MgO	0.24	0.25	0.48	0.25	0.26	0.31	0.23	0.28	0.47	0.34	0.33	0.42	0.30	0.36	0.21	0.35	0.32	0.24	0.19
CaO	0.43	0.19	0.62	0.20	0.26	0.48	0.32	0.44	1.32	1.31	0.54	1.02	0.63	0.54	0.17	0.45	0.28	0.09	0.18
Na_2O	0.06	0.07	0.08	0.09	0.08	0.07	0.07	0.07	0.08	0.09	0.09	0.07	0.07	0.04	0.04	0.05	0.05	0.06	0.03
K_2O	0.41	0.54	0.56	0.61	0.49	0.44	0.39	0.47	0.38	0.43	0.39	0.37	0.33	0.31	0.41	0.67	0.62	0.63	0.41
P_2O_5	0.23	0.15	0.15	0.23	0.22	0.33	0.17	0.31	0.44	0.81	0.33	0.37	0.25	0.07	0.05	0.06	0.10	0.05	0.09
H_2O^-	1.22	1.15	1.12	1.05	1.10	1.18	1.15	1.19	1.17	1.00	1.12	1.38	1.19	0.91	1.34	1.12	1.04	1.05	0.56
LOI	42.49	37.91	34.70	26.64	33.06	38.17	41.93	38.44	43.69	36.34	47.84	50.15	43.07	16.16	30.59	31.53	24.84	24.87	18.84
Total	99.04	98.89	98.89	99.38	99.67	98.96	99.03	99.44	99.75	99.97	98.89	99.61	99.82	99.98	98.73	98.99	99.29	99.38	99.58
Mn	129.9	149.1	306.9	29.8	82.9	106.5	98.7	73.5	226.1	96.5	115.2	171.1	79.8	46.1	30.2	164.0	68.8	21.6	28.6
S	2827.3	3887.4	4519.0	1622.5	2333.0	3093.3	3457.0	3984.5	5680.9	2773.1	2507.3	2318.1	1939.4	370.5	1735.5	1991.1	1273.3	1485.3	859.6
Ba	864.1	683.5	576.8	917.4	776.7	842.0	1254	1017	1084	653.0	1215.3	1022	759.0	216.5	193.8	323.5	425.8	242.5	293.2
Sc	13.5	11.1	12.4	17.4	15.8	16.0	13.0	17.0	14.0	15.2	16.4	15.5	17.0	14.1	35.6	21.4	20.8	25.9	19.4
Rb	37.9	42.2	33.6	66.2	48.6	51.9	45.4	52.5	50.2	34.2	35.7	30.5	26.7	23.9	33.2	62.6	57.7	49.6	29.4
Sr	488.7	351.5	417.6	441.6	424.7	293.6	332.6	270.4	259.3	342.8	471.1	376.5	279.8	56.4	34.5	66.1	99.2	37.4	73.2
Y	46.0	43.9	42.5	42.0	43.2	45.2	42.6	27.9	34.7	45.9	46.9	46.4	39.4	34.5	62.0	58.5	52.8	72.7	41.0
Zr	289.2	300.8	265.4	319.8	277.2	262.2	203.1	199.2	189.8	274.8	275.1	277.8	308.3	472.8	477.8	361.7	348.1	465.2	624.8
Nb	26.6	29.3	27.5	32.9	26.9	28.3	20.5	22.3	19.2	30.9	27.5	28.5	30.4	43.6	46.6	40.4	37.2	50.6	29.6
Mo	1.0	1.3	0.9	1.3	1.0	1.1	1.0	1.3	1.0	1.1	0.8	1.4	0.6	2.7	3.3	5.5	3.2	4.8	0.8
Co	3.8	4.2	4.7	2.8	3.8	2.9	4.6	3.9	6.2	6.1	4.3	4.0	4.2	5.8	5.1	5.3	5.4	7.1	15.3
Cr	49.2	50.0	43.6	67.9	61.1	63.8	49.0	64.2	56.8	57.2	76.7	65.8	65.3	48.8	178.8	87.3	83.5	106.1	132.4
V	59.7	57.6	50.0	87.9	83.4	85.6	68.6	90.4	73.2	76.6	85.2	88.3	87.5	63.3	171.5	95.0	92.1	97.7	62.8
Zn	17.5	17.4	17.3	24.3	23.6	19.2	20.8	23.9	29.8	15.7	14.7	10.7	12.1	17.8	16.7	15.9	13.3	17.9	44.6
Cu	19.8	21.1	18.5	29.6	19.2	14.9	14.8	23.1	19.7	25.1	24.8	20.0	20.3	21.1	32.8	18.4	23.6	27.2	24.1
Ni	5.3	9.6	15.1	6.7	8.2	12.4	5.2	4.6	4.8	21.0	14.8	11.2	11.8	41.2	26.6	12.9	19.0	20.2	39.5
Ge	0.9	1.2	0.9	0.9	1.1	0.7	0.6	0.7	0.8	0.9	< 0.7	< 0.7	< 0.7	< 0.7	< 0.7	< 0.7	< 0.7	< 0.7	< 0.7
W	5.7	6.8	7.4	8.5	9.9	7.7	7.2	8.1	7.5	6.7	6.3	6.8	6.0	8.4	10.3	8.4	8.2	8.3	6.1
U	7.2	6.6	7.7	7.9	6.1	6.5	5.5	4.2	4.3	8.4	7.2	6.6	7.5	9.3	8.2	8.5	7.8	8.6	6.2
Th	34.7	30.9	27.1	32.9	28.6	30.4	23.9	24.3	20.3	30.8	32.3	24.9	33.4	36.9	51.9	34.8	32.0	37.3	35.5
Pb	180.9	176.8	140.0	39.8	30.9	28.0	23.0	25.0	18.1	128.1	46.0	39.3	43.4	56.1	47.6	124.7	139.2	109.5	123.7
As	< 0.9	< 0.9	< 0.9	1.9	2.3	1.3	< 0.6	< 0.7	1.3	< 0.9	< 0.7	< 0.6	< 0.6	< 0.8	< 0.7	< 0.9	< 0.9	< 0.9	8.5
Se	1.4	2.1	2.2	2.8	1.7	1.8	0.9	1.2	1.1	2.5	2.2	2.0	2.2	8.4	4.6	2.3	2.9	3.6	1.4
Bi	< 2.2	< 2.3	3	5	3	< 2.3	< 2.1	< 2.3	< 2.5	< 2.3	< 2.1	< 2.0	4	3	6	< 2.3	3	6	< 2.5
Br	< .8	< .9	< .9	< .9	< .9	< .9	< .8	< .9	< 1.0	< .9	< .8	< .8	< .8	< .9	< .9	< .9	< .9	< .9	< .9
La	47.7	39.9	40.0	54.4	51.2	50.4	60.3	60.0	49.9	43.8	65.6	55.0	49.8	28.2	32.6	39.4	56.1	24.4	50.1
Ce	100.7	81.3	79.3	115.9	112.2	113.7	133.0	131.9	103.0	91.4	147.0	115.9	106.2	56.6	86.8	78.1	111.3	62.0	104.7
Nd	42.2	34.6	32.1	47.9	45.1	42.7	55.9	53.6	44.1	38.3	62.3	47.7	43.8	21.8	39.0	34.3	43.9	33.1	36.9
Cs	7.8	8.8	8.2	6.7	5.7	7.7	8.2	9.9	7.2	7.5	6.2	7.2	3.9	4.2	6.4	11.2	6.9	10.3	4.0
D	-61.22	-62.73	-63.52	-63.76	-64.47	-65	-65.35	-65.7	-66.54	-67.18	-67.54	-69.03	-69.14	-74.3	-74.64	-75.34	-76.27	-78.16	-79.19

Table II.3 Whole-rock major and trace element compositions of mudstones and carbonaceous mudstones (borehole 136 and 137) re-calculated to a 100% major element volatile-free. Majors are reported in weight % oxide and trace elements in ppm. All Fe is calculated as FeO. Elements which have concentrations less than lower limit of detection are reported as blank values. *nd* = not determined. D = depth (m) with respect to the topmost coal seam in the Grootegeluk Fm (negative value below and positive above). <LLD = below lower limit of detection. Sample numbering and position in boreholes are explained in Appendix I.

136	0a	0b	0c	1ba	1bb	1bc	1bd	1ca	1cb	1cc	1cd	1ce	1da	1db	1dc	1dd	2a	2b	2c
SiO_2	73.57	73.48	70.08	72.18	75.87	74.57	74.64	73.35	70.96	70.50	70.44	73.64	71.63	72.82	72.64	72.72	73.19	69.77	73.25
TiO_2	0.82	0.86	0.80	0.76	0.71	0.76	0.80	0.79	0.84	0.79	0.85	0.77	0.77	0.83	0.63	0.81	0.88	0.89	0.75
Al_2O_3	19.96	21.00	19.45	18.89	18.38	19.57	19.64	19.66	22.53	23.13	24.00	20.74	23.15	21.27	22.35	21.64	21.12	22.61	16.78
FeO	2.98	2.66	7.56	4.66	1.44	1.64	1.21	1.88	1.98	1.59	1.19	1.22	1.19	1.31	1.36	1.24	1.27	2.42	6.42
MgO	0.83	0.43	0.48	0.56	0.59	0.62	0.50	0.73	0.62	0.60	0.51	0.51	0.47	0.50	0.40	0.45	0.46	0.69	0.48
CaO	0.43	0.16	0.38	0.19	0.20	0.32	0.15	0.30	0.28	0.26	0.21	0.19	0.19	0.22	0.17	0.20	0.22	0.28	0.58
Na_2O	0.06	0.06	0.06	0.10	0.09	0.08	0.12	0.12	0.11	0.14	0.12	0.14	0.12	0.15	0.13	0.15	0.16	0.18	0.12
K_2O	1.32	1.31	1.15	2.60	2.66	2.40	2.91	3.10	2.64	2.96	2.62	2.76	2.43	2.86	2.26	2.73	2.65	3.08	1.57
P_2O_5	0.03	0.05	0.05	0.07	0.06	0.03	0.03	0.08	0.04	0.04	0.06	0.04	0.05	0.04	0.08	0.06	0.04	0.08	0.05
TOTAL	100.00	100.00	100.00	100.00	100.00	100.00	100.00	100.00	100.00	100.00	100.00	100.00	100.00	100.00	100.00	100.00	100.00	100.00	100.00
Mn	76.2	42.4	60.7	43.1	34.9	54.7	34.3	57.0	89.5	65.4	53.0	61.9	66.1	65.8	47.2	50.6	66.2	119.9	114.8
S	0.2800	0.6440	2.3600	1.2890	0.0900	0.0550	0.2770	0.0910	0.4410	0.0880	0.2070	0.4340	0.3590	0.2650	0.9420	0.2660	0.3590	0.2230	3.8200
Ba	248.4	243.1	236.8	389.4	351.6	335.2	652.4	437.9	411.1	440.7	409.2	441.4	405.7	478.4	431.8	437.6	471.4	649.8	323.3
Sc	17.4	16.8	16.4	14.6	16.8	12.9	11.3	15.7	13.6	14.8	13.3	13.6	13.6	15.5	11.8	13.0	13.2	17.9	18.5
Rb	125.9	119.2	97.6	178.2	204.3	162.1	174.7	211.6	171.0	199.3	176.1	186.1	169.5	192.7	143.8	172.1	186.0	203.9	128.8
Sr	98.1	135.9	117.5	289.4	236.2	137.5	136.1	328.1	154.5	159.0	224.5	145.8	179.2	154.6	308.8	236.3	143.8	277.3	135.8
Y	50.4	54.7	51.1	58.3	51.0	42.6	40.8	57.9	47.1	43.5	52.9	48.4	58.1	51.1	55.9	52.4	47.8	80.8	113.9
Zr	370.1	372.3	311.0	274.0	381.0	306.9	245.8	319.8	283.9	264.9	249.1	256.1	248.4	271.2	221.9	252.1	297.9	351.3	503.1
Nb	34.6	36.8	31.5	29.4	31.0	31.2	26.0	31.6	26.6	30.3	25.9	22.0	22.7	29.8	12.7	24.8	29.0	28.3	20.4
Mo	3.6	8.8	18.2	9.7	1.9	2.0	1.6	1.9	2.6	1.6	1.0	1.4	1.5	1.9	1.2	1.3	1.6	1.5	8.2
Co	8.0	6.7	16.5	16.4	4.9	2.1	2.8	3.2	11.8	2.3	2.5	4.3	<lld	3.9	7.9	2.5	6.5	5.6	17.7
Cr	64.0	71.1	62.4	48.3	55.9	48.4	44.5	53.7	48.5	48.1	43.1	49.6	46.3	51.7	40.5	48.4	58.4	66.0	58.0
V	112.4	136.8	82.4	70.7	74.7	69.3	49.7	97.5	63.0	59.3	58.4	69.7	53.6	62.4	45.9	53.7	75.4	91.5	102.0
Zn	99.8	70.1	79.4	100.3	55.1	36.4	38.1	88.8	67.4	56.1	37.0	63.6	53.5	54.6	59.2	39.3	70.7	80.2	95.7
Cu	18.3	23.3	25.4	40.1	19.4	6.2	17.0	33.4	14.8	23.7	11.8	21.6	17.2	16.5	25.0	18.7	22.5	60.2	18.8
Ni	10.9	15.6	31.4	30.1	7.4	4.4	6.6	7.6	18.2	5.8	4.5	7.3	8.7	8.2	11.0	8.9	11.6	18.4	19.9
Ge	<LLD	<LLD	<LLD	<LLD	<LLD	<LLD	<LLD	<LLD	<LLD	<LLD	<LLD	<LLD	<LLD	<LLD	<LLD	<LLD	<LLD	<LLD	4.2
W	5.8	10.1	10.5	7.6	8.0	4.8	9.1	6.9	4.7	6.0	6.9	8.4	8.0	11.6	1.8	9.4	9.6	11.5	10.6
U	24.4	52.4	26.4	7.0	4.6	5.6	4.3	9.3	5.7	5.0	6.9	4.7	9.1	4.9	5.0	5.6	6.0	7.8	7.7
Th	27.6	29.3	30.3	29.5	24.5	25.4	24.7	30.7	32.0	30.6	41.4	28.3	40.1	28.5	32.0	28.6	28.4	34.9	24.0
Pb	598.7	45.3	69.5	766.7	23.9	233.0	13.6	136.1	95.1	22.5	88.2	23.7	32.6	30.7	50.1	21.5	20.5	40.1	108.0
As	15.5	14.9	80.2	29.1	2.4	2.8	3.5	0.6	6.0	1.7	0.6	1.6	8.0	2.7	3.1	3.8	6.6	4.0	12.9
Se	2.4	6.5	7.9	1.9	<LLD	<LLD	<LLD	<LLD	1.5	<LLD	<LLD	<LLD	<LLD	<LLD	<LLD	<LLD	<LLD	<LLD	2.2
Bi	<LLD	<LLD	<LLD	<LLD	<LLD	<LLD	<LLD	<LLD	<LLD	<LLD	<LLD	<LLD	<LLD	<LLD	<LLD	<LLD	<LLD	<LLD	<LLD
Br	<LLD	<LLD	<LLD	<LLD	<LLD	<LLD	<LLD	<LLD	<LLD	<LLD	<LLD	<LLD	<LLD	<LLD	<LLD	<LLD	<LLD	<LLD	<LLD
La	35.4	53.9	51.6	56.4	69.3	47.7	41.9	68.8	57.1	49.9	58.1	55.8	70.0	58.8	78.5	55.6	55.6	80.7	72.7
Ce	77.9	121.5	106.3	117.8	148.1	95.4	81.9	146.8	111.5	104.9	116.9	116.3	149.7	124.2	159.5	112.6	117.3	164.3	136.3
Nd	35.4	52.2	48.7	60.5	57.5	36.8	38.0	69.9	49.5	48.2	52.8	52.8	70.5	57.3	76.5	53.3	49.8	77.8	65.1
D	0.23	0.04	0	-0.74	-0.89	-1.3	-2.1	-2.5	-3.15	-4.53	-4.92	-5.27	-5.73	-5.9	-6.38	-6.69	-7.53	-8.24	-8.74

136	2d	2e	3a	3b	4	5	6	7a	7b	8a	8b	8c	8d	8e	9a	9b	9c	10a	10b
SiO_2	73.21	71.01	74.86	71.82	71.77	74.26	73.76	72.28	71.73	70.42	70.69	70.03	74.35	73.05	75.98	75.21	74.24	71.53	69.63
TiO_2	0.83	0.77	0.76	0.90	0.92	0.90	0.82	0.96	0.96	0.97	1.01	0.97	0.91	0.91	0.77	0.85	0.86	0.97	0.93
Al_2O_3	22.34	19.95	20.63	23.31	23.12	21.29	21.13	23.84	24.39	25.45	24.88	25.96	22.14	23.08	20.76	21.79	22.20	24.01	25.96
FeO	0.85	3.36	0.88	1.15	1.28	0.90	2.35	0.68	0.72	0.93	1.09	0.82	0.51	0.70	0.54	0.46	0.77	1.22	1.29
MgO	0.40	1.19	0.41	0.41	0.42	0.36	0.29	0.33	0.31	0.35	0.37	0.34	0.29	0.35	0.29	0.24	0.28	0.41	0.38
CaO	0.16	1.72	0.16	0.19	0.17	0.16	0.15	0.16	0.15	0.17	0.18	0.15	0.13	0.14	0.21	0.13	0.14	0.23	0.17
Na_2O	0.13	0.13	0.13	0.13	0.13	0.13	0.12	0.12	0.12	0.11	0.12	0.11	0.13	0.12	0.11	0.11	0.11	0.12	0.12
K_2O	2.06	1.84	2.14	2.05	2.13	1.94	1.35	1.58	1.57	1.55	1.62	1.58	1.52	1.61	1.30	1.18	1.33	1.45	1.48
P_2O_5	0.04	0.04	0.04	0.04	0.06	0.05	0.04	0.05	0.04	0.06	0.05	0.05	0.03	0.05	0.05	0.03	0.06	0.07	0.04
TOTAL	100.00	100.00	100.00	100.00	100.00	100.00	100.00	100.00	100.00	100.00	100.00	100.00	100.00	100.00	100.00	100.00	100.00	100.00	100.00
Mn	46.4	192.5	47.6	68.1	64.7	67.0	36.1	35.9	39.9	100.1	131.9	52.3	29.0	37.6	35.0	29.2	33.3	86.7	81.5
S	0.5740	2.9380	0.9600	0.6240	0.3470	0.3310	1.3800	0.1710	0.1870	0.1870	0.1190	0.1670	0.1910	0.2940	0.3450	0.3040	0.4360	0.2180	0.0750
Ba	337.2	370.8	347.3	338.0	341.8	439.5	279.5	727.7	313.8	376.4	609.1	296.6	301.0	332.9	253.2	247.1	281.7	323.1	404.4
Sc	12.8	16.7	13.2	16.2	17.1	13.4	11.8	16.1	14.8	20.8	19.7	17.7	9.6	10.8	10.1	8.8	12.8	18.1	18.4
Rb	146.9	130.8	149.4	152.3	158.8	149.2	124.7	130.9	131.1	129.7	134.6	132.0	118.9	138.6	97.5	98.4	109.4	126.4	124.8
Sr	117.3	179.0	148.1	127.5	152.0	168.4	120.5	124.7	98.8	128.2	108.7	90.7	82.2	161.3	156.5	89.0	139.3	180.0	88.0
Y	44.0	52.0	48.6	53.7	57.8	47.6	44.5	51.5	53.9	71.6	62.5	68.5	44.1	42.3	39.8	35.7	49.4	61.4	53.5
Zr	250.1	297.3	269.4	295.6	312.1	283.5	269.3	307.6	286.1	328.8	341.6	317.1	256.1	269.7	229.0	249.1	329.9	414.9	366.8
Nb	23.1	22.8	20.0	28.2	33.7	28.3	21.5	34.5	34.2	36.8	38.6	35.6	25.4	30.3	20.6	23.3	26.3	36.9	37.0
Mo	1.2	2.7	1.1	0.9	1.8	1.7	1.9	1.2	1.5	1.3	2.4	2.0	1.3	1.5	0.9	0.9	2.2	3.5	1.4
Co	4.3	15.8	8.0	6.1	2.7	3.3	4.5	2.8	3.5	4.5	4.3	4.1	3.0	2.6	2.2	4.7	8.7	3.9	8.4
Cr	49.8	57.2	54.5	59.5	66.0	54.5	46.9	62.5	61.9	69.0	74.3	74.2	40.1	50.4	37.5	36.5	48.0	66.9	65.9
V	60.7	96.0	81.6	82.4	84.1	60.8	55.5	83.2	79.1	102.7	105.1	99.2	42.2	57.6	44.8	39.5	71.1	102.9	91.6
Zn	39.0	85.3	40.6	46.5	51.3	38.5	31.6	50.6	41.9	68.7	59.6	57.2	25.8	34.1	37.9	20.1	51.2	64.1	65.3
Cu	16.2	23.4	25.1	22.5	30.6	22.9	13.5	22.8	22.7	32.7	30.7	21.7	15.9	17.9	28.9	14.4	33.3	30.6	31.2
Ni	7.1	16.4	8.0	10.4	12.2	7.5	9.3	7.4	8.3	12.0	16.2	14.4	5.0	4.5	5.4	8.9	13.4	13.8	29.4
Ge	<LLD	<LLD	<LLD	<LLD	<LLD	<LLD	<LLD	<LLD	<LLD	<LLD	<LLD	<LLD	<LLD	<LLD	<LLD	<LLD	<LLD	<LLD	<LLD
W	4.4	5.1	6.8	7.9	16.4	9.7	5.2	7.3	8.1	12.5	14.6	11.8	5.5	7.8	5.4	5.3	8.1	7.5	12.5
U	6.0	6.2	6.9	7.7	7.0	6.7	7.2	7.5	7.0	9.9	7.3	8.8	5.2	5.5	6.0	5.4	8.7	10.0	7.7
Th	35.3	26.4	29.7	29.9	34.8	32.3	31.0	32.3	30.1	36.1	34.7	34.6	23.9	34.7	27.1	26.8	32.9	35.5	42.0
Pb	54.8	44.8	108.4	64.3	41.6	34.4	137.7	84.6	32.0	60.4	56.5	53.6	41.9	49.5	56.8	150.6	58.7	120.1	48.1
As	2.3	8.4	1.3	1.6	2.2	0.5	10.5	1.6	6.4	3.6	3.2	2.4	1.2	1.9	1.5	1.8	3.1	4.0	4.8
Se	<LLd	<LLd	<LLd	<LLd	<LLd	<LLd	<LLd	<LLd	<LLd	<LLd	<LLd	1.5	<LLd	<LLd	<LLd	<LLd	2.2	2.4	0.9
Bi	<LLD	<LLD	<LLD	<LLD	<LLD	<LLD	<LLD	<LLD	<LLD	<LLD	<LLD	<LLD	<LLD	<LLD	<LLD	<LLD	<LLD	<LLD	<LLD
Br	<LLD	<LLD	<LLD	<LLD	<LLD	<LLD	<LLD	<LLD	<LLD	<LLD	<LLD	<LLD	<LLD	<LLD	<LLD	<LLD	<LLD	<LLD	<LLD
La	60.2	59.4	59.7	61.2	68.2	59.3	65.7	60.2	54.0	85.3	63.4	74.0	42.9	65.0	57.0	40.2	62.0	74.8	50.8
Ce	130.1	118.2	127.7	129.9	148.7	126.8	129.6	123.5	115.2	179.3	138.0	148.1	87.6	140.0	122.7	84.3	134.2	152.2	96.9
Nd	58.2	55.3	55.7	59.4	67.9	58.6	53.7	55.0	48.8	79.9	62.6	66.7	35.7	60.9	53.0	35.1	60.0	73.5	47.0
D	-9.55	-9.94	-10.52	-11.14	-12.46	-14.06	-16.16	-17.83	-19.05	-19.69	-20.69	-21.34	-22	-22.89	-23.48	-24.04	-24.93	-25.21	-25.37

XRF data re-calculated volatile-free!

136	10c	10d	11a	11b	12a	12b	12c	12d	12e	13a	14a	14b	14c	14d	14e	15aa	15ab	15ac	15ad
SiO_2	72.04	71.57	71.19	76.39	72.13	71.97	69.47	72.83	70.49	71.52	71.10	71.04	71.56	73.11	68.65	70.77	69.92	71.67	71.06
TiO_2	0.97	0.98	0.93	0.86	0.96	0.97	0.90	0.98	0.94	0.97	1.02	0.90	0.90	0.88	0.94	0.99	0.85	0.97	0.95
Al_2O_3	23.91	24.72	25.59	20.59	23.77	25.12	27.03	23.91	26.61	25.45	25.53	23.94	24.57	21.73	25.19	25.99	26.35	24.57	25.40
FeO	0.87	0.74	0.57	0.57	1.51	0.39	1.10	0.66	0.50	0.43	0.58	1.16	1.01	2.50	3.63	0.56	1.18	0.82	0.91
MgO	0.36	0.32	0.28	0.23	0.24	0.23	0.25	0.25	0.23	0.25	0.28	0.50	0.33	0.31	0.26	0.26	0.27	0.31	0.28
CaO	0.15	0.15	0.14	0.15	0.19	0.13	0.15	0.16	0.13	0.13	0.15	1.07	0.37	0.31	0.16	0.13	0.16	0.13	0.17
Na_2O	0.11	0.11	0.09	0.11	0.12	0.11	0.10	0.13	0.12	0.14	0.15	0.15	0.16	0.15	0.15	0.14	0.14	0.15	0.12
K_2O	1.56	1.35	1.16	1.07	1.03	1.03	0.95	1.03	0.94	1.07	1.13	1.16	1.02	0.96	0.94	1.07	1.05	1.27	1.01
P_2O_5	0.04	0.05	0.05	0.04	0.05	0.05	0.06	0.06	0.05	0.07	0.08	0.08	0.08	0.06	0.08	0.09	0.08	0.11	0.09
TOTAL	100.00	100.00	100.00	100.00	100.00	100.00	100.00	100.00	100.00	100.00	100.00	100.00	100.00	100.00	100.00	100.00	100.00	100.00	100.00
Mn	58.7	65.9	58.0	32.3	33.9	22.6	26.3	53.6	38.8	22.5	29.7	113.3	73.2	88.9	432.4	37.6	125.9	51.0	83.4
S	0.1370	0.0800	0.1880	0.2910	0.7680	0.1360	0.4750	0.4100	0.2960	0.2220	0.3190	1.3390	1.2230	2.1950	1.2680	0.2550	0.4400	0.2460	0.5260
Ba	347.6	413.9	252.2	342.6	276.6	279.6	285.0	290.3	291.3	374.6	420.5	473.9	466.2	314.4	444.4	571.6	491.9	675.4	530.9
Sc	20.2	16.7	15.2	13.3	16.5	17.0	11.5	13.0	10.4	12.7	13.4	23.9	19.4	17.1	14.9	13.6	12.4	12.9	15.7
Rb	137.1	111.1	98.3	94.4	95.4	94.0	94.7	99.8	83.8	98.5	112.2	110.9	100.1	98.7	96.5	102.4	96.2	109.1	94.6
Sr	66.0	111.9	124.2	96.2	120.6	117.4	150.0	156.6	135.9	173.3	182.9	242.3	224.3	175.2	203.0	202.0	181.2	222.6	204.6
Y	81.0	56.7	57.2	57.8	66.6	62.4	49.6	54.8	47.1	50.0	48.9	76.9	62.2	65.2	55.6	49.1	52.5	48.5	59.6
Zr	370.0	322.1	309.9	258.8	381.8	347.3	269.3	282.1	285.3	292.4	314.3	347.5	318.4	314.9	305.2	282.4	257.9	252.1	290.2
Nb	39.0	34.8	34.2	24.9	32.0	38.6	28.0	23.7	24.3	30.7	32.5	21.3	20.3	18.6	17.6	31.3	23.7	29.3	25.4
Mo	2.1	1.0	0.9	1.4	2.2	1.0	1.0	1.4	1.4	0.3	0.8	2.3	1.9	2.7	2.0	1.6	1.4	1.4	1.2
Co	1.0	2.6	2.4	4.3	8.4	1.9	3.9	6.4	2.4	2.9	3.0	12.2	12.3	28.0	11.8	3.7	5.8	5.0	7.1
Cr	66.9	58.3	58.7	45.5	68.8	61.7	46.7	51.0	42.4	50.9	63.9	65.1	65.5	60.7	59.1	51.7	47.5	49.4	53.2
V	90.4	77.9	84.6	47.3	92.6	86.3	53.8	61.6	45.4	61.3	75.8	92.1	87.7	76.5	84.4	60.3	55.2	50.7	68.2
Zn	63.6	46.6	53.8	41.8	34.2	23.7	32.1	44.5	19.4	20.1	25.4	55.2	33.9	52.4	34.4	18.5	37.1	27.4	49.9
Cu	20.5	27.7	23.0	18.2	24.6	20.8	14.3	22.6	14.1	21.9	22.0	23.8	25.1	14.7	32.7	23.4	16.8	23.5	24.5
Ni	9.9	7.6	8.2	13.3	12.7	6.3	6.9	12.3	5.2	5.6	9.1	17.0	15.5	28.8	14.1	9.4	10.5	13.5	16.3
Ge	<LLD	<LLD	<LLD	<LLD	<LLD	<LLD	<LLD	<LLD	<LLD	<LLD	<LLD	<LLD	<LLD	<LLD	<LLD	<LLD	<LLD	<LLD	<LLD
W	12.5	8.5	7.3	9.0	11.9	5.6	5.6	10.8	4.7	5.9	9.2	11.8	8.8	9.4	11.4	9.0	8.2	9.6	6.0
U	10.7	7.4	8.9	5.5	8.6	8.1	8.3	6.8	6.4	7.5	9.1	6.4	5.3	5.0	7.7	6.8	6.0	6.6	6.5
Th	42.3	33.1	36.3	25.1	41.8	41.4	34.9	29.9	50.4	32.8	33.5	28.2	27.3	36.3	29.3	27.5	32.7	33.6	31.3
Pb	56.9	121.2	84.1	31.6	57.6	65.3	63.7	33.2	28.9	75.3	43.0	32.5	27.0	46.4	28.7	35.4	28.2	34.8	113.8
As	1.7	2.5	3.0	4.5	7.7	2.8	10.0	5.4	1.9	1.8	3.8	7.2	5.2	14.1	4.0	5.2	7.0	14.7	15.5
Se	<LLD	<LLD	<LLD	0.9	1.1	0.9	2.8	<LLD	<LLD	<LLD	<LLD	<LLD	<LLD	<LLD	<LLD	<LLD	<LLD	1.2	1.1
Bi	0.6	0.6	0.6	0.6	0.6	0.6	0.6	0.6	0.6	0.6	0.6	0.8	0.8	0.9	0.8	0.6	0.6	0.6	0.6
Br	<LLD	<LLD	<LLD	<LLD	<LLD	<LLD	<LLD	<LLD	<LLD	<LLD	<LLD	<LLD	<LLD	<LLD	<LLD	<LLD	<LLD	<LLD	<LLD
La	77.4	60.2	68.7	62.5	75.5	70.4	70.8	73.0	61.9	65.5	67.8	88.8	93.3	91.2	82.0	64.0	64.7	62.0	65.6
Ce	152.8	128.8	147.3	124.9	159.8	143.1	149.1	155.0	135.7	136.9	143.6	187.9	190.0	184.4	169.7	135.3	131.6	129.5	143.9
Nd	72.1	58.3	62.5	53.3	76.9	62.7	59.2	66.8	62.9	58.7	58.4	87.6	79.6	82.7	67.1	56.6	60.0	61.6	64.9
D	-26.51	-27.08	-27.63	-28.22	-29.53	-29.77	-30.95	-31.14	-31.49	-31.68	-32.99	-33.42	-33.77	-34.17	-35.04	-35.5	-36.19	-36.86	-37.36

136	15ba	15bb	15bc	15bd	16a	16b	17a	17b	17c	17d	18	19a	19b	19c	19d	19e	20a	20b	21a
SiO_2	71.88	69.97	69.43	69.78	69.35	71.30	70.49	70.35	69.86	70.19	69.62	65.83	69.56	68.22	67.25	66.36	66.43	67.80	66.56
TiO_2	1.00	0.91	1.00	0.97	1.07	1.05	1.05	1.01	1.02	0.88	1.09	1.04	1.15	1.06	1.10	1.21	1.17	1.14	1.27
Al_2O_3	24.96	26.26	27.33	27.13	27.61	25.78	26.58	26.53	27.12	26.93	27.16	27.66	27.45	28.03	29.57	29.72	30.16	28.47	29.75
FeO	0.61	1.28	0.66	0.60	0.55	0.52	0.49	0.56	0.53	0.76	0.68	3.87	0.45	1.15	0.85	1.17	0.71	1.21	0.56
MgO	0.27	0.28	0.27	0.25	0.24	0.22	0.22	0.24	0.24	0.21	0.23	0.30	0.23	0.25	0.18	0.24	0.24	0.22	0.38
CaO	0.18	0.15	0.16	0.12	0.13	0.13	0.11	0.11	0.16	0.12	0.13	0.15	0.16	0.13	0.11	0.13	0.16	0.14	0.66
Na_2O	0.12	0.11	0.11	0.11	0.10	0.09	0.09	0.10	0.10	0.09	0.11	0.13	0.11	0.11	0.11	0.13	0.11	0.11	0.13
K_2O	0.91	0.96	0.97	0.97	0.89	0.83	0.90	1.01	0.88	0.76	0.91	0.94	0.82	0.98	0.75	0.96	0.91	0.82	0.62
P_2O_5	0.07	0.09	0.08	0.08	0.07	0.08	0.08	0.09	0.09	0.07	0.08	0.09	0.08	0.08	0.07	0.09	0.10	0.10	0.08
TOTAL	100.00	100.00	100.00	100.00	100.00	100.00	100.00	100.00	100.00	100.00	100.00	100.00	100.00	100.00	100.00	100.00	100.00	100.00	100.00
Mn	51.3	159.9	52.7	40.0	20.2	38.9	19.3	26.0	32.6	23.2	26.6	312.7	29.7	53.8	30.7	61.0	29.8	52.2	66.6
S	0.2900	0.4340	0.1800	0.2350	0.1250	0.2000	0.2550	0.3870	0.5450	0.5960	0.3210	0.4540	0.3380	1.6690	0.7220	0.4020	0.7240	1.8400	0.2350
Ba	420.1	479.5	463.4	459.6	386.8	429.3	485.1	537.2	467.0	371.5	459.9	421.2	388.6	419.2	384.0	494.3	509.1	440.2	452.8
Sc	19.2	17.8	15.7	16.5	16.5	12.0	13.0	13.8	17.2	15.1	14.7	14.5	19.7	21.8	16.0	17.6	22.5	23.8	16.8
Rb	95.6	94.1	96.4	89.8	92.9	90.9	85.5	103.4	97.7	77.4	99.0	94.5	83.4	114.1	77.8	107.3	99.5	108.9	70.5
Sr	150.1	181.9	150.9	157.2	107.1	143.1	144.6	183.1	170.2	133.3	152.9	187.1	152.5	146.3	130.6	168.7	191.9	229.9	129.0
Y	67.3	64.4	58.1	65.4	54.6	45.2	51.3	49.1	55.3	53.5	47.4	58.2	59.8	81.6	52.1	56.3	65.4	96.4	52.6
Zr	337.6	300.1	319.1	291.8	352.0	286.4	266.4	259.3	287.4	254.9	299.1	277.4	326.1	307.3	293.1	323.5	384.9	382.5	363.9
Nb	37.3	28.8	39.3	30.8	40.0	33.9	34.0	27.8	27.6	21.3	34.8	33.6	41.1	28.2	37.1	42.5	43.4	29.6	44.4
Mo	1.4	1.1	1.2	0.8	1.3	0.9	1.5	1.3	1.6	1.8	1.5	1.6	2.2	2.6	1.5	1.2	2.3	4.3	1.7
Co	5.0	5.9	2.9	3.2	3.0	3.2	4.0	8.3	7.5	3.8	3.0	6.0	4.1	10.2	4.2	4.1	5.5	13.9	4.5
Cr	61.8	50.7	58.5	46.5	62.6	51.4	41.9	44.3	52.5	38.0	51.8	47.0	74.6	62.6	46.6	62.0	79.8	71.9	69.1
V	100.5	79.1	82.4	58.3	94.7	58.6	48.4	52.0	71.3	48.3	66.0	61.0	95.7	87.5	56.8	76.9	114.4	89.8	99.4
Zn	32.6	46.3	24.9	24.6	18.9	23.1	33.8	24.0	48.2	15.3	19.8	71.0	27.8	31.2	30.9	30.3	28.0	75.3	13.7
Cu	23.6	20.1	25.4	23.6	21.6	26.1	30.4	26.5	30.2	19.9	30.8	35.6	36.8	29.7	25.2	33.9	37.9	27.4	35.0
Ni	10.9	15.6	7.4	11.0	7.1	12.8	10.4	15.5	16.4	10.2	11.9	16.1	13.5	15.6	11.0	15.5	18.7	23.7	14.7
Ge	<LLD	<LLD	<LLD	<LLD	<LLD	<LLD	<LLD	<LLD	<LLD	<LLD	<LLD	<LLD	<LLD	<LLD	<LLD	<LLD	<LLD	<LLD	<LLD
W	8.1	8.6	8.7	8.1	6.8	7.1	9.9	7.4	7.7	5.6	8.6	9.7	8.2	10.3	9.5	7.6	8.8	12.0	8.6
U	8.1	7.7	9.6	8.7	8.7	9.0	7.3	8.1	8.4	8.6	8.4	9.7	10.1	8.9	10.1	9.9	11.5	11.6	10.8
Th	31.6	28.0	44.7	36.7	40.3	33.5	37.3	29.3	33.7	27.1	41.7	37.0	37.6	34.8	40.7	36.5	44.8	52.1	43.9
Pb	96.4	94.8	72.8	65.9	58.2	50.4	34.6	91.2	52.5	63.1	45.0	44.9	52.1	72.3	43.8	63.3	54.5	69.3	59.9
As	8.2	16.4	6.1	12.4	3.2	8.9	10.0	20.2	13.9	10.1	5.8	17.2	7.9	11.8	7.6	14.7	16.8	12.0	10.5
Se	<LLD	<LLD	<LLD	1.4	<LLD	<LLD	<LLD	1.0	<LLD	<LLD	<LLD	2.1	1.0	1.1	1.8	1.7	3.3	<LLD	1.7
Bi	<LLD	<LLD	<LLD	<LLD	<LLD	<LLD	<LLD	<LLD	<LLD	<LLD	<LLD	<LLD	<LLD	<LLD	<LLD	<LLD	<LLD	<LLD	<LLD
Br	<LLD	<LLD	<LLD	<LLD	<LLD	<LLD	<LLD	<LLD	<LLD	<LLD	<LLD	<LLD	<LLD	<LLD	<LLD	<LLD	<LLD	<LLD	<LLD
La	65.5	73.8	69.7	65.7	64.0	56.2	54.5	62.2	67.1	64.6	56.4	76.6	75.0	96.6	61.4	66.2	83.6	103.6	52.1
Ce	136.4	156.8	143.0	134.8	142.7	115.2	120.7	128.4	140.6	136.2	115.9	153.4	160.9	193.5	130.9	138.5	174.6	212.4	110.1
Nd	62.8	64.4	58.8	65.0	63.5	48.7	56.8	52.9	65.0	60.0	55.1	71.8	70.6	83.4	56.0	63.1	74.1	104.5	48.8
D	-38.17	-38.6	-39.02	-39.5	-40.09	-41.09	-41.72	-42.34	-43.54	-44.66	-44.88	-45.87	-46.2	-46.87	-47.17	-47.68	-47.99	-48.46	-49.43

XRF data re-calculated volatile-free!

136	21b	21c	21d	22aa	22ab	22ac	22ad	22ae	22ba	22bb	22bc	22bd	22be	22ca	22cb	22cc	22da	22db	22dc
SiO_2	67.31	66.71	65.73	63.75	64.48	64.58	65.64	64.85	65.33	68.40	65.05	66.99	64.59	62.79	66.44	64.98	64.71	62.26	63.70
TiO_2	1.22	1.13	1.34	1.16	1.18	1.23	1.15	1.19	1.20	1.18	1.20	1.15	1.17	1.28	1.29	1.35	1.32	1.29	1.32
Al_2O_3	29.68	30.36	30.70	31.41	30.77	31.76	30.38	30.49	29.59	28.34	31.45	29.67	29.96	31.23	29.06	30.99	31.39	30.13	30.41
FeO	0.42	0.59	0.63	2.17	2.03	0.57	0.79	1.32	1.58	0.43	0.51	0.41	2.19	2.28	1.30	0.80	0.65	3.74	2.66
MgO	0.22	0.21	0.28	0.28	0.28	0.36	0.42	0.29	0.45	0.26	0.28	0.27	0.32	0.43	0.34	0.27	0.30	0.49	0.44
CaO	0.14	0.17	0.30	0.17	0.17	0.44	0.64	0.61	0.55	0.21	0.26	0.25	0.50	0.58	0.38	0.33	0.29	1.10	0.40
Na_2O	0.11	0.10	0.11	0.12	0.12	0.11	0.12	0.15	0.13	0.12	0.13	0.12	0.12	0.12	0.13	0.14	0.11	0.12	0.11
K_2O	0.81	0.67	0.82	0.82	0.85	0.81	0.78	0.97	1.02	0.88	0.92	0.85	0.71	0.87	0.79	0.82	0.91	0.66	0.94
P_2O_5	0.09	0.08	0.10	0.12	0.12	0.14	0.10	0.14	0.17	0.20	0.20	0.29	0.46	0.42	0.28	0.33	0.31	0.22	0.22
TOTAL	100.00	100.00	100.00	100.00	100.00	100.00	100.00	100.00	100.00	100.00	100.00	100.00	100.00	100.00	100.00	100.00	100.00	100.00	100.30
Mn	21.6	25.9	49.9	150.4	129.0	53.9	59.2	64.8	81.3	28.1	28.9	27.0	181.7	203.3	106.2	70.8	49.3	433.4	250.4
S	0.4100	1.0030	0.4610	0.5020	0.5960	0.4200	0.5140	2.7360	1.0520	0.6560	0.6940	0.3440	0.4690	0.2060	0.3400	0.5300	0.3250	0.3970	0.4270
Ba	395.8	340.3	470.0	513.4	547.6	602.9	425.6	661.9	722.4	834.6	880.2	1175.3	1404.5	1401.7	1017.9	1225.4	1189.4	878.9	871.4
Sc	26.6	18.9	17.6	19.0	17.7	25.4	27.3	22.1	29.9	22.4	23.2	23.9	18.2	22.2	24.8	20.7	24.4	19.2	17.4
Rb	85.2	67.6	82.2	88.6	91.7	84.8	83.1	105.7	99.1	90.7	86.4	95.6	69.4	89.1	75.8	87.9	90.1	64.4	98.3
Sr	141.1	140.0	193.1	207.6	228.8	261.9	158.5	273.4	262.1	341.7	332.9	500.5	699.4	680.3	454.1	589.8	468.8	342.5	370.2
Y	75.0	66.6	59.7	54.2	64.2	74.0	75.8	72.9	66.8	71.0	64.5	53.0	58.5	57.5	65.6	65.2	64.7	47.7	38.2
Zr	393.0	366.3	361.3	317.8	281.0	397.1	379.4	390.1	343.5	388.4	378.8	375.1	321.6	375.4	392.2	336.4	413.9	305.1	278.6
Nb	42.4	30.0	41.6	35.5	30.7	40.2	35.2	30.2	36.7	39.3	36.0	38.7	34.3	41.6	38.9	35.1	43.8	35.6	30.3
Mo	2.2	2.3	1.8	2.3	3.0	2.6	2.2	5.6	2.2	2.3	1.8	1.6	2.0	1.4	1.6	2.3	1.3	1.9	2.2
Co	3.9	7.2	6.3	5.9	13.9	5.4	6.5	33.5	6.3	7.8	7.0	2.8	4.5	3.5	5.0	7.2	4.1	5.3	3.8
Cr	96.3	61.3	66.3	68.9	47.8	73.7	74.4	76.2	75.2	78.9	88.1	78.4	65.5	85.9	94.4	82.5	90.6	76.3	58.3
V	142.3	74.9	102.8	100.5	61.1	130.8	91.5	111.2	116.1	121.8	128.8	101.4	79.0	111.2	108.0	91.8	125.0	98.8	73.6
Zn	21.8	40.4	21.7	48.1	73.4	33.8	31.4	69.7	41.2	23.7	25.6	14.1	22.8	32.2	26.6	39.6	24.1	40.6	25.0
Cu	39.2	28.9	45.8	40.2	33.1	43.3	35.6	40.7	29.4	35.5	25.0	24.3	28.7	35.1	22.3	31.0	33.6	34.0	27.4
Ni	16.0	16.5	15.6	16.1	29.2	22.0	23.4	38.9	25.1	23.0	17.9	11.4	14.9	16.0	18.5	20.8	12.3	16.8	9.7
Ge	<LLD	1.2	<LLD	<LLD	<LLD	<LLD	<LLD	<LLD	<LLD	<LLD	<LLD	<LLD	<LLD	<LLD	<LLD	1.3	<LLD	<LLD	<LLD
W	12.7	10.1	9.1	8.6	11.5	11.6	10.1	8.5	9.8	10.0	11.0	6.5	10.3	8.9	9.2	8.4	11.0	7.4	7.7
U	11.4	11.3	10.7	10.3	9.2	10.6	10.5	10.1	10.8	10.8	10.2	10.0	9.0	9.4	9.8	10.0	10.1	8.5	7.2
Th	42.5	46.2	47.5	41.3	34.8	43.4	41.6	36.4	37.4	46.6	43.7	53.2	45.1	45.2	43.8	38.2	45.7	38.4	37.3
Pb	60.6	46.7	40.6	64.2	64.8	47.8	44.9	99.2	36.0	46.5	49.1	62.3	41.2	50.5	33.9	46.3	50.8	142.5	24.7
As	9.3	8.2	11.7	13.5	30.1	19.4	14.7	31.5	25.0	21.1	8.2	5.5	4.8	5.3	3.6	4.5	1.2	4.4	3.2
Se	2.2	1.7	2.7	3.5	17.1	3.0	3.7	3.7	2.0	2.4	1.7	<LLD	1.7	1.6	<LLD	1.7	<LLD	1.3	<LLD
Bi	<LLD	<LLD	<LLD	<LLD	<LLD	<LLD	<LLD	<LLD	<LLD	<LLD	<LLD	<LLD	<LLD	<LLD	<LLD	<LLD	<LLD	<LLD	<LLD
Br	6.0	<LLD	<LLD	<LLD	<LLD	<LLD	<LLD	<LLD	<LLD	<LLD	<LLD	<LLD	<LLD	<LLD	<LLD	5.0D	<LLD	4.5	<LLD
La	95.7	76.6	80.3	72.2	68.0	83.1	81.8	71.4	77.9	81.4	70.1	72.8	67.7	73.0	58.4	73.2	76.9	63.0	64.9
Ce	197.2	156.0	169.1	148.5	141.6	180.4	161.4	146.6	163.4	171.9	153.5	160.5	146.9	153.6	134.8	155.0	148.4	121.9	126.2
Nd	88.3	73.9	77.9	67.7	66.7	85.4	76.8	70.1	74.8	82.0	69.0	64.9	67.6	67.6	55.2	73.6	57.7	50.5	46.6
D	-49.73	-50.15	-51.24	-52.15	-52.53	-52.8	-53.52	-54.39	-55.09	-55.39	-56.38	-57	-57.53	-59.05	-59.77	-60.21	-60.64	-61.59	-62.49

136	22dd	22de	22ea	22eb	22ec	22ed	22ee	22fsa	22fsb	22fsc	23asa	23asb	23asc	23asd	23ase	23bsa	0a	0b	0c
SiO_2	63.99	64.29	63.40	59.56	62.09	55.93	54.73	57.78	54.53	54.46	61.70	60.99	65.54	65.24	63.90	68.21	74.60	72.21	57.24
TiO_2	1.27	1.38	1.31	1.32	1.46	1.37	1.70	1.79	1.80	1.79	2.13	2.17	1.84	1.88	2.01	1.18	0.91	0.76	0.52
Al_2O_3	31.00	27.42	31.64	31.21	33.16	33.15	31.01	35.04	36.31	39.26	34.53	34.46	30.22	30.64	32.38	28.96	20.26	20.55	11.09
FeO	1.23	3.31	0.98	3.34	0.98	5.24	5.13	1.74	3.12	1.95	0.49	0.73	0.67	0.70	0.51	0.72	2.32	4.74	25.22
MgO	0.52	0.73	0.47	0.98	0.43	0.96	0.99	0.53	0.77	0.48	0.25	0.30	0.36	0.33	0.27	0.16	0.41	0.38	1.46
CaO	0.89	1.89	0.87	2.07	0.63	2.06	4.56	1.34	1.92	0.88	0.12	0.58	0.13	0.13	0.12	0.11	0.13	0.15	3.47
Na_2O	0.12	0.14	0.14	0.15	0.14	0.16	0.18	0.19	0.18	0.15	0.06	0.07	0.08	0.07	0.07	0.04	0.06	0.06	0.06
K_2O	0.68	0.63	0.83	0.69	0.73	0.65	0.57	0.79	0.72	0.60	0.66	0.64	1.11	0.96	0.70	0.53	1.26	1.11	0.87
P_2O_5	0.29	0.21	0.35	0.68	0.38	0.49	1.14	0.81	0.66	0.44	0.07	0.06	0.05	0.06	0.05	0.09	0.05	0.05	0.06
TOTAL	100.00	100.00	100.00	100.00	100.00	100.00	100.00	100.00	100.00	100.00	100.00	100.00	100.00	100.00	100.00	100.00	100.00	100.00	100.00
Mn	107.5	420.3	72.6	321.4	73.9	455.7	660.1	154.9	311.6	173.7	28.5	55.4	35.5	40.1	25.6	45.1	38.6	64.3	174.5
S	0.4970	0.2980	0.3820	0.6120	0.4020	0.7380	0.5210	0.4120	0.5120	0.4480	0.4720	0.1840	0.1000	0.2920	0.1340	0.0880	1.1920	2.1350	12.1070
Ba	1056.8	634.3	1388.9	2138.8	282.8	285.7	371.1	361.5	318.0	331.9	1431.6	1501.5	622.3	1762.9	1492.4	1100.9	281.0	289.4	571.3
Sc	20.5	21.4	23.1	26.3	58.4	29.4	33.6	55.8	42.6	25.3	30.5	24.1	20.0	28.0	25.5	28.3	17.4	15.1	13.5
Rb	56.1	51.3	76.7	63.3	53.3	71.0	144.9	95.1	69.6	46.8	62.0	43.8	33.6	59.9	48.0	41.1	117.4	99.3	67.3
Sr	411.9	247.4	565.4	903.2	63.2	76.7	71.7	59.8	55.8	81.8	519.4	535.8	309.9	697.6	560.1	449.4	137.7	129.7	214.6
Y	55.4	53.4	54.0	88.4	117.7	87.7	102.6	134.1	109.8	57.2	68.3	40.5	51.7	72.7	67.4	66.7	63.5	75.3	118.8
Zr	363.2	353.3	370.5	480.1	710.8	874.6	736.2	636.3	713.7	706.2	521.6	344.0	321.1	489.1	432.2	523.0	352.8	311.7	601.9
Nb	41.5	40.8	39.8	44.6	71.2	93.4	85.6	69.3	79.1	41.1	47.1	35.6	35.6	49.1	44.2	51.4	38.1	26.0	21.1
Mo	1.8	1.6	1.5	1.8	6.1	7.5	10.3	7.2	7.0	1.8	1.1	1.5	1.6	1.9	2.1	1.3	9.0	4.5	13.4
Co	7.1	5.7	5.9	5.6	4.8	7.6	7.2	4.9	9.3	7.2	7.5	7.5	5.0	3.7	8.0	18.9	27.2	11.2	108.7
Cr	80.2	79.2	80.1	95.1	124.7	106.9	80.6	130.5	127.0	131.1	297.2	155.4	106.4	204.0	142.3	135.6	71.1	62.2	61.4
V	102.5	89.8	116.6	128.8	167.5	147.2	97.6	151.0	172.9	175.9	238.6	123.9	112.8	244.2	126.8	71.4	117.5	92.9	143.7
Zn	27.3	28.5	23.7	38.2	19.7	42.8	24.9	17.8	25.4	45.1	23.0	25.4	15.1	20.3	20.3	20.1	95.6	107.7	104.9
Cu	24.2	26.1	35.6	30.6	42.4	76.3	47.0	32.1	50.3	33.1	34.0	22.9	33.9	38.3	28.0	37.8	23.2	23.0	21.0
Ni	20.6	23.6	19.1	19.8	32.9	71.2	31.1	34.7	53.8	50.7	21.9	25.0	27.4	29.2	24.8	29.0	35.6	11.7	160.6
Ge	<LLD	<LLD	<LLD	<LLD	2.5	2.2	2.4	1.9	3.2	1.4	<LLD	<LLD	1.2	1.2	1.1	1.2	<LLD	<LLD	60.0
W	10.1	10.2	9.0	11.6	15.8	23.3	23.8	14.3	21.4	7.1	9.4	8.8	9.2	11.9	9.1	14.0	7.8	8.0	15.2
U	9.3	9.3	10.4	15.3	14.0	16.4	12.7	13.0	12.1	9.5	10.6	9.4	9.6	14.1	11.3	13.1	27.2	11.4	8.7
Th	42.0	46.6	42.8	50.6	85.6	85.9	68.8	54.5	64.3	54.1	47.4	42.0	35.0	49.4	40.4	52.6	32.6	30.0	20.1
Po	42.0	32.9	54.7	75.3	72.0	92.0	68.7	60.3	40.7	39.2	68.5	51.7	39.2	62.4	59.9	76.1	135.3	102.9	75.3
As	2.3	2.1	2.8	2.2	2.9	4.2	6.3	3.0	4.4	8.2	2.7	3.1	4.8	3.3	2.5	2.8	35.2	42.2	245.1
Se	1.6	1.2	<LLD	2.3	5.0	10.1	4.9	4.4	4.1	4.4	3.0	1.4	0.9	2.4	1.9	2.8	3.7	1.3	3.9
Br	<LLD	<LLD	<LLD	<LLD	<LLD	<LLD	<LLD	<LLD	<LLD	<LLD	<LLD	<LLD	<LLD	<LLD	<LLD	<LLD	<LLD	<LLD	<LLD
Bi	<LLD	<LLD	<LLD	<LLD	5.3	7.0	6.8	4.4	6.4	<LLD	3.9	<LLD	<LLD	5.6	4.6	4.7	<LLD	<LLD	
La	64.0	44.4	84.9	118.2	92.7	94.4	65.0	119.0	106.3	97.8	51.0	32.6	31.0	32.7	28.5	45.8	77.2	77.2	53.4
Ce	130.9	92.7	178.1	245.8	194.6	189.6	134.9	247.5	222.2	201.5	151.8	77.5	66.8	81.9	64.2	86.8	183.2	156.7	105.6
Nd	58.7	40.1	75.1	111.3	86.1	82.8	57.4	102.7	92.1	83.6	75.1	39.7	39.4	48.2	36.2	31.7	74.0	70.2	43.5
Cs																	9.7	5.6	3.5
D	-62.8	-63.44	-64.04	-64.36	-65.02	-65.62	-66.2	-66.54	-67	-68.07	-73.53	-73.69	-74.89	-75.89	-77.23	-78.84	0.35	0.12	0

XRF data re-calculated volatile-free! Samples 137_0a, _0b and 0c presented on previous page.

137	1Ba	1Bb	1Bc	1Bd	1Be	1Ca	1Cb	1Cc	1Cd	1Ce	1Cf	1Cg	1Da	1Db	1Dc	1Dd	2a	2b	2c
SiO_2	73.43	76.37	71.66	70.49	73.93	73.20	74.18	71.38	71.47	70.76	72.69	74.31	72.78	73.65	72.85	73.47	68.57	71.51	73.34
TiO_2	0.82	0.76	0.65	0.97	0.79	0.69	0.83	0.80	0.82	0.83	0.75	0.77	0.81	0.85	0.82	0.86	0.83	0.82	0.88
Al_2O_3	20.39	18.84	16.32	24.11	20.10	17.22	20.18	22.16	22.09	23.55	21.66	20.28	21.21	21.13	21.33	20.63	23.83	20.30	21.22
FeO	2.26	1.09	5.69	1.28	1.54	3.21	1.01	1.84	1.59	1.25	1.26	1.27	1.40	1.18	1.21	1.36	2.57	2.92	1.13
MgO	0.53	0.50	1.91	0.59	0.57	1.36	0.57	0.50	0.61	0.54	0.52	0.51	0.51	0.39	0.51	0.52	0.66	0.73	0.47
CaO	0.21	0.21	1.73	0.20	0.18	1.43	0.18	0.18	0.25	0.20	0.19	0.23	0.22	0.17	0.22	0.33	0.31	0.35	0.24
Na_2O	0.08	0.08	0.08	0.07	0.10	0.11	0.10	0.13	0.13	0.11	0.12	0.12	0.14	0.14	0.15	0.15	0.18	0.21	0.15
K_2O	2.18	2.09	1.90	2.22	2.74	2.71	2.90	2.98	2.99	2.71	2.76	2.46	2.88	2.43	2.84	2.63	2.92	3.09	2.53
P_2O_5	0.11	0.07	0.04	0.07	0.05	0.07	0.04	0.04	0.05	0.07	0.04	0.06	0.05	0.07	0.08	0.05	0.12	0.07	0.03
TOTAL	100.00	100.00	100.00	100.00	100.00	100.00	100.00	100.00	100.00	100.00	100.00	100.00	100.00	100.00	100.00	100.00	100.00	100.00	100.00
Mn	40.6	28.3	124.7	27.8	54.4	122.3	33.2	36.4	67.3	58.7	59.7	67.6	53.5	37.8	60.1	68.5	77.4	139.5	53.2
S	0.6340	0.1110	0.1350	0.4380	0.3330	0.0600	0.2170	0.4880	0.1660	0.1520	0.3650	0.8330	0.3350	0.7940	0.2560	0.3580	0.3090	0.2050	0.2110
Ba	582.9	347.2	331.5	302.2	452.3	439.1	445.9	603.2	481.2	440.9	540.0	437.6	611.8	544.8	489.6	456.3	515.3	508.3	432.8
Sc	15.7	12.0	15.8	13.3	11.9	13.7	15.9	12.6	14.9	12.8	12.8	16.5	14.2	10.3	12.4	12.2	17.3	22.3	16.9
Rb	158.1	171.4	150.7	157.7	174.9	182.8	196.6	190.3	199.6	183.7	185.9	173.0	204.2	155.0	178.6	189.8	201.4	201.3	169.9
Sr	340.5	229.5	160.0	176.5	165.1	308.9	148.3	152.2	169.3	257.0	152.8	195.9	160.5	231.8	274.0	165.2	411.8	171.1	85.0
Y	63.2	47.0	46.0	34.6	40.1	53.6	57.9	46.5	49.2	61.6	49.8	68.9	49.5	49.6	51.8	48.4	90.0	89.5	68.6
Zr	304.2	312.4	332.2	299.5	257.2	337.7	334.6	277.0	286.0	239.3	245.9	298.3	287.4	262.1	251.7	286.4	338.5	484.2	394.2
Nb	32.4	31.1	26.8	42.7	25.4	28.4	31.4	26.7	30.2	28.0	22.8	24.0	31.5	18.7	23.7	29.7	30.1	34.6	30.9
Mo	3.9	1.4	1.7	3.8	1.2	1.5	1.7	1.3	1.8	1.9	0.8	2.1	1.9	0.8	0.9	1.4	1.5	1.2	2.1
Co	26.8	5.0	5.4	5.6	4.6	4.4	3.2	4.5	3.1	2.2	<LLD	4.4	3.1	7.8	4.9	4.6	4.6	18.5	5.1
Cr	56.5	53.1	48.9	63.6	54.0	50.4	60.4	48.4	51.2	42.4	47.6	54.1	50.1	47.6	49.7	50.4	61.8	59.1	63.1
V	77.5	74.8	60.3	108.0	56.1	64.7	83.2	54.4	63.2	59.8	62.2	79.5	67.5	52.4	59.4	62.8	80.9	99.4	91.6
Zn	87.3	89.5	64.4	55.9	47.9	51.9	79.7	60.1	61.6	54.6	55.8	69.2	51.7	60.0	60.9	50.8	79.4	59.2	61.0
Cu	37.5	18.8	16.3	14.8	28.8	15.7	10.0	12.6	20.1	12.3	18.8	25.2	12.0	17.8	23.3	12.0	56.8	26.9	16.4
Ni	24.1	4.9	3.8	<LLD	2.5	3.9	1.6	3.1	1.5	<LLD	<LLD	3.0	2.4	3.4	4.4	5.3	14.9	38.3	0.7
Ge	<LLD	<LLD	<LLD	<LLD	<LLD	<LLD	<LLD	<LLD	<LLD	<LLD	<LLD	<LLD	<LLD	<LLD	<LLD	<LLD	<LLD	<LLD	<LLD
W	7.2	5.8	6.6	7.6	8.2	7.4	6.8	8.6	7.1	7.0	7.0	7.1	1.7	4.5	4.0	6.9	10.9	11.6	7.9
U	7.1	7.7	5.5	12.3	5.7	7.0	7.4	5.5	6.5	10.6	6.4	9.4	5.7	6.1	6.2	6.5	10.1	8.3	8.3
Th	30.5	27.9	23.2	41.1	28.4	24.3	25.7	30.4	30.4	44.4	31.0	34.2	29.2	26.8	29.1	25.7	35.2	31.2	28.5
Pb	78.7	39.9	51.4	17.8	18.3	26.1	32.6	15.6	17.4	25.5	26.7	36.1	29.2	34.0	25.4	20.3	46.8	49.8	32.7
As	11.9	4.1	4.6	2.8	5.7	3.3	2.5	2.5	1.9	1.8	1.7	3.1	4.1	3.6	3.2	5.0	4.7	11.6	2.2
Se	2.0	<LLD	<LLD	<LLD	<LLD	<LLD	<LLD	<LLD	<LLD	<LLD	<LLD	<LLD	<LLD	<LLD	<LLD	<LLD	<LLD	<LLD	<LLD
Br	<LLD	<LLD	<LLD	<LLD	<LLD	<LLD	<LLD	<LLD	<LLD	<LLD	<LLD	<LLD	<LLD	<LLD	<LLD	<LLD	<LLD	<LLD	<LLD
Bi	4.0	<LLD	<LLD	<LLD	<LLD	<LLD	<LLD	<LLD	<LLD	<LLD	<LLD	3.8	<LLD	<LLD	<LLD	<LLD	<LLD	<LLD	<LLD
La	58.2	66.5	28.2	84.5	47.9	62.0	62.3	53.3	53.3	59.6	55.1	83.8	53.8	56.1	57.6	57.3	82.1	47.6	42.0
Ce	126.3	139.6	65.5	169.3	105.5	137.2	136.5	110.8	121.3	123.5	120.4	171.1	116.2	118.6	121.5	121.0	176.5	110.0	92.8
Nd	62.7	61.2	26.6	38.1	45.5	55.5	60.8	46.4	53.0	54.1	53.9	79.2	53.3	55.9	57.0	51.6	93.0	51.0	42.2
Cs	6.4	9.2	10.3	13.8	7.7	10.2	15.8	12.3	13.4	13.9	15.0	13.3	13.7	10.9	6.9	14.2	8.4	10.0	10.8
D	-0.85	-1.07	-1.84	-2.38	-2.7	-3.5	-3.98	-4.54	-4.89	-5.3	-5.66	-6.13	-6.28	-6.74	-7.09	-7.37	-8	-8.58	-9.16

137	2d	2e	3a	3b	4	5	6a	7a	7b	7c	8a	8b	8c	8d	8e	9a	9b	9c	10a
SiO_2	74.04	75.17	74.31	71.41	71.35	72.74	74.80	71.84	72.42	74.22	71.80	71.14	71.67	77.44	72.93	74.22	74.93	70.42	72.11
TiO_2	0.82	0.73	0.82	0.87	0.91	0.89	0.80	0.95	0.96	0.89	0.96	0.93	0.89	0.83	0.88	0.91	0.81	0.90	0.95
Al_2O_3	21.04	20.43	21.03	23.83	23.63	22.72	21.89	24.17	23.59	21.94	23.58	24.90	24.55	19.01	23.28	22.21	21.29	23.83	23.58
FeO	1.17	0.91	0.86	1.04	1.15	0.89	0.67	0.79	0.81	0.71	1.23	0.94	0.93	0.67	0.76	0.63	1.15	2.68	1.13
MgO	0.42	0.39	0.41	0.41	0.43	0.39	0.27	0.33	0.32	0.32	0.40	0.33	0.27	0.27	0.32	0.28	0.25	0.30	0.34
CaO	0.23	0.22	0.16	0.20	0.19	0.18	0.18	0.16	0.16	0.15	0.20	0.15	0.14	0.13	0.14	0.14	0.13	0.16	0.18
Na_2O	0.14	0.14	0.13	0.13	0.13	0.13	0.12	0.12	0.13	0.13	0.13	0.11	0.11	0.13	0.12	0.12	0.11	0.13	0.13
K_2O	2.12	1.95	2.23	2.06	2.17	1.99	1.23	1.60	1.57	1.58	1.64	1.45	1.40	1.48	1.54	1.45	1.28	1.47	1.53
P_2O_5	0.04	0.05	0.06	0.05	0.05	0.07	0.04	0.05	0.05	0.06	0.07	0.06	0.05	0.04	0.04	0.05	0.05	0.11	0.05
TOTAL	100.00	100.00	100.00	100.00	100.00	100.00	100.00	100.00	100.00	100.00	100.00	100.00	100.00	100.00	100.00	100.00	100.00	100.00	100.00
Mn	45.1	53.0	45.1	49.8	56.2	49.7	39.9	132.2	99.4	48.5	236.9	215.8	200.7	44.0	37.0	33.3	34.8	421.2	46.8
S	0.9020	1.5240	0.4140	0.4260	0.3920	0.2950	1.0920	0.1830	0.2420	0.3990	0.1450	0.1810	0.1730	0.5250	0.2300	0.1720	0.7060	0.5100	0.0710
Ba	375.2	396.6	378.7	356.5	353.7	362.5	285.1	611.8	322.2	327.5	415.1	317.6	308.5	323.7	584.7	504.0	346.0	961.2	310.9
Sc	12.8	13.0	13.1	14.6	15.2	13.5	10.1	15.6	15.4	12.9	19.9	31.6	14.9	11.9	10.1	11.7	9.5	7.5	14.7
Rb	150.0	142.5	157.2	150.3	161.2	153.9	121.5	129.8	130.2	126.8	145.0	117.0	136.0	130.8	121.3	114.5	115.6	116.4	133.0
Sr	143.6	148.1	137.7	139.1	132.3	204.2	130.0	101.7	103.3	166.0	163.1	129.9	113.6	123.5	119.4	123.3	96.9	237.4	65.9
Y	42.1	45.8	48.0	52.0	50.4	47.5	37.7	58.8	62.9	54.8	70.1	65.6	66.8	51.0	50.7	46.8	47.9	35.8	48.4
Zr	278.3	269.4	240.7	285.2	296.1	287.3	272.2	319.3	330.3	264.1	337.7	320.0	316.8	257.7	253.3	265.9	251.5	285.1	334.2
Nb	21.2	16.6	22.8	29.7	31.7	29.6	17.0	35.2	35.4	25.5	34.9	32.9	32.4	20.7	28.5	31.3	20.0	24.5	35.2
Mo	1.3	1.6	1.1	1.3	1.0	1.3	1.5	1.4	1.6	0.9	1.9	1.5	1.5	1.1	1.1	1.0	2.3	1.3	2.3
Co	6.9	11.8	4.2	5.9	4.1	2.8	4.6	3.9	5.1	4.1	3.6	<LLD	1.9	7.1	2.1	2.8	6.0	6.4	4.9
Cr	59.2	54.0	51.9	56.1	58.2	56.6	49.7	64.1	61.2	51.7	68.2	57.9	55.9	47.9	44.1	53.5	37.1	47.1	60.1
V	73.1	75.1	59.7	78.3	71.7	69.4	67.2	94.1	98.3	60.8	90.8	84.7	64.3	52.8	46.4	63.2	39.4	48.1	84.1
Zn	45.0	52.3	32.2	43.9	51.6	38.7	44.8	51.4	38.9	54.7	60.5	56.3	45.9	39.9	26.1	26.9	27.5	44.7	35.4
Cu	22.2	20.8	18.0	24.2	24.5	17.9	18.8	24.9	21.4	22.4	26.1	24.7	13.0	19.9	28.7	21.7	17.1	27.7	15.6
Ni	3.4	3.7	3.4	4.6	6.7	<LLD	<LLD	3.9	3.2	1.7	4.0	2.2	<LLD	<LLD	<LLD	<LLD	<LLD	6.2	5.5	9.2
Ge	<LLD	<LLD	<LLD	<LLD	<LLD	<LLD	<LLD	<LLD	<LLD	<LLD	<LLD	<LLD	<LLD	<LLD	<LLD	<LLD	<LLD	<LLD	<LLD
W	6.4	7.7	10.0	7.2	5.4	5.4	4.3	7.7	8.5	6.7	10.2	8.6	6.8	7.6	9.0	8.0	8.0	9.7	8.7
U	5.9	6.3	6.3	7.3	8.0	5.6	6.7	7.3	7.5	6.8	8.3	8.0	6.8	5.8	7.1	7.2	6.9	4.7	9.0
Th	36.1	24.5	30.1	31.9	32.2	30.0	27.5	29.6	32.9	34.0	37.7	36.9	43.2	24.4	29.4	31.2	23.8	31.7	34.6
Pb	28.2	17.5	24.6	27.6	69.9	132.1	96.0	102.7	69.4	70.8	61.6	54.8	0.3	21.0	23.8	25.4	25.7	14.5	33.9
As	1.9	2.7	<LLD	3.1	6.9	4.2	3.3	2.9	3.8	2.1	2.4	1.6	22.9	1.4	2.0	1.5	3.5	5.2	4.4
Se	<LLD	<LLD	<LLD	<LLD	<LLD	<LLD	<LLD	<LLD	<LLD	<LLD	<LLD	<LLD	<LLD	<LLD	<LLD	<LLD	<LLD	1.5	2.5
Bi	<LLD	<LLD	<LLD	<LLD	<LLD	<LLD	<LLD	<LLD	<LLD	<LLD	<LLD	<LLD	<LLD	<LLD	<LLD	<LLD	<LLD	<LLD	<LLD
Br	<LLD	<LLD	<LLD	<LLD	<LLD	<LLD	1.9	3.3	<LLD	<LLD	<LLD	<LLD	<LLD	<LLD	<LLD	<LLD	<LLD	<LLD	4.2
La	62.3	59.4	58.3	59.9	60.1	56.4	58.4	61.1	56.8	62.5	83.7	62.8	67.6	56.1	53.8	47.7	51.8	44.5	48.0
Ce	134.9	133.4	124.0	136.6	131.0	122.4	121.9	128.2	123.9	132.8	185.5	135.7	145.0	116.7	119.4	103.8	108.1	95.5	107.1
Nd	58.4	58.8	58.2	61.4	57.8	58.0	52.4	55.5	55.8	66.2	89.3	63.0	67.0	55.3	51.1	45.9	44.8	41.4	44.9
Cs	11.6	10.1	11.5	11.2	12.0	10.4	13.3	10.7	11.4	9.0	11.6	7.0	14.0	10.0	8.8	8.8	7.8	8.8	8.8
D	-10.11	-10.48	-11.13	-11.77	-13.24	-14.7	-17.15	-19.46	-20.22	-21.43	-21.88	-22.72	-22.88	-23.19	-24.22	-24.71	-25.23	-25.75	-26.38

XRF data re-calculated volatile-free!

137	10b	10c	10d	11a	11b	12a	12b	12c	12d	12e	13	14a	14b	14c	14d	14e	15Aa	15Ab	15Ac
SiO_2	70.72	69.79	72.41	71.90	74.55	72.63	71.77	72.62	72.31	69.33	71.56	71.43	59.88	71.75	74.26	69.14	71.07	70.02	70.77
TiO_2	0.97	0.88	0.95	0.93	0.85	0.96	0.98	0.91	0.92	0.93	0.98	0.99	0.79	0.91	1.03	0.85	0.95	0.95	0.97
Al_2O_3	24.86	26.60	23.95	24.93	22.76	24.54	25.26	23.71	24.17	27.41	25.28	25.19	20.29	24.84	22.67	25.02	25.56	26.44	25.21
FeO	1.23	0.73	0.66	0.54	0.41	0.40	0.40	1.01	0.98	0.61	0.51	0.57	11.43	0.78	0.54	3.07	0.56	0.79	1.11
MgO	0.35	0.31	0.29	0.26	0.20	0.23	0.23	0.29	0.24	0.26	0.25	0.27	0.76	0.27	0.25	0.34	0.30	0.29	0.32
CaO	0.18	0.15	0.15	0.14	0.14	0.15	0.13	0.21	0.16	0.21	0.13	0.14	5.61	0.13	0.16	0.30	0.17	0.13	0.16
Na_2O	0.12	0.10	0.11	0.10	0.10	0.11	0.11	0.12	0.14	0.11	0.14	0.15	0.14	0.14	0.15	0.14	0.14	0.13	0.12
K_2O	1.52	1.39	1.41	1.15	0.95	0.94	1.06	1.07	1.03	1.08	1.09	1.18	1.02	1.10	0.90	1.04	1.16	1.18	1.24
P_2O_5	0.05	0.06	0.08	0.06	0.05	0.04	0.06	0.06	0.05	0.07	0.07	0.08	0.09	0.08	0.06	0.09	0.09	0.09	0.11
TOTAL	100.00	100.00	100.00	100.00	100.00	100.00	100.00	100.00	100.00	100.00	100.00	100.00	100.00	100.00	100.00	100.00	100.00	100.00	100.00
Mn	55.4	41.0	39.3	33.4	24.5	24.2	20.3	45.9	32.9	32.1	27.4	27.1	0.3	59.3	34.6	449.0	40.6	46.0	92.9
S	0.1110	0.1000	0.1880	0.2810	0.2760	0.2390	0.2310	0.9280	0.6190	0.3530	0.4210	0.3140	2.7070	1.1620	0.4500	1.8110	0.5210	0.4030	0.7060
Ba	304.2	268.8	343.8	280.0	230.7	262.9	312.6	319.4	306.8	334.8	385.8	430.2	445.7	461.3	350.7	512.6	517.2	587.9	675.0
Sc	16.1	14.2	15.6	14.7	12.0	12.1	15.6	17.0	12.0	14.0	12.6	13.8	16.2	17.1	13.4	15.2	15.5	12.1	14.3
Rb	124.3	112.1	118.0	98.7	82.8	84.6	96.3	111.1	102.4	92.5	102.7	107.6	106.1	104.9	98.5	100.9	111.7	106.9	111.6
Sr	73.9	61.2	127.0	136.8	90.1	73.5	109.5	120.3	136.8	141.4	161.6	157.2	239.3	179.1	136.5	217.6	180.3	179.1	210.5
Y	48.2	57.2	59.4	61.7	47.8	41.8	58.5	60.7	54.5	50.8	56.6	48.6	79.9	64.9	63.1	61.0	56.0	50.5	53.3
Zr	338.0	316.9	334.1	333.8	298.1	301.8	332.7	350.1	278.2	286.6	318.5	318.5	278.9	303.3	342.1	330.7	318.3	269.9	284.3
Nb	39.1	36.8	33.6	33.2	29.2	31.3	36.4	26.2	25.2	27.3	29.9	34.3	17.3	17.4	31.5	23.8	29.4	29.0	27.7
Mo	2.9	1.9	1.3	1.1	1.3	1.1	1.3	1.2	1.6	1.0	0.9	1.0	3.9	1.2	1.8	1.9	1.2	1.4	1.4
Co	9.5	3.0	3.5	3.0	1.9	2.3	3.4	9.1	4.2	3.8	2.8	3.6	15.3	17.1	5.6	13.4	5.1	6.4	12.7
Cr	63.8	53.1	63.7	55.6	45.8	46.7	59.1	61.2	53.8	49.7	65.2	56.0	53.1	57.6	52.4	61.8	58.9	48.4	57.1
V	95.0	78.0	93.0	79.3	62.1	57.9	83.7	95.0	62.4	51.7	75.2	77.2	71.1	73.6	70.3	102.2	77.3	49.4	67.5
Zn	47.5	39.9	56.6	49.2	27.5	18.7	28.1	37.7	34.3	34.9	32.3	27.3	75.2	35.6	21.6	36.3	26.0	36.8	101.0
Cu	18.2	8.4	27.3	23.0	15.9	14.7	23.2	19.3	18.3	18.5	27.2	20.6	22.4	20.3	16.0	23.0	19.9	18.5	24.8
Ni	29.8	1.9	2.6	0.7	0.7	0.7	0.7	3.1	2.1	0.7	1.5	1.7	10.4	5.0	1.7	8.0	2.6	5.4	12.1
Ge	<LLD	<LLD	<LLD	<LLD	<LLD	<LLD	<LLD	<LLD	<LLD	<LLD	<LLD	<LLD	<LLD	<LLD	<LLD	<LLD	<LLD	<LLD	<LLD
W	9.3	9.6	9.3	8.9	7.8	6.7	6.2	5.1	8.4	8.6	6.7	10.1	10.4	9.2	9.1	2.3	5.5	7.6	7.2
U	9.2	9.0	8.7	9.1	6.6	7.1	9.2	6.6	7.6	8.7	7.8	7.6	7.7	8.8	8.2	7.7	7.8	8.3	7.6
Th	35.3	39.3	34.5	36.8	29.0	35.2	46.1	35.7	34.0	34.4	34.2	30.6	26.4	32.0	37.0	34.6	39.3	34.3	35.2
Pb	55.3	47.3	41.4	1099.0	265.0	234.2	240.0	205.2	38.0	41.9	38.6	40.3	64.3	25.4	24.1	202.3	601.7	342.4	307.1
As	7.2	2.5	2.7	13.7	3.1	2.0	1.9	7.1	5.4	6.8	3.4	3.4	12.3	2.4	2.7	6.7	12.1	14.8	10.6
Se	5.4	<LLD	<LLD	<LLD	<LLD	<LLD	<LLD	<LLD	<LLD	1.9	<LLD	<LLD	<LLD	<LLD	<LLD	<LLD	<LLD	<LLD	<LLD
Bi	<LLD	<LLD	<LLD	<LLD	<LLD	<LLD	<LLD	<LLD	<LLD	<LLD	<LLD	<LLD	<LLD	<LLD	<LLD	<LLD	<LLD	<LLD	<LLD
Br	<LLD	<LLD	<LLD	<LLD	<LLD	<LLD	<LLD	<LLD	<LLD	<LLD	<LLD	<LLD	2.9	2.1	2.0	2.3	<LLD	<LLD	<LLD
La	47.2	63.7	61.9	73.6	53.0	47.6	66.8	68.0	65.2	72.3	74.0	53.8	69.1	92.1	60.7	76.1	67.8	61.3	60.4
Ce	103.4	131.8	137.8	153.4	113.3	102.3	148.5	142.8	144.7	153.6	158.0	115.0	147.8	195.9	137.7	163.4	146.2	135.6	132.5
Nd	43.2	56.7	62.1	62.2	47.8	42.1	69.3	62.3	65.1	61.3	67.6	48.5	68.4	81.0	58.6	74.1	62.7	55.9	58.4
Cs	9.0	9.2	9.6	6.9	8.2	14.5	10.8	18.5	11.0	10.7	8.5	8.8	7.3	12.9	21.4	11.9	11.9	9.4	11.0
D	-26.55	-27.28	-27.81	-28.43	-29.21	-29.92	-30.39	-31.32	-31.52	-31.91	-32.18	-33.46	-33.74	-34.26	-34.43	-35.32	-36.02	-36.72	-37.42

137	15Ad	15Ba	15Bb	15Bc	15Bd	16a	16b	17a	17b	17c	17d	18	19a	19b	19c	19d	19e	20a	20b
SiO_2	72.71	72.43	71.88	70.23	71.94	69.91	71.36	70.76	71.28	69.99	68.36	69.02	67.38	68.76	67.44	66.79	64.48	68.32	64.43
TiO_2	0.96	1.01	0.93	0.98	0.98	1.08	1.03	1.00	1.02	1.02	0.95	1.08	1.11	1.13	1.09	1.07	1.06	1.23	1.09
Al_2O_3	23.98	24.40	24.80	26.60	24.85	26.98	25.78	26.30	25.60	26.95	27.94	27.62	29.41	28.29	29.38	29.63	31.91	28.12	29.91
FeO	0.63	0.59	0.87	0.73	0.74	0.56	0.51	0.46	0.51	0.62	1.24	0.86	0.58	0.44	0.53	1.19	1.16	0.66	3.27
MgO	0.28	0.27	0.24	0.25	0.24	0.25	0.22	0.24	0.27	0.24	0.27	0.26	0.26	0.24	0.27	0.22	0.25	0.29	0.23
CaO	0.13	0.14	0.13	0.18	0.13	0.13	0.13	0.12	0.14	0.13	0.16	0.13	0.12	0.12	0.14	0.11	0.13	0.14	0.14
Na_2O	0.12	0.11	0.11	0.10	0.11	0.10	0.09	0.09	0.10	0.10	0.09	0.11	0.10	0.10	0.10	0.11	0.09	0.11	0.10
K_2O	1.12	0.98	0.95	0.86	0.94	0.91	0.80	0.95	1.01	0.86	0.91	0.86	0.95	0.85	0.96	0.80	0.83	1.03	0.74
P_2O_5	0.08	0.08	0.08	0.08	0.08	0.07	0.07	0.08	0.08	0.08	0.08	0.08	0.09	0.08	0.10	0.08	0.10	0.11	0.10
TOTAL	100.00	100.00	100.00	100.00	100.00	100.00	100.00	100.00	100.00	100.00	100.00	100.00	100.00	100.00	100.00	100.00	100.00	100.00	100.00
Mn	47.8	41.7	86.2	67.2	57.5	23.4	28.8	23.4	26.5	28.7	56.1	66.9	34.4	24.9	29.9	23.7	61.0	45.2	44.0
S	0.4510	0.3340	0.3280	0.2640	0.2720	0.1190	0.2420	0.3560	0.4310	0.5790	0.8890	0.1680	0.1860	0.2600	1.6070	0.6530	0.5540	0.4390	2.0310
Ba	512.8	476.7	489.5	424.6	445.1	426.6	444.0	475.5	523.7	468.0	473.0	463.9	534.1	427.9	546.4	445.1	522.8	607.1	489.2
Sc	14.9	17.0	13.7	18.1	16.8	15.8	14.2	13.5	15.4	16.1	20.0	13.0	17.2	18.2	25.7	14.9	18.4	22.9	19.2
Rb	104.2	101.8	91.5	82.6	90.6	94.3	85.8	95.9	106.3	92.4	92.1	97.3	99.8	87.3	116.3	86.4	92.2	111.5	82.5
Sr	167.9	146.0	176.6	141.9	130.2	112.8	133.3	145.1	153.1	144.7	141.2	131.8	160.0	134.0	147.7	146.2	176.9	183.7	204.6
Y	60.8	63.7	64.2	66.5	66.5	57.1	49.1	50.3	55.3	54.3	67.5	44.3	53.2	62.3	102.6	54.1	61.5	74.7	79.1
Zr	282.0	340.7	281.1	340.6	309.9	349.9	285.0	285.6	263.2	279.2	284.3	286.7	340.7	333.5	361.2	287.7	327.5	365.8	354.4
Nb	27.4	36.5	29.7	35.7	33.4	39.8	34.6	31.2	28.5	28.8	21.9	35.2	41.5	42.1	26.9	33.5	40.4	41.3	30.3
Mo	0.9	1.6	1.5	1.4	1.1	1.1	0.9	1.0	1.2	1.3	1.7	1.0	1.7	1.7	3.2	2.0	2.0	2.2	5.1
Co	7.6	4.7	6.9	4.6	5.2	3.9	4.3	4.5	6.0	4.1	10.3	3.0	3.8	3.0	26.6	5.4	6.6	7.0	14.3
Cr	51.0	68.2	52.0	55.6	58.5	60.5	59.5	50.1	46.3	45.2	45.8	43.8	56.8	67.5	73.0	44.3	60.2	79.1	60.8
V	59.5	86.2	68.1	86.4	80.3	83.8	68.4	58.2	58.0	59.9	56.4	56.7	82.2	103.5	104.3	51.4	78.0	114.8	83.1
Zn	25.4	30.0	35.9	42.2	37.9	20.0	24.4	24.4	24.6	20.2	39.4	21.1	29.4	27.4	44.2	44.5	42.7	25.7	44.6
Cu	23.1	23.4	24.3	26.0	22.7	20.4	23.3	22.6	25.1	22.7	24.1	23.5	30.6	29.0	34.1	29.9	33.8	38.8	30.4
Ni	6.8	5.7	10.3	3.7	6.5	2.0	4.8	5.5	7.4	5.0	10.3	3.5	7.1	6.6	17.2	7.5	11.0	14.8	15.7
Ge	<LLD	<LLD	<LLD	<LLD	<LLD	<LLD	<LLD	<LLD	<LLD	<LLD	<LLD	<LLD	<LLD	<LLD	<LLD	<LLD	<LLD	<LLD	<LLD
W	7.5	10.2	11.6	11.9	9.3	10.3	8.1	7.1	8.0	7.3	6.0	7.4	10.0	10.1	10.2	8.6	10.2	7.3	10.0
U	6.5	7.4	7.3	9.9	8.2	8.7	7.4	7.6	7.5	7.4	7.4	7.8	10.0	10.1	11.2	8.8	10.6	11.1	9.3
Th	31.9	30.9	31.3	47.3	34.5	38.1	35.7	34.5	32.7	29.9	32.7	33.5	43.9	41.6	37.8	33.7	49.4	37.5	42.6
Pb	281.8	45.8	39.2	47.3	45.1	48.0	212.0	132.9	136.2	161.9	156.3	151.0	170.6	52.2	55.6	44.0	53.6	48.8	58.8
As	8.6	6.9	14.7	3.8	8.0	<LLD	<LLD	3.4	3.3	<LLD	3.5	<LLD	<LLD	4.4	8.7	5.7	13.2	17.4	29.2
Se	<LLD	<LLD	<LLD	1.5	1.9	2.1	1.8	2.0	1.3	2.5	1.1	1.6	2.3	1.5	1.8	1.9	2.5	1.6	3.9
Bi	<LLD	<LLD	<LLD	<LLD	<LLD	<LLD	<LLD	<LLD	<LLD	<LLD	<LLD	<LLD	<LLD	<LLD	<LLD	<LLD	<LLD	<LLD	<LLD
Br	<LLD	<LLD	<LLD	<LLD	<LLD	3.1	<LLD	4.6	<LLD	4.1	<LLD	<LLD	4.9	3.5	<LLD	3.5	<LLD	<LLD	4.6
La	61.1	64.4	62.4	59.8	68.1	60.1	57.1	61.0	61.7	65.6	72.8	49.8	65.9	66.3	98.4	63.8	75.3	86.4	83.1
Ce	128.7	135.6	137.4	134.1	149.6	133.9	126.6	133.4	132.3	142.4	151.5	109.8	142.1	143.3	207.7	142.2	163.6	183.3	170.9
Nd	57.9	56.9	57.1	61.7	66.2	61.3	54.0	57.4	54.8	57.6	67.5	46.3	61.7	62.0	94.6	56.9	71.0	78.2	81.1
Cs	9.6	11.2	6.5	7.0	9.5	8.2	10.2	11.6	9.6	11.4	10.3	11.3	8.2	12.6	23.8	9.0	8.3	16.7	16.0
D	-37.92	-38.76	-39.22	-39.67	-40.2	-40.84	-41.85	-42.46	-43.11	-44.21	-45.38	-45.58	-46.52	-47.27	-47.82	-48.13	-48.67	-49.18	-49.51

XRF data re-calculated volatile-free!

137	21a	21b	21c	21d	21e	22Aa	22Ab	22Ac	22Ad	22Ae	22Ba	22Bb	22Bc	22Bd	22Be	22Bf	22Ca	22Cb	22Cc
SiO_2	67.45	67.32	66.30	64.31	64.19	65.42	63.38	65.71	67.42	65.15	63.70	65.91	67.22	66.14	65.73	64.00	64.53	63.56	66.48
TiO_2	1.32	1.27	1.08	1.14	1.20	1.34	1.24	1.27	1.14	1.22	1.12	1.22	1.17	1.16	1.17	1.25	1.33	1.24	1.33
Al_2O_3	29.50	29.59	30.56	32.61	29.61	31.13	33.49	30.99	29.35	30.46	32.90	30.21	29.57	30.73	29.38	32.11	31.67	31.05	30.25
FeO	0.40	0.41	0.89	0.72	3.37	0.65	0.51	0.52	0.70	1.11	0.57	0.88	0.49	0.37	1.67	0.81	0.61	1.87	0.47
MgO	0.22	0.24	0.21	0.21	0.32	0.25	0.24	0.27	0.23	0.34	0.28	0.32	0.25	0.28	0.38	0.25	0.26	0.46	0.26
CaO	0.15	0.13	0.12	0.12	0.16	0.15	0.13	0.14	0.14	0.43	0.13	0.32	0.22	0.19	0.52	0.22	0.28	0.63	0.17
Na_2O	0.11	0.10	0.08	0.08	0.11	0.10	0.09	0.10	0.12	0.11	0.09	0.11	0.11	0.10	0.11	0.10	0.10	0.11	0.10
K_2O	0.76	0.86	0.70	0.73	0.92	0.84	0.78	0.89	0.79	1.00	1.01	0.83	0.76	0.80	0.68	0.81	0.85	0.73	0.73
P_2O_5	0.09	0.09	0.08	0.09	0.12	0.13	0.14	0.11	0.12	0.19	0.20	0.21	0.22	0.24	0.38	0.46	0.39	0.36	0.28
TOTAL	100.00	100.00	100.00	100.00	100.00	100.00	100.00	100.00	100.00	100.00	100.00	100.00	100.00	100.00	100.00	100.00	100.00	100.00	100.00
Mn	22.3	24.2	61.4	40.4	270.8	46.8	39.5	29.0	34.1	59.8	22.0	107.5	34.2	21.4	180.0	58.0	41.9	197.0	27.3
S	0.1890	0.1730	0.4890	0.6320	0.5540	0.2860	0.3430	0.2120	0.9910	1.1470	0.3680	0.6850	0.6890	0.2610	0.5320	0.3140	0.1950	0.2630	0.2450
Ba	212.3	402.0	396.6	426.7	560.2	624.7	613.0	587.5	494.5	919.9	1009.3	943.1	1017.9	1056.5	1544.1	1890.2	1374.5	1403.8	1097.6
Sc	6.9	17.6	14.8	15.3	15.5	20.7	23.6	22.7	22.9	23.5	18.5	23.2	21.6	18.2	19.0	19.5	20.4	25.3	23.7
Rb	82.0	88.3	72.7	69.5	100.2	86.7	81.7	96.0	84.3	105.4	100.2	86.3	73.3	90.3	66.5	80.8	75.5	51.6	58.3
Sr	141.4	121.9	123.6	162.0	221.8	213.0	244.2	144.7	214.7	312.1	319.7	351.8	349.0	393.6	683.9	800.0	410.3	366.2	446.1
Y	56.4	62.7	59.0	57.6	60.4	68.5	80.5	68.8	79.9	76.4	59.9	77.5	64.2	45.4	57.6	44.6	56.2	55.8	55.8
Zr	368.4	363.7	329.5	315.7	306.7	392.9	422.6	397.6	355.0	370.8	336.0	391.5	396.0	362.4	334.5	363.4	411.0	365.2	336.7
Nb	46.7	45.6	29.9	31.7	31.8	43.3	44.0	41.9	30.6	36.3	38.7	38.7	37.3	42.3	34.1	43.4	44.0	42.1	35.9
Mo	1.9	2.2	2.0	2.1	2.2	2.4	1.9	1.4	1.9	3.1	1.7	2.9	1.8	1.4	1.7	1.5	1.6	1.4	1.3
Co	4.0	2.3	6.8	10.5	18.1	6.4	7.7	5.2	17.4	14.1	6.0	8.1	11.7	2.6	7.1	4.9	4.0	4.1	5.3
Cr	74.7	74.6	44.5	60.7	59.8	77.7	77.6	89.6	76.5	78.8	67.5	86.5	82.9	64.5	71.7	81.6	88.5	95.1	95.2
V	117.9	118.4	57.1	83.7	75.8	132.1	127.0	123.5	89.8	119.4	103.4	133.6	130.7	79.7	92.0	108.2	120.5	129.1	100.3
Zn	14.4	12.2	22.7	45.3	65.7	33.2	46.4	26.8	65.6	54.4	23.3	37.2	29.0	12.4	27.0	25.6	18.2	29.8	29.7
Cu	34.3	42.5	23.3	39.3	31.9	44.1	43.3	41.3	30.7	38.2	41.2	38.9	27.0	24.2	24.1	30.9	26.8	35.5	29.2
Ni	10.5	8.1	8.2	13.9	22.0	15.3	19.6	13.8	27.3	22.6	14.8	16.2	19.0	4.6	8.3	5.9	9.3	19.2	13.2
Ge	<LLD	<LLD	1.3	<LLD	0.5	0.5	1.1	1.1	2.0	<LLD	<LLD	1.1	<LLD	<LLD	1.5	<LLD	1.1	0.5	<LLD
W	13.5	9.4	13.2	10.0	11.6	10.9	11.0	8.9	13.7	11.2	8.7	10.0	9.6	10.4	8.6	7.9	10.5	8.0	8.2
U	11.9	8.2	8.4	9.8	9.1	10.5	11.1	9.9	8.6	8.5	11.4	9.1	9.9	9.6	9.8	7.9	8.4	8.2	8.5
Th	42.6	39.9	41.5	39.7	44.0	43.1	50.6	47.3	37.7	35.5	50.9	44.8	44.8	50.2	42.7	47.3	44.3	46.4	42.8
Pb	55.5	48.5	34.6	43.5	59.6	48.6	59.9	260.2	192.3	165.5	47.3	184.4	158.8	87.7	68.6	69.8	50.9	593.1	627.3
As	8.8	5.2	8.1	11.5	18.4	10.3	14.0	<LLD	18.8	24.4	18.8	7.4	5.2	2.4	2.6	2.9	<LLD	<LLD	<LLD
Se	3.0	2.3	2.1	3.7	14.2	3.1	3.7	7.2	5.5	2.9	2.3	2.4	2.4	2.3	2.3	2.0	2.3	2.8	1.8
Bi	<LLD	<LLD	<LLD	<LLD	<LLD	<LLD	<LLD	<LLD	<LLD	<LLD	<LLD	<LLD	<LLD	<LLD	<LLD	<LLD	<LLD	<LLD	<LLD
Br	3.3	3.9	<LLD	<LLD	<LLD	<LLD	<LLD	<LLD	<LLD	<LLD	<LLD	<LLD	<LLD	<LLD	<LLD	<LLD	3.2	3.9	<LLD
La	62.1	68.3	65.3	83.8	74.5	73.8	92.1	74.8	96.8	84.3	72.2	87.1	71.3	58.3	71.9	70.6	60.0	68.7	56.8
Ce	130.2	148.8	141.9	178.8	156.0	157.4	192.9	166.4	200.5	176.7	145.9	179.4	156.6	120.9	159.0	145.2	134.6	153.8	135.4
Nd	55.2	64.3	63.2	72.7	70.8	68.3	86.9	73.2	90.1	82.0	68.9	77.4	66.9	50.0	73.3	60.2	57.0	71.2	59.5
Cs	13.1	13.3	9.1	9.1	14.4	13.4	10.5	10.1	11.1	10.0	7.1	12.8	15.8	14.7	8.3	10.6	10.3	12.0	10.8
D	-50.65	-50.92	-51.41	-52.24	-53.12	-53.76	-53.98	-54.31	-55.09	-55.96	-56.39	-56.56	-57.35	-57.99	-58.44	-59.51	-59.98	-60.38	-60.84

137	22Da	22Db	22Dc	22Dd	22De	22Ea	22Eb	22Ec	22Ed	22Ee	22FSa	22FSb	22FSc	23ASa	23ASb	23ASc	23ASd	23ASe	23BS
SiO_2	63.95	63.04	61.65	65.65	64.23	60.67	65.99	60.91	56.56	56.96	56.61	53.99	54.13	55.78	57.74	64.02	63.21	66.95	67.44
TiO_2	1.19	1.22	1.11	1.28	1.31	1.28	1.46	1.42	1.49	1.64	1.78	1.88	1.56	1.47	2.07	1.86	1.52	2.25	1.32
Al_2O_3	30.31	30.34	28.66	30.57	30.17	33.22	29.26	32.82	31.90	34.93	35.88	36.70	40.23	40.76	38.13	29.64	32.41	28.79	29.54
FeO	2.08	3.40	5.58	0.59	2.30	2.09	1.20	2.24	5.16	1.74	2.38	2.77	1.24	0.40	0.75	2.09	0.99	0.57	0.55
MgO	0.44	0.41	0.77	0.35	0.40	0.53	0.40	0.47	0.86	0.54	0.65	0.86	0.55	0.44	0.32	0.53	0.44	0.32	0.23
CaO	0.79	0.32	0.99	0.27	0.39	0.80	0.57	0.74	2.40	2.09	1.07	2.11	1.14	0.65	0.25	0.68	0.38	0.13	0.23
Na_2O	0.11	0.12	0.13	0.12	0.12	0.12	0.12	0.11	0.14	0.14	0.18	0.15	0.12	0.05	0.06	0.08	0.06	0.08	0.05
K_2O	0.73	0.89	0.89	0.85	0.75	0.74	0.70	0.78	0.69	0.68	0.79	0.77	0.60	0.37	0.62	1.01	0.85	0.86	0.57
P_2O_5	0.41	0.26	0.23	0.32	0.33	0.55	0.31	0.51	0.80	1.30	0.66	0.76	0.45	0.09	0.07	0.09	0.14	0.06	0.12
TOTAL	100.00	100.00	100.00	100.00	100.00	100.00	100.00	100.00	100.00	100.00	100.00	100.00	100.00	100.00	100.00	100.00	100.00	100.00	100.20
Mn	234.8	249.3	486.8	41.6	126.6	178.6	176.5	122.9	412.1	154.1	230.8	355.9	143.6	55.6	45.2	247.3	93.7	29.4	35.7
S	0.5110	0.6500	0.7170	0.2260	0.3560	0.5190	0.6180	0.6660	1.0360	0.4430	0.5020	0.4820	0.3490	0.0450	0.2600	0.3000	0.1730	0.2020	0.1070
Ba	1562.4	1142.7	914.9	1279.7	1185.8	1412.6	2240.9	1701.7	1976.5	1042.9	2434.7	2127.2	1366.2	261.1	290.1	487.8	580.1	330.1	365.6
Sc	24.4	18.5	19.6	24.3	24.1	26.9	23.2	28.5	25.5	24.3	32.8	32.1	30.6	17.0	53.2	32.2	28.3	35.3	24.2
Rb	68.5	70.5	53.3	92.3	74.3	87.0	81.1	87.8	91.4	54.6	71.4	63.5	48.1	28.9	49.7	94.4	78.5	67.5	36.7
Sr	883.5	587.7	662.4	616.1	648.5	492.5	594.5	452.3	472.7	547.4	943.8	783.3	503.7	68.0	51.6	99.6	135.2	50.9	91.3
Y	83.2	73.4	67.4	58.5	65.9	75.9	76.2	46.6	63.2	73.3	94.0	96.5	70.9	41.7	92.8	88.2	71.9	99.0	51.2
Zr	522.9	502.9	420.9	446.1	423.1	439.8	363.1	333.2	345.9	438.8	551.1	577.9	555.0	570.3	715.2	545.3	474.2	633.2	779.2
Nb	48.1	49.1	43.6	45.8	41.1	47.5	36.6	37.2	35.1	49.3	55.1	59.2	54.7	52.6	69.7	61.0	50.7	68.9	36.9
Mo	1.8	2.1	1.4	1.8	1.6	1.9	1.7	2.2	1.8	1.7	1.6	2.9	1.1	3.2	5.0	8.3	4.3	6.5	1.8
Co	6.9	7.0	7.4	3.9	5.8	4.9	8.3	6.4	11.3	9.8	8.6	8.3	7.5	7.0	7.7	8.0	7.4	9.7	19.2
Cr	88.9	83.6	69.2	94.6	93.3	106.9	87.5	107.3	103.5	91.4	153.6	136.9	117.5	58.9	267.6	131.7	113.7	144.4	165.2
V	108.0	96.3	79.3	122.6	127.3	143.6	122.5	151.3	133.5	122.3	170.6	183.7	157.4	76.3	256.8	143.3	125.4	133.0	78.3
Zn	31.6	29.0	27.4	33.9	36.1	32.3	37.3	39.9	54.3	25.0	29.4	22.3	21.7	21.4	24.9	24.0	18.1	24.4	55.6
Cu	35.7	35.2	29.3	41.3	29.3	25.0	26.4	38.7	35.8	40.1	49.7	41.5	36.6	25.5	49.1	27.7	32.1	37.0	30.8
Ni	9.5	16.1	24.0	9.4	12.5	20.8	9.3	7.7	8.8	33.6	29.7	23.3	21.2	49.7	39.7	19.4	25.9	27.5	49.2
Ge	1.5	1.8	1.5	1.2	1.6	1.2	0.6	1.2	0.7	1.5	<LLD	<LLD	<LLD	<LLD	<LLD	<LLD	<LLD	<LLD	<LLD
W	10.3	11.4	11.8	11.9	15.2	12.9	12.8	13.6	13.7	10.8	12.6	14.1	10.8	10.1	15.4	12.7	11.2	11.2	7.6
U	13.1	11.0	12.2	11.0	9.3	10.9	9.7	7.0	7.8	13.4	14.5	13.8	13.5	11.3	12.3	12.8	10.6	11.7	7.7
Th	62.7	51.7	43.0	45.9	43.7	51.0	42.8	40.7	37.0	49.2	64.7	51.9	60.1	44.5	77.8	52.5	43.7	50.8	44.2
Pb	327.1	295.6	222.1	55.5	47.1	46.9	41.1	41.8	33.0	204.6	92.1	81.8	78.1	67.6	71.2	187.9	189.6	149.0	154.3
As	<LLD	<LLD	<LLD	2.7	3.5	2.2	<LLD	<LLD	2.4	<LLD	<LLD	<LLD	<LLD	<LLD	<LLD	<LLD	<LLD	<LLD	10.6
Se	2.5	3.5	3.5	3.9	2.6	3.0	1.5	2.0	1.9	4.0	4.5	4.1	3.9	10.1	6.9	3.4	4.0	4.9	1.7
Bi	<LLD	<LLD	<LLD	<LLD	<LLD	<LLD	<LLD	<LLD	<LLD	<LLD	<LLD	<LLD	<LLD	<LLD	<LLD	<LLD	<LLD	<LLD	<LLD
Br	<LLD	<LLD	4.2	6.7	4.2	<LLD	<LLD	<LLD	<LLD	<LLD	<LLD	<LLD	6.9	3.9	8.5	<LLD	3.7	7.9	
La	86.2	66.7	63.5	75.9	78.2	84.6	107.7	100.4	90.9	69.9	131.5	114.3	89.6	34.1	48.8	59.4	76.4	33.2	62.4
Ce	182.0	136.0	125.8	161.6	171.2	190.7	237.8	220.5	187.7	146.0	294.4	241.1	191.1	68.3	129.9	117.7	151.6	84.3	130.5
Nd	76.3	57.9	50.9	66.8	68.9	71.6	99.9	89.6	80.4	61.1	124.8	99.2	78.9	26.3	58.4	51.8	59.8	45.0	46.2
Cs	14.1	14.8	13.1	9.3	8.6	13.0	14.7	16.5	13.2	12.0	12.3	15.0	7.0	5.1	9.5	16.9	9.5	14.1	5.2
D	-61.22	-62.73	-63.52	-63.76	-64.47	-65	-65.35	-65.7	-66.54	-67.18	-67.54	-69.03	-69.14	-74.3	-74.64	-75.34	-76.27	-78.16	-79.35

Table II.4 Analytical results of samples that were leached in duplicate and triplicate. Negative numbers indicate that the result was below the lower limit of determination. ICP-OES was used to analyse the concentrations of Na to Zn (ppm) and the rest of the elements were analysed by ICP-MS (ppb). The values analysed by ICP-OES are reported either to one or two decimal places depending on the lower limit of determination for the element (Chapter 3).

	137 0c i	137 0c ii	137 0c iii	136 2b i	136 2b ii	137 12a i	137 12a ii	137 14b i	137 14b ii	136 19c i	136 19c ii	137 22ad i	137 22ad ii	FA i	FA ii	BA i	BA ii
Na	7.3	7.4	7.0	26	27	16.0	15.0	19.0	19.0	6.3	6.3	13.0	12.0	1.1	1.1	0.7	0.7
Mg	505	497	501	114	109	40	40	36	35	33	32	38	38	0.4	0.4	0.1	0.1
Al	13.0	7.3	8.1	1.2	0.3	0.6	0.3	0.7	0.3	73.0	70.0	0.3	0.0	40.0	36.0	6.2	5.7
P	1.0	1.0	1.0	0.3	0.3	-0.2	0.2	0.5	0.5	-0.2	-0.2	-0.2	-0.2	408	405	29	25
S	3380	3120	3220	29	33	10.0	10.0	299	300	278	272	47	47	-3.6	-5.8	-4.9	-8.5
K	2.9	2.3	2.5	121.0	113.0	32.0	30.0	27.0	25.0	5.9	5.6	16.0	16.0	24	24	22	20
Ca	1630	1580	1600	458	447	274	273	920	910	181	179	172	174	2.1	2.1	0.0	0.0
V	0.20	0.17	0.17	0.06	0.03	0.03	0.03	0.06	0.04	0.02	-0.01	0.02	0.01	1140	1400	243	242
Cr	0.43	0.39	0.38	0.06	0.04	0.03	0.02	0.05	0.03	0.04	-0.02	-0.02	-0.02	-0.02	3.50	-0.02	0.02
Fe	2450	2170	2100	0.79	4.40	0.07	0.52	0.12	1.30	45	45	0.13	0.63	0.62	0.67	0.16	0.17
Ni	18.0	17.0	18.0	0.4	0.4	0.2	0.2	0.5	0.5	1.3	1.3	1.0	1.0	0.4	0.5	0.0	-0.2
Zn	2.30	2.20	2.10	0.38	0.35	0.27	0.27	0.45	0.43	2.70	2.60	0.62	0.56	106	115	27	24
B	-58	539	-10	-91	-26	-92	-36	172	386	-4	-33	298	-47	16	-6	-5	-6
Be	-6	-8	21	-3	-7	-5	-4	0	-3	100	110	-11	-4	5	11	-2	-1
Co	13009	12484	12590	98	35	6	63	9	17	374	391	398	397	1416	1237	118	-9
Cu	196	129	132	-4	-5	-8	-8	-16	-11	950	967	81	-36	0	0	-1	0
As	43	-1	-15	0	-1	-2	-6	0	-3	-6	-19	-7	0	2223	2239	2742	1574
Mo	-5	90	-3	-1	-19	-3	-25	25	53	20	-17	0	-13	6	5	0	0
Cd	41	40	48	-3	-2	-11	-2	-4	-5	52	36	-4	-9	-4	-4	-5	-10
Sb	0	13	-2	-1	-3	-2	-3	-1	-1	0	4	-3	-2	211	192	11	2
Ba	349	390	365	4631	4797	2051	2069	1252	1292	891	835	2659	2864	2223	2239	2742	1574
Tl	419	380	484	6	3	2	5	2	3	2	2	3	6	18614	18385	670	275
Bi	-1	-1	-1	-1	-1	-2	-1	-1	0	0	-1	3	2	256	252	-3	-2
U	4	2	3	-2	-1	17	2	37	35	19	25	2	0	174	182	36	-4

Table II.5 Analyses of leachates that were obtained according to the method of von Prüeß et al. (1991), described in Chapter 3. In the case of samples that were leached in duplicate the average value is presented, and if a value of an element from one of the duplicate leachates was below the lower limit of determination the other value is reported. Negative numbers indicate that the value was below the lower limit of determination. ICP-OES was used to analyse the concentrations of Na to Zn (ppm) and the rest of the elements were analsed by ICP-MS (ppb). The samples analysed by ICP-OES are reported either to one or two decimal places depending on the lower limit of determination for the element (Chapter 3).

	136_0a	136_0b	137_0b	137_0c	136_0c	136_1bd	136_1ca	136_2b	137_6a	137_7c	137_8b	137_12a	136_14b	137_14b	136_19a
Na	17.0	20.0	4.5	7.3	12.0	25.0	24.0	26.0	13.0	14.0	16.0	16.0	22.0	19.0	16.0
Mg	115	100	106	501	207	116	147	114	27	36	38	40	30	36	46
Al	0.3	2.3	244.0	9.5	26.0	0.6	0.6	0.7	0.6	0.3	0.5	0.5	0.3	0.5	0.6
P	0.3	-0.2	0.4	1.0	0.4	-0.2	0.3	0.3	-0.2	-0.2	-0.2	0.2	0.4	0.5	-0.2
S	27	100	954	3240	656	52	15	30	41	16	12	10	28	299	78
K	77.0	105.0	1.3	2.6	50.0	205.0	123.0	117.0	24.0	44.0	50.0	32.0	37.0	27.0	23.0
Ca	378	287	255	1603	577	273	482	453	215	239	254	274	583	920	223
V	0.03	0.02	0.26	0.18	0.04	0.03	0.05	0.04	0.04	0.02	0.03	0.03	0.04	0.06	0.03
Cr	0.04	0.03	0.18	0.40	0.08	0.04	0.06	0.06	0.03	0.03	0.02	0.03	0.04	0.05	0.03
Fe	0.35	0.25	553.00	2240.00	126.00	2.60	1.20	2.60	0.55	-0.02	-0.02	0.30	0.26	0.70	0.12
Ni	0.4	0.6	3.6	18.0	2.5	0.3	0.4	0.4	0.2	0.2	0.2	0.2	0.4	0.5	0.5
Zn	0.31	0.81	7.80	2.20	1.60	0.28	0.38	0.38	0.49	0.50	0.27	0.27	0.35	0.45	0.49
B	220	149	-19	539	-96	205	756	-91	139	-75	-78	-92	200	279	-52
Be	-7	-6	143	21	23	-1	28	-3	-4	-1	-1	-5	-1	0	-6
Co	12	196	2039	12694	1238	43	9	67	21	23	11	35	-6	13	127
Cu	-3	-6	1805	152	-28	-35	52	-4	0	-13	-2	-8	-5	-16	-37
As	-14	-14	87	43	-15	-6	-9	0	-6	-7	-4	-2	-7	0	-1
Mo	-5	-2	-10	90	0	-3	-5	-1	-11	-6	-9	-3	-4	39	-4
Cd	-5	-5	37	43	-7	-3	-8	-3	0	-2	-1	-11	-2	-4	-2
Sb	5	-1	6	13	-2	-1	-2	-1	5	-2	4	-2	-3	-1	5
Ba	1827	2181	168	368	1417	3663	2789	4714	2237	2903	2590	2051	2765	1272	1800
Tl	7	17	65	428	66	9	4	5	2	1	2	4	-1	2	5
Pb	1010	49	6311	24	129	51	91	-19	1759	335	99	5667	-9	22	43
Bi	-1	-1	-1	-1	-1	-2	3	-1	-2	-1	-1	-2	-1	-1	-1
U	0	8	382	3	31	1	10	-2	0	-1	-1	17	21	36	0
D	0.5	0.3	0.2	0.1	0	-2.1	-2.5	-8.24	-19.46	-21.43	-22.72	-30	-33.42	-33.74	-45.87

	136_19c	136_20b	137_21a	137_21d	137_22ad	136_22ae	136_22eb	137_22eb	136_22ec	136_22ee	137_22ee	136_22fsa	136_22fsb	136_22fsc
Na	6.3	14.0	33.0	16.0	13.0	11.0	6.5	28.0	18.0	8.6	17.0	37.0	17.0	32.0
Mg	33	38	48	68	38	40	49	62	66	72	69	65	63	70
Al	73.0	23.0	0.3	0.5	0.3	0.2	0.4	0.3	0.3	0.3	0.2	0.3	0.6	0.3
P	-0.2	-0.2	-0.2	0.2	-0.2	0.3	0.2	0.3	0.3	0.3	0.3	0.3	0.3	0.3
S	278	276	16	44	47	160	13	19	9	19	32	11	7	14
K	5.9	17.0	51.0	24.0	16.0	11.0	9.2	27.0	20.0	13.0	18.0	36.0	18.0	28.0
Ca	181	170	243	281	172	562	295	481	370	398	402	464	457	411
V	0.02	0.02	0.02	0.03	0.02	0.03	0.03	0.04	0.04	0.04	0.03	0.04	0.04	0.04
Cr	0.04	0.03	0.02	0.04	-0.02	0.03	0.03	0.03	0.04	0.04	0.03	0.04	0.04	0.03
Fe	45.00	85.00	0.08	0.07	0.13	-0.02	-0.02	-0.02	0.08	0.02	-0.02	0.09	-0.02	0.03
Ni	1.3	0.7	0.2	0.3	1.0	0.7	0.3	0.3	0.3	0.3	0.3	0.3	0.3	0.3
Zn	2.70	0.95	0.17	0.21	0.62	0.36	0.21	0.30	0.28	0.26	0.26	0.30	0.28	0.27
B	-4	-53	324	-46	298	-7	-7	-95	-75	-51	258	-57	-82	157
Be	105	54	-9	-9	-11	-3	-3	-5	-4	-3	0	-5	-11	-6
Co	382	445	15	12	398	181	51	-1	-4	-5	-6	-1	-2	-1
Cu	960	61	-18	-4	81	-5	-3	-31	-14	84	-1	-8	-10	-1
As	-6	-1	-6	-1	0	-2	-5	-6	-3	-15	-1	0	-7	-5
Mo	20	-4	-3	24	0	23	-16	24	-3	-11	25	38	-7	15
Cd	52	42	-6	0	-4	-9	-3	-4	-2	-8	-2	-2	-2	-2
Sb	4	-5	-2	-5	-3	-3	-1	4	-1	4	-2	26	-1	16
Ba	863	1937	5612	2085	2762	1444	4208	10583	9777	5961	9838	14222	10284	11274
Tl	2	17	4	1	5	14	0	-1	0	1	2	3	0	-1
Pb	3028	452	66	23	2179	-1	-5	-9	-25	-2	-13	19	-6	52
Bi	0	0	0	-1	3	-1	-1	-1	-1	-1	-1	0	-1	-1
U	22	7	-1	2	2	8	12	17	8	13	3	12	29	9
D	-46.87	-48.46	-50.65	-52.24	-55.09	-56.39	-64.36	-65.35	-66.02	-66.2	-66.3	-67.54	-68	-69